I. THE 3.7 Å CRYSTAL STRUCTURE OF HORSE HEART FERRICYTOCHROME C

II. THE APPLICATION OF THE KARLE-HAUPTMAN TANGENT FORMULA TO PROTEIN PHASING

Thesis by

Jon Edward Weinzierl

In Partial Fulfillment of the Requirements

For the Degree of

Doctor of Philosophy

California Institute of Technology

Pasadena, California

1969

(Submitted July 8, 1968)

ACKNOWLEDGMENTS

I am most deeply indebted to Dr. R. E. Dickerson for his continual interest, guidance and assistance throughout the course of the research presented in this Thesis. His comprehensive knowledge of the field of protein crystallography and his unending patience and interest in myself are largely responsible for the completion of my graduate studies at Caltech.

I also wish to thank one of my coauthors, Dr. D. S. Eisenberg, for his extensive contribution to the investigation into the application of the Karle-Hauptman tangent formula to protein phasing.

I am also indebted to the following people for their invaluable contributions to the investigation into the crystal structure of horse heart cytochrome c: Mary L. Kopka, Joan C. Varnum, Dr. Charles L. Borders, Jr., Kathryn Christiansen, and Roberta Pratl.

The initial crystals of cytochrome c, and many of the initial heavy atom derivatives were supplied by Dr. Emanuel Margoliash to whom I also wish to express my thanks.

Finally, I wish to express my gratitude to the California Institute of Technology and to the National Institute of Health for the financial support which I have received during my graduate work.

SECTIONS OF THIS PROJECT SPECIFICALLY PERFORMED BY THE AUTHOR

Since many people have contributed to the research reported in this Thesis, I must specifically identify my contributions to the project.

I have participated in all areas of this project, with the exception of the heavy atom derivative preparation and chemistry. My major contributions, however, have been in the areas of the three dimensional structure analysis and the applications of the Karle-Hauptman tangent formula to protein phasing.

In these areas one of my main contributions has been the writing of the major computer programs used, with the exception of the phase-refinement program. All of the work, in the three dimensional structure determination, from the point of the measured intensities to the final Fourier map, is mine. I shared equally in the work concerning the tangent formula with Dr. Eisenberg and Dr. Dickerson.

USE OF THE PREVIOUSLY PUBLISHED PAPERS CONCERNING THIS RESEARCH PROJECT

Four papers have been published concerning the two and three dimensional structure determinations of cytochrome c and one paper concerning the application of the Karle-Hauptman tangent formula to protein phase refinement. Rather than duplicate the information contained in these papers, I have included them as appendices and have referred to them whenever possible in the main body of this Thesis. When making reference to one of these papers I have used the notation I, II, III, IV, or V and a page number, in contrast to the notation for the other appendices: Appendix I, etc.

ABSTRACT

I. The 3.7 Å Crystal Structure of Horse Heart Ferricytochrome C.

The crystal structure of horse heart ferricytochrome c has been determined to a resolution of 3.7 Å using the multiple isomorphous replacement technique. Two isomorphous derivatives were used in the analysis, leading to a map with a mean figure of merit of 0.458. The quality of the resulting map was extremely high, even though the derivative data did not appear to be of high quality.

Although it was impossible to fit the known amino acid sequence to the calculated structure in an unambiguous way, many important features of the molecule could still be determined from the 3.7 Å electron density map. Among these was the fact that cytochrome c contains little or no α-helix. The polypeptide chain appears to be wound about the heme group in such a way as to form a loosely packed hydrophobic core in the molecule.

The heme group is located in a cleft on the molecule with one edge exposed to the solvent. The fifth coordinating ligand is His 18 and the sixth coordinating ligand is probably neither His 26 nor His 33.

The high resolution analysis of cytochrome c is now in progress and should be completed within the next year.

II. The Application of the Karle-Hauptman Tangent Formula to Protein Phasing.

The Karle-Hauptman tangent formula has been shown to be applicable to the refinement of previously determined protein phases. Tests were made with both the cytochrome c data from Part I and a theoretical structure based on the myoglobin molecule. The refinement process was found to be highly dependent upon the manner in which the tangent formula was applied. Iterative procedures did not work well, at least at low resolution.

The tangent formula worked very well in selecting the true phase from the two possible phase choices resulting from a single isomorphous replacement phase analysis. The only restriction on this application is that the heavy atoms form a non-centric cluster in the unit cell.

Pages 156 through 284 in this Thesis consist of previously published papers relating to the above two sections. References to these papers can be found on page 155.

TABLE OF CONTENTS

PART I

THE 3.7 Å CRYSTAL STRUCTURE OF HORSE HEART FERRICYTOCHROME C

INTRODUCTION

The general composition and sequence of amino acids in a protein can now, in principle, be determined using standard organic and biochemical techniques. The biological properties of a protein, however, do not directly depend on the simple sequence of amino acids in the polypeptide chain, but on the three dimensional arrangement of these amino acids which comprises the enzymatically active protein. To obtain the three dimensional arrangement of amino acids in a protein one must resort to a direct measurement of the atomic positions.

At present, the only method for obtaining the spatial arrangement of amino acids in a protein molecule is x-ray crystallography. In theory the x-ray analysis of a crystalline protein should produce unequivocal results concerning the type and location of every atom in the protein molecule. In practice, however, this is seldom true, and chemical information, in particular the amino acid sequence, is invariably used as an aid in interpreting the results of the x-ray analysis.

This Thesis is concerned with the x-ray analysis and subsequent interpretation of the structure of a respiratory protein, horse heart cytochrome c. Cytochrome c is a heme-containing protein occurring in the mitochondria of almost all aerobic organisms. It is one of a number of cytochromes which are involved in the transfer of free energy, released from the metabolism of sugars, into high energy intermediate compounds such as ATP. The entire system of cytochromes

is known as the "electron transport" system and operates through the reversible oxidation-reduction of the iron atoms located in the heme groups of the constituent cytochromes. Cytochrome c has been widely studied and has been obtained in a crystalline form from a wide variety of organisms (14).

A great deal is already known or suspected concerning the structure of horse heart cytochrome c from chemical and physical chemical evidence. Of primary importance to the crystallographer is the amino acid sequence (Fig. 1), determined by Margoliash (13) and others. The primary structure consists of 104 amino acids with a heme group covalently attached to two cysteines at positions 14 and 17. The mode of attachment of the heme is through the α-carbons of its vinyl side chains and occurs in such a way that, looking into the heme plane with the propionic acid groups at the bottom, one of the bonds points to the side of the heme and the other points upward, as in Fig. 2. It has been further shown by solvent perturbation studies (19) that the heme is on the surface of the protein, partially buried in a crevice-like structure. Kabat (8) and Eaton & Hochstrasser (6) have also shown that for horse heart cytochrome c in the space group $P4_1$, the space group used in this study, the heme normal is at an angle of about 70° to the c axis of the crystal.

Electron microscope studies (11, 12) have indicated that the cytochrome c molecule is an oblate spheroid of approximate dimensions (38 to 40 Å) x 28 Å. This study also implied that the structure consists of three rods running parallel to each other and connected by

FIGURE 1

The amino acid sequence of horse heart cytochorme c (14).

```
    1                                       10
Ac-Gly-Asp-Val-Glu-Lys-Gly-Lys-Lys-Ilu-Phe-Val-Gln-Lys-Cys-Ala-

                  20                                        30
Gln-Cys-His-Thr-Val-Glu-Lys-Gly-Gly-Lys-His-Lys-Thr-Gly-Pro-Asn-

                                    40
Leu-His-Gly-Leu-Phe-Gly-Arg-Lys-Thr-Gly-Gln-Ala-Pro-Gly-Phe-Thr-

        50                                              60
Tyr-Thr-Asp-Ala-Asn-Lys-Asn-Lys-Gly-Ilu-Thr-Try-Lys-Glu-Glu-Thr-

                           70
Leu-Met-Glu-Tyr-Leu-Glu-Asn-Pro-Lys-Lys-Tyr-Ilu-Pro-Gly-Thr-Lys-

80                                          90
Met-Ilu-Phe-Ala-Gly-Ilu-Lys-Lys-Lys-Thr-Glu-Arg-Glu-Asp-Leu-Ilu-

                  100
Ala-Tyr-Leu-Lys-Lys-Ala-Thr-Asn-Glu-COOH
```

The heme group is covalently attached through the α-carbons of its vinyl side chains to Cys 14 and Cys 17.

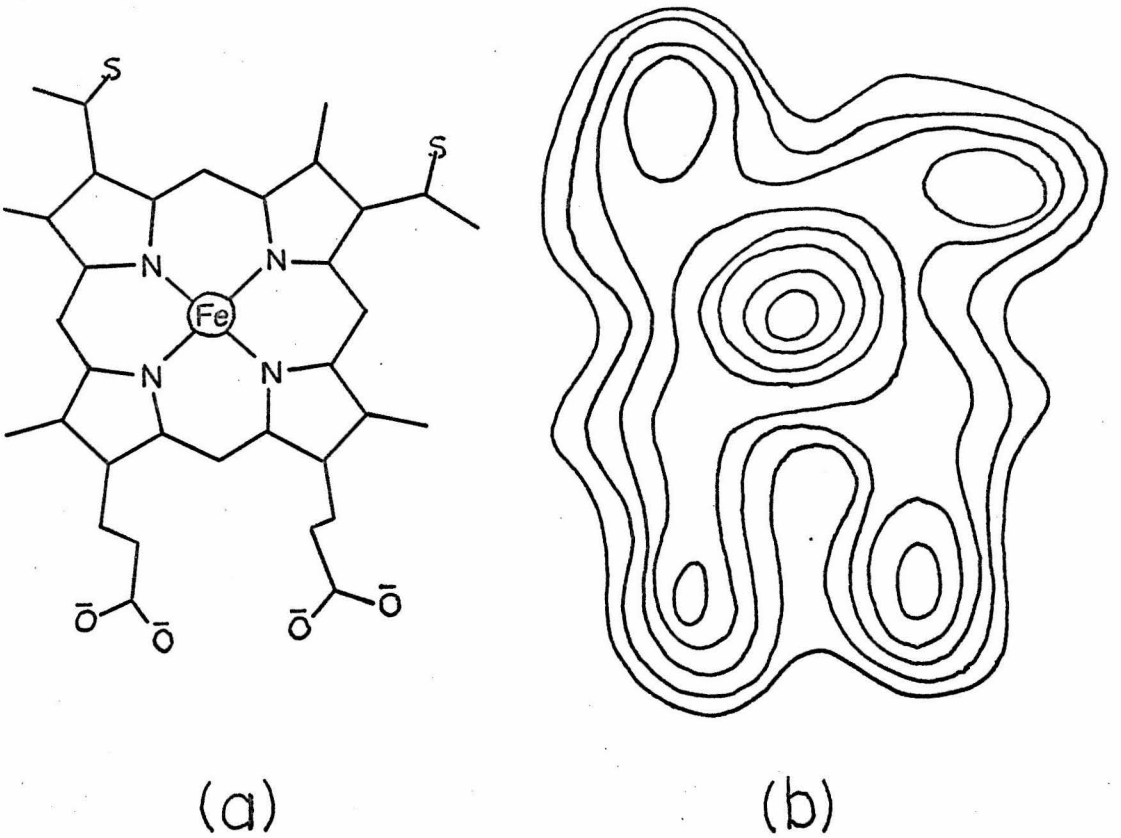

FIGURE 2

(a) The skeletal arrangement of the heme group contained in horse heart cytochrome c. The heme is attached to Cys (14) and Cys (17) in the protein at the points marked "s".

(b) The heme group in (a) as it would appear in a 3.7 Å resolution Fourier map.

two short turns of polypeptide chain. Interpreting these rods in terms of α-helix, the structure would consist of 85% or more α-helix. This is very high compared to that predicted by the Cotton effect at 235 mμ of 41 to 45% (14). The minimal amount of α-helix, calculated on the basis of the length of segments containing 6 or more helix forming residues in sequence is 35% (2).

Much additional structural evidence comes from the comparative sequence studies of the cytochrome c's taken from a variety of different organisms. This information is relevant to the structure of horse heart cytochrome c because the tertiary structures of the various cytochrome c's used in these studies are almost certainly the same as that of the horse heart form. This can be shown by the fact that cytochrome c taken from one species of animal can replace that of another species, in vitro, with little or no loss of activity in the enzyme systems utilizing cytochrome c (14).

One of the most striking results of these studies is the presence of the so called "invariant regions" in the amino acid sequence. These are presumably required to maintain the general tertiary structure of the protein or are involved in providing a specific environment for the heme group. They may also be required as specific "active sites" for the interaction of the cytochrome c molecule with the other proteins of the electron transport system or with the mitochondrial matrix protein.

Among the cytochrome c's of the higher animals the following amino acids are invariant: two histidines at 18 and 26, two arginines at

38 and 91, a tryptophan at 59, three of the three to five prolines, four of the four to five tyrosines, and eleven out of the twelve to fourteen glycines (14). The positions of the three constant prolines and positions 25 and 44, which contain proline in certain species, can be located in an α-helix only at the N-terminal end of the helix. Most of the eleven constant glycines occur in the region of the heme attachment and may be the points of close approach between different regions of the peptide chain.

The longest invariant region in the cytochrome c sequence occurs from Asn 70 to Met 80. This region is invariant even in the plant, fungal and yeast cytochrome c's studied to date and is certainly non-helical, since it contains two prolines and several other helix breakers. One possible reason for the constancy of this region is the implied participation of Met 80 as the sixth coordinating ligand of the iron atom in the heme (1, 7).

In examining the sequences of the various cytochrome c's, another property of the sequence seems to remain invariant. Most of the hydrophobic amino acids are clustered in eight regions: 9 to 12, 32 to 36, 46 to 48, 57 to 59, 64 to 68, 74 to 75, 80 to 85, and 94 to 98. Almost every one of these hydrophobic areas is next to, or one amino acid removed from, a basic residue or cluster of basic residues. The acidic amino acids do not seem to be clustered at all (14). These hydrophobic regions of the protein are probably not exposed to

the solvent due to the large, positive change in entropy which results if they can be arranged to form a non-polar region in the interior of the molecule, and thus, isolate the non-polar groups from the solvent (10).

On the other hand, the four residues at the carboxy-terminal end of the protein vary widely in the different species with the only apparent restriction that they be non-hydrophobic. These residues can be removed enzymatically without loss of biological activity (21). They almost certainly are located at the surface of the protein.

Up to 90% of the ε-amino groups of lysine can be blocked by acetylation with acetic anhydride (16). This results in the complete loss of activity in the succinate oxidase and cytochrome oxidase systems, but causes no change in the absorption spectrum, ascorbic acid oxidase activity, hydroxylamine reductase activity, nor the reactivity with carbon monoxide. The protein does, however, become auto-oxidizable. Guanidinated derivatives, however, retain their activity in the above mentioned systems (20). This indicates that the main function of the lysyl residues is to provide basic groups, and that the structure of these groups is not important. This also indicates that the lysine positions are involved in the sites required for binding cytochrome oxidase and succinate oxidase and therefore are positioned on the surface of the protein. It has been further shown that blocking either Lys 72 or Lys 73, which both occur in the Asn 70 to Met 80 constant region, results in the loss of about 50% of the activity with cytochrome oxidase (17). Thus, this eleven-residue long

invariant region is also related to the interaction of cytochrome c with cytochrome oxidase.

Positions 89 and 92 are occupied in the various species studied by basic, acidic, neutral, and hydrophobic groups. With this variability in functional groups, these positions are also probably on the surface of the molecule, or at least distant from the heme.

In yeast and fungal cytochromes, the N-terminal acetyl group is replaced by four or five extra residues. Their sequence is highly variable and they are also probably on the surface of the molecule. The function of the N-acetyl group of the extra residues seems to be merely to remove the positive charge ordinarily found on the N-terminal amino acid from the vicinity of the heme.

THEORY OF PROTEIN PHASE ANALYSIS

An x-ray structure analysis is based on the fact that when a crystalline substance is placed in a monochromatic, collimated x-ray beam, x-rays are diffracted in certain, discrete directions by the atoms of the crystal. The directions of diffraction are related only to the interval and directions between the repeating units making up the crystal, while the magnitudes or intensities of the diffracted rays are only a function of the atomic arrangement within a repeating unit.*

This set of diffracted rays is most generally thought of as a three dimensional lattice of points called the weighted reciprocal lattice, each point in the lattice being assigned a number, or weight, proportional to the square root of the intensity of the associated diffracted ray.

Since x-rays are electromagnetic radiation, and thus possess a wave nature, another parameter is needed to completely describe the diffraction of x-rays by a crystal. Each individual diffracted ray has a certain phase relationship to the original x-ray beam. Therefore, each point of the

*The measured intensities also depend on certain experimental factors such as the type of device used to record the reflections (Lorentz and Polarization factors) and the size of the crystal (absorption effects).

weighted reciprocal lattice must also be assigned a certain phase angle between 0 and 2π.

It is this phase information that is lost during the process of recording the diffraction pattern, and which must be recovered in order to calculate the structure of the repeating unit in the crystal.

The intensity of a reciprocal lattice point is related to the crystal structure by the following equations:

$$I(h,k,l) \propto |\vec{F}(h,k,l)|^2 \tag{1}$$

$$\vec{F}(h,k,l) = \sum_{j=1}^{N} f_j(h,k,l) \cdot e^{2\pi i(hx_j + ky_j + lz_j)} \tag{2}$$

where, (h,k,l) = Miller indices of the reciprocal lattice point (or reflection).

$I(h,k,l)$ = Intensity of the (h,k,l) reflection.

$\vec{F}(h,k,l)$ = Structure Factor of the (h,k,l) reflection.

N = Total number of atoms in the unit cell.

$f_j(h,k,l)$ = Scattering power of the j'th atom for this particular (h,k,l). (known parameter)

(x_j,y_j,z_j) = The coordinates of the j'th atom expressed as fractions of the unit cell edge.

Each individual term in Equation (2) is a complex number and the summation can be viewed as a summation of vectors of length, $f_j(h,k,l)$, and angle, $\Phi_j(h,k,l) = 2\pi(hx_j + ky_j + lz_j)$, as in Fig. 3.

In this way, the resultant of Equation (2) can be written:

$$\vec{F}(h,k,l) = |\vec{F}(h,k,l)| \cdot e^{i\Phi(h,k,l)} \tag{3}$$

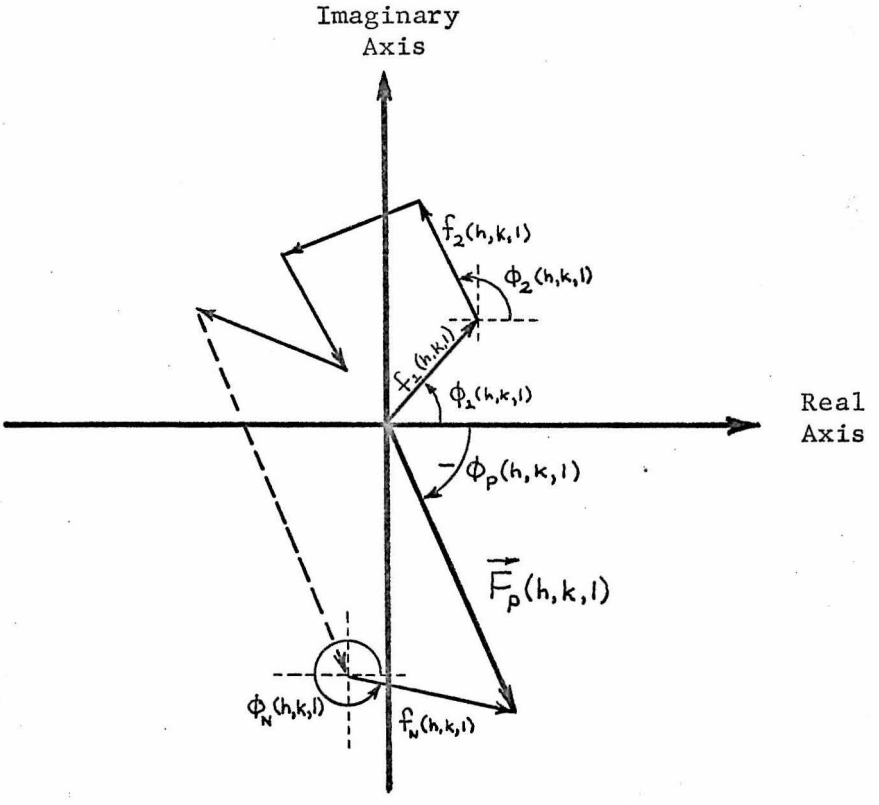

FIGURE 3

Vector summation of Equation 2.

where, $\Phi(h,k,l)$ is the phase angle for the reflection which was lost during the process of recording the intensity.

For a protein structure, the magnitudes of the structure factors will seldom be as large as their maximum possible value (when all of the individual vectors in Eq. (2) are colinear and in phase). Because of this, the addition of a single heavy atom to the protein molecule can cause fairly large changes in the observed diffraction pattern. If the heavy atom can be attached to the protein in the crystal without disturbing the original protein structure or the packing of the protein molecules within the crystal, the resulting diffraction pattern can be described by Eq. (1) and Eq. (2) with the addition of a single term to the sum in Eq. (2) for the heavy atom contribution. Symbolically, this can be written:

$$\vec{F}_{PH}(h,k,l) = \vec{F}_{P}(h,k,l) + \vec{F}_{H}(h,k,l) \tag{4}$$

where, $\vec{F}_{PH}(h,k,l)$ = Structure factor for the protein atoms plus the heavy atom.

$\vec{F}_{P}(h,k,l)$ = Structure factor for the protein atoms alone.

$\vec{F}_{H}(h,k,l)$ = Structure factor for the heavy atom alone.

This is graphically illustrated in Fig. 4. Equation (4) is the basis of the isomorphous replacement method.

In general, there will be more than one heavy atom in the unit cell contributing to the heavy atom term in Eq. (4). This can be due to one of two reasons. First, the heavy atom may be bound to more

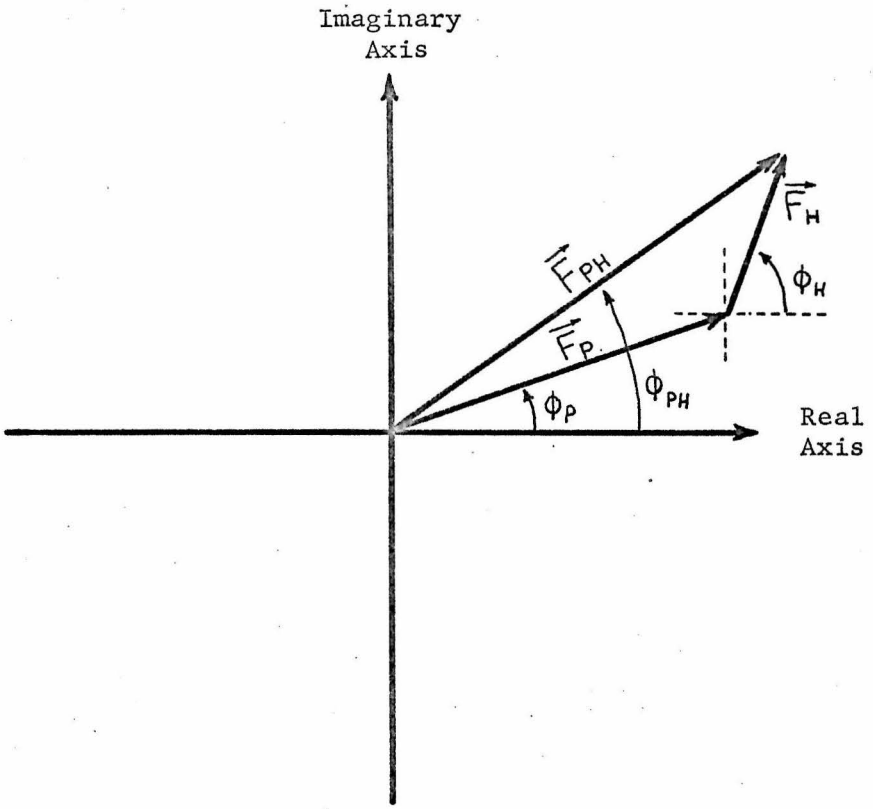

FIGURE 4

The vector summation of $\vec{F}_P$ and $\vec{F}_H$ to form $\vec{F}_{PH}$.

than one site on a given protein molecule in the cell, and second, the unit cell of a protein crystal usually contains several protein molecules related to each other by symmetry operations. In the space group, $P4_1$, for instance, each repeating unit in the crystal consists of four molecules related to each other by a four-fold screw axis. In this case, there would be four symmetry equivalent heavy atoms, one for each of the symmetry equivalent protein molecules.

Each of the terms in Eq. (4) can be expressed in terms of a magnitude and a phase, as in Eq. (3). The only parameters in the resulting expression which can be experimentally measured are the magnitudes of the derivative structure factors and the native protein structure factors, $|\vec{F}_{PH}(h,k,l)|$ and $|\vec{F}_{P}(h,k,l)|$.

The heavy atom term in Eq. (4), $\vec{F}_{H}(h,k,l)$, is a function of both the heavy atom positions, (x_H, y_H, z_H), and the heavy atom form factor, $f_H(h,k,l)$ (see Eq. (2)). The heavy atom positions can generally be calculated (if not, the derivative is useless) from the known parameters, $|\vec{F}_{PH}(h,k,l)|$ and $|\vec{F}_{P}(h,k,l)|$, using standard crystallographic techniques, such as ΔF Patterson functions ($\Delta F(h,k,l) = |\vec{F}_{PH}(h,k,l)| - |\vec{F}_{P}(h,k,l)|$). An empirical expression for the heavy atom form factor, $f_H(h,k,l)$, can be obtained from a statistical comparison of the magnitudes of the observed $\Delta F(h,k,l)$'s to the magnitudes of the corresponding $\vec{F}_{H}(h,k,l)$'s, calculated from Eq. (2) and the known heavy atom positions (since $f_H(h,k,l)$ is the same for all the symmetry related heavy atoms, it can be factored out of the summation in Eq. (2), leaving only the exponential component in the sum).

Thus, both the magnitude and phase of $\vec{F}_H(h,k,l)$ can be calculated for each reflection.

The phase angle for the native protein reflection, $\Phi_P(h,k,l)$, can now be limited to one of two possible choices, as in Fig. 5. If another derivative can be prepared and its diffraction pattern measured, the same process will, in the same manner, produce two possible phase choices, one of which will be close to one of the phase choices from the first derivative, as in Fig. 6. The two phase angles which overlap represent the true native protein phase angle. The addition of more derivatives to the analysis leads to a more accurate determination of the true phase angle.

The errors contributing to the inexact phase determination are of two general types: errors in measuring the required diffraction patterns, and errors pertaining to the heavy atom group and its effect on the crystal. The errors due to the heavy atom group are of two types: incomplete knowledge of the structure of the heavy atom group (and thus errors in calculating $\vec{F}_H(h,k,l)$), and perturbations of the original protein structure by the heavy atom group (in which case $\vec{F}_{PH}(h,k,l) \neq \vec{F}_P(h,k,l) + \vec{F}_H(h,k,l)$). Errors of the second type cannot, generally, be corrected for. If they are serious, the derivative will not be useful in multiple isomorphous replacement. Errors of the first type can often be removed with high resolution data from which the structure of the heavy atom group can be more accurately deduced.

Errors in measuring the intensities can be removed by

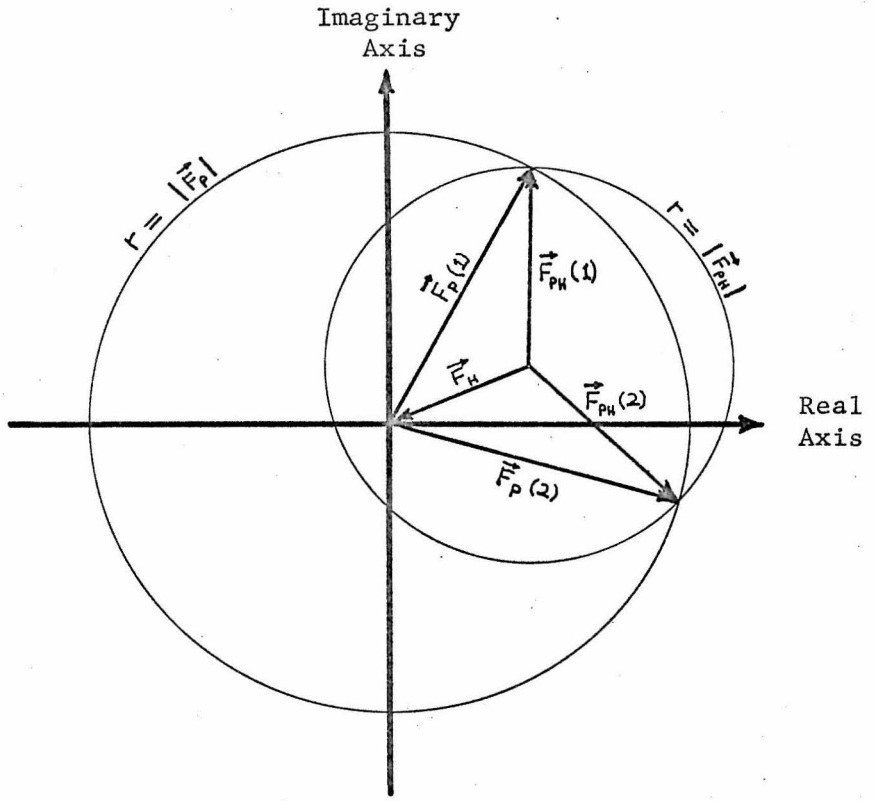

FIGURE 5

A phase circle diagram showing the two possible values of $\vec{F}_P$ determined by a single isomorphous derivative.

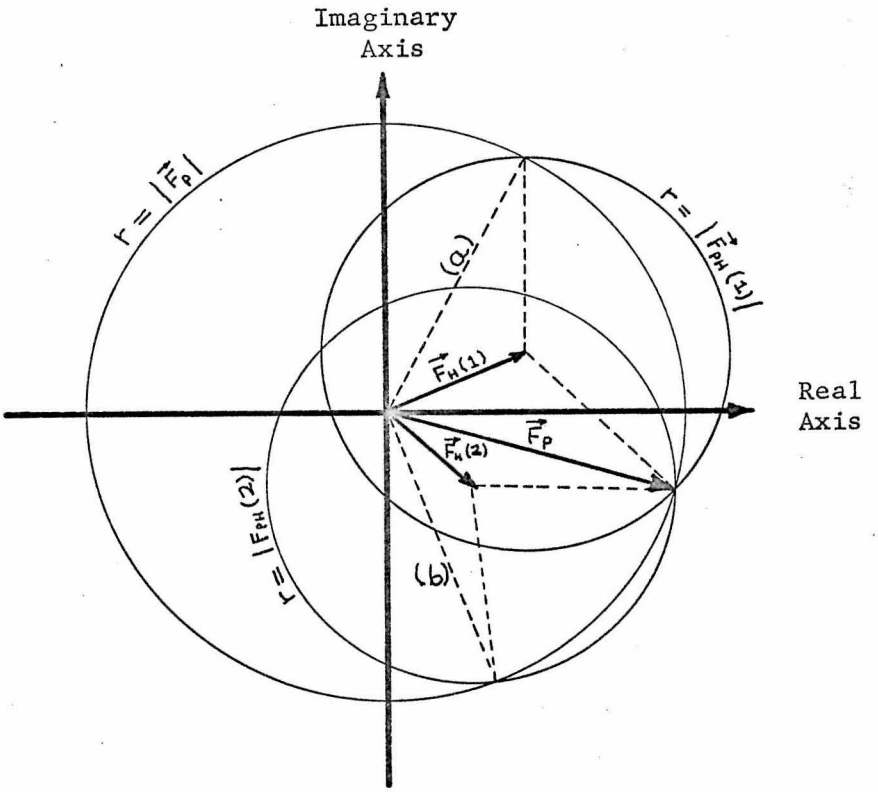

FIGURE 6

Phase circle diagram for two isomorphous derivatives. Derivative (1) limits the native protein structure factor to the two values marked (a) and $\vec{F}_P$. Derivative (2) limits the native protein structure factors to the two values marked (b) and $\vec{F}_P$. The value common to both derivatives, $\vec{F}_P$, is the true native structure factor.

re-collecting the intensity data several times. This is not generally done for a protein structure, however, because of the massive amounts of data which have to be collected. It is generally more profitable to collect the data for another derivative than to collect the data for an existing derivative twice. If the number of available derivatives is small, however, data re-collection may be profitable in terms of the phase analysis.

Once both the magnitudes and phases of the reflections in the native protein diffraction pattern are known, they can be combined in a Fourier series to produce a picture of the electron density distribution within the crystal:

$$\rho(x,y,z) = \frac{1}{V_C} \sum_h \sum_k \sum_l |\vec{F}(hkl)| \cos [2\pi(hx+ky+lz) - \Phi(hkl)] \qquad (5)$$

where, $\rho(x,y,z)$ = Electron density at the point (x,y,z) within the unit cell.

$|\vec{F}(h,k,l)|$ = Magnitude of the structure factor of the (h,k,l) reflection.

$\Phi(h,k,l)$ = Phase angle of the structure factor of the (h,k,l) reflection.

V_C = Volume of the unit cell.

The higher the values of (h,k,l) used in the summations (the further out the diffraction pattern is measured), the finer will be the resultant detail in the electron density map.

A second kind of map, the Patterson map, can be calculated without knowledge of the phases of the structure factors:

$$P(x,y,z) = \frac{1}{V_C} \sum_h \sum_k \sum_l |F(hkl)|^2 \cos 2\pi(hx+ky+lz) \quad . \tag{6}$$

This function does not produce a picture of the electron density, but represents the set of interatomic vectors between atoms in the structure, each vector being weighted by the product of the number of scattering electrons in the two atoms defining the vector. This is illustrated in Fig. 7. Maps of this type can sometimes be used to completely solve the structures of smaller compounds, but are much too complicated to allow the solution of a protein structure. Patterson maps are used in a protein structure analysis to determine the positions of the heavy atoms in the heavy atom derivative compounds. In a centric zone of data, where the structure factors are limited to real numbers ($\Phi = 0$ or π), the heavy atom structure factors are exactly related to the native protein and derivative structure factors by:

$$|\vec{F}_H(h,k,l)|^2 = \Delta F(h,k,l)^2 = (|\vec{F}_{PH}(h,k,l)| - |\vec{F}_P(h,k,l)|)^2 \tag{7}$$

except in the case when $\vec{F}_{PH}(h,k,l)$ and $\vec{F}_P(h,k,l)$ have different signs. Since the perturbing effect of the heavy atom is small, this rarely happens. Thus, the interatomic vectors between the heavy atoms can be calculated using Eq. (6) (substituting $\Delta F(h,k,l)^2$ for $|\vec{F}(h,k,l)|^2$), from which the heavy atom positions can be deduced.

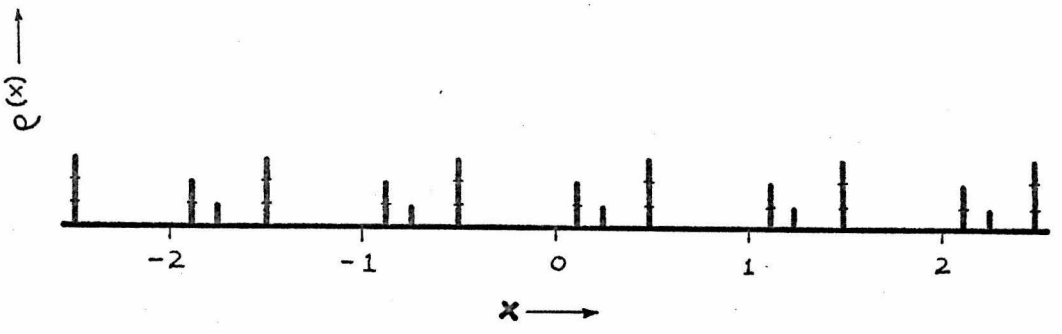

Periodic Electron Density

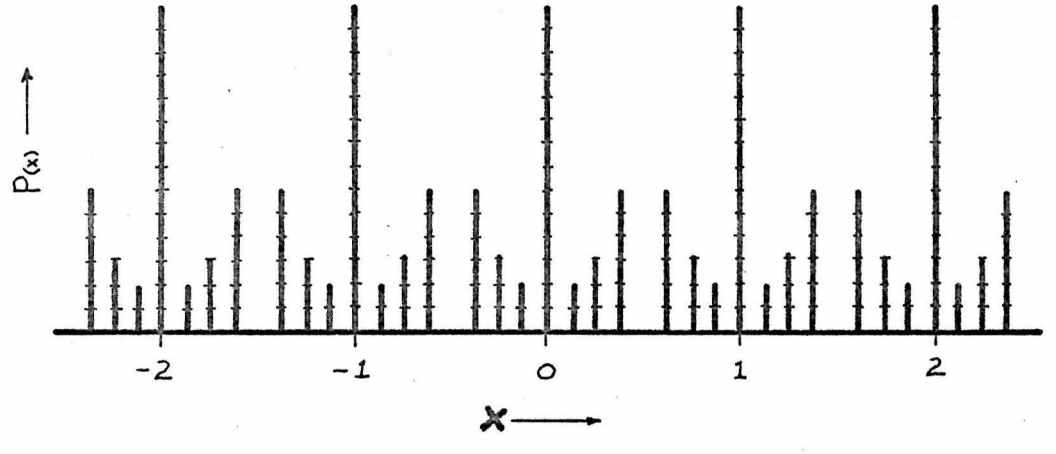

Periodic Patterson Function

FIGURE 7

The relationship between a periodic, one-dimensional electron density function, $\rho(x)$, and the corresponding periodic Patterson function, $P(x)$.

EXPERIMENTAL

EXTRACTION, PURIFICATION & CRYSTALLIZATION

See: I (512), II (78) & III (3015)*

The extraction, purification and crystallization of horse heart cytochrome c were carried out using the procedure of Margoliash & Walasek (15). Essentially, this is an acidic extraction utilizing aluminum sulfate, rather than trichloroacetic acid or sulfuric acid, for solubilizing the protein, followed by a purification using column exchange chromatography, and finally a crystallization from ammonium sulfate solution. This isolation procedure has the distinct advantage of minimizing deamidation of the cytochrome during the extraction step.

A brief outline of this procedure is given in Appendix I.

CRYSTAL SURVEY AND SPACE GROUP DETERMINATION

See: I (512), II (78) & III (3015)

Cytochrome c crystallizes in the tetragonal system, $P4_1$, with the following cell dimensions:

$$a = 58.45 \text{ Å}$$
$$b = 58.45 \text{ Å}$$
$$c = 42.34 \text{ Å}$$
$$V = 144{,}700 \text{ Å}^3$$

*The Roman Numerals refer to the previously published papers, reproduced at the end of this Thesis.

The calculated density of the crystals, as measured by flotation in chlorobenzene/bromobenzene, is 1.264 g/cm^3, which corresponds to 4 molecules per cell (MW = 12,400) and a weight percent of protein of 44.9%, or else 8 molecules per cell and a weight percent of protein of 90%. The cell almost certainly contains only 4 molecules, since only four heavy atom sites are indicated for the two isomorphous derivatives which have been obtained, and because a weight percent of protein of 90% is much too high, when compared to other crystalline proteins.

DERIVATIVE SURVEY

See: I (512), II (78-81) & III (3015)

Among the many derivatives screened, three derivatives, $PtCl_4^{-2}$, HO-Hg-CH_2-CH(O-CH_3)-CH_2-NH-CO-(o-C_6H_4)-O-CH_2COONa (mersalyl), and the simultaneous substitution of both compounds, satisfied the requirements for being useful in isomorphous phasing. The unit cell dimensions for each derivative were essentially identical with those of the native protein. In the centric (hk0) zone, the mean value of $|\Delta F|$ divided by the mean value of $|\vec{F}_P|$ was 0.328 for the Pt derivative, 0.196 for the mersalyl derivative, and 0.295 for the mixed derivative. The Patterson maps for the first two derivatives can be completely interpreted in terms of single site substitutions, at least at 3.7 Å resolution, and the map for the mixed derivative as a two site derivative, the two sites being identical to those of the single derivatives.

A summary of the procedure for preparing derivatives and a list of the various derivatives tested to date are given in Appendix II.

2-D DATA COLLECTION AND INITIAL DATA PROCESSING

See: I (512) & II (81-82)

The centric (hk0) zone was collected to a resolution of 3.7 Å for the native protein and the three derivatives on Buerger precession cameras with Cu Kα radiation (Ni filter) using the multiple film technique. The intensities were measured using a Joyce-Loebl Mark III microdensitometer and were corrected for Lorentz and polarization factors. Reflections too weak to be accurately measured were given a value of one-half the minimum observed structure factor.

A list of the observed structure factors for the native protein and the three derivatives is given in I (513) or II (82). Radial plots of $\langle \vec{F}_P \rangle$, $\langle \Delta F_{Pt} \rangle$, $\langle \Delta F_{Hg} \rangle$, and $\langle \Delta F_{Pt+Hg} \rangle$ are given in II (81).

PHASE DETERMINATION

See: I (515-521) & II (83-89)

After the initial data processing, a $(\Delta F)^2$ Patterson map, where $\Delta F = |\vec{F}_{PH}| - |\vec{F}_P|$, was calculated for each of the derivatives. These maps are shown in I(514,519) and II(84). All three maps can be interpreted in terms of a single Pt site and a single Hg site, with the possibility of a weaker secondary Pt site. "Cross ΔF Fouriers", that is, ΔF's

calculated from the native and one of the derivatives and signs calculated from the native and another of the derivatives, confirm the single site nature of these substitutions. The cross maps are shown in I (516) and II (85). Based on these same considerations, a fourth derivative, $PdCl_4^{-2}$, was rejected as being either non-isomorphous or as binding in a non-specific manner (see I (517)).

Each of the derivatives was refined using the method of Blow & Crick (3, 5). The initial input parameters were obtained from the Patterson maps and from Wilson plots. During the refinement process the existence of the secondary Pt site was confirmed. The input data and the final parameters after refinement are given in I (513) and II (86). Both derivatives were found to have form factors which best fitted $A \cdot e^{-Bs}$ rather than the usual $A \cdot e^{-Bs^2}$, where A and B are constants and $s = 2 \sin \theta$.

The results of the refinements are given in I (512-521) and II (83-89). The final 2-D Fourier is shown in II (89-93).

3-D DATA COLLECTION AND INITIAL DATA PROCESSING

Three dimensional data sets were collected to a resolution of 3.7 Å for the native protein (henceforth called the old native), the platinum derivative and the mercury derivative with Buerger precession cameras using the multiple film technique. Fifteen layers, parallel to the c axis, were collected for each data set, containing approximately 98% of the total reflections in the 3.7 Å sphere. A different crystal was used for each layer, in order to minimize the effects of

x-ray damage. The intensities were measured by means of a Joyce-Loebl Mark III microdensitometer and all symmetry related reflections on a given film were manually scaled together (the films contained only horizontal and vertical mirror planes as symmetry elements, so the Lorentz and polarization factors for the symmetry related reflections were the same). Reflections on a film which were too weak to be accurately measured were given a value of one-half the minimum observed intensity on the film. Each film was then corrected for Lorentz and polarization factors and the 15 films were scaled together by means of the overlapping rows of reflections on the various films using the method of Dickerson (4). Individual temperature factors were not applied to the films in this scaling process as they were negligible.

A second native data set (henceforth called new native) was later collected from crystals which were of much higher quality than those used in the first collection. This, plus the original platinum and mercury sets, was used to produce the final 3-D Fourier map of the protein.

A listing of the structure factor amplitudes for the four data sets is given in Appendix III.

DATA SCALING AND DETERMINATION OF THE HEAVY ATOM PARAMETERS

The platinum, mercury and old native data sets were initially scaled to the new native data set by means of Wilson plots of the type:

$$\ln \frac{\langle | \vec{F}_N(hkl) | \rangle_s}{\langle | \vec{F}_D(hkl) | \rangle_s} = \ln A_D + B_{D^*} \left\langle (2 \sin \theta(hkl))^2 \right\rangle_s \qquad (8)$$

where, N = new native; D = platinum, mercury, or old native; and s = a small radial zone of data with s = 2 sin θ approximately a constant (intervals in s of 0.021 were used).

The A_D values reflect differing exposure times and crystal sizes, and to a lesser extent, the quality of the crystals. The B_D values, on the other hand, reflect almost entirely the effects of crystal quality and x-ray damage. The B_D values needed to scale the three data sets to the new native data set were:

Data Set	B_D	$e^{B_D*(2 \sin \theta_{3.7 Å})^2}$
Old Native	0.500	1.091
Platinum	1.100	1.210
Mercury	0.475	1.086

The column on the right represents the factor by which a reflection at the 3.7 Å data edge would be corrected, compared to a value of 1.0 at the origin. From these values it can be seen that the old native and mercury data sets are of roughly equal quality, but not as good as the new native data set, and that the platinum data set has the most rapid rate of falloff of intensity with s and is of the poorest quality.

The heavy atom positions were determined in three dimensions by the calculation of $(\Delta F)^2$ Patterson maps. These maps could both be interpreted in terms of single site substitutions of Pt and Hg atoms. The maps are shown in Appendices IV and V. The coordinates were found to be:

Atom			
Pt	0.219 (0.219)	0.203 (0.199)	0.000 (0.000)
Hg	0.021 (0.021)	0.396 (0.400)	----------

(The values in parentheses are the refined 2-D values)

The relative z coordinate of the Hg atom was calculated from a "cross" ($\Delta F_{Pt} \Delta F_{Hg}$) Patterson map. This map and its explanation are given in Appendix VI. The peaks in this map correspond to a separation of the Pt and Hg atoms of ±0.376. The value of +0.376 was chosen on the basis of an earlier calculated old native vs platinum, single isomorphous replacement map which allowed the determination of the molecular boundaries in three dimensions. The choice of $z_{Hg} = +0.376$ placed the mercury atom on the exterior of the same molecule binding the Pt atom. The other possible site occurred between two molecules in a region probably occupied by solvent. A three dimensional view of the single isomorphous replacement map is shown in Fig. 8. The actual Fourier sections are shown in Appendix VII.

The form factors of the heavy atoms were shown, in the two-dimensional work (I (512) and II (83)), to be of the form:

$$f_H(hkl) = A_H * e^{-B_H * (2 \sin \theta\ (hkl))} \quad . \tag{9}$$

The heavy atom contribution to $\vec{F}_{PH}(h,k,l)$ is then:

$$\vec{F}_H(hkl) = A_H * e^{-B_H * (2 \sin \theta\ (hkl))} \sum_{j=1}^{4} e^{2\pi i (hx_j + ky_j + lz_j)} \quad . \tag{10}$$

Values for A_H and B_H were obtained from plots of the form:

$$\ln \left\{ \frac{\left| |\vec{F}_{PH}(hkl)| - |\vec{F}_P(hkl)| \right|}{\sum_{j=1}^{4} e^{2\pi i (kx_j + ky_j + lz_j)}} \right\} = \ln\left(\frac{2}{\pi} * A_H\right) - B_H * (2 \sin\theta (hkl)) \quad . \tag{11}$$

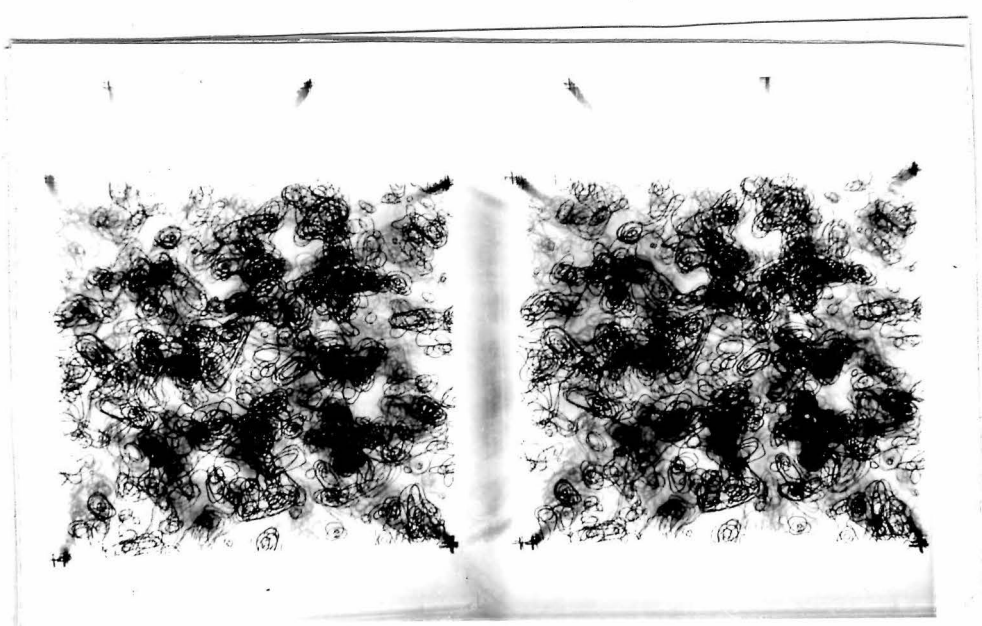

FIGURE 8 (a)

View of the Pt derivative SIR Fourier map along the z axis. One complete cell is shown.

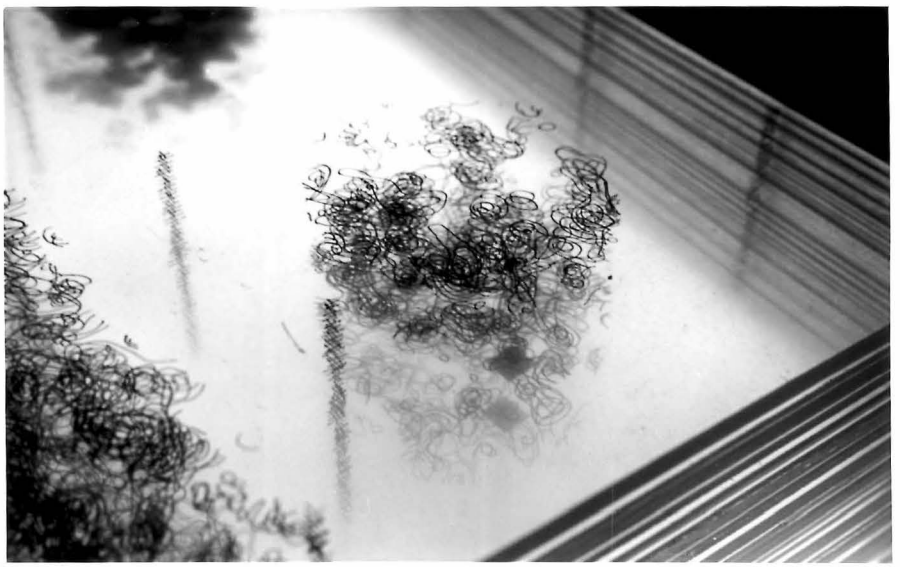

FIGURE 8 (b)

View of one molecule in the SIR map. The two possible Hg sites are indicated by the dark squares. The upper site was chosen as correct.

The factor, $2/\pi$, arises because in the acentric case, the observed difference between $|\vec{F}_{PH}|$ and $|\vec{F}_{P}|$ is equal to, or less than, the heavy atom contribution, $|\vec{F}_{H}|$. This is shown in Fig. 9. The relationship between $|\Delta F|$ and $|\vec{F}_{H}|$ is of the approximate form:

$$|\Delta F| = |\vec{F}_{H}| * |\cos(\theta)| \quad . \tag{12}$$

The mean value of the cosine factor is $2/\pi$ when averaged over a large number of reflections. A least squares fit to the points determined by Eq. (11) gave:

Heavy Atom	A	B
Pt	9.94 (7.99)	7.78 (7.46)
Hg	3.41 (5.33)	2.88 (8.64)

(The values in parentheses are the refined 2-D values)

These heavy atom parameters were then directly used to calculate a set of "centroid" protein phases.

REFINEMENT OF THE HEAVY ATOM PARAMETERS

Several attempts were made to refine the heavy atom parameters by the method of Blow & Crick (3, 5). The positional parameters of the heavy atoms behaved normally during refinement when refined alone, and did not move appreciably from their initial values. The form factor parameters, however, would not refine normally.

The first new native refinement run began with starting parameters taken from the end of a set of refinements based on the old native data set. The refinement took the following path:

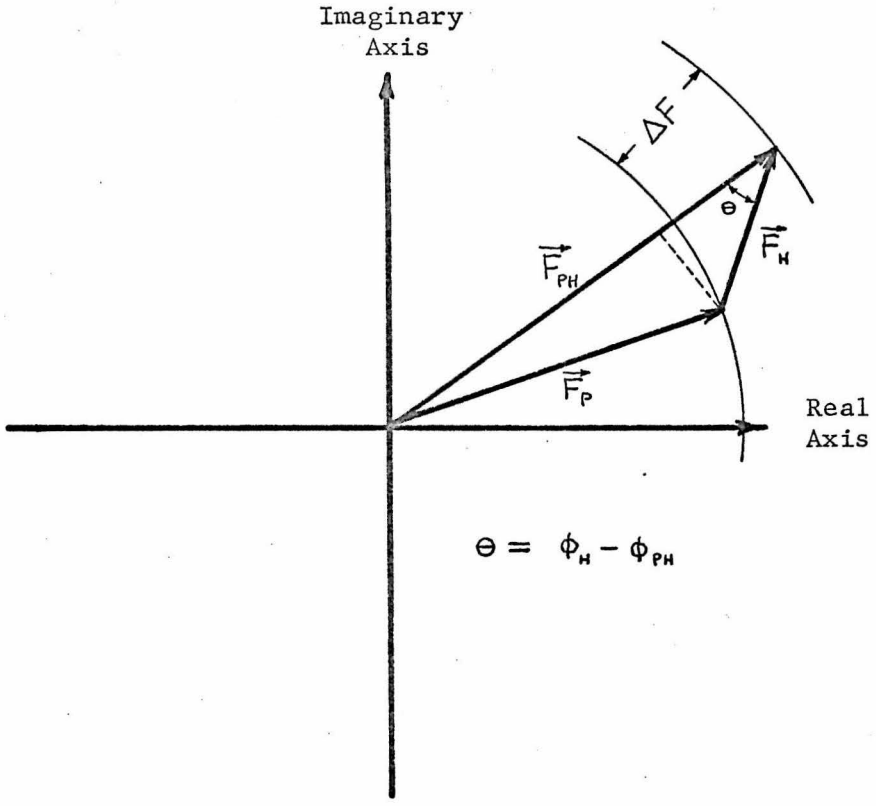

FIGURE 9

The relationship between $\Delta F(hkl)$ and $|\vec{F}_H(hkl)|$.

		Input Parameters	I	II
Pt	x	0.218	0.214	0.212
	y	0.198	0.196	0.193
	z	0.000	0.000	0.000
	B	2.800	2.800	2.800
	A	6.710	6.021	5.461
	E_{LS}*	4.623	5.741	4.441
	E_{RMS}	6.16	5.12	4.90
	R	8.37	8.54	9.15
Hg	x	0.022	0.027	0.034
	y	0.401	0.404	0.404
	z	0.375	0.380	0.385
	B	1.150	1.150	1.150
	A	2.981	2.162	1.910
	E_{LS}	3.985	5.355	3.814
	E_{RMS}	4.01	3.40	3.40
	R	7.34	7.51	7.68
	FM	0.441	0.412	0.458

(*The three R-factors are defined in I (513-514))

The effect of this refinement run was to decrease systematically the heavy atom contributions from both the Pt and Hg atoms, as was the case in the old native refinement runs. The quantity, E_{LS}, is the R-factor related to the refinement process. After an initial increase it dropped below its initial value (for both derivatives). The movement of the heavy atom positions is coupled to the systematic decrease of the heavy atom substitution numbers. If the refinement had been continued, both heavy atom substitution numbers would have refined to zero. It should be noted that the temperature factor parameter was not refined for either derivative. In the earlier 2-D work it had been shown that it was impossible to refine both A_H and

B_H at the same time at this resolution, even in the centric case, as was verified in a later run for the acentric data.

A second set of runs was next made using the derivative B values found in the two dimensional work:

		Input Parameters	I	II	III	IV	V
Pt	x	0.219	0.214	0.213	0.215	0.219	0.216
	y	0.199	0.195	0.194	0.196	0.194	0.193
	z	0.000	0.000	0.000	0.000	0.000	0.000
	B	7.500	7.500	7.500	7.500	7.500	7.500
	A	8.000	7.314	6.890	6.271	6.052	5.812
	E_{LS}	5.272	5.455	5.620	3.981	5.721	4.708
	E_{RMS}	4.58	4.09	3.99	3.97	4.23	4.06
	R	9.64	9.82	10.07	10.47	11.01	11.36
Hg	x	0.021	0.025	0.027	0.027	0.030	0.028
	y	0.400	0.399	0.398	0.398	0.407	0.408
	z	0.375	0.385	0.370	0.362	0.331	0.332
	B	8.650	8.650	8.650	8.650	8.650	8.650
	A	5.330	4.129	3.400	2.816	2.407	2.196
	E_{LS}	3.932	4.041	4.473	3.280	3.089	3.370
	E_{RMS}	3.68	3.29	3.16	3.14	3.19	3.21
	R	7.87	8.13	8.56	8.91	9.31	9.36
	FM	0.450	0.467	0.490	0.490	0.479	0.444

This refinement run behaved similarly to the first run. The heavy atom substitution numbers were systematically refined toward zero at about the same rate as before. The least squares error factor rose during the first two cycles and then oscillated for both of the derivatives. On the basis of these, and other similar runs, it was decided that the refinement of the heavy atom parameters was probably impossible in this case. This conclusion can be justified by the following argument. The minimal number of derivatives necessary

to uniquely determine a phase angle is two. Since the refinement process makes use of the protein phase angles calculated in the phasing cycle immediately prior to the refinement cycle, and these phases are highly dependent upon the parameters of either heavy atom derivative, a solid base does not exist from which the derivatives can be refined. If more than two derivatives were used in calculating the phases in the phasing cycle of the process, slight changes in the parameters of any one of the derivatives would not cause a large change in the phase angles calculated in the next phasing cycle, and the refinement would have a much better chance of converging. Thus, using only two derivatives, refinement of the heavy atom form factor parameters may well be impossible, particularly at low resolution.

Since refinement of the heavy atom parameters appeared to be impossible, it was decided to calculate phases on the basis of the most probable set of input parameters. The positional parameters used were the refined two-dimensional parameters. The form factor constants for the heavy atoms were those obtained from the least squares fit mentioned above. The input parameters and final refinement parameters for this run were:

Pt		Hg	
x	= 0.219	x	= 0.019
y	= 0.199	y	= 0.405
z	= 0.000	z	= 0.377
B	= 7.780	B	= 2.280
A	= 9.940	A	= 3.410
E_{LS}	= 4.211	E_{LS}	= 3.629
E_{RMS}	= 4.86	E_{RMS}	= 3.99
R	= 7.81	R	= 6.06

FM = 0.458

The phases produced in this run were used to produce the final 3.7 Å Fourier map.

THREE DIMENSIONAL FOURIER MAPS

The first Fourier map calculated was a platinum derivative single isomorphous replacement map based on the old native data set. The phases for this map were obtained from a simple phasing run of the phase-refinement program. The mean figure of merit was 0.302. A three dimensional view of this map is shown in Fig. 8. The individual Fourier sections are given in Appendix VII.

The resulting map clearly shows the outlines of the four molecules in the cell. The iron atom of the heme group (verified in the two derivative map) is the highest point on the map. The main features of the map are the same as those of the two compound map (Fig. 10 and Appendix VIII) although the connections between regions of high electron density are quite different in the two maps. This map allowed the determination of the relative z coordinate of the mercury atom of the second derivative (mentioned earlier).

The two derivative map, based on the new native data set, is shown in Fig. 10 and Appendix VIII. The mean figure of merit for the data in this map was 0.458. A discussion of the interpretation of this map and its general features is given in the next section and in III (3015-3017) and IV (7-23). The most important features of the map are the lack of alpha helix and the occurrence of a hydrophobic core in the molecule.

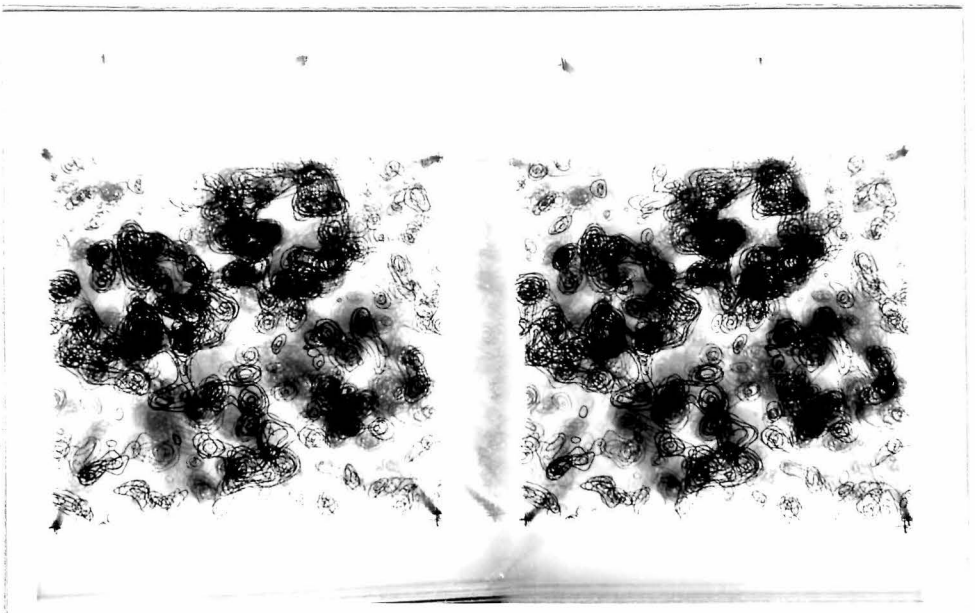

FIGURE 10 (a)

View of the two derivative Fourier map along the z axis. One complete cell is shown.

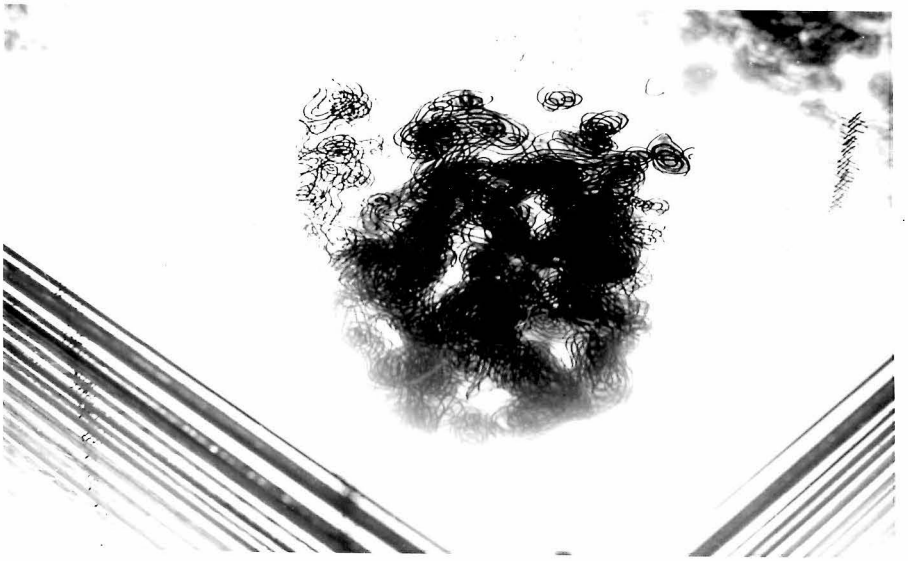

FIGURE 10 (b)

View of one molecule in the two derivative map.
The contours assigned to the molecule are shaded.

CONCLUSIONS

Although the structure of cytochrome c reported in this Thesis has not been calculated at atomic resolution, many important features of the molecule can still be deduced from the electron density map. These can be divided into two groups: features which can be unequivocally demonstrated in the structure, and features which are based on a very tentative fitting of the known amino acid sequence to the structure seen in the 3.7 Å Fourier map.

The most remarkable feature of the map is the appearance of the heme group shown in Fig. 11 (also in: III (3016) and IV (Figs. 2, 4, 5, 6)). The contours of the heme group and the region of polypeptide chain from Lys 13 through Thr 19 correspond extremely well to a space filling model of this region, constructed on steric considerations. The heme is situated in a crevice on the surface of the molecule with one edge exposed to the solvent (Fig. 12), in agreement with the solvent perturbation studies of Stellwagen(19). The heme normal makes an angle of 70° to the z axis, in agreement with the values obtained by Kabat (8) and Eaton & Hochstrasser (6) of 65-70° and 72±3°. The propionic acid side chains of the heme can be seen trailing off into the interior of the molecule.

It is quite clear from the map that the fifth coordinating ligand to the heme is the imidazol group of His 18. On the other side of the heme there is a vertical column of density in the proper position to provide the sixth coordinating ligand (Fig. 12), but the

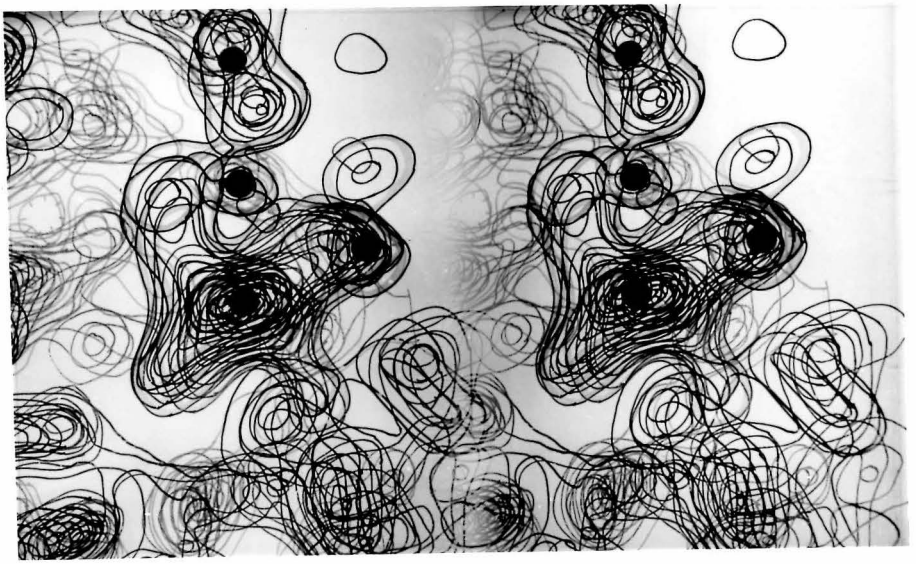

FIGURE 11

Electron density around the heme group. This figure should be compared to Fig. 2.

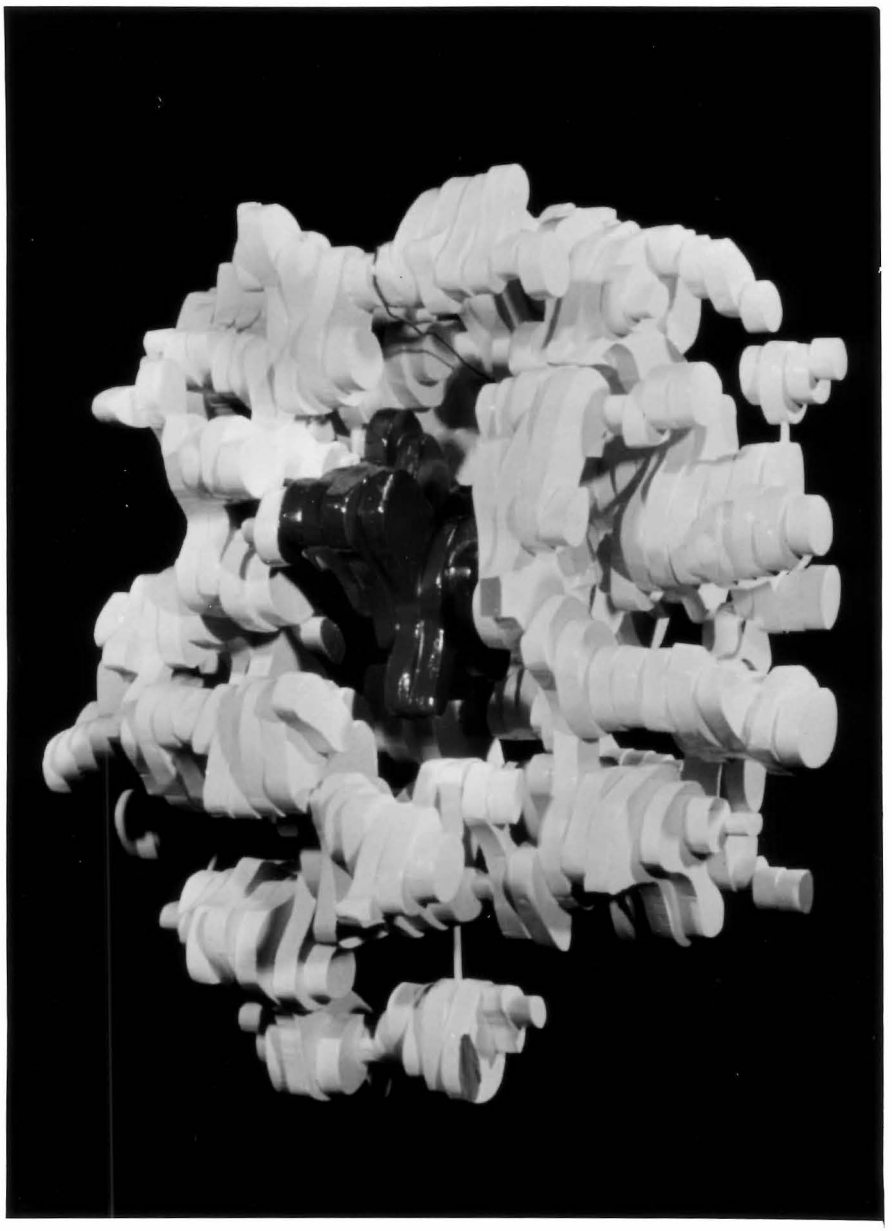

FIGURE 12

View of a plywood model of the two derivative cytochrome c structure. The heme group is the dark object in the center of the picture.

nature of this group cannot be established from the map. All that can be said is that it probably does not involve His 26 or His 33, the two remaining histidines in the structure (III (3016)).

The calculated cytochrome c structure conforms quite well to the "hydrophobic drop" model for proteins, in which the molecular interior consists of loosely packed hydrophobic side chains. This is indicated in the Fourier map by the presence of highly negative electron density throughout the interior of the molecule, giving it the appearance of a hollow oblate spheroid. The dimensions of the molecule are approximately 25 x 25 x 37 Å. There are two apparent channels from the surface of the molecule to its interior. These are, in reality, probably the same as the interior of the molecule, loosely packed side chains.

One of the most interesting features of the gross structure of the molecule is that it contains little or no α-helical structure. At one site, on the side of the molecule opposite His 18, there is a possibility of 1 to 1½ turns of α-helix, however, there is no indication of helical structure anywhere else in the molecule. Thus, the predictions of α-helix content by various authors (14) of from 35 to 85% α-helix are wrong.

Assuming that the sixth coordinating ligand to the heme iron atom is Met 80 (1, 7), almost the entire stretch of polypeptide from Asn 70 to Met 80, the longest invariant region in the sequence, lies on or near the surface of the molecule. This is in good agreement with the fact that it is an invariant region and that blocking of either Lys 72

or Lys 73 results in a loss of about 50% of the activity with cytochrome oxidase (17).

The total running length of continuous electron density in the map corresponds quite well with the expected length of the polypeptide chain. Several attempts have been made to fit the amino acid sequence to the observed structure but this can not be done with much certainty at this point. One such interpretation is presented in IV (14-23).

In summary, the 3.7 Å x-ray analysis of cytochrome c has provided a surprisingly large amount of useful information concerning the structure of the cytochrome c molecule. Most of its gross features have been determined, as well as the path of the polypeptide chain in the region of the heme attachment. The remainder of the structure can only be determined by the high resolution analysis, which is planned for the summer and fall of 1968.

PART II

THE APPLICATION OF THE KARLE-HAUPTMAN TANGENT FORMULA TO PROTEIN PHASE REFINEMENT

INTRODUCTION

The single most important problem in the field of x-ray crystallography is the fact that the phase angles associated with each reflection of the diffraction pattern are lost during the process of recording the intensities of the various reflections. Without this phase information, it is impossible to calculate the Fourier transform of the diffraction pattern directly, and thus calculate the electron density distribution associated to the observed diffraction pattern. This is the so called "phase problem" in protein crystallography.

Given the types and positions of the various atoms constituting a crystal structure, there exists a unique Fourier transform or set of structure factors, determined by the structure, and conversely, given the complete Fourier transform of a crystal structure, the structure itself is uniquely determined. If, however, only the magnitudes of the structure factors are known, and not the phases, there exists an infinite number of density functions which will correspond to these structure factor magnitudes, or structure amplitudes, each having its own particular set of associated phase angles. Only one of this infinite set represents the true structure.

Most of these phase sets, however, correspond to purely mathematical structures which can be ruled out on the basis of known chemical information. For instance, no real structure can have a negative electron density. Also, any real crystal structure will consist of atoms, that is, the electron density must be concentrated

into small areas around the centers of the atoms which are bonded together, and not randomly spread out over the unit cell. Limitations on the electron density of this sort have led most crystallographers to believe that for any reasonably complicated structure, there probably exists only one solution to the phase problem which will produce a chemically reasonable structure, this solution corresponding to the real structure.

This implies that the phase information needed to calculate the crystal structure is not completely lost in the process of recording the intensities: it must still exist in the intensity distribution itself, and perhaps could be extracted by the application of the structure limitations mentioned above. A practical method for doing this has recently been developed by Karle & Karle (9), called the symbolic addition method, by which many small structures have now been solved.

This Thesis is concerned with the application of one aspect of this method, tangent formula refinement, to the refinement of previously determined protein phases. The method has been tested on a trial structure at 4 Å resolution, and on the cytochrome c structure described in the preceeding part of this Thesis. The method produced favorable results in both cases and, particularly at high resolution, should provide a powerful tool for protein structure analyses in the future.

BASIS OF THE TANGENT FORMULA

The tangent formula is based on the phase relationships imposed on the diffraction pattern of a real crystal by the restrictions on the structure that the electron density be zero or positive everywhere in the crystal and that the electron density be concentrated into small spherical regions about the atomic centers. This can be physically interpreted in the following way:

Consider a one dimensional, theoretical structure composed of unitary, point atoms. In other words, each atom in the structure consists of a single, point electron. The structure factor expression for this theoretical structure is, then:

$$\vec{F}(h) = \sum_{j=1}^{N} e^{2\pi i h x_j} = |\vec{F}(h)| e^{i\Phi(h)} \qquad (1)$$

The Fourier transform of the structure factors, or the electron density function, can then be written:

$$\rho(x) = \frac{1}{X} \sum_{h} \vec{F}(h)\ e^{-2\pi i h x} \qquad (2)$$

where, X is the length of the repeating unit in the x direction. Since we are considering a unitary, point atomic atomic structure, the electron density must be zero or positive everywhere in space, and

furthermore, it must be either zero or one. Thus, the square of the electron density and the true electron density at any point in space must be equal to each other and must equal zero or one. Mathematically, this can be expressed:

$$\frac{1}{X}\sum_{h}\vec{F}(h)\ e^{-2\pi ihx} = \left[\frac{1}{X}\sum_{h}\vec{F}(h)\ e^{-2\pi ihx}\right]^2 \quad . \tag{3}$$

Expanding the right hand side of Eq. (3) in terms of a double sum:

$$\frac{1}{X}\sum_{h}\vec{F}(h)\ e^{-2\pi ihx} = \frac{1}{X^2}\sum_{h}\sum_{h'}\vec{F}(h)\vec{F}(h')\ e^{-2\pi i(h\ +\ h')x} \quad . \tag{4}$$

With a change of variable, the right hand side of Eq. (4) becomes:

$$\frac{1}{X}\sum_{h}\vec{F}(h)\ e^{-2\pi ihx} = \frac{1}{X^2}\sum_{h}\sum_{h'}\vec{F}(h')\vec{F}(h\ -\ h')\ e^{-2\pi ihx} \quad . \tag{5}$$

By a comparison of the left and right hand sides of Eq. (5), it is obvious that the following relationship must be true if the equality is to be preserved:

$$\vec{F}(h) = \frac{1}{X}\sum_{h'}\vec{F}(h')\vec{F}(h\ -\ h') \tag{6}$$

This is the basis of the tangent formula. Each term on the right hand side of Eq. (6) is a complex number which can be visualized as a vector in the complex plane. To properly sum a series of complex numbers, one

must sum their real and imaginary components separately. The length of the resultant vector is merely the square root of the sum of the squares of the real and imaginary components, and the phase angle of the resultant vector in the imaginary plane is merely the arc tangent of the ratio of the imaginary to the real component of the vector. By expressing Eq. (6) in terms of Eq. (1) and applying the relationship: $e^{ix} = \cos(x) + i \sin(x)$, the tangent formula can be written:

$$\Phi(h) = \tan^{-1}\left\{ \frac{\sum_{h'} |\vec{F}(h')| \cdot |\vec{F}(h-h')| \sin[\Phi(h')+\Phi(h-h')]}{\sum_{h'} |\vec{F}(h')| \cdot |\vec{F}(h-h')| \cos[\Phi(h')+\Phi(h-h')]} \right\} . \qquad (7)$$

Since no real structure consists of unitary, point atoms, but of atoms of varying atomic numbers which occupy a finite amount of space, the above relationships do not strictly apply to the real case. The structure factor expression for a real crystal can be written:

$$\vec{F}(hkl) = \sum_{j=1}^{N} f_j(hkl)\, e^{2\pi i(hx_j+ky_j+lz_j)} = |\vec{F}(hkl)|\, e^{i\Phi(hkl)} . \qquad (8)$$

Comparing this to the one-dimensional example in Eq. (1), the only difference is in the atomic scattering factors, the $f_j(h,k,l)$'s. These are known parameters for each type of atom and are a function of the distance of the (h,k,l) reflection to the origin of reciprocal space (measured by $s = 2 \sin \theta$ (h,k,l)). As the angle of diffraction (Bragg angle) increases from 0° to 90°, the scattering factors

decrease monotonically from a value of the atomic number of the atom involved to a value of zero. This is related to the fact that real atoms have a finite volume, and destructive interference can occur between x-rays scattered from opposite sides of the atom. Since the scattering power of the atoms in a structure falls off with increasing scattering angle, the mean value of the structure factors will also fall off.

This falloff effect can be exactly corrected for in the case where all the atoms in the structure are of the same type. In that case the scattering factor can be factored out of the summation in Eq. (8) and the observed structure factors can be normalized to those of the equivalent point atomic structure by dividing each structure factor by the known scattering factor for that particular (h,k,l) value.

For a real structure composed of more than one type of atom, a good approximation to the corresponding unitary point atomic structure can be obtained by normalizing the observed structure factors by an average value of the different scattering factors. The average generally used is the root mean square average. The normalized structure factors obtained by using this average are known as the E's:

$$\vec{E}(hkl) = \vec{F}(hkl) \Big/ \mathcal{E}\left[\sum_{j=1}^{N} f_j^{\,2}(hkl)\right]^{\frac{1}{2}} \qquad (9)*$$

*The E's in Eq. (9) differ from the F's in Eq. (1) by the constant N.

where, $\mathcal{E}$ is a number which corrects for space group extinctions and other factors. The errors introduced by this approximation are small for a protein structure except for reflections with very small values of $|E|$.

In deriving the tangent formula expression, it was assumed that an infinite amount of data was included in the summations. In a real application of the tangent formula, however, only a very limited amount of data is available. This is the most serious cause of error in the use of the tangent formula. It can also be shown that the accuracy of $\Phi(h,k,l)$, using a constant amount of data, increases with increasing $|E(h,k,l)|$. The relationship of these two effects determines the accuracy of the tangent formula in a given phase determination.

EXPERIMENTAL

The experimental details concerned with this section have already been carefully described in V (4-19). Rather than to duplicate this paper, only a general outline of the experimental procedure is given in this section of the Thesis.

MODEL PROTEIN CALCULATIONS

See: V (5-11, 14-17)

The main chain and β-carbon atoms of myoglobin were used to produce a structure factor set, complete to a resolution of 4 Å, of known magnitude and phase. This model protein structure will hence-forth be called "modelglobin". The structure factor magnitudes were normalized to the corresponding E's, which were used, along with the known phases, to test the accuracy of the tangent formula in calculating the phases of a protein structure at 4 Å resolution.

The first test of the tangent formula was simply to insert the known E's and phases on the right hand side of the tangent formula equation and compare the calculated phases to the true phases. The results of the calculation are shown in V (p. 7 and Fig. 1). As expected, the tangent formula works best for reflections of large $|E|$ and is more accurate at 4 Å than at 5 Å resolution.

Random errors were introduced into the phase data to simulate the conditions occurring in the phase determination of a real protein.

Two error decks were produced, one with a mean error of 32° over all the reflections, and the second with a mean error of 56° for the 100 largest reflections and a mean error of 32° for the remainder. Application of the tangent formula to each of these decks showed marked phase improvement in both cases (V: p. 10 and Fig. 6).

A second possibility for the use of the tangent formula is a method of selecting the proper phase angle from the two possible phase angles resulting from a single isomorphous phase analysis. The single isomorphous phases and the corresponding centroid phase angle (V: 14) were calculated for the modelglobin structure based on a theoretical two site mercury derivative. The centroid phases were used, along with the known E's to calculate a new phase angle which was then compared to the two possible phase choices. The choice which was nearest the calculated phase was taken as being correct. The results of this calculation are shown in V (15-17 and Fig. 13). The mean phase error was lowered from about 45° to about 15° over about half the data deck.

CYTOCHROME C CALCULATIONS

See: V (11-14 and 17-19)

Having demonstrated that the Karle-Hauptman tangent formula could, in theory, be successfully applied to the phase refinement of low resolution protein data sets, it was decided to attempt the refinement of a real set of protein diffraction data, that of the 3.7 Å cytochrome c structure reported in the first part of this Thesis.

Before this refinement was even attempted it was recognized that without a good refinement criterion it would be impossible to tell whether the new, calculated phases were, in fact, better than the original double isomorphous replacement phases. Since no reliable mathematical refinement criterion was found from the modelglobin refinement trials, it was decided to use the appearance of the heme region in the Fourier map, as a basis for deciding whether the refinement was proceeding satisfactorily or not.

The refinement of cytochrome c gave much less favorable results than did the test structure. The refinement path was dependent upon the nature of the refinement procedure used. When the newly calculated phases were immediately inserted into the phase set, and thus contributed to the phase determination of the remainder of the reflections, the quality of the resulting Fourier map degenerated, with most of the electron density piling up at the position of the iron atom.

When the newly calculated phases were not inserted into the phase deck (and thus all calculations were made on the basis of the original multiple isomorphous replacement phases), however, the resulting Fourier map showed significant improvement in certain regions around the heme group. The features in the remainder of the map remained about the same as in the multiple isomorphous replacement map, with only minor changes in the low electron density regions (Appendix IX).

The most encouraging results from the cytochrome c refinements came from the application of the tangent formula to the platinum

derivative, single isomorphous replacement phases. The procedure used was the same as in the modelglobin trials. The 800 reflections of highest $|E|$ were processed (out of a total of 1439) which led to a map almost as good as the original multiple isomorphous replacement map.

CONCLUSIONS

The most important conclusion which can be drawn from this study is that the Karle-Hauptman tangent formula can, in fact, be successfully applied to the refinement of protein phases. Although there is no "a priori" mathematical reason why this should not be true, at least at high resolution, many people have still maintained the belief that the restrictions of non-negative electron density and discreet atomic structure, which are the physical basis for the tangent formula, would not cause strong enough limitations on the phase angles to allow a protein structure to be refined by this method.

The fact that the tangent formula can be applied to protein phases, at low resolution, can be explained in the following way:

There is much more information contained in a set of protein structure factors than can be seen in the corresponding Fourier map. Using the relationship between intensity and atomic positions:

$$I(hkl) = |\vec{F}(hkl)|^2 = \sum_{j=1}^{N} \sum_{k=1}^{N} f_j(hkl)\ f_k(hkl) \cdot$$

$$\cdot \cos 2\pi[h(x_j - x_k) + k(y_j - y_k) + l(z_j - z_k)] \qquad (10)$$

where, N will be about 2000 atoms for a protein structure, the atomic positions can, in theory, be exactly determined (neglecting atomic temperature factor parameters) with 3N, or 6000, independent

reflections, by the solution of 3N equations defined by Eq. (10). To obtain the same information (exact coordinates) from a Fourier map, an infinite number of structure factors would have to be used. Even to obtain approximate atomic coordinates, high resolution data would have to be used, probably on the order of 20,000 independent reflections. Thus, the Fourier map is a very inefficient way of extracting information from a set of structure factors. This explains the fact that the tangent formula is valid for protein phase refinement, even when the data has not been collected to atomic resolution. The tangent formula is based on relationships between reciprocal space parameters, the structure factors, which still contain the maximum amount of positional information. In calculating the corresponding Fourier map, much of this information is lost.

The tests on the 4 Å modelglobin structure showed that, in theory, the tangent formula will work for a protein structure at this resolution. Although the self-consistent set of phases (invariant upon application of the tangent formula) were different from the true set, they were not far off and the structure would have still appeared about the same in a Fourier map. When errors were introduced into the theoretical phase set, the tangent formula refined the phases back toward the self-consistent set, with the largest correction occurring during the first pass of the data through the tangent formula. Before the original condition of self-consistency was reached, however, the tangent formula started to refine the phases away from the original self-consistent set.

There are two possible explanations for this. First, since the reflections with low $|E|$ were not refined, the constant errors in this group of reflections could produce a new point of self-consistency, occurring farther from the true set of phases than the original self-consistent set. Second, and more probable, is that the intensity errors lower the amount of useful phase information in the data deck to the point where the tangent formula sees information related mainly to the most dense features of the structure, and as a result will try to produce a self-consistent set of phases based on these features alone. This was borne out in the first refinements of the cytochrome c data where the effect was to pile the electron density at the position of the iron atom of the heme group.

The application of the tangent formula to the cytochrome c data set demonstrated that extreme care must be taken when attempting the refinement of a real protein structure, especially at low resolution. The pile-up of density at the iron position, mentioned above, was due primarily to the way in which the tangent formula was applied to the data. When a newly calculated phase was immediately substituted into the primary phase deck, and thus, contributed in the calculation of the remaining phases (accelerated cycling), pile-up occurred. When the newly calculated phases were not included in subsequent phase calculations (block cycling), however, pile-up did not occur and the effect of the refinement was to produce a somewhat improved electron density map. This effect has been explained in the following way:

As a result of the limited amount of data in the 3.7 Å cytochrome

c data set and the significant phase errors contained in this data, the strong features of the map (heme area) will be more strongly determined than the weak features (general polypeptide areas). Thus, any self-consistent set of phases obtained by repeated cycling of the data through the tangent formula will probably be based only on the heme region of the map. The maximum amount of useful phase angle correction will, thus, be obtained from a non-iterative application of the tangent formula to the approximate multiple isomorphous replacement protein phases (a single block cycle, rather than accelerated cycling or repeated block cycling). This will result in large corrections of the phase angles of reflections which are greatly in error with only a very small drift in the remainder of the phases toward the phases determined by the strong features in the map.

The most successful application of the tangent formula to protein phase refinement was in its use in breaking the phase ambiguity of the two possible phase choices from a single isomorphous replacement phase analysis. In this procedure, the tangent formula is only required to predict which of two known phases is more probably correct, not to predict the exact phase itself. Approximately one-half of the model-globin phases could be determined by this method with good accuracy (the mean error dropped from 45° to 15° with one pass through the tangent formula). The same procedure, applied to the single isomorphous replacement cytochrome c data, determined by the platinum derivative, produced a Fourier map which was almost equal in quality to the double isomorphous replacement map.

This method has not yet been applied to high resolution protein data. On the basis of the results presented here, however, one can expect that with high resolution data the power of the tangent formula refinement procedure will be extremely great. The self-consistency problem will probably disappear (due to the large amount of data available) and iterative refinement procedures will probably be practical. It may well be possible to completely solve a protein structure on the basis of one heavy atom derivative, using the tangent formula to break the phase ambiguity.

APPENDIX I

ISOLATION PROCEDURE FOR CYTOCHROME C

PREPARATION OF BIO-REX 70 RESIN (200-400 MESH) FOR CYTOCHROME C

FOR NEW RESIN

1. Add 6 N NaOH to 1-2 lbs of resin and stir with propeller blade stirrer for 30 minutes.
2. Wash with distilled H_2O.
3. Allow to settle and pour off H_2O and fines.
4. Wash with bottled distilled H_2O and stir adjusting pH to 8.3 - 8.5 by titrating with approximately 43% H_3PO_4.
5. Allow to settle and pour off.
6. Add bottled distilled H_2O and stir again adjusting pH with H_3PO_4. (Fine adjustment.)

FOR USED RESIN

1. Add 6 N NaOH and stir with stirrer for 30 minutes.
2. Pour off NaOH and add tap distilled H_2O and stir by hand.
3. Allow to settle and pour off.
4. Repeat steps 2 and 3 two more times.
5. Add 6 N HCl and stir with stirrer for 30 minutes.
6. Pour off HCl and add tap distilled H_2O and stir by hand.
7. Allow to settle and pour off.
8. Repeat steps 6 and 7 twice more.
9. Add 6 N NaOH and stir for 30 minutes.

10. Allow to settle and pour off.
11. Add bottled distilled H_2O, stir with stirrer while adjusting pH with H_3PO_4 (43%) to pH 8.3 - 8.5.
12. Allow to settle, pour off and repeat step 11 (fine adjustment of pH).

CYTOCHROME C EXTRACTION PROCEDURE (33 lb. run)

REAGENTS

2 lb Bio-Rex 70 resin equilibrated at pH 8.3 - 8.4 with phosphate

2 liters 10% sat. $(NH_4)_2SO_4$ adjusted to pH 7.5 - 7.8 with NH_4OH

100 cc 70% sat. $(NH_4)_2SO_4$

100 cc saturated Na_2HPO_4

100 cc $K_3Fe(CN)_6$ saturated

1 liter 1.0 M NaCl

1 liter .04 M Na_2HPO_4

5 liters 4% $Al_2(SO_4)_3$

EXTRACTION (RT)

1. When ordering horse heart, have linings, fat and any extraneous tissues removed, as well as blood.
2. Chop fairly small with hatchet or knife in semi-frozen state. Put through meat grinder.
3. Homogenize in a gal. size Waring Blender for 15 to 20 sec. at high speed. Fill blender 1/2 full with ground meat and bring to 7/8 full with distilled water at room temperature.
4. Add 50% water by volume to homogenate.
5. Adjust pH with 4% $Al_2(SO_4)_3$ to pH 4.5 with continuous stirring.

6. Let stand for 2 hours at room temperature.

FILTRATION - Cold Room (5°C)

1. Set up 1 dozen 1-liter funnels (gravity) and 1 dozen ten-fifteen liter containers to receive filtrate.
2. Filter through coarse, rapid-flow filter paper. (Schleicher and Schuell #478½, size 50 cm. hand folded.) Takes 6 - 8 hours
3. After 2 hours collect filtrate from receivers. Adjust pH of filtrate with NH_4OH to 8.2 - 8.7.
4. Let stand 20 minutes.
5. Add diatomaceous earth (Hiflow) 10 g/1. Let stand for 15 min.
6. Set up three large gravity funnels over three 10 - 15 liter containers. Collect first 2 to 3 minutes of filtrate and then transfer to another receiver. Put initial filtrate through filter again.
7. Set up two columns of approximately 7 inches diameter with a resin bed depth of approximately 4 - 5 inches. Pour in a quite thick slurry of Bio-Rex 70 (200 Mesh) adjusted to pH 8.3 - 8.4 with H_3PO_4.
8. Put a piece of Filter paper with holes in it on top of column to prevent formation of hole in resin bed. A vacuum on the receiver speeds rate 3 - 4 fold.
9. After about half of the solution has gone through, the column tends to slow up. It may be necessary to start a new column at this time.
10. After cytochrome is collected on column, wash the column with

1 - 2 liters of distilled water.

11. Scrape out the cytochrome layer into a beaker. Add 10% sat. $(NH_4)_2SO_4$ adjusted to pH 7.5 - 7.8 with NH_4OH.
12. Filter through sintered glass funnel with a vacuum. (Repeat steps 10 and 11 for second column and combine filtrates.)
13. Add 1 ml. of sat. $K_3Fe(CN)_6$ to filtrate.
14. Bring concentration of $(NH_4)_2SO_4$ to 70% saturated. Let stand for 20 minutes. Filter by gravity in cold room through S + S filter paper. Wash filter with 70% sat. $(NH_4)_2SO_4$. Keep cold.

N.B. At this point, cytochrome c is at a safe point in the extraction procedure and can be left until the next day.

DIALYSIS (5°C)

1. Prepare dialysis tubing by soaking in distilled water for half hour. Some tubing will not work. Each roll should be tested with some cytochrome solution.
2. Fill tubing 1/2 to 2/3 full. Add 1 ml sat. $K_3Fe(CN)_6$ and 2% by volume of sat. Na_2HPO_4. Add a small amount (1 cc) of NH_4OH to dialysis water to keep pH about 7.5 - 8.5.
3. Dialyze for 2 days with a minimum of 5 changes of water.

COLUMN CHROMATOGRAPHY

1. Put solution on column 1¼ inches diameter and 12 inches long. Fill resin to depth of 6 - 7 inches. Prepare column carefully using the same resin (8.2 - 8.5) and making sure the column is vertical. Add resin in a fairly thin slurry, so that it settles

uniformly. When adding more resin, be careful not to disturb resin already settled.

2. Put a piece of filter paper with holes in it on top of column to break the fall of liquid over bed. Use a vacuum carefully.
3. Since the volume going through this column is 3 - 4 liters, it will take 6 hours to adsorb. The purpose of this first column is to concentrate the cytochrome and, therefore, it is not eluted but scraped out and 100 - 200 cc of 1 M NaCl added.
4. This slurry is filtered through sintered glass and the solution analyzed spectrophotometrically for yield and purity.

CALCULATION OF YIELD AND PURITY

Take spectra of oxidized form at 280 mμ

Take spectra of reduced form at 550 mμ . (Reduction is effected by a small amount of $Na_2S_2O_4$.)

If pure $\frac{550 \text{ red.}}{280 \text{ oxid.}} = 1.23$ If ratio is lower (1.19 to 1.20), the cytochrome is not pure.

$$g_{Cyt.} = \frac{(O.D.)\ (dil.)\ (V)\ (MW)}{\varepsilon}$$

WHERE O.D. = Optical Density at 550

dil. = dilution

V = total volume taken off column

MW = Molecular Wt (12.4)

ε = extinction

5. This solution is then dialyzed for 2 days and again adsorbed on a Bio-Rex Column, 1-inch diameter and resin height to 6 inches.
6. This solution is spread and eluted from the column by using a concentration gradient of 0% NaCl to 1.0 M NaCl in 0.015 M - 0.030 M Na_2HPO_4 (total volume = 1 l.).
7. A fraction collector is used to collect the samples after the cytochrome has been spread down the column with the gradient.
8. All fractions are read to 280 mμ oxid and 550 mμ reduced and all having a 1.23 ratio are combined for crystallization after testing for % autoxidizability. All fractions showing 1% or greater autoxidizability should not be used for crystallization. The % autoxidizability is measured by passing a current of CO through the reduced Cyt and measuring the O.D. at 550 mμ .

$$\% \text{ Autoxidizable} = 162 \frac{(O.D._{red.} - O.D._{red.} + CO)}{O.D._{red.}}$$

CRYSTALLIZATION

1. Determine the % Cyt C solution that has come off the column. g/cc (100) = %
2. Dilute the solution to 1.1 - 1.3% Cyt C using a 90 - 100% sat. $(NH_4)_2SO_4$ solution. (Methods in Enzymology, Vol. 1, p. 76.)
3. Recalculate the amount of saturation of $(NH_4)_2SO_4$ after the addition of Cyt C solution.

   e.g. If one has 10 cc of 5% Cyt C, then for a final solution of 1.2% Cyt

$$(10cc)\ (5\%) = (xcc)\ (1.2\%)$$

$$x = 41.66\ cc$$

$$\begin{array}{r} 41.66 \\ -10.00 \\ \hline 31.66\ cc\ H_2O \end{array}$$

For a 90% sat $(NH_4)_2SO_4$ need 66.2 g $(NH_4)_2SO_4$ to 100 mlH_2 0

$$\frac{66.2g}{100} = \frac{X}{31.66}$$

X = 21 g $(NH_4)_2SO_4$ to add to 31.66 cc of H_2O

but there are 10 cc of Cyt C solution to be added.

Final concentration of $(NH_4)_2SO_4$ =

$$\frac{21g}{41.66} = \frac{Xg}{100}$$

Xg = 50.5 g = approximately 74% sat. $(NH_4)_2SO_4$

4. Allow to stand for 2 to 3 days.

4a.*Bring to 90% sat. Allow to stand overnight. Centrifuge at 4°C if sediment forms.

5. Slowly bring from 90 - 92.5% sat. by adding solid $(NH_4)_2SO_4$. Crystals should begin forming in 1 to 2 weeks and should be allowed to grow for 4 - 6 weeks before using.

N.B. At cytochrome concentration greater than 1.3%, the crystals tend to come down in clumps.

At salt concentrations greater than 92.5% sat., say 95%, the crystals tend to come down as fine needles.

---

*Centrifugation is necessary to remove a fine sticky sediment which forms on the bottom of the container. If crystallization occurs without removal of this sediment, the crystals will stick to this and be hard to remove.

APPENDIX II

HEAVY ATOM DERIVATIVE PREPARATION AND HEAVY ATOMS TESTED TO DATE

PREPARATION OF HEAVY METAL DERIVATIVES IN SAN OR PHOSPHATE

PtIl -K_2PtCl_4

1. Determine concentration of cytochrome crystal preparation to be used for making derivatives.

$$\frac{(O.D._{550\ m\mu\ red.})\ (dil.)}{29.5} = \mu\text{-moles/cc}$$

2. Measure out 5 cc of 95% sat $(NH_4)_2SO_4$ - 1 M NaCl (SAN) into a test tube.
3. Weigh out on analytical balance 50 - 75 mg. of PtIl and add to SAN.
4. Adjust pH with NH_4OH diluted 1/50 to pH 6.5 - 7.0.
5. Calculate concentration of Heavy Metal.

e.g. $\frac{50mg}{5cc} = 10\ mg/cc = .010\ g/cc$

$$\frac{.010g/cc\ (10^6)}{\text{MW of Heavy Metal}} = \mu\text{-moles/cc of PtIl}$$

6. Calculate total amount of cytochrome used.

e.g. (μ-moles/cc cyt) (# of cc of cyt) = total # of μ-moles.

7. For Pt 11 either a 2:1 or 1:1 μM ratio has been used. Measure out amount needed with a syringe and add to crystals.

8. Take final pH.

N.B. pH is extremely important with HgI, the best diffusion of Heavy Metal occurring at pH 6.8. At pH less than 6.0, little HgI diffuses in.

DERIVATIVE LIST

I. Mercury

Salyrganic acid
Neohydrin
p-aminophenylmercuric acetate
6-acetoxymercuir-2,4-dinitrophenol
Phenylmercuric nitrate
Mercurochrome
Phenylmercuric hydroxide
p-chloromercuribenzoate "PCMB"
p-chloromercuriphenyl-1-azo-2-naphthol
p-chloromercuribenzene sulfonate, "PCMBS"
Mercury iodide, K_2HgI_4
p-hydroxymercuribenzoate

II. Platinum

$(PtEn_2ClBr)^{+2}Cl_2^{-2}$
$(PtEn_3)^{+4}Cl_4^{-4}$
$(Pt(NH_3)_3Cl_3)^{+}Cl^{-}$
$(PtEn_2Cl_2)^{+2}Cl_2^{-2}$
$(PtEn_2)^{+2}Cl_2^{-2}$
$(Pt(NH_3)_6)^{+4}Cl_4^{-4}$
H_2PtCl_6
K_2PtBr_6
$Na_2Pt(CN)_6$
$K_2Pt(CNS)_6$
K_2PtCl_4
K_2PtI_6
$Pt(NH_3)_2Cl_2$
Dinitro dichloro diamino Pt
Tetramino $PtCl_2$
$(PtDiI)^{+}L^{-}$

En = $H_2N\text{-}CH_2\text{-}CH_2\text{-}NH_2$

Di = $H_2N\text{-}C_2H_4\text{-}NH\text{-}C_2H_4\text{-}NH_2$

Tr = $(C_2H_5)_2N\text{-}C_2H_4\text{-}NH\text{-}C_2H_4\text{-}N(C_2H_5)_2$

III. Palladium

$(Pd(En)_2)^{+2}Cl_2^{-2}$

$(Pd(NH_3)_4)^{+2}Cl_2^{-2}$

$(PdDiI)^{+}I^{-}$

$(PdTrSCN)^{+}SCN^{-}$

K_2PdCl_4

K_2PdBr_4

Pd oxalate

K_2PdCl_6

Pt dipyridine nitrate

IV. Uranium

Uranyl acetate

Uranyl hexafluoride $K_4UO_2F_6$

Uranyl nitrate

V. Gold

$(AuDiCl)^{+2}Cl_2^{-2}$

$(AuEnCl_2)^{+}AuCl_4^{-}$

$(H_3Di)^{+3}(AuCl_4)_3^{-3}$

$(AuDiCl)^{+}AuCl_4^{-}$

AuCl

$KAu(CN)_2$

VI. Silver

$KAg(CN)_2$

AgOAc

AgCN

VII. Miscellaneous

$(Rh(NH_3)_6)^{+3}Cl_3^{-3}$

$(Ir(NH_3)_6)^{+3}(NO_3)_3^{-3}$

APPENDIX III

The following table contains the three dimensional structure factor magnitudes for the old native, new native, platinum derivative and mercury derivative data sets. All four data sets are on the same arbitrary scale. Undetermined reflections are indicated by a value of -1.

H	K	L	NEW NATIVE	OLD NATIVE	PT	HG	H	K	L	NEW NATIVE	OLD NATIVE	PT	HG	H	K	L	NEW NATIVE	OLD NATIVE	PT	HG
0	0	1	0.	0.	0.	0.	1	7	10	35.9	38.4	42.9	35.5	2	3	2	57.8	65.9	65.0	54.6
0	0	2	0.	0.	0.	0.	1	8	0	62.2	60.7	60.0	58.9	2	3	3	13.8	15.0	27.2	13.4
0	0	3	0.	0.	0.	0.	1	8	1	10.5	12.3	19.5	18.6	2	3	4	11.1	7.7	7.3	5.9
0	0	4	100.4	101.8	77.7	109.3	1	8	2	14.9	15.4	9.5	16.6	2	3	5	30.7	30.1	27.4	24.4
0	0	5	0.	0.	0.	0.	1	8	3	30.4	29.6	18.3	24.4	2	3	6	17.5	17.3	10.3	14.0
0	0	6	0.	0.	0.	0.	1	8	4	8.3	12.2	12.0	7.9	2	3	7	24.0	25.4	32.1	21.9
0	0	7	0.	0.	0.	0.	1	8	5	30.0	30.2	28.4	31.9	2	3	8	34.4	33.2	36.6	32.1
0	0	8	67.0	69.8	76.4	73.6	1	8	6	15.6	15.6	14.5	12.0	2	3	9	24.3	23.6	17.6	22.9
0	0	9	0.	0.	0.	0.	1	8	7	45.3	47.2	44.3	38.0	2	3	10	18.9	19.2	12.6	22.0
0	0	10	0.	0.	0.	0.	1	8	8	22.5	23.0	18.7	22.4	2	3	11	-1.0	24.2	12.7	17.6
0	0	11	0.	0.	0.	0.	1	8	9	18.9	21.2	18.1	28.3	2	4	0	163.0	160.5	189.9	174.4
1	0	0	-1.0	28.4	24.9	-1.0	1	9	0	16.9	16.3	9.9	22.2	2	4	1	12.6	13.4	27.5	18.4
1	0	1	-1.0	31.4	22.2	30.4	1	9	1	20.8	22.9	16.4	25.4	2	4	2	39.6	40.3	48.8	39.2
1	0	2	55.7	53.8	51.8	59.1	1	9	2	6.1	7.5	9.1	5.5	2	4	3	63.4	62.4	45.2	60.3
1	0	3	10.2	8.8	26.0	11.4	1	9	3	10.9	16.4	11.1	14.9	2	4	4	23.8	21.4	18.7	25.1
1	0	4	43.1	44.4	43.6	41.3	1	9	4	47.7	48.9	49.3	45.8	2	4	5	29.4	28.6	38.8	27.9
1	0	5	28.9	28.9	37.6	26.1	1	9	5	17.5	18.3	21.0	14.0	2	4	6	39.9	38.6	33.9	39.3
1	0	6	23.5	25.0	22.1	22.7	1	9	6	32.7	32.5	16.5	31.8	2	4	7	48.1	48.1	50.3	51.4
1	0	7	38.7	38.6	39.1	36.4	1	9	7	41.3	42.0	39.5	39.6	2	4	8	34.5	34.9	38.3	37.9
1	0	8	22.7	25.5	18.8	23.7	1	9	8	19.8	22.0	20.8	22.8	2	4	9	41.6	42.9	42.4	44.6
1	0	9	45.3	45.2	38.3	44.1	1	9	9	27.5	27.8	29.7	30.9	2	4	10	10.6	8.5	9.4	11.0
1	0	10	4.1	11.0	4.7	8.1	1	10	0	32.8	33.2	36.5	33.4	2	5	0	23.7	19.7	4.9	19.9
1	0	11	19.7	16.5	13.9	13.2	1	10	1	41.4	45.2	56.1	41.2	2	5	1	76.7	69.5	72.3	74.0
1	1	0	-1.0	6.6	5.5	21.4	1	10	2	38.6	39.4	29.8	37.0	2	5	2	40.3	39.0	50.3	38.9
1	1	1	38.5	47.4	44.1	32.4	1	10	3	59.6	56.1	48.8	49.2	2	5	3	27.3	24.6	37.0	23.6
1	1	2	51.5	55.2	62.9	50.3	1	10	4	14.1	14.5	22.6	10.3	2	5	4	39.9	36.1	39.9	37.8
1	1	3	38.7	41.6	44.9	36.2	1	10	5	33.6	34.1	29.5	29.1	2	5	5	49.3	46.8	39.7	48.8
1	1	4	20.2	20.8	17.5	15.2	1	10	6	35.7	35.1	34.1	32.1	2	5	6	18.4	17.6	21.4	15.1
1	1	5	12.7	11.8	5.8	16.6	1	10	7	13.9	15.7	19.4	16.5	2	5	7	31.2	27.6	22.5	28.8
1	1	6	18.1	19.6	27.2	20.4	1	10	8	18.9	16.9	22.4	17.5	2	5	8	46.7	49.	43.3	46.7
1	1	7	41.1	43.5	36.7	39.3	1	11	0	62.1	62.0	45.7	61.2	2	5	9	55.8	59.8	59.4	62.9
1	1	8	48.0	50.7	58.2	55.7	1	11	1	12.1	13.4	11.0	10.8	2	5	10	18.7	16.8	18.3	23.0
1	1	9	34.5	40.5	43.3	41.7	1	11	2	36.4	37.1	50.5	29.5	2	6	0	52.9	49.7	51.4	51.7
1	1	10	17.0	15.2	9.8	21.7	1	11	3	37.7	37.6	39.4	35.3	2	6	1	40.5	46.6	47.7	45.9
1	1	11	24.1	24.1	23.4	26.1	1	11	4	8.7	14.8	12.6	6.0	2	6	2	10.6	11.5	24.9	13.4
1	2	0	28.7	33.8	6.5	22.0	1	11	5	14.4	13.5	16.8	10.6	2	6	3	37.5	35.5	32.7	41.5
1	2	1	40.4	33.4	50.9	25.4	1	11	6	24.7	25.1	32.7	21.6	2	6	4	23.7	20.5	21.7	27.3
1	2	2	17.5	19.3	27.7	19.5	1	11	7	13.3	13.8	4.4	19.6	2	6	5	23.	22.	19.7	24.3
1	2	3	52.	53.9	31.8	46.6	1	11	8	31.6	33.0	31.8	31.1	2	6	6	15.4	15.2	1.6	1.8
1	2	4	36.1	38.0	41.9	36.7	1	12	0	38.5	40.2	45.2	29.6	2	6	7	16.4	16.7	23.7	14.4
1	2	5	61.	60.5	66.5	60.4	1	12	1	26.6	27.1	39.3	28.4	2	6	8	30.2	32.6	31.8	34.5
1	2	6	4.4	7.3	3.9	6.3	1	12	2	14.4	17.3	17.7	13.5	2	6	9	22.8	20.1	24.5	24.2
1	2	7	20.	21.7	34.8	24.2	1	12	3	15.1	17.7	24.5	21.9	2	6	10	14.1	11.6	2.6	14.5
1	2	8	49.7	47.2	52.2	47.2	1	12	4	17.9	20.4	20.9	15.1	2	7	0	17.2	17.9	-1.	13.1
1	2	9	11.	10.4	14.6	13.9	1	12	5	9.3	11.9	14.8	12.4	2	7	1	-1.0	13.4	-1.0	29.5
1	2	10	13.6	14.5	13.6	18.4	1	12	6	31.0	34.7	33.9	27.0	2	7	2	29.4	28.0	13.5	31.3
1	2	11	5.	6.5	33.1	23.8	1	12	7	46.8	49.8	45.4	43.2	2	7	3	21.5	27.5	32.0	17.7
1	3	0	20.4	27.6	11.1	21.0	1	13	0	17.4	15.3	11.6	14.6	2	7	4	34.2	36.9	40.0	33.1
1	3	1	72.0	75.2	80.6	59.8	1	13	1	16.2	16.5	18.8	14.5	2	7	5	36.6	37.0	32.0	44.0
1	3	2	36.6	38.3	19.5	38.3	1	13	2	19.2	18.9	17.9	19.4	2	7	6	8.5	23.7	24.3	13.4
1	3	3	9.	10.8	23.7	38.7	1	13	3	0.5	4.3	6.6	10.6	2	7	7	7.0	6.9	4.7	11.6
1	3	4	22.	20.1	10.1	20.9	1	13	4	4.4	9.7	4.3	6.2	2	7	8	52.8	52.5	50.4	54.1
1	3	5	44.4	43.1	44.3	46.9	1	13	5	29.4	22.6	16.3	19.5	2	7	9	11.7	17.9	12.5	19.6
1	3	6	2.	11.	1.9	6.8	1	13	6	34.7	28.9	30.9	22.3	2	7	10	17.5	19.9	17.1	21.4
1	3	7	16.7	14.8	19.7	17.3	1	14	0	4.7	7.4	13.7	8.7	2	8	0	19.7	14.1	7.4	11.6
1	3	8	41.1	46.4	42.7	43.9	1	14	1	32.8	32.2	39.2	32.3	2	8	1	47.9	41.3	41.7	46.3
1	3	9	36.	35.8	36.2	32.2	1	14	2	40.2	42.7	34.9	37.2	2	8	2	39.1	37.1	34.7	37.5
1	3	10	7.	10.1	41.4	34.3	1	14	3	20.8	20.2	16.3	19.6	2	8	3	14.4	12.9	19.2	11.9
1	3	11	20.7	22.	21.7	28.8	1	14	4	12.8	14.4	17.2	12.4	2	8	4	29.1	31.0	27.9	28.5
1	4	0	32.8	34.5	41.1	23.1	1	14	5	36.7	40.1	38.0	32.4	2	8	5	19.7	19.2	19.5	18.0
1	4	1	-1.0	-1.0	42.9	58.7	1	15	0	20.5	21.4	21.6	21.7	2	8	6	11.9	9.6	7.7	8.2
1	4	2	56.3	55.1	59.6	57.9	1	15	1	29.3	30.8	27.5	28.9	2	8	7	31.8	29.7	36.0	30.5
1	4	3	15.1	15.4	2.7	16.3	1	15	2	32.4	34.0	33.1	27.3	2	8	8	55.7	56.3	58.1	54.8
1	4	4	14.7	11.3	31.5	20.3	1	15	3	7.8	10.6	4.2	8.6	2	8	9	19.9	19.0	16.0	18.2
1	4	5	22.4	22.3	27.4	25.7	2	0	0	2.5	-1.0	32.1	15.6	2	9	0	52.7	53.4	44.2	42.1
1	4	6	49.6	47.3	60.9	50.9	2	0	1	2.6	-1.0	16.3	3.2	2	9	1	29.2	29.3	9.1	26.4
1	4	7	20.8	18.5	16.3	25.1	2	0	2	13.7	12.2	10.8	17.4	2	9	2	36.7	34.1	32.6	36.3
1	4	8	6.2	6.5	9.2	7.8	2	0	3	68.7	67.0	50.9	67.4	2	9	3	33.8	33.4	34.1	28.1
1	4	9	51.5	55.5	48.4	54.2	2	0	4	76.5	81.4	68.7	71.8	2	9	4	24.8	24.8	26.6	13.0
1	4	10	9.7	10.1	3.0	9.5	2	0	5	69.1	69.0	62.2	64.5	2	9	5	23.4	22.7	13.2	23.0
1	5	0	15.0	16.5	9.5	14.4	2	0	6	29.1	28.1	29.0	31.0	2	9	6	28.6	30.6	27.2	27.1
1	5	1	7.4	7.0	13.8	4.4	2	0	7	39.6	40.6	46.3	41.1	2	9	7	34.5	35.8	23.6	29.3
1	5	2	16.1	17.5	13.0	19.9	2	0	8	30.8	32.1	38.6	29.3	2	9	8	16.9	17.8	20.3	17.4
1	5	3	53.0	52.5	54.1	46.0	2	0	9	18.3	20.5	17.9	21.6	2	9	9	27.1	27.5	18.9	28.8
1	5	4	33.9	34.5	29.9	36.3	2	0	10	26.7	28.2	28.3	25.6	2	10	0	20.3	19.7	31.0	16.7
1	5	5	29.8	28.7	13.5	30.2	2	0	11	37.8	42.2	41.0	37.8	2	10	1	27.8	27.3	29.8	25.3
1	5	6	46.6	47.2	49.4	43.6	2	1	0	8.9	11.6	2.4	3.2	2	10	2	25.3	24.6	33.5	19.5
1	5	7	35.3	34.7	36.4	33.8	2	1	1	21.1	23.9	42.9	30.7	2	10	3	41.5	40.2	41.5	41.9
1	5	8	21.7	23.7	24.0	26.8	2	1	2	34.9	38.1	19.6	36.5	2	10	4	59.7	59.7	50.4	62.2
1	5	9	66.2	64.7	63.3	66.2	2	1	3	40.8	41.3	56.8	37.0	2	10	5	46.9	42.2	41.8	37.1
1	5	10	21.6	20.2	19.4	22.0	2	1	4	18.3	19.5	18.6	20.3	2	10	6	13.5	6.7	14.1	8.7
1	6	0	52.9	50.7	41.1	44.3	2	1	5	20.5	21.9	15.2	22.3	2	10	7	30.0	31.3	33.1	30.8
1	6	1	26.5	26.2	31.2	32.0	2	1	6	31.1	32.8	40.9	31.5	2	10	8	33.5	32.4	31.7	31.4
1	6	2	19.8	20.3	3.0	21.2	2	1	7	52.4	53.0	41.4	48.5	2	11	0	19.3	19.2	20.3	24.4
1	6	3	11.9	11.7	10.3	10.9	2	1	8	42.7	44.2	44.3	45.8	2	11	1	15.4	16.7	27.3	14.6
1	6	4	23.0	21.9	26.5	18.7	2	1	9	25.3	27.2	26.0	22.9	2	11	2	32.5	32.1	31.3	34.5
1	6	5	34.0	35.1	32.3	36.0	2	1	10	22.9	23.6	29.5	20.9	2	11	3	54.9	52.5	46.4	55.3
1	6	6	21.9	23.1	6.2	23.2	2	1	11	27.4	30.9	32.7	28.8	2	11	4	43.6	39.2	41.5	46.5
1	6	7	45.1	45.7	49.3	42.3	2	2	0	19.2	20.8	11.7	13.3	2	11	5	26.9	23.5	17.9	22.8
1	6	8	12.8	13.5	23.7	12.3	2	2	1	27.8	30.6	44.5	29.3	2	11	6	11.2	6.9	10.4	8.8
1	6	9	65.1	67.3	62.8	58.8	2	2	2	58.0	58.8	58.0	53.0	2	11	7	30.2	30.1	35.6	28.0
1	6	10	15.9	16.4	21.5	13.8	2	2	3	41.2	41.8	36.0	35.7	2	11	8	29.5	30.0	27.0	28.3
1	7	0	17.0	17.3	9.8	18.4	2	2	4	40.6	40.9	44.4	35.6	2	12	0	22.0	22.2	8.5	23.9
1	7	1	11.8	13.1	3.3	14.3	2	2	5	35.6	35.7	31.8	27.9	2	12	1	25.5	22.5	16.4	27.2
1	7	2	24.4	22.7	28.4	22.6	2	2	6	13.0	12.8	8.1	13.1	2	12	2	50.8	46.6	53.0	48.9
1	7	3	24.0	21.2	20.4	25.6	2	2	7	24.6	23.6	23.3	25.0	2	12	3	79.2	71.2	75.7	75.7
1	7	4	19.0	21.4	30.2	23.6	2	2	8	18.2	19.6	11.7	14.7	2	12	4	26.0	24.8	19.6	23.7
1	7	5	41.2	42.0	52.6	44.3	2	2	9	35.6	35.4	41.3	36.8	2	12	5	14.7	11.9	23.2	8.8
1	7	6	4.6	4.1	4.1	6.0	2	2	10	32.1	34.5	29.9	32.4	2	12	6	9.8	7.0	10.7	9.0
1	7	7	39.8	40.2	42.8	34.8	2	2	11	31.5	35.2	32.3	30.2	2	12	7	31.2	30.0	33.6	25.7
1	7	8	34.5	34.5	40.4	33.2	2	3	0	34.8	36.1	45.5	40.6	2	13	0	61.0	60.2	61.6	53.0
1	7	9	26.8	29.0	32.2	26.1	2	3	1	25.2	29.7	37.9	32.7	2	13	1	35.9	34.0	25.9	36.3

H	K	L	NEW NATIVE	OLD NATIVE	PT	HG	H	K	L	NEW NATIVE	OLD NATIVE	PT	HG	H	K	L	NEW NATIVE	OLD NATIVE	PT	HG
2	13	2	16.5	19.4	20.8	19.9	3	7	7	7.9	11.1	10.1	10.0	4	3	6	45.9	49.2	63.1	51.1
2	13	3	59.3	55.8	50.6	49.4	3	7	8	32.3	33.6	37.6	41.8	4	3	7	37.2	35.5	43.6	33.9
2	13	4	28.2	25.8	25.2	24.8	3	7	9	14.9	18.8	5.2	19.6	4	3	8	10.8	12.6	14.8	10.8
2	13	5	15.8	19.9	16.1	16.0	3	8	0	8.8	10.1	8.9	9.1	4	3	9	48.2	46.6	45.3	46.9
2	13	6	33.9	33.3	24.2	31.6	3	8	1	45.7	43.6	47.0	50.0	4	3	10	47.4	43.8	54.6	54.3
2	14	0	58.6	59.0	63.3	54.7	3	8	2	48.5	45.7	41.3	46.5	4	4	0	18.9	18.4	18.4	9.0
2	14	1	15.6	16.8	17.5	16.6	3	8	3	22.5	18.6	11.1	20.3	4	4	1	54.9	59.1	65.1	52.2
2	14	2	24.2	24.9	19.5	27.8	3	8	4	30.3	27.3	23.6	25.1	4	4	2	63.8	66.8	69.3	66.0
2	14	3	28.2	28.6	24.6	26.8	3	8	5	5.1	6.1	8.8	10.6	4	4	3	21.2	18.2	33.6	17.2
2	14	4	11.2	7.1	12.5	15.6	3	8	6	9.2	6.7	5.7	6.8	4	4	4	36.1	40.8	36.3	31.5
2	14	5	11.2	7.1	3.9	9.0	3	8	7	26.7	26.6	25.2	30.6	4	4	5	59.3	62.7	61.2	56.6
2	15	0	22.8	23.7	26.2	22.8	3	8	8	59.0	62.4	64.9	59.9	4	4	6	20.9	19.1	23.8	18.7
2	15	1	28.8	26.9	25.5	27.0	3	8	9	9.5	6.4	5.3	9.9	4	4	7	26.9	26.4	30.6	24.9
2	15	2	19.3	19.5	22.1	17.1	3	9	0	15.3	16.0	35.7	12.1	4	4	8	43.4	45.1	43.2	40.1
2	15	3	26.2	23.1	22.0	19.1	3	9	1	-1.0	-1.0	18.6	17.4	4	4	9	43.1	44.3	40.6	42.5
3	0	0	18.4	18.0	10.8	23.7	3	9	2	-1.0	-1.0	25.7	21.8	4	4	10	31.1	29.6	39.1	32.4
3	0	1	28.3	28.9	27.9	33.3	3	9	3	33.7	33.6	34.2	39.9	4	5	0	10.5	6.3	4.8	11.0
3	0	2	52.2	50.3	41.5	44.0	3	9	4	13.1	17.2	20.3	17.6	4	5	1	22.0	26.5	32.2	25.3
3	0	3	41.0	40.1	29.7	32.9	3	9	5	29.9	28.7	32.3	26.1	4	5	2	23.9	25.9	24.2	12.6
3	0	4	63.9	59.5	72.3	67.3	3	9	6	28.2	29.3	22.3	25.5	4	5	3	62.1	73.5	60.1	62.8
3	0	5	27.4	28.0	38.0	29.4	3	9	7	54.7	52.9	53.4	57.3	4	5	4	18.2	25.0	22.2	18.1
3	0	6	16.0	17.6	20.1	20.0	3	9	8	33.0	35.1	22.6	34.4	4	5	5	19.5	18.2	19.5	18.0
3	0	7	10.6	11.4	16.6	10.2	3	9	9	32.8	34.7	31.9	34.3	4	5	6	33.5	34.9	43.7	34.8
3	0	8	38.6	41.6	39.9	45.4	3	10	0	5.0	4.4	3.6	6.5	4	5	7	17.7	19.1	9.7	17.1
3	0	9	12.5	15.0	15.8	18.5	3	10	1	7.1	9.3	3.6	7.0	4	5	8	32.6	31.6	25.6	34.1
3	0	10	21.6	24.1	20.2	20.1	3	10	2	42.6	40.7	39.7	41.8	4	5	9	23.7	23.6	28.9	23.7
3	0	11	28.2	32.3	20.0	33.7	3	10	3	21.4	22.4	31.2	23.7	4	5	10	26.3	32.3	32.5	19.1
3	1	0	31.4	36.6	29.3	38.9	3	10	4	14.1	17.2	27.4	19.2	4	6	0	7.4	11.9	6.6	12.9
3	1	1	28.2	-1.0	10.4	33.1	3	10	5	17.3	20.4	23.2	19.5	4	6	1	13.1	12.1	20.3	13.6
3	1	2	23.8	-1.0	27.1	30.3	3	10	6	9.0	14.3	4.8	9.2	4	6	2	53.4	53.1	64.7	58.4
3	1	3	41.1	39.8	55.3	42.8	3	10	7	44.5	43.2	49.4	44.0	4	6	3	30.8	27.9	37.2	33.7
3	1	4	8.6	10.7	9.2	9.8	3	10	8	17.1	18.6	19.9	19.3	4	6	4	15.2	14.3	11.3	7.6
3	1	5	32.5	31.8	41.6	36.0	3	11	0	6.1	5.0	4.1	6.0	4	6	5	32.1	28.9	31.4	30.3
3	1	6	17.0	17.6	25.3	22.9	3	11	1	34.2	33.1	30.2	35.5	4	6	6	14.0	15.1	21.2	11.6
3	1	7	45.5	43.7	51.1	43.8	3	11	2	29.9	27.8	20.0	24.3	4	6	7	12.9	14.3	5.2	14.8
3	1	8	28.4	28.4	27.7	26.4	3	11	3	28.1	29.0	34.5	28.7	4	6	8	21.3	22.0	26.9	16.6
3	1	9	37.8	39.5	40.3	41.7	3	11	4	53.0	55.3	47.4	61.8	4	6	9	23.5	23.1	26.1	19.6
3	1	10	30.9	33.1	23.4	28.4	3	11	5	38.7	43.3	34.7	45.7	4	6	10	32.4	32.2	25.5	29.2
3	1	11	15.9	16.1	17.9	14.7	3	11	6	14.6	15.4	14.6	20.7	4	7	0	30.0	28.1	23.6	25.3
3	2	0	17.9	16.6	41.9	20.2	3	11	7	28.3	26.2	19.4	21.4	4	7	1	33.2	27.7	38.5	30.2
3	2	1	56.5	-1.0	62.7	59.2	3	12	0	43.4	44.9	33.6	38.8	4	7	2	13.6	14.3	16.0	10.4
3	2	2	45.9	46.0	40.0	45.2	3	12	1	35.4	34.0	26.5	34.3	4	7	3	45.9	38.3	32.2	38.9
3	2	3	57.4	62.0	51.1	54.6	3	12	2	16.1	15.6	12.0	12.3	4	7	4	25.2	17.0	20.2	21.4
3	2	4	29.8	31.4	41.9	25.2	3	12	3	47.4	44.1	51.4	41.1	4	7	5	25.3	19.1	22.4	21.8
3	2	5	35.1	33.9	22.7	36.0	3	12	4	64.6	61.0	66.5	65.3	4	7	6	20.7	16.1	23.0	19.0
3	2	6	5.1	8.3	3.8	8.1	3	12	5	45.5	48.9	51.5	48.8	4	7	7	23.5	23.1	15.6	22.8
3	2	7	22.4	21.2	16.9	19.9	3	12	6	27.6	26.7	27.2	25.5	4	7	8	15.0	13.0	16.4	13.4
3	2	8	20.3	21.9	32.1	24.3	3	12	7	28.4	29.9	26.4	28.7	4	7	9	8.4	7.3	11.7	7.8
3	2	9	28.5	30.0	25.1	26.7	3	13	0	35.7	37.1	26.0	34.3	4	8	0	42.7	37.7	31.7	35.4
3	2	10	20.3	23.4	18.2	21.6	3	13	1	19.9	18.3	19.7	19.3	4	8	1	37.0	31.4	30.1	33.1
3	2	11	12.2	11.4	17.4	9.2	3	13	2	32.9	34.4	35.6	41.2	4	8	2	11.1	8.9	10.4	12.2
3	3	0	70.5	76.9	80.7	77.9	3	13	3	27.4	27.3	33.6	28.4	4	8	3	36.4	33.1	32.3	36.6
3	3	1	56.8	60.1	72.8	62.7	3	13	4	32.8	32.8	29.9	27.8	4	8	4	7.8	4.3	12.6	10.1
3	3	2	8.9	6.0	5.5	9.3	3	13	5	6.7	6.3	5.2	9.7	4	8	5	16.4	13.8	13.7	12.6
3	3	3	32.1	32.9	41.2	34.0	3	13	6	16.4	6.5	5.5	14.1	4	8	6	18.9	17.7	8.5	18.6
3	3	4	49.8	48.7	37.4	51.7	3	14	0	57.5	63.2	46.6	67.6	4	8	7	28.0	27.5	25.9	26.0
3	3	5	32.4	32.9	40.5	30.1	3	14	1	21.6	20.2	17.1	25.1	4	8	8	12.5	13.4	8.3	9.4
3	3	6	27.1	26.3	15.4	27.2	3	14	2	41.7	40.6	34.7	41.4	4	8	9	23.2	18.9	16.7	22.1
3	3	7	28.9	29.5	36.3	26.7	3	14	3	41.6	43.3	38.2	44.5	4	9	0	34.5	35.1	27.3	30.8
3	3	8	8.5	7.2	6.2	7.6	3	14	4	30.0	33.7	21.4	36.9	4	9	1	28.7	25.8	13.8	33.0
3	3	9	68.7	70.0	78.6	75.0	3	15	0	9.0	12.6	5.3	19.6	4	9	2	25.8	22.8	19.9	23.4
3	3	10	44.7	44.8	40.6	45.6	3	15	1	12.6	12.0	12.9	6.9	4	9	3	26.3	23.0	24.1	32.7
3	4	0	15.3	16.6	35.5	16.6	3	15	2	18.9	19.2	14.5	17.1	4	9	4	20.7	19.5	14.2	27.6
3	4	1	16.6	19.4	20.5	9.3	4	0	0	50.5	50.3	60.1	55.4	4	9	5	13.4	14.9	18.0	20.1
3	4	2	42.3	39.9	41.9	39.6	4	0	1	58.3	57.9	56.5	56.8	4	9	6	11.0	11.9	14.7	12.0
3	4	3	20.2	17.8	15.2	15.6	4	0	2	38.4	38.9	26.4	40.2	4	9	7	9.1	13.5	13.1	11.5
3	4	4	29.9	27.2	17.3	26.0	4	0	3	11.6	12.0	5.5	18.1	4	9	8	18.2	16.2	17.3	20.6
3	4	5	23.0	21.0	25.9	21.1	4	0	4	44.0	45.2	29.1	42.7	4	10	0	9.4	10.5	7.9	9.4
3	4	6	18.4	16.6	23.1	18.2	4	0	5	9.0	12.8	6.5	14.7	4	10	1	20.4	17.3	19.3	17.2
3	4	7	28.9	27.9	25.0	24.1	4	0	6	16.1	14.9	17.8	23.9	4	10	2	16.1	14.2	17.0	12.3
3	4	8	20.5	20.9	15.1	23.4	4	0	7	33.2	36.7	20.1	33.9	4	10	3	42.0	39.6	36.7	40.9
3	4	9	35.3	35.8	39.6	37.1	4	0	8	21.4	25.0	15.9	23.3	4	10	4	13.1	14.7	7.0	14.3
3	4	10	18.4	21.3	16.9	25.1	4	0	9	22.7	25.7	22.1	26.6	4	10	5	19.4	15.1	23.5	17.2
3	5	0	38.0	29.2	18.9	36.8	4	0	10	26.5	28.3	29.7	23.3	4	10	6	16.7	17.4	27.9	18.5
3	5	1	27.9	23.4	10.7	25.0	4	1	0	45.6	44.8	28.6	36.2	4	10	7	12.7	15.8	8.5	11.6
3	5	2	50.6	42.0	51.1	40.5	4	1	1	-1.0	-1.0	45.7	51.4	4	10	8	27.6	-1.0	18.1	27.4
3	5	3	28.3	24.9	35.5	30.4	4	1	2	13.2	15.1	37.3	14.3	4	11	0	12.7	12.0	-1.0	4.8
3	5	4	23.3	21.9	24.6	18.8	4	1	3	51.2	55.1	39.2	53.3	4	11	1	-1.0	-1.0	-1.0	47.7
3	5	5	43.6	40.3	50.9	42.2	4	1	4	31.6	31.9	27.6	41.6	4	11	2	25.9	27.6	-1.0	26.0
3	5	6	48.0	46.0	50.7	45.7	4	1	5	28.0	28.4	35.4	29.4	4	11	3	35.8	36.9	38.3	31.8
3	5	7	16.4	17.1	15.7	20.0	4	1	6	22.2	23.7	5.9	25.4	4	11	4	11.0	14.7	4.4	8.7
3	5	8	75.8	72.3	82.4	66.7	4	1	7	35.9	36.6	43.2	33.4	4	11	5	53.5	53.7	51.5	59.6
3	5	9	42.0	39.0	48.3	35.8	4	1	8	15.3	15.0	19.5	17.7	4	11	6	16.7	15.6	20.6	19.2
3	5	10	16.9	20.3	14.2	18.2	4	1	9	35.1	34.9	37.4	33.2	4	11	7	40.8	41.4	47.5	39.9
3	6	0	13.4	13.7	19.5	17.7	4	1	10	24.3	23.3	23.5	23.1	4	12	0	4.9	5.7	9.6	5.2
3	6	1	22.3	16.8	12.9	23.0	4	2	0	15.3	17.2	26.4	21.0	4	12	1	15.5	14.1	10.6	9.8
3	6	2	27.8	23.8	17.0	22.6	4	2	1	26.1	26.2	7.6	23.2	4	12	2	16.3	15.8	14.1	14.3
3	6	3	27.4	24.1	36.2	24.5	4	2	2	43.7	37.1	42.8	31.6	4	12	3	14.8	15.3	18.3	10.1
3	6	4	16.1	14.5	11.8	17.0	4	2	3	17.9	20.0	26.8	23.0	4	12	4	45.1	43.1	36.0	48.4
3	6	5	11.2	9.5	5.9	7.0	4	2	4	16.2	14.6	15.3	14.2	4	12	5	46.3	44.9	44.9	48.7
3	6	6	21.6	20.5	13.5	22.1	4	2	5	16.1	14.3	27.3	12.8	4	12	6	22.4	22.1	24.2	22.8
3	6	7	46.8	45.8	48.4	45.5	4	2	6	49.4	48.5	50.6	54.8	4	13	0	19.2	19.7	15.3	20.8
3	6	8	25.8	21.5	28.6	21.7	4	2	7	15.2	14.4	18.5	14.6	4	13	1	35.1	33.5	30.9	32.7
3	6	9	46.3	48.9	51.2	49.1	4	2	8	13.5	15.3	16.8	15.7	4	13	2	38.7	36.0	41.9	39.9
3	6	10	21.5	27.5	22.2	32.5	4	2	9	60.6	64.7	64.7	63.7	4	13	3	41.9	40.3	43.9	37.9
3	7	0	49.6	44.8	25.9	42.4	4	2	10	35.7	38.8	38.7	36.2	4	13	4	31.8	31.2	38.4	28.5
3	7	1	22.2	17.4	21.5	23.0	4	3	0	55.5	52.6	56.7	57.5	4	13	5	24.1	21.0	25.6	19.6
3	7	2	14.5	13.9	6.0	16.2	4	3	1	65.1	66.2	70.3	61.9	4	14	0	22.0	24.4	15.8	25.1
3	7	3	31.9	27.3	30.7	27.4	4	3	2	31.8	31.6	22.3	33.3	4	14	1	21.7	17.9	22.1	21.0
3	7	4	30.4	25.1	12.9	37.9	4	3	3	40.2	40.7	35.2	34.7	4	14	2	9.8	7.1	5.3	10.5
3	7	5	19.6	16.9	24.9	14.9	4	3	4	35.0	37.7	32.9	38.0	4	14	3	31.5	29.3	30.8	23.5
3	7	6	20.4	19.2	14.1	19.8	4	3	5	14.2	13.2	17.8	15.3	4	14	4	21.6	21.3	19.5	20.9

H	K	L	NEW NATIVE	OLD NATIVE	PT	HG	H	K	L	NEW NATIVE	OLD NATIVE	PT	HG	H	K	L	NEW NATIVE	OLD NATIVE	PT	HG
4	15	0	11.4	7.4	15.4	14.5	5	9	3	27.5	23.9	22.6	27.3	6	5	6	31.0	29.7	32.9	31.3
4	15	1	23.5	21.7	20.0	26.3	5	9	4	48.2	39.9	45.3	43.8	6	5	7	59.5	56.5	61.9	61.4
4	15	2	27.0	25.8	15.7	30.0	5	9	5	25.1	20.7	22.1	25.2	6	5	8	34.7	34.9	35.1	38.1
5	0	0	86.0	82.1	61.9	76.8	5	9	6	34.0	32.7	26.2	33.0	6	5	9	15.1	7.3	5.8	14.5
5	0	1	10.2	11.3	14.0	15.4	5	9	7	23.4	22.8	19.9	19.8	6	6	0	23.5	19.7	17.0	15.5
5	0	2	31.8	32.0	40.1	30.4	5	9	8	-1.0	-1.0	-1.0	-1.0	6	6	1	16.9	16.7	4.6	12.0
5	0	3	34.4	35.1	27.0	30.2	5	10	0	40.0	36.7	34.0	38.2	6	6	2	24.5	23.6	13.5	21.0
5	0	4	20.9	24.3	29.4	22.3	5	10	1	19.5	13.8	8.2	15.1	6	6	3	41.9	41.5	48.4	42.3
5	0	5	38.3	41.2	34.7	38.0	5	10	2	19.2	19.0	17.1	21.7	6	6	4	16.7	17.9	17.4	16.6
5	0	6	5.7	11.0	14.6	8.9	5	10	3	15.2	13.8	18.4	22.5	6	6	5	16.6	16.3	18.8	13.8
5	0	7	7.0	13.3	16.0	8.7	5	10	4	14.5	20.0	7.1	23.7	6	6	6	42.8	42.7	42.7	35.8
5	0	8	48.6	53.1	63.1	50.8	5	10	5	24.6	22.0	22.3	22.6	6	6	7	61.9	65.2	58.3	63.1
5	0	9	8.0	9.0	12.3	12.0	5	10	6	21.1	20.3	15.0	22.7	6	6	8	26.2	27.8	19.0	28.8
5	0	10	7.5	10.6	6.4	6.8	5	10	7	20.4	14.4	21.7	12.2	6	6	9	26.8	25.6	21.9	24.3
5	1	0	66.9	63.7	67.2	68.7	5	10	8	-1.0	-1.0	-1.0	-1.0	6	7	0	34.3	35.9	25.4	33.0
5	1	1	31.3	28.6	9.6	29.3	5	11	0	25.7	25.2	27.0	21.6	6	7	1	24.5	29.1	11.2	25.7
5	1	2	59.8	59.4	51.3	58.2	5	11	1	34.8	27.4	20.3	37.6	6	7	2	8.1	7.7	13.6	10.8
5	1	3	31.3	31.7	41.3	31.0	5	11	2	32.0	31.0	21.0	31.0	6	7	3	23.6	20.7	24.3	26.6
5	1	4	22.4	22.2	16.9	25.5	5	11	3	43.1	39.3	27.9	36.9	6	7	4	42.2	45.1	32.0	39.5
5	1	5	8.4	11.0	23.4	9.9	5	11	4	32.4	28.0	17.7	28.0	6	7	5	29.0	27.4	30.9	28.6
5	1	6	12.5	15.3	12.1	24.7	5	11	5	35.8	29.7	28.4	36.2	6	7	6	20.4	26.1	17.7	19.6
5	1	7	19.5	19.1	16.3	20.6	5	11	6	-1.0	-1.0	24.0	-1.0	6	7	7	26.2	25.8	29.6	27.9
5	1	8	29.2	32.1	30.5	30.0	5	11	7	-1.0	-1.0	-1.0	-1.0	6	7	8	18.9	19.5	19.8	15.9
5	1	9	56.3	59.1	60.4	59.0	5	12	0	7.3	10.7	3.4	6.8	6	7	9	21.8	-1.0	-1.0	-1.0
5	1	10	28.8	31.8	31.5	28.0	5	12	1	31.6	28.3	29.2	38.3	6	8	0	15.2	13.8	16.6	14.4
5	2	0	77.2	70.8	47.8	84.1	5	12	2	19.7	16.5	19.1	14.1	6	8	1	14.9	16.2	15.4	13.2
5	2	1	36.5	32.4	32.1	35.8	5	12	3	14.7	12.3	11.5	13.8	6	8	2	13.0	16.2	21.4	15.3
5	2	2	52.3	46.2	45.6	51.2	5	12	4	5.8	-1.0	-1.0	-1.0	6	8	3	38.1	32.7	40.9	41.3
5	2	3	18.9	17.1	18.0	23.1	5	12	5	-1.0	-1.0	-1.0	17.6	6	8	4	26.2	23.9	30.1	25.4
5	2	4	17.8	16.4	34.0	18.4	5	12	6	-1.0	-1.0	-1.0	-1.0	6	8	5	33.7	30.7	32.5	34.0
5	2	5	15.5	16.4	14.1	14.9	5	13	0	29.9	34.5	-1.0	27.8	6	8	6	16.1	16.5	25.4	17.9
5	2	6	15.0	16.8	15.2	16.1	5	13	1	-1.0	-1.0	-1.0	-1.0	6	8	7	30.9	32.6	35.3	29.6
5	2	7	7.3	5.6	4.7	7.8	5	13	2	-1.0	-1.0	-1.0	-1.0	6	8	8	27.6	25.6	32.3	24.9
5	2	8	41.1	43.7	42.4	40.8	5	13	3	-1.0	-1.0	-1.0	-1.0	6	9	0	5.6	4.1	4.0	6.6
5	2	9	50.9	50.8	52.6	47.8	5	13	4	-1.0	-1.0	-1.0	-1.0	6	9	1	19.3	17.9	4.2	13.1
5	2	10	30.6	32.0	29.8	30.2	5	13	5	-1.0	-1.0	-1.0	-1.0	6	9	2	32.9	31.6	34.3	32.8
5	3	0	36.0	36.8	37.2	32.5	5	14	0	21.0	22.3	-1.0	11.6	6	9	3	36.0	38.4	31.8	41.7
5	3	1	44.3	45.1	27.2	49.4	5	14	1	-1.0	-1.0	-1.0	-1.0	6	9	4	45.7	48.4	47.7	45.6
5	3	2	33.2	30.7	29.1	33.0	5	14	2	-1.0	-1.0	-1.0	-1.0	6	9	5	10.3	11.6	7.4	11.6
5	3	3	45.1	42.9	57.0	45.5	5	14	3	-1.0	-1.0	-1.0	-1.0	6	9	6	14.5	11.7	13.2	12.9
5	3	4	33.9	33.0	34.8	32.8	5	15	0	40.5	-1.0	-1.0	-1.0	6	9	7	12.3	10.2	11.1	10.9
5	3	5	28.9	28.6	32.1	22.3	6	0	0	22.3	22.5	27.2	21.7	6	9	8	37.3	-1.0	41.2	48.2
5	3	6	28.0	21.1	18.0	20.1	6	0	1	43.5	46.3	30.0	49.2	6	10	0	8.5	10.3	3.5	7.8
5	3	7	11.7	14.1	16.6	14.7	6	0	2	36.1	38.8	28.5	45.2	6	10	1	44.5	41.8	48.9	45.6
5	3	8	27.5	27.9	22.1	26.9	6	0	3	46.8	49.1	42.8	45.7	6	10	2	16.1	16.2	22.7	16.9
5	3	9	18.3	18.6	25.4	18.4	6	0	4	22.8	26.2	24.9	25.0	6	10	3	20.3	24.1	28.9	20.7
5	3	10	21.8	23.9	21.3	27.6	6	0	5	23.8	27.1	23.5	19.3	6	10	4	41.1	42.6	47.8	43.0
5	4	0	9.2	6.3	14.1	8.1	6	0	6	21.0	23.3	24.8	24.8	6	10	5	50.1	52.4	52.4	54.0
5	4	1	57.1	61.5	59.8	63.2	6	0	7	19.5	23.4	10.0	25.7	6	10	6	-1.0	-1.0	-1.0	13.6
5	4	2	48.1	48.4	44.6	53.4	6	0	8	25.4	30.4	30.0	24.0	6	10	7	-1.0	-1.0	-1.0	-1.0
5	4	3	59.7	60.8	59.3	66.2	6	0	9	31.3	38.1	38.5	31.9	6	11	0	36.2	37.1	29.5	38.6
5	4	4	22.8	22.1	38.4	23.4	6	0	10	14.7	20.2	23.2	18.6	6	11	1	27.8	25.0	14.1	26.7
5	4	5	33.5	33.5	40.3	27.9	6	1	0	4.4	2.9	6.3	15.7	6	11	2	28.2	27.0	18.3	28.4
5	4	6	17.7	13.7	17.0	15.2	6	1	1	4.4	3.0	9.1	5.7	6	11	3	34.4	31.0	24.3	23.1
5	4	7	36.9	34.9	32.5	33.5	6	1	2	37.5	35.3	62.0	37.4	6	11	4	7.9	-1.0	2.7	9.0
5	4	8	23.7	25.8	30.0	24.6	6	1	3	24.6	23.6	23.5	22.9	6	11	5	24.7	-1.0	-1.0	-1.0
5	4	9	39.8	39.9	43.3	45.0	6	1	4	14.9	15.8	15.9	14.7	6	11	6	-1.0	-1.0	-1.0	20.0
5	4	10	13.1	7.1	5.7	14.6	6	1	5	18.1	19.0	22.4	22.8	6	12	0	51.0	49.1	39.2	48.6
5	5	0	42.3	42.2	52.1	47.6	6	1	6	6.4	4.0	13.4	6.0	6	12	1	43.8	42.0	26.7	40.7
5	5	1	4.9	6.4	15.6	5.3	6	1	7	10.6	11.4	13.9	15.9	6	12	2	57.6	56.7	49.0	46.9
5	5	2	55.7	57.4	53.6	48.5	6	1	8	14.9	17.1	22.1	12.3	6	12	3	37.9	37.9	25.1	32.0
5	5	3	38.9	40.0	45.2	38.8	6	1	9	49.1	51.9	48.2	50.9	6	12	4	43.1	45.0	30.8	41.1
5	5	4	33.7	36.5	44.9	26.8	6	1	10	7.1	4.4	4.3	6.2	6	12	5	24.6	23.7	21.2	20.0
5	5	5	13.1	11.9	19.8	12.4	6	2	0	4.6	9.0	2.8	4.4	6	12	6	-1.0	-1.0	-1.0	-1.0
5	5	6	34.5	33.0	28.0	30.1	6	2	1	36.1	34.0	42.6	38.9	6	13	0	9.7	13.5	2.4	9.8
5	5	7	14.7	15.8	20.2	12.7	6	2	2	38.9	38.6	40.7	44.0	6	13	1	24.9	21.9	13.0	-1.0
5	5	8	12.0	10.2	13.9	8.8	6	2	3	20.7	19.2	3.1	20.6	6	13	2	40.8	35.8	23.4	-1.0
5	5	9	24.5	22.9	22.2	26.9	6	2	4	28.6	30.2	27.6	32.2	6	13	3	-1.0	-1.0	-1.0	-1.0
5	5	10	-1.0	-1.0	37.4	23.2	6	2	5	15.3	16.5	3.2	14.9	6	13	4	-1.0	-1.0	-1.0	-1.0
5	6	0	33.0	35.0	46.1	31.2	6	2	6	32.9	31.8	31.7	36.9	6	14	0	36.3	38.9	-1.0	31.7
5	6	1	33.3	37.8	35.4	30.6	6	2	7	22.0	23.9	29.0	23.4	6	14	1	-1.0	-1.0	-1.0	-1.0
5	6	2	37.9	45.0	35.7	30.7	6	2	8	57.3	55.4	59.1	54.8	6	14	2	-1.0	-1.0	-1.0	-1.0
5	6	3	27.7	28.3	21.8	20.7	6	2	9	37.1	38.9	43.2	36.3	6	14	3	-1.0	-1.0	-1.0	-1.0
5	6	4	43.7	49.6	51.7	39.4	6	2	10	26.3	29.8	27.4	29.1	7	0	0	21.1	24.6	39.6	18.9
5	6	5	22.6	27.0	17.7	20.7	6	3	0	9.1	12.4	4.0	10.4	7	0	1	46.1	54.3	61.2	48.1
5	6	6	27.0	29.7	27.6	24.0	6	3	1	41.2	41.8	46.5	43.5	7	0	2	16.3	20.5	18.2	16.9
5	6	7	40.5	44.8	40.7	38.9	6	3	2	25.2	23.5	43.1	27.7	7	0	3	8.4	13.0	13.1	16.4
5	6	8	33.5	30.1	24.6	31.9	6	3	3	12.1	12.6	5.9	17.6	7	0	4	20.1	24.2	32.1	23.5
5	6	9	6.5	-1.0	11.3	-1.0	6	3	4	37.1	43.2	41.4	44.0	7	0	5	14.7	19.4	19.7	23.0
5	7	0	19.0	17.5	34.0	14.0	6	3	5	31.5	31.1	26.6	28.6	7	0	6	35.6	43.9	40.0	43.7
5	7	1	15.7	14.9	9.7	15.0	6	3	6	56.5	55.9	46.9	55.4	7	0	7	33.4	42.5	41.9	37.1
5	7	2	33.4	30.7	26.1	34.6	6	3	7	51.4	51.6	46.9	51.2	7	0	8	8.6	14.0	21.2	12.5
5	7	3	11.1	12.4	8.6	14.6	6	3	8	50.2	56.9	53.3	56.7	7	0	9	21.2	27.9	23.0	24.9
5	7	4	11.0	14.2	26.8	18.6	6	3	9	47.9	47.4	42.5	49.1	7	0	10	-1.0	23.0	-1.0	-1.0
5	7	5	20.8	19.3	16.8	22.9	6	3	10	38.9	43.1	45.6	41.0	7	1	0	27.1	28.3	34.4	22.9
5	7	6	36.5	26.1	29.6	27.8	6	4	0	10.3	13.6	13.3	7.6	7	1	1	17.0	15.5	25.2	17.3
5	7	7	15.8	15.2	6.9	13.3	6	4	1	44.9	39.6	35.5	41.8	7	1	2	39.6	38.9	42.9	44.4
5	7	8	40.2	38.5	50.5	37.0	6	4	2	17.9	16.9	22.3	18.1	7	1	3	28.4	28.9	17.6	36.6
5	7	9	19.7	19.4	22.5	18.8	6	4	3	18.8	18.5	32.6	21.2	7	1	4	26.4	29.1	31.8	30.2
5	8	0	38.4	34.8	37.4	33.0	6	4	4	34.1	34.3	31.3	32.9	7	1	5	30.8	31.9	41.9	29.6
5	8	1	8.8	4.3	15.7	9.1	6	4	5	27.6	27.8	29.5	34.2	7	1	6	12.8	12.8	14.8	17.1
5	8	2	22.7	20.4	25.3	20.5	6	4	6	16.6	17.2	21.5	15.0	7	1	7	33.3	35.1	35.1	34.9
5	8	3	44.2	38.4	31.9	46.0	6	4	7	37.3	35.9	27.8	30.9	7	1	8	27.8	27.4	25.6	27.0
5	8	4	36.9	33.7	31.1	39.6	6	4	8	55.5	51.9	53.8	51.9	7	1	9	14.9	16.9	7.0	17.6
5	8	5	14.2	11.7	13.8	13.0	6	4	9	44.4	42.6	39.9	41.9	7	1	10	13.8	17.4	18.9	10.7
5	8	6	22.9	20.2	21.3	18.4	6	4	10	19.5	20.6	27.9	21.1	7	2	0	6.4	12.6	-1.0	13.2
5	8	7	30.6	28.4	35.1	31.8	6	5	0	32.4	31.5	24.6	31.6	7	2	1	6.7	-1.0	-1.0	19.2
5	8	8	15.3	10.2	7.8	11.3	6	5	1	21.7	25.9	13.4	24.0	7	2	2	52.3	51.5	44.6	53.6
5	8	9	25.8	-1.0	28.8	27.5	6	5	2	46.3	46.6	50.8	42.1	7	2	3	30.1	30.6	19.9	29.1
5	9	0	51.4	48.0	31.6	49.6	6	5	3	55.5	58.1	62.2	61.0	7	2	4	22.7	23.3	38.5	16.7
5	9	1	3.5	8.9	2.9	7.1	6	5	4	38.9	36.5	37.9	37.6	7	2	5	25.7	28.4	30.1	28.5
5	9	2	19.5	16.9	20.4	16.8	6	5	5	32.4	24.3	37.1	28.9	7	2	6	32.4	32.1	28.0	34.7

H	K	L	NEW NATIVE	OLD NATIVE	PT	HG	H	K	L	NEW NATIVE	OLD NATIVE	PT	HG	H	K	L	NEW NATIVE	OLD NATIVE	PT	HG
7	2	7	32.9	35.3	28.4	33.9	8	0	4	24.8	33.7	23.1	25.5	8	11	5	4.2	-1.0	7.8	5.7
7	2	8	61.6	65.8	67.7	66.0	8	0	5	5.7	7.7	7.0	4.6	8	12	0	11.1	12.4	-1.0	7.8
7	2	9	41.9	45.5	43.3	44.9	8	0	6	42.1	54.9	44.1	45.7	8	12	1	-1.0	-1.0	-1.0	-1.0
7	2	10	15.9	20.4	17.2	21.2	8	0	7	7.9	12.8	17.9	7.3	8	12	2	-1.0	-1.0	-1.0	-1.0
7	3	0	6.2	6.2	2.6	6.4	8	0	8	11.2	16.0	15.5	16.4	8	12	3	-1.0	-1.0	-1.0	-1.0
7	3	1	16.7	14.1	29.0	19.9	8	0	9	37.6	52.4	46.9	49.3	8	12	4	-1.0	-1.0	-1.0	-1.0
7	3	2	39.4	35.0	30.9	40.3	8	1	0	17.0	18.8	21.9	18.8	8	13	0	52.1	58.3	-1.0	49.1
7	3	3	42.4	38.7	40.6	37.5	8	1	1	55.9	56.2	48.4	56.9	8	13	1	-1.0	-1.0	-1.0	-1.0
7	3	4	6.8	6.1	2.9	9.5	8	1	2	24.8	26.7	34.0	35.2	8	13	2	-1.0	-1.0	-1.0	-1.0
7	3	5	22.0	18.4	11.0	13.2	8	1	3	12.2	14.3	21.0	16.2	8	13	3	-1.0	-1.0	-1.0	-1.0
7	3	6	51.6	46.3	46.1	48.3	8	1	4	16.6	16.6	18.2	14.8	9	0	0	4.7	10.6	6.7	8.5
7	3	7	50.6	45.7	58.4	39.9	8	1	5	18.0	18.1	17.7	24.0	9	0	1	16.4	23.2	34.4	17.9
7	3	8	34.7	35.2	30.7	39.7	8	1	6	4.6	4.1	19.7	8.5	9	0	2	15.9	26.1	21.8	19.0
7	3	9	20.3	28.2	29.3	28.7	8	1	7	30.3	33.5	29.0	31.8	9	0	3	19.6	27.6	16.7	24.1
7	4	0	24.6	27.3	36.9	26.0	8	1	8	49.2	56.3	53.3	56.8	9	0	4	29.9	37.3	25.6	23.2
7	4	1	25.3	24.6	29.4	29.3	8	1	9	47.0	52.6	53.2	54.2	9	0	5	19.7	30.6	22.2	36.9
7	4	2	10.6	8.2	10.0	11.0	8	2	0	26.1	23.5	5.6	13.8	9	0	6	16.8	24.4	15.1	17.4
7	4	3	24.0	23.1	20.1	25.8	8	2	1	63.8	64.1	67.9	54.0	9	0	7	17.3	25.4	32.3	23.6
7	4	4	61.1	63.5	44.8	60.0	8	2	2	31.1	30.5	29.6	25.6	9	0	8	42.2	59.4	55.3	51.2
7	4	5	17.8	16.3	19.9	11.6	8	2	3	44.2	44.7	37.5	39.3	9	0	9	21.7	31.5	27.1	16.7
7	4	6	25.0	25.0	26.9	25.2	8	2	4	56.1	57.6	45.8	51.1	9	1	0	23.3	25.9	33.5	31.7
7	4	7	17.7	20.4	16.7	15.8	8	2	5	15.7	17.3	19.7	13.6	9	1	1	13.1	12.8	21.3	14.6
7	4	8	31.3	31.3	39.3	31.5	8	2	6	23.7	23.3	26.8	19.2	9	1	2	25.5	25.3	36.3	26.2
7	4	9	22.4	21.1	25.9	19.6	8	2	7	41.2	39.6	52.5	36.7	9	1	3	28.4	28.4	43.0	32.4
7	5	0	14.4	14.1	3.4	13.0	8	2	8	36.7	38.8	43.7	37.6	9	1	4	45.3	44.2	36.7	40.5
7	5	1	9.3	5.1	3.4	10.1	8	2	9	48.5	51.7	52.2	47.5	9	1	5	12.1	11.3	9.1	14.0
7	5	2	18.7	18.4	27.5	20.2	8	3	0	10.0	7.9	12.8	8.6	9	1	6	9.2	7.4	9.6	12.4
7	5	3	36.7	36.1	30.7	43.9	8	3	1	30.1	29.6	33.2	36.8	9	1	7	16.5	17.8	18.5	21.9
7	5	4	52.9	45.8	64.3	56.6	8	3	2	40.5	40.4	44.1	43.9	9	1	8	32.1	35.4	38.1	31.5
7	5	5	25.6	19.0	23.2	19.7	8	3	3	8.9	8.3	8.1	8.0	9	1	9	31.5	32.2	31.2	32.0
7	5	6	48.4	44.1	40.3	54.0	8	3	4	19.6	18.2	17.3	20.7	9	2	0	40.4	39.0	37.0	36.3
7	5	7	39.6	37.6	31.4	39.1	8	3	5	6.0	8.5	7.3	14.5	9	2	1	9.2	12.9	7.1	10.4
7	5	8	44.8	41.5	41.9	43.3	8	3	6	53.4	49.0	57.7	56.3	9	2	2	28.7	26.4	23.7	27.4
7	5	9	10.4	11.5	4.2	10.9	8	3	7	58.6	52.8	52.6	57.8	9	2	3	6.9	9.0	10.1	8.1
7	6	0	9.1	8.8	8.3	5.0	8	3	8	49.5	41.9	43.8	41.0	9	2	4	9.1	9.0	14.7	7.8
7	6	1	24.9	24.4	19.9	24.8	8	3	9	30.4	30.6	32.2	33.2	9	2	5	9.1	8.8	24.3	10.8
7	6	2	15.7	11.5	14.1	11.6	8	4	0	33.1	28.9	18.6	32.1	9	2	6	22.3	24.2	17.5	20.1
7	6	3	32.0	33.4	27.9	32.3	8	4	1	45.9	43.8	51.9	44.4	9	2	7	27.4	32.2	20.7	22.5
7	6	4	5.0	6.3	39.1	48.9	8	4	2	5.7	4.8	4.4	7.9	9	2	8	14.8	21.7	26.5	19.4
7	6	5	48.1	40.7	40.6	47.2	8	4	3	27.4	24.4	15.4	25.2	9	2	9	40.0	37.9	34.1	37.9
7	6	6	45.0	44.3	54.8	48.0	8	4	4	33.4	32.7	41.0	33.2	9	3	0	22.6	27.8	-1.0	30.1
7	6	7	8.8	7.9	6.1	8.7	8	4	5	19.9	21.7	28.9	19.8	9	3	1	-1.0	-1.0	-1.0	-1.0
7	6	8	26.7	24.6	27.4	28.7	8	4	6	29.6	31.4	33.0	31.1	9	3	2	-1.0	-1.0	-1.0	16.4
7	6	9	23.1	-1.0	23.9	-1.0	8	4	7	15.1	18.1	9.0	19.4	9	3	3	43.5	40.9	32.3	41.1
7	7	0	12.6	8.1	4.7	6.0	8	4	8	14.1	14.0	18.9	11.5	9	3	4	13.8	9.7	10.3	11.7
7	7	1	22.3	22.1	25.5	24.5	8	4	9	41.4	45.2	44.9	46.1	9	3	5	8.2	5.2	4.2	1.0
7	7	2	35.6	35.2	31.6	35.3	8	5	0	28.8	30.9	31.8	29.1	9	3	6	12.3	5.6	9.6	10.4
7	7	3	26.3	24.5	26.6	23.1	8	5	1	26.8	29.1	16.3	24.3	9	3	7	12.9	15.7	13.3	17.8
7	7	4	30.3	27.6	36.4	24.4	8	5	2	10.6	8.3	19.2	9.4	9	3	8	52.1	49.3	51.6	47.4
7	7	5	16.6	16.0	21.4	17.3	8	5	3	25.3	27.6	28.5	27.9	9	3	9	29.4	29.4	31.8	27.0
7	7	6	28.2	28.4	25.7	26.9	8	5	4	57.5	57.4	50.4	53.1	9	4	0	16.7	13.9	23.1	11.9
7	7	7	14.2	7.0	16.5	13.3	8	5	5	41.0	40.2	27.8	40.5	9	4	1	23.8	19.0	15.5	24.3
7	7	8	44.5	40.4	39.1	47.9	8	5	6	32.8	30.5	26.3	27.5	9	4	2	14.4	8.9	8.1	13.0
7	8	0	35.8	36.1	37.3	36.9	8	5	7	33.3	32.6	28.2	31.7	9	4	3	40.1	34.6	40.3	42.2
7	8	1	43.4	44.2	48.6	39.2	8	5	8	23.3	18.7	27.8	20.0	9	4	4	15.0	16.5	18.6	18.7
7	8	2	19.4	17.9	16.9	11.2	8	5	9	48.8	-1.0	53.0	48.4	9	4	5	30.7	30.7	33.8	30.9
7	8	3	34.5	37.2	40.6	39.7	8	6	0	12.3	12.4	3.9	11.3	9	4	6	14.8	14.6	21.3	12.7
7	8	4	14.3	17.0	13.8	9.5	8	6	1	12.8	14.1	6.3	17.6	9	4	7	23.9	21.9	19.7	24.4
7	8	5	29.7	33.4	30.0	35.9	8	6	2	12.3	11.6	9.9	14.1	9	4	8	14.2	12.8	22.4	14.1
7	8	6	28.1	26.2	31.8	27.4	8	6	3	23.9	18.8	27.9	23.9	9	5	0	37.7	41.6	30.7	41.1
7	8	7	39.7	37.8	44.5	32.6	8	6	4	33.1	28.3	38.1	37.2	9	5	1	21.9	22.2	22.4	24.0
7	8	8	4.7	-1.0	-1.0	5.1	8	6	5	50.8	45.9	51.9	55.1	9	5	2	4.4	6.3	15.2	9.9
7	9	0	24.6	25.2	19.5	22.5	8	6	6	21.1	17.6	20.1	18.3	9	5	3	45.8	49.3	47.1	42.1
7	9	1	11.7	17.8	4.3	12.3	8	6	7	11.5	6.1	4.4	8.8	9	5	4	32.7	24.8	30.9	24.8
7	9	2	30.2	33.5	36.3	37.8	8	6	8	25.3	22.4	35.1	26.7	9	5	5	17.1	20.2	21.4	13.3
7	9	3	16.2	19.1	22.5	12.9	8	7	0	59.8	60.8	66.2	70.5	9	5	6	29.3	31.4	25.6	22.7
7	9	4	70.9	77.2	84.4	84.4	8	7	1	26.1	22.3	16.3	24.8	9	5	7	12.6	14.1	-1.0	14.2
7	9	5	4.5	6.3	9.7	6.5	8	7	2	21.2	23.7	17.4	21.9	9	5	8	-1.0	-1.0	-1.0	-1.0
7	9	6	27.3	21.5	24.4	22.9	8	7	3	25.2	25.9	28.8	26.4	9	6	0	46.4	43.4	58.3	50.7
7	9	7	14.5	16.4	20.2	18.6	8	7	4	24.1	24.1	14.9	30.3	9	6	1	31.0	25.6	24.8	26.0
7	9	8	27.2	26.6	29.5	26.1	8	7	5	11.7	8.0	12.5	9.5	9	6	2	23.5	17.6	29.5	19.3
7	10	0	27.2	26.6	29.5	26.1	8	7	6	30.7	32.2	32.4	32.1	9	6	3	44.6	40.3	53.2	44.4
7	10	1	49.4	43.6	49.8	46.2	8	7	7	29.5	28.0	29.1	28.0	9	6	4	69.7	61.6	70.4	64.6
7	10	2	16.7	11.8	23.6	12.7	8	7	8	21.9	-1.0	19.2	16.8	9	6	5	32.7	24.8	36.2	24.6
7	10	3	14.2	16.1	19.4	19.2	8	8	0	16.0	15.7	22.1	6.2	9	6	6	4.2	8.2	14.6	5.8
7	10	4	27.6	27.1	23.1	32.3	8	8	1	10.7	7.3	13.5	6.0	9	6	7	26.1	21.0	24.4	28.4
7	10	5	49.2	48.0	51.4	52.9	8	8	2	31.2	30.2	30.7	29.0	9	6	8	17.9	-1.0	21.6	15.0
7	10	6	31.7	31.6	26.9	37.8	8	8	3	32.0	30.9	34.9	26.5	9	7	0	4.8	6.8	4.2	6.8
7	10	7	26.4	-1.0	36.5	27.5	8	8	4	42.5	42.4	42.6	38.6	9	7	1	52.3	44.2	58.8	59.8
7	11	0	17.4	17.6	-1.0	11.5	8	8	5	30.9	31.0	29.7	29.9	9	7	2	10.0	6.1	15.2	9.6
7	11	1	-1.0	-1.0	-1.0	-1.0	8	8	6	21.2	16.6	23.9	13.7	9	7	3	39.0	34.8	36.7	45.0
7	11	2	-1.0	-1.0	-1.0	-1.0	8	8	7	18.4	17.2	12.4	19.5	9	7	4	45.3	38.9	46.0	47.1
7	11	3	-1.0	-1.0	-1.0	-1.0	8	9	0	22.0	25.0	27.2	19.5	9	7	5	31.8	27.0	28.4	36.4
7	11	4	-1.0	-1.0	-1.0	-1.0	8	9	1	16.4	16.1	17.2	10.1	9	7	6	10.8	12.3	13.7	19.6
7	11	5	-1.0	-1.0	-1.0	-1.0	8	9	2	45.0	49.6	47.7	41.8	9	7	7	16.4	14.3	23.1	12.6
7	11	6	-1.0	-1.0	-1.0	-1.0	8	9	3	17.3	11.3	13.1	19.3	9	8	0	15.1	17.0	14.1	20.4
7	12	0	37.1	35.2	41.8	31.6	8	9	4	35.1	42.9	43.3	35.0	9	8	1	7.4	8.0	6.2	8.5
7	12	1	33.6	35.6	37.0	-1.0	8	9	5	26.9	27.0	23.2	22.3	9	8	2	16.6	12.5	21.4	20.9
7	12	2	49.9	51.4	-1.0	-1.0	8	9	6	30.0	31.4	34.6	29.7	9	8	3	36.4	35.9	42.7	42.1
7	12	3	-1.0	-1.0	-1.0	-1.0	8	9	7	19.9	-1.0	-1.0	-1.0	9	8	4	36.7	37.0	42.4	41.9
7	12	4	-1.0	-1.0	-1.0	-1.0	8	10	0	33.2	30.7	39.0	33.2	9	8	5	35.7	33.4	40.4	35.8
7	12	5	-1.0	-1.0	-1.0	-1.0	8	10	1	33.2	32.8	33.6	34.4	9	8	6	36.2	34.7	40.1	44.7
7	13	0	10.6	13.5	-1.0	12.7	8	10	2	18.7	14.8	23.0	16.5	9	8	7	-1.0	-1.0	5.2	-1.0
7	13	1	-1.0	-1.0	-1.0	-1.0	8	10	3	63.9	56.9	67.0	69.0	9	9	0	19.4	17.2	19.7	12.5
7	13	2	-1.0	-1.0	-1.0	-1.0	8	10	4	20.1	20.9	18.8	23.3	9	9	1	32.5	34.3	34.5	28.4
7	13	3	-1.0	-1.0	-1.0	-1.0	8	10	5	34.0	30.4	39.2	31.1	9	9	2	23.8	23.1	19.8	18.4
7	13	4	-1.0	-1.0	-1.0	-1.0	8	10	6	18.0	16.4	21.4	19.8	9	9	3	42.6	41.2	45.9	34.4
7	14	0	5.4	-1.0	-1.0	-1.0	8	11	0	18.0	17.4	24.8	17.5	9	9	4	33.7	33.5	33.4	27.0
7	14	1	-1.0	-1.0	-1.0	-1.0	8	11	1	19.7	12.9	17.1	17.0	9	9	5	16.6	26.9	29.4	26.0
8	0	0	35.8	38.2	27.2	44.3	8	11	2	27.3	26.0	28.1	32.4	9	9	6	25.2	10.5	14.7	12.6
8	0	1	10.1	14.8	9.7	8.5	8	11	3	43.0	45.6	45.6	49.4	9	10	0	19.9	19.5	17.4	17.9
8	0	2	5.8	9.7	18.0	10.3	8	11	4	29.8	24.4	31.6	29.4	9	10	1	14.7	20.9	16.4	12.0
8	0	3	10.7	16.1	24.0	10.6														

H	K	L	NEW NATIVE	OLD NATIVE	PT	HG	H	K	L	NEW NATIVE	OLD NATIVE	PT	HG	H	K	L	NEW NATIVE	OLD NATIVE	PT	HG
9	10	2	11.2	7.9	9.5	7.8	10	10	4	29.4	26.5	26.8	20.1	12	1	2	28.1	29.4	28.2	24.6
9	10	3	29.9	39.5	33.1	26.1	10	10	5	15.5	-1.0	-1.0	-1.0	12	1	3	30.8	32.1	23.6	34.3
9	10	4	31.5	35.2	29.9	30.3	10	11	0	24.9	23.8	14.4	24.2	12	1	4	33.8	35.3	37.2	33.2
9	10	5	9.7	7.0	11.5	-1.0	10	11	1	33.4	42.8	36.6	27.7	12	1	5	10.9	12.6	18.4	8.7
9	11	0	5.4	6.1	4.4	9.9	10	11	2	28.7	30.5	28.1	-1.0	12	1	6	42.7	47.6	40.3	42.9
9	11	1	16.0	14.9	8.6	14.3	10	11	3	21.6	-1.0	-1.0	-1.0	12	1	7	6.4	4.4	4.3	6.1
9	11	2	25.3	20.9	26.9	20.6	10	12	0	50.5	45.9	54.6	50.8	12	2	0	22.9	25.4	38.4	23.7
9	11	3	24.2	21.4	22.0	25.9	10	12	1	14.4	5.4	15.4	10.7	12	2	1	21.9	22.5	20.0	16.5
9	11	4	23.2	21.6	24.1	22.9	11	0	0	18.4	25.2	20.7	21.7	12	2	2	29.5	28.9	35.2	24.7
9	11	5	9.1	-1.0	-1.0	8.9	11	0	1	21.2	31.7	39.2	22.6	12	2	3	17.5	19.0	23.5	16.7
9	12	0	5.1	7.0	4.8	5.7	11	0	2	7.5	14.8	13.2	10.3	12	2	4	13.0	16.4	24.2	8.7
9	12	1	10.2	4.5	7.8	5.8	11	0	3	16.7	23.4	13.3	15.2	12	2	5	55.9	55.8	49.8	52.6
9	12	2	27.7	24.3	26.2	29.7	11	0	4	4.4	7.0	7.1	4.5	12	2	6	30.5	32.7	25.3	33.0
9	12	3	17.3	-1.0	19.2	8.7	11	0	5	9.5	17.5	7.1	12.4	12	2	7	25.3	25.5	20.9	24.4
9	13	0	-1.0	-1.0	-1.0	-1.0	11	0	6	23.1	34.0	34.8	24.9	12	3	0	30.1	32.3	24.9	27.2
10	0	0	11.4	12.3	6.8	8.8	11	0	7	19.2	34.7	33.1	22.9	12	3	1	32.8	28.6	19.8	27.3
10	0	1	28.9	40.9	35.1	38.6	11	0	8	-1.0	42.5	41.0	-1.0	12	3	2	18.3	-1.0	18.2	21.3
10	0	2	13.6	20.9	26.7	14.8	11	1	0	14.5	15.2	28.9	6.5	12	3	3	30.0	26.2	29.5	24.2
10	0	3	6.1	11.3	15.4	13.2	11	1	1	21.0	24.6	22.4	28.2	12	3	4	72.7	69.2	65.6	63.4
10	0	4	4.5	3.9	18.7	4.5	11	1	2	14.4	14.4	26.5	14.0	12	3	5	30.9	28.4	21.3	25.0
10	0	5	22.4	33.6	28.4	24.0	11	1	3	13.4	13.7	14.5	14.6	12	3	6	31.9	31.3	20.5	32.2
10	0	6	23.8	33.0	26.1	28.7	11	1	4	22.2	24.7	17.7	19.1	12	3	7	36.4	39.0	29.7	33.2
10	0	7	14.0	24.6	19.0	17.0	11	1	5	18.5	20.8	24.3	25.0	12	4	0	29.8	31.2	13.5	29.7
10	0	8	27.7	42.1	38.4	30.1	11	1	6	18.9	22.5	24.1	23.2	12	4	1	22.9	23.0	18.0	19.7
10	1	0	4.8	5.7	8.5	6.0	11	1	7	8.0	6.9	12.0	6.2	12	4	2	35.4	37.5	33.6	36.1
10	1	1	25.4	26.2	10.4	27.1	11	1	8	6.9	6.9	11.9	6.1	12	4	3	24.4	27.0	27.4	31.3
10	1	2	28.1	28.8	26.2	31.4	11	2	0	9.5	15.3	13.2	11.1	12	4	4	16.6	19.7	5.0	12.9
10	1	3	30.3	29.1	33.3	35.2	11	2	1	5.1	6.1	11.4	7.9	12	4	5	36.0	38.4	43.9	39.6
10	1	4	36.3	35.7	41.0	36.5	11	2	2	14.4	15.1	14.0	19.7	12	4	6	21.2	22.8	17.5	21.8
10	1	5	12.4	9.4	6.5	13.5	11	2	3	57.9	57.5	40.0	58.4	12	5	0	29.5	29.5	28.4	34.7
10	1	6	26.5	27.4	29.1	21.3	11	2	4	5.4	6.5	8.0	5.9	12	5	1	35.7	29.7	32.9	36.0
10	1	7	26.9	25.6	27.0	27.1	11	2	5	15.1	18.9	22.2	20.3	12	5	2	71.7	58.7	96.6	72.0
10	1	8	14.8	15.2	23.1	6.1	11	2	6	33.9	32.9	35.0	29.8	12	5	3	30.5	28.3	34.0	32.0
10	2	0	11.5	13.0	25.4	5.7	11	2	7	5.6	7.0	3.9	6.3	12	5	4	30.2	-1.0	22.0	-1.0
10	2	1	6.7	5.7	10.8	5.3	11	2	8	15.9	17.6	20.0	15.8	12	5	5	-1.0	-1.0	-1.0	24.9
10	2	2	5.0	9.0	3.1	5.9	11	3	0	17.2	17.9	21.7	23.2	12	5	6	-1.0	-1.0	-1.0	-1.0
10	2	3	31.3	28.2	30.0	27.0	11	3	1	39.2	39.5	33.6	36.5	12	6	0	31.8	31.0	14.3	29.5
10	2	4	16.3	19.7	3.4	11.5	11	3	2	17.2	16.6	25.7	16.3	12	6	1	23.3	-1.0	17.0	13.6
10	2	5	13.6	13.0	14.0	13.4	11	3	3	22.1	21.6	14.0	21.0	12	6	2	41.8	45.5	47.0	45.0
10	2	6	19.8	21.6	25.7	20.4	11	3	4	42.0	36.6	30.9	34.0	12	6	3	10.1	10.5	8.2	8.3
10	2	7	11.2	8.5	16.1	11.0	11	3	5	21.6	20.9	16.0	20.4	12	6	4	15.6	16.5	12.0	15.6
10	2	8	29.6	31.3	22.6	30.1	11	3	6	13.1	19.2	21.9	23.5	12	6	5	29.4	-1.0	31.8	27.6
10	3	0	6.1	4.4	3.6	5.5	11	3	7	10.3	6.3	5.3	6.9	12	6	6	-1.0	-1.0	-1.0	-1.0
10	3	1	4.9	4.5	17.7	8.6	11	4	0	5.1	4.4	-1.0	4.8	12	7	0	4.4	7.8	-1.0	6.0
10	3	2	37.2	24.0	25.0	37.8	11	4	1	22.0	22.4	-1.0	15.1	12	7	1	43.5	40.6	-1.0	-1.0
10	3	3	40.6	40.6	36.4	39.7	11	4	2	45.5	57.6	62.7	49.4	12	7	2	29.8	-1.0	-1.0	-1.0
10	3	4	33.7	31.2	33.9	31.0	11	4	3	19.9	19.1	17.1	21.6	12	7	3	-1.0	-1.0	-1.0	-1.0
10	3	5	31.0	29.5	32.7	24.6	11	4	4	34.2	33.1	34.9	34.1	12	7	4	-1.0	-1.0	-1.0	-1.0
10	3	6	16.0	15.5	15.3	12.9	11	4	5	36.6	37.4	35.8	41.3	12	7	5	-1.0	-1.0	-1.0	-1.0
10	3	7	16.7	19.4	8.0	12.8	11	4	6	32.6	34.9	28.6	37.0	12	8	0	37.8	39.4	-1.0	21.6
10	3	8	47.2	45.4	43.6	42.8	11	4	7	8.3	7.4	8.9	17.4	12	8	1	-1.0	-1.0	-1.0	-1.0
10	4	0	4.9	36.4	23.1	37.1	11	5	0	34.0	31.0	24.3	33.2	12	8	2	-1.0	-1.0	-1.0	-1.0
10	4	1	27.0	26.3	29.8	34.2	11	5	1	35.0	31.8	32.8	40.8	12	8	3	-1.0	-1.0	-1.0	-1.0
10	4	2	16.3	20.1	18.4	22.5	11	5	2	6.6	6.4	15.9	5.3	12	8	4	-1.0	-1.0	-1.0	-1.0
10	4	3	24.1	28.1	20.5	21.1	11	5	3	15.8	16.1	19.2	20.0	12	9	0	36.1	39.5	44.0	39.4
10	4	4	27.3	25.3	38.6	24.6	11	5	4	44.9	35.1	36.6	42.8	12	9	1	5.9	4.9	4.8	8.1
10	4	5	27.4	26.2	26.4	24.3	11	5	5	30.0	28.6	27.8	30.3	12	9	2	15.5	6.7	14.8	12.8
10	4	6	23.9	19.5	24.0	16.6	11	5	6	-1.0	-1.0	-1.0	-1.0	12	9	3	60.6	-1.0	53.2	57.2
10	4	7	16.0	16.8	13.0	14.4	11	5	7	-1.0	-1.0	-1.0	-1.0	12	10	0	24.5	23.4	-1.0	29.3
10	4	8	26.3	25.3	26.0	26.5	11	6	0	59.8	63.4	52.8	60.1	12	10	1	24.1	20.1	-1.0	27.1
10	5	0	12.8	13.7	17.6	15.3	11	6	1	30.2	32.3	18.7	30.4	13	0	0	8.3	3.9	11.1	9.3
10	5	1	33.2	34.1	41.6	30.6	11	6	2	21.7	26.1	15.8	22.3	13	0	1	16.6	25.3	29.7	23.3
10	5	2	9.9	12.4	13.5	14.1	11	6	3	18.7	19.7	22.8	20.9	13	0	2	14.9	22.0	16.5	13.5
10	5	3	15.1	13.3	12.2	16.3	11	6	4	40.1	41.3	34.3	36.6	13	0	3	20.2	34.4	16.3	20.2
10	5	4	14.5	16.9	17.2	17.1	11	6	5	52.6	55.3	49.7	49.8	13	0	4	19.9	32.4	27.9	24.6
10	5	5	39.8	42.7	48.1	47.3	11	6	6	-1.0	-1.0	-1.0	17.7	13	0	5	18.8	31.0	31.9	20.6
10	5	6	25.0	31.6	28.6	30.5	11	7	0	37.2	34.2	-1.0	31.1	13	0	6	14.5	25.4	20.7	-1.0
10	5	7	32.9	43.0	35.2	42.5	11	7	1	-1.0	-1.0	-1.0	-1.0	13	1	0	8.0	4.3	4.2	6.2
10	5	8	-1.0	-1.0	-1.0	-1.0	11	7	2	-1.0	-1.0	-1.0	-1.0	13	1	1	24.0	25.8	23.5	29.8
10	6	0	33.6	32.1	21.7	27.0	11	7	3	-1.0	-1.0	-1.0	-1.0	13	1	2	18.8	19.9	32.3	19.8
10	6	1	33.0	27.9	24.9	32.8	11	7	4	-1.0	-1.0	-1.0	-1.0	13	1	3	21.9	26.2	28.2	18.5
10	6	2	16.5	18.1	13.0	8.7	11	7	5	-1.0	-1.0	-1.0	-1.0	13	1	4	9.7	6.9	10.6	6.2
10	6	3	54.2	49.5	44.5	42.8	11	7	6	-1.0	-1.0	-1.0	-1.0	13	1	5	21.2	25.1	29.8	24.8
10	6	4	28.2	32.6	30.6	29.3	11	8	0	13.0	8.4	11.3	5.9	13	1	6	18.2	20.5	23.8	17.4
10	6	5	18.9	13.4	3.4	8.8	11	8	1	42.2	32.3	43.2	34.6	13	2	0	37.2	38.5	27.7	29.3
10	6	6	-1.0	-1.0	-1.0	48.1	11	8	2	15.8	12.8	13.3	17.1	13	2	1	27.2	27.6	33.5	24.7
10	6	7	-1.0	-1.0	-1.0	-1.0	11	8	3	24.4	18.7	20.8	20.7	13	2	2	15.5	17.0	17.0	15.2
10	7	0	8.8	8.1	4.6	15.9	11	8	4	41.0	34.9	38.2	38.8	13	2	3	7.8	6.8	21.6	13.7
10	7	1	31.1	23.3	21.3	24.0	11	8	5	37.0	27.6	31.9	27.9	13	2	4	15.7	19.5	25.2	12.5
10	7	2	17.4	12.9	14.9	13.4	11	9	0	18.6	19.9	22.5	23.2	13	2	5	63.7	63.9	58.9	57.2
10	7	3	59.4	49.5	54.9	53.1	11	9	1	13.5	8.6	10.5	15.4	13	2	6	57.4	58.0	54.2	56.0
10	7	4	55.8	47.0	48.8	51.6	11	9	2	35.3	29.6	37.2	39.6	13	3	0	23.0	23.4	13.1	19.5
10	7	5	25.6	19.4	22.0	24.9	11	9	3	30.9	26.7	33.5	36.4	13	3	1	16.6	13.0	15.5	12.2
10	7	6	24.9	21.7	22.1	26.7	11	9	4	17.9	12.8	22.8	14.2	13	3	2	38.7	35.9	23.3	31.7
10	7	7	8.2	-1.0	4.8	5.6	11	9	5	24.2	-1.0	-1.0	24.3	13	3	3	38.6	36.8	32.7	36.6
10	8	0	48.6	45.8	41.9	53.8	11	10	0	6.1	7.1	8.0	4.6	13	3	4	32.9	28.1	31.7	26.1
10	8	1	12.3	8.7	16.9	14.0	11	10	1	12.7	15.0	11.3	16.4	13	3	5	18.8	15.4	15.7	16.9
10	8	2	30.5	24.2	30.9	32.8	11	10	2	30.6	27.7	34.0	38.4	13	3	6	29.5	29.1	19.0	24.4
10	8	3	36.3	32.1	33.8	44.2	11	10	3	-1.0	13.9	13.6	14.3	13	4	0	30.9	34.1	39.2	26.4
10	8	4	17.2	12.3	21.1	24.9	11	11	0	22.9	-1.0	26.0	15.1	13	4	1	39.3	39.6	41.4	40.9
10	8	5	37.9	34.1	47.2	40.5	11	11	1	25.0	-1.0	23.2	23.2	13	4	2	25.1	23.3	23.5	25.7
10	8	6	15.6	13.5	4.1	16.8	11	11	2	15.3	-1.0	-1.0	12.6	13	4	3	48.6	47.4	41.2	48.7
10	9	0	13.2	14.3	21.8	11.1	12	0	0	9.6	14.3	24.8	9.7	13	4	4	30.6	30.2	34.5	33.7
10	9	1	21.9	25.6	26.1	25.9	12	0	1	20.8	32.3	29.5	22.8	13	4	5	39.0	40.9	35.3	41.8
10	9	2	29.5	28.0	33.8	34.7	12	0	2	38.6	57.8	51.3	51.4	13	5	0	69.4	72.7	-1.0	67.0
10	9	3	15.5	15.5	14.8	17.5	12	0	3	5.6	11.0	7.0	14.9	13	5	1	-1.0	-1.0	-1.0	-1.0
10	9	4	27.5	30.7	25.4	31.8	12	0	4	5.8	11.5	7.1	11.9	13	5	2	-1.0	-1.0	-1.0	-1.0
10	9	5	30.7	31.3	38.8	39.7	12	0	5	19.4	34.2	31.1	28.7	13	5	3	-1.0	-1.0	-1.0	-1.0
10	10	0	29.7	28.5	27.0	24.7	12	0	6	25.4	41.1	29.0	33.0	13	5	4	-1.0	-1.0	-1.0	-1.0
10	10	1	16.6	15.9	13.9	16.3	12	0	7	22.5	35.4	30.8	-1.0	13	5	5	-1.0	-1.0	-1.0	-1.0
10	10	2	43.1	45.0	44.0	32.7	12	1	0	5.8	4.2	4.3	6.1	13	6	0	25.5	26.2	18.9	20.9
10	10	3	30.3	28.6	24.6	20.3	12	1	1	38.8	41.0	50.6	40.9	13	6	1	10.1	-1.0	12.3	-1.0

H	K	L	NEW NATIVE	OLD NATIVE	PT	HG	H	K	L	NEW NATIVE	OLD NATIVE	PT	HG	H	K	L	NEW NATIVE	OLD NATIVE	PT	HG
13	6	2	-1.0	-1.0	32.6	-1.0	14	1	5	25.0	29.5	29.6	25.8	14	6	3	-1.0	-1.0	-1.0	-1.0
13	6	3	-1.0	-1.0	-1.0	-1.0	14	2	0	27.5	29.7	19.4	21.7	14	7	0	17.7	-1.0	-1.0	-1.0
13	6	4	-1.0	-1.0	-1.0	-1.0	14	2	1	23.8	23.8	16.8	21.6	14	7	1	-1.0	-1.0	-1.0	-1.0
13	7	0	12.5	15.2	-1.0	5.6	14	2	2	5.6	6.9	6.0	8.9	15	0	0	10.8	15.6	18.9	10.5
13	7	1	-1.0	-1.0	-1.0	-1.0	14	2	3	38.6	38.7	33.2	34.1	15	0	1	23.2	41.9	35.1	34.6
13	7	2	-1.0	-1.0	-1.0	-1.0	14	2	4	27.2	27.0	34.4	22.6	15	0	2	4.6	9.0	9.4	8.0
13	7	3	-1.0	-1.0	-1.0	-1.0	14	2	5	52.6	54.1	43.5	47.3	15	0	3	-1.0	5.6	5.8	-1.0
13	7	4	-1.0	-1.0	-1.0	-1.0	14	3	0	9.2	6.1	5.1	11.6	15	1	0	8.0	4.4	4.4	6.9
13	8	0	4.1	6.4	-1.0	5.3	14	3	1	13.0	14.4	10.1	13.4	15	1	1	17.4	17.4	25.4	16.6
13	8	1	-1.0	-1.0	-1.0	-1.0	14	3	2	49.9	43.3	46.2	40.3	15	1	2	32.4	36.6	31.0	31.4
13	8	2	-1.0	-1.0	-1.0	-1.0	14	3	3	20.5	18.8	8.1	16.2	15	1	3	12.1	13.7	17.1	13.7
13	8	3	-1.0	-1.0	-1.0	-1.0	14	3	4	25.9	26.5	17.2	23.1	15	2	0	12.1	7.0	20.6	6.3
13	9	0	-1.0	-1.0	-1.0	-1.0	14	4	0	7.9	14.0	11.8	6.5	15	2	1	28.5	25.9	29.8	24.6
14	0	0	23.2	31.2	31.6	25.2	14	4	1	20.5	20.0	18.1	22.0	15	2	2	36.4	37.5	37.6	32.1
14	0	1	15.4	24.8	17.5	23.3	14	4	2	26.5	25.8	39.1	30.9	15	2	3	22.6	22.1	26.6	23.2
14	0	2	22.4	37.1	31.3	28.9	14	4	3	26.0	25.8	23.0	26.4	15	3	0	10.9	15.4	14.4	14.7
14	0	3	30.7	20.2	12.8	19.6	14	4	4	23.3	23.1	26.6	26.0	15	3	1	32.2	33.1	31.9	32.9
14	0	4	27.0	37.8	22.5	28.3	14	5	0	4.3	5.6	-1.0	5.5	15	3	2	26.7	25.8	22.8	24.1
14	0	5	-1.0	29.4	-1.0	-1.0	14	5	1	-1.0	-1.0	-1.0	-1.0	15	4	0	24.5	27.4	34.5	30.6
14	1	0	16.0	16.8	22.2	16.1	14	5	2	-1.0	-1.0	-1.0	-1.0	15	4	1	19.5	17.8	17.3	17.3
14	1	1	11.7	4.3	14.0	11.1	14	5	3	-1.0	-1.0	-1.0	-1.0	15	4	2	20.1	20.9	18.9	17.1
14	1	2	26.5	27.6	17.9	20.2	14	6	0	24.0	27.6	-1.0	19.6	15	5	0	21.9	-1.0	-1.0	-1.0
14	1	3	16.4	18.2	21.4	18.6	14	6	1	-1.0	-1.0	-1.0	-1.0	56	56	56	-0.0	-0.0	-0.0	-0.0
14	1	4	19.6	25.1	20.9	25.9	14	6	2	-1.0	-1.0	-1.0	-1.0	56	56	56	-0.0	-0.0	-0.0	-0.0

APPENDIX IV

PLATINUM DERIVATIVE $(\Delta F)^2$ PATTERSON MAP

The following Patterson map was calculated on the basis of the new native data set and the platinum derivative data set. The contour interval was taken at 50 beginning at a contour level of 50. One eighth of the cell is shown: x from 0.0 to 0.5, y from 0.0 to 0.5, and z from 0.0 to 0.5.

In the space group $P4_1$, the following arrangement of Patterson peaks occurs for a single site derivative:

x'	y'	z'	x'	y'	z'	x'	y'	z'
2x	2y	½	(x+y)	(y-x)	-¼	(x+y)	(y-x)	¼
-2y	2x	½	-(y-x)	(x+y)	-¼	-(y-x)	(x+y)	¼
-2x	-2y	½	-(x+y)	-(y-x)	-¼	-(x+y)	-(y-x)	¼
2y	-2x	½	(y-x)	-(x+y)	-¼	(y-x)	-(x+y)	¼

where: x, y, z is the position of one of the four symmetry related platinum atoms in the cell. For a single derivative, the z coordinate is arbitrary and has been assigned a value of 0.0 for the platinum derivative.

Two peaks at (0.75/48, 20.25/48, 12/48) and (21/48, 19.5/48, 24/48) are present in the octant of the unit cell shown here, leading to a platinum position of (0.219, 0.203, 0.000).

This is an example of an exceptionally clean Patterson map.

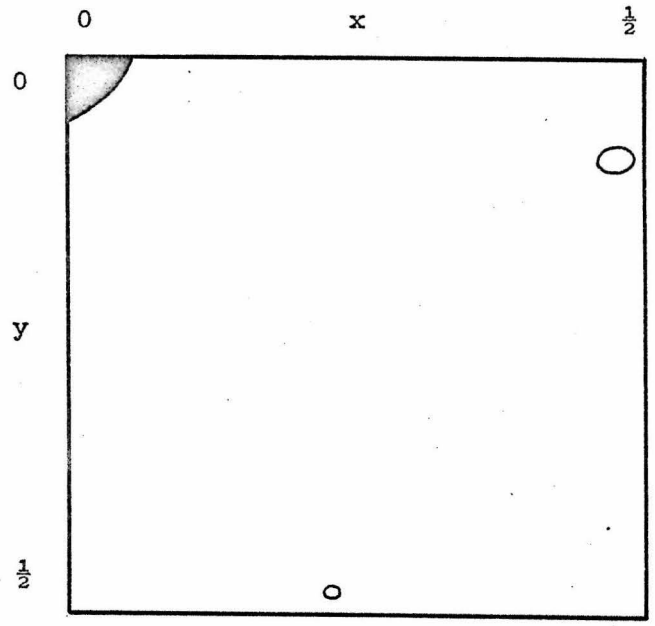

z= 0/48

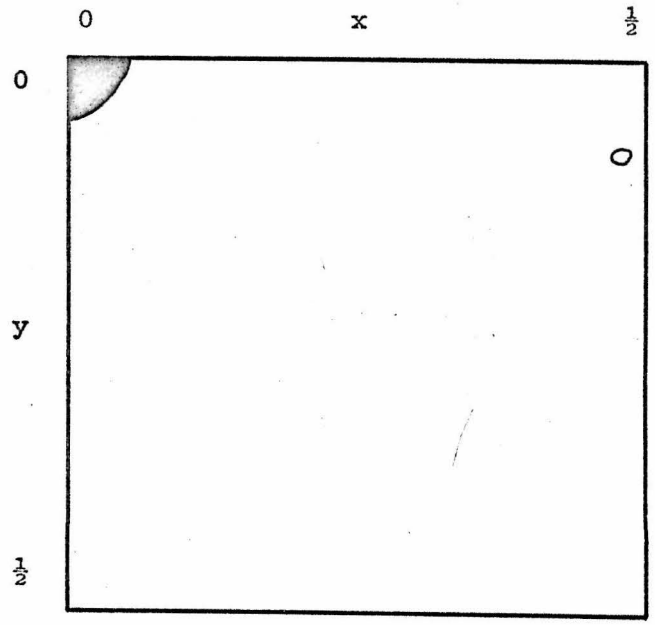

z= 1/48

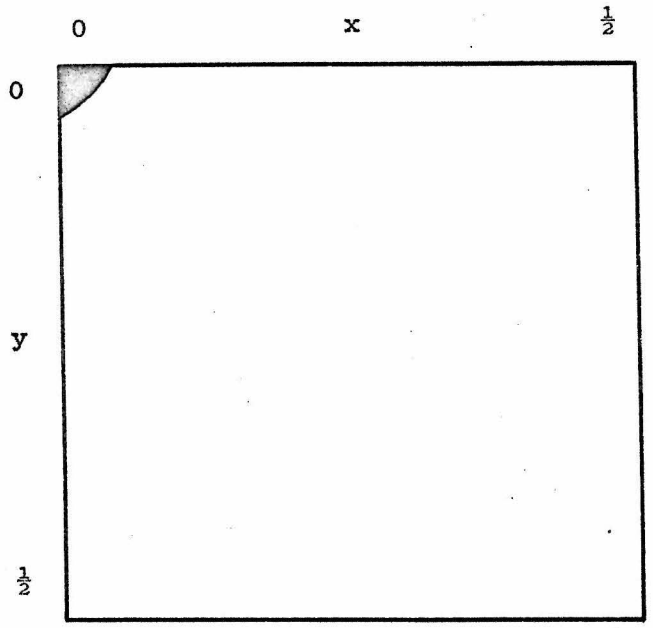

z= 2/48

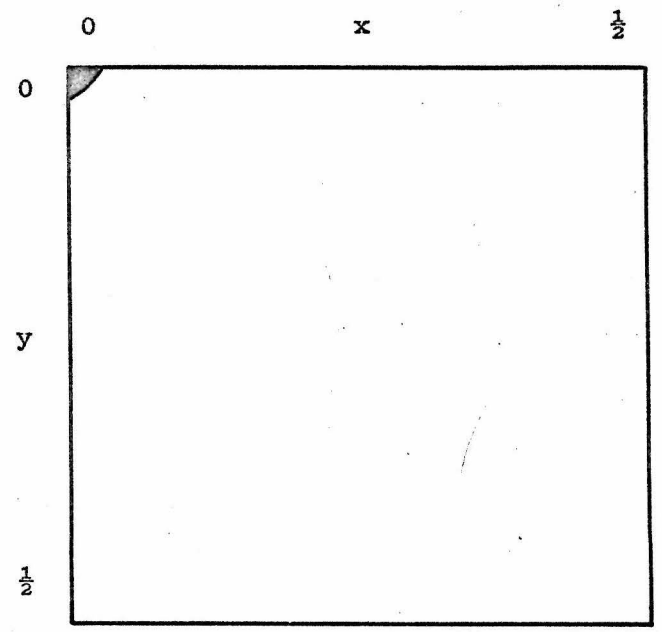

z= 3/48

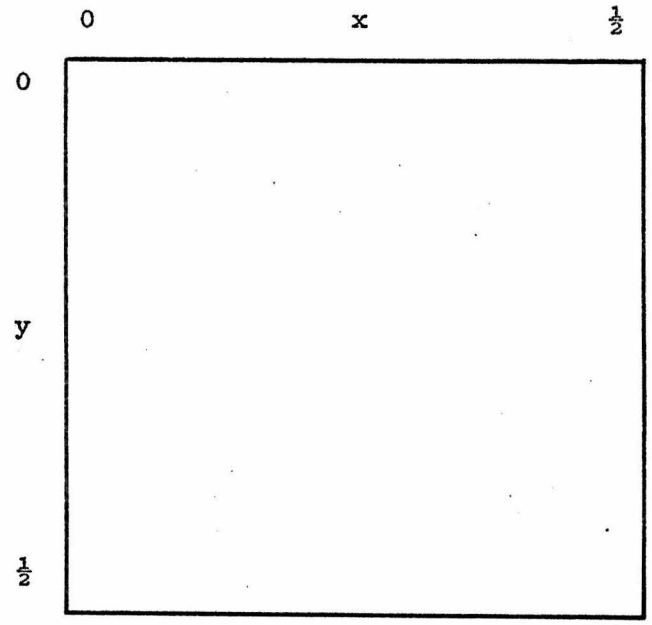

z= 4/48 to 9/48

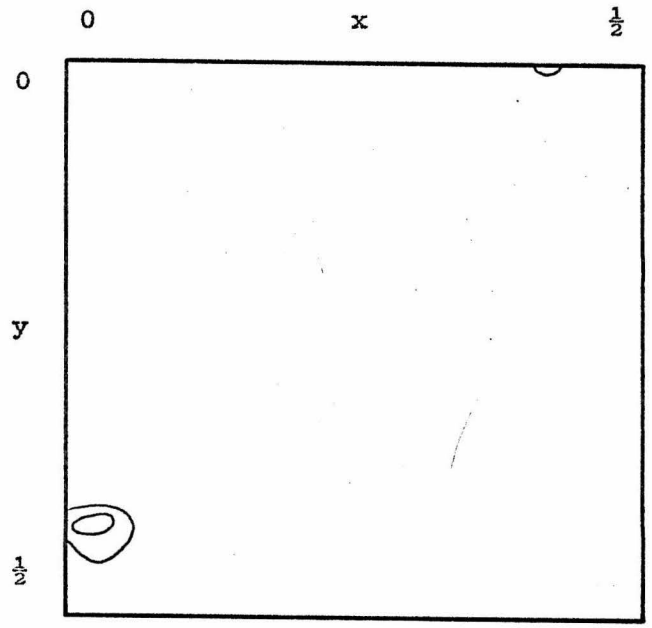

z= 10/48

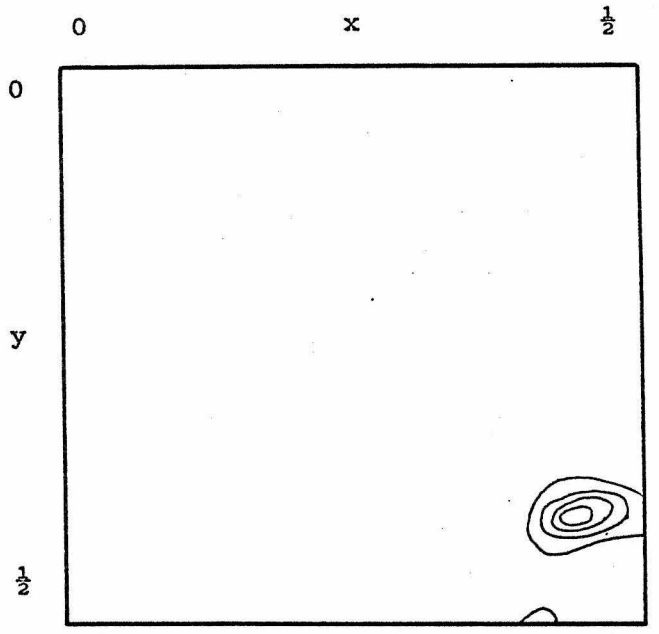

z= 23/48

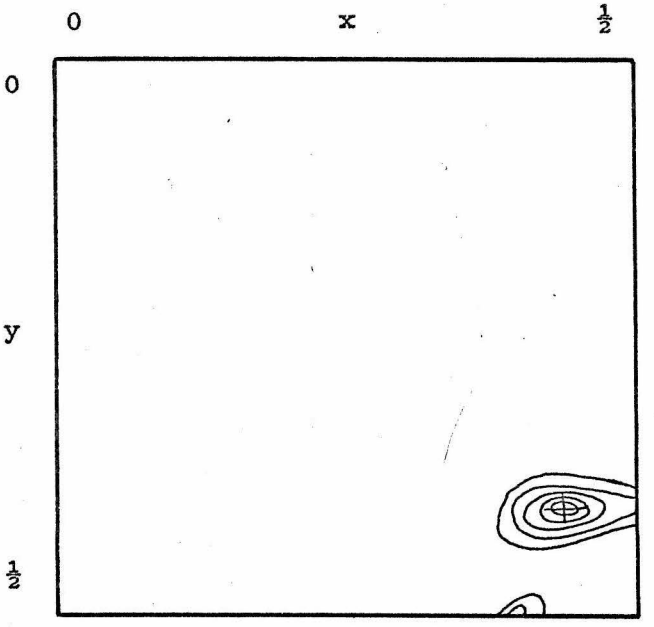

z= 24/48

+ = Single Weight Peak

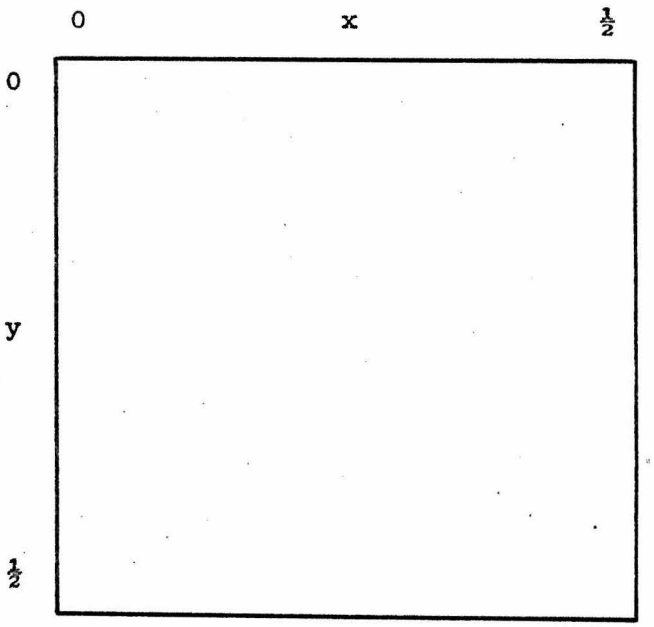

z= 15/48 to 21/48

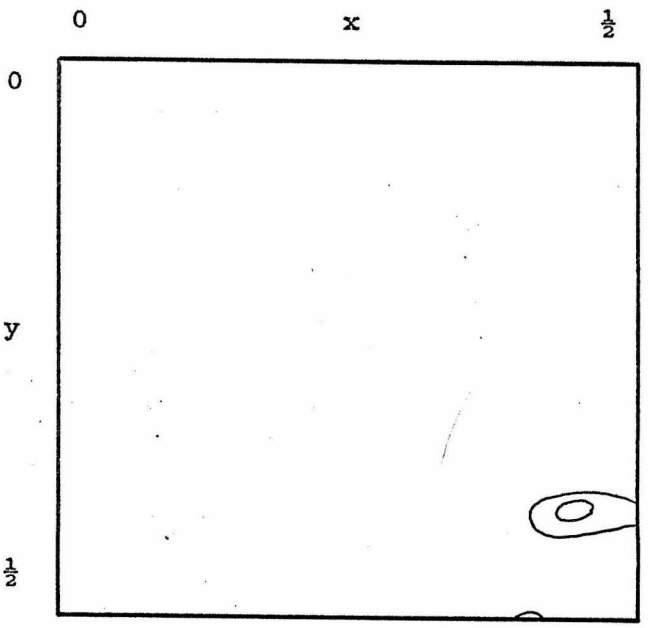

z= 22/48

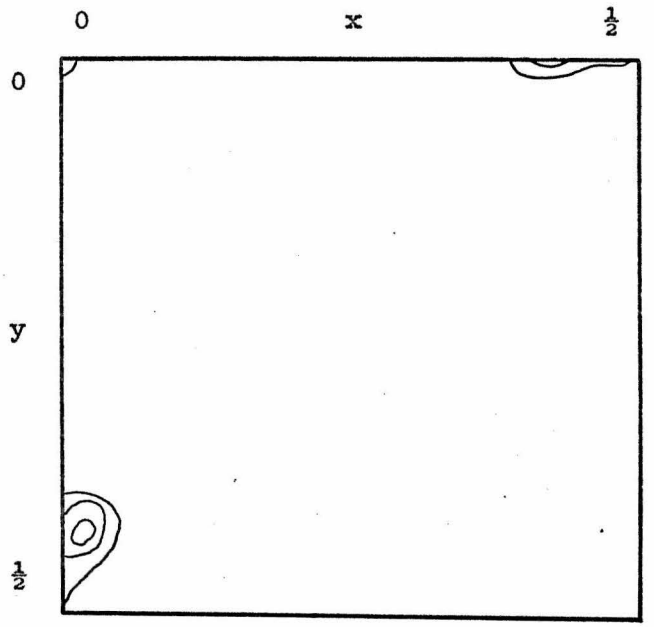

z= 13/48

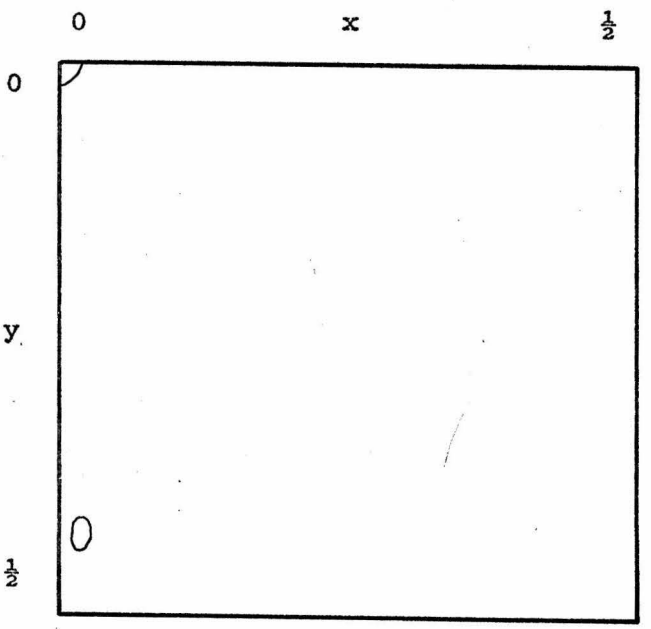

z= 14/48

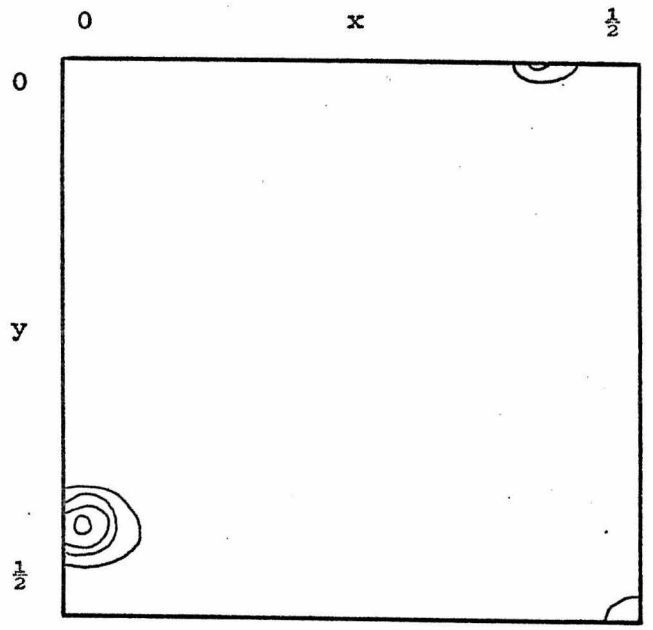

z= 11/48

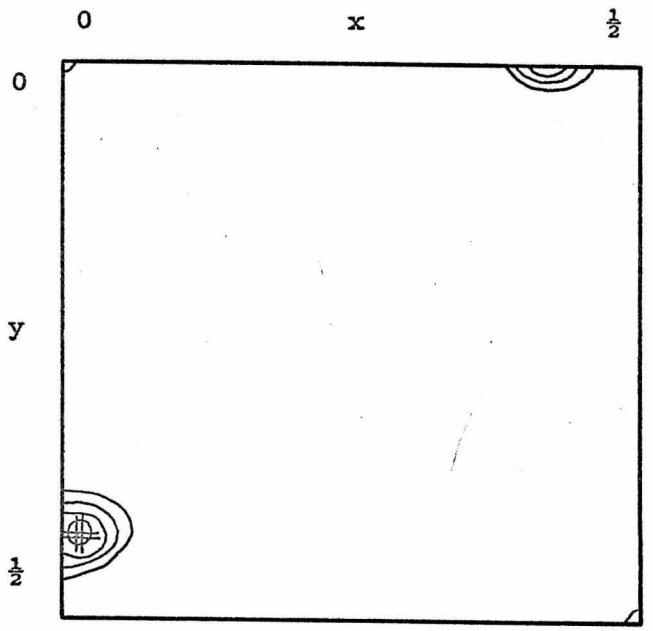

z= 12/48

= Double Weight Peak

APPENDIX V

MERCURY DERIVATIVE $(\Delta F)^2$ PATTERSON MAP

The following Patterson map was calculated on the basis of the new native data set and the mercury derivative data set. The contour interval was taken at 20 beginning at a contour height of 20. One eighth of the cell is shown: x from 0.0 to 0.5, y from 0.0 to 0.5, and z from 0.0 to 0.5.

The noise level in this map is extremely high. The double and single weight peak positions correspond well to those found in the two dimensional work, however. These are marked on their corresponding sections and occur at: D = (20/48, 18/48, 12/48) and S = (10/48, 2/48, 24/48). This corresponds to a mercury atom position of (0.021, 0.396, z), where z represents the displacement from the Pt atom in the c direction.

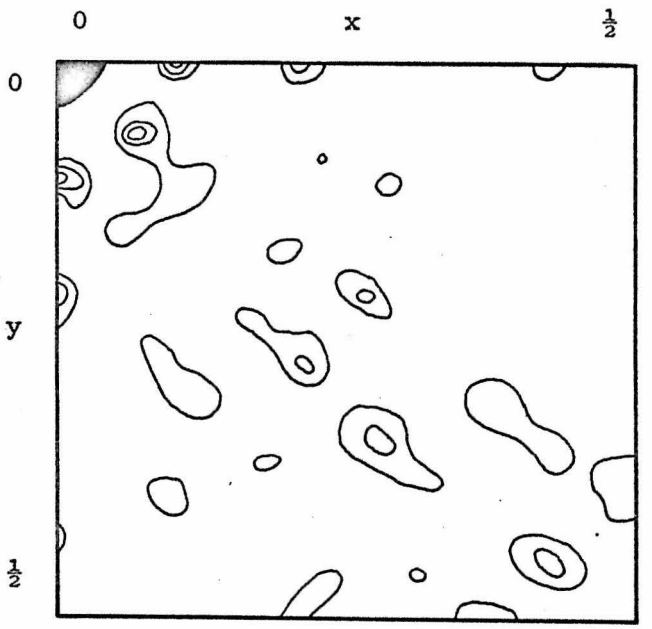

z= 0/48

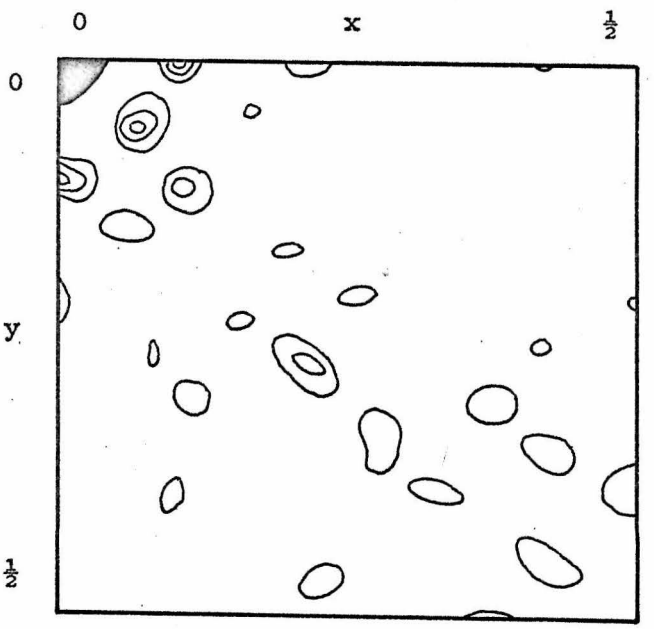

z= 1/48

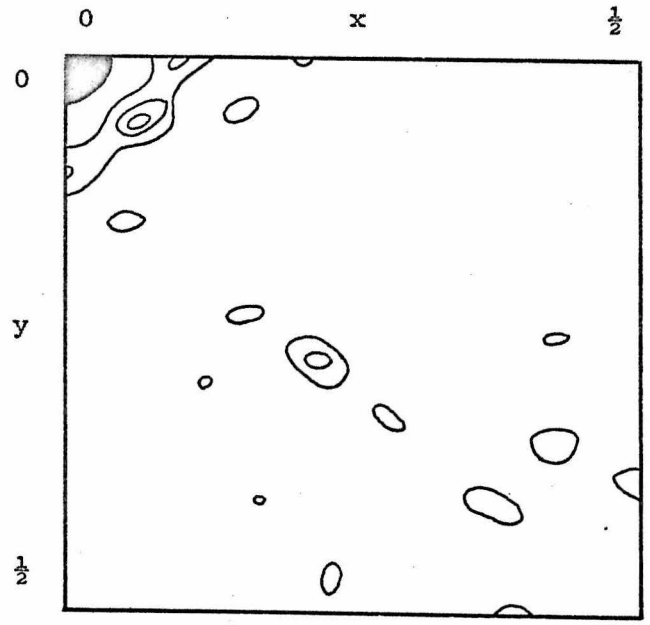

z= 2/48

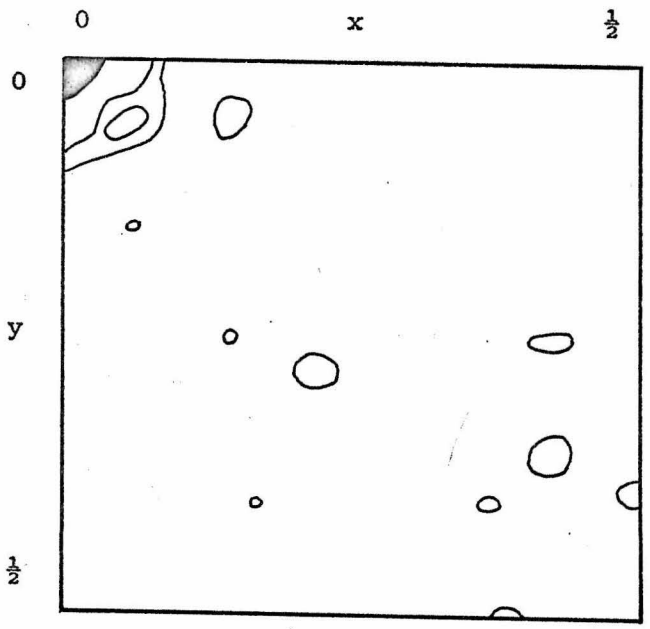

z= 3/48

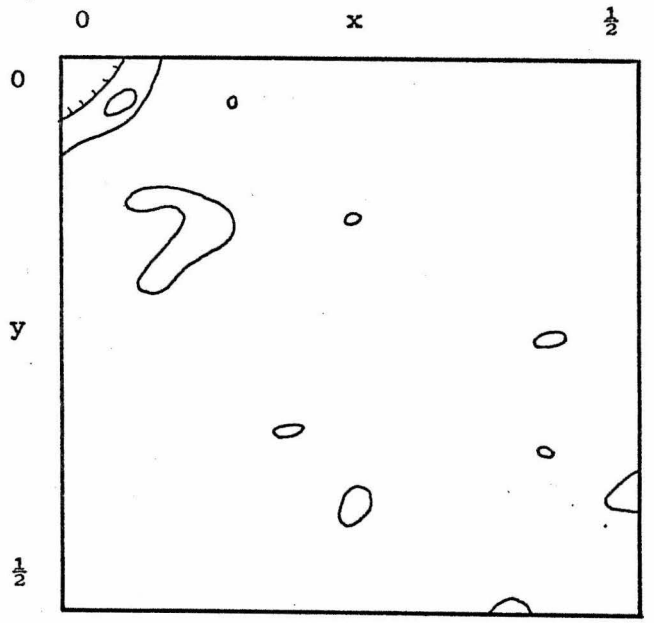

z= 4/48

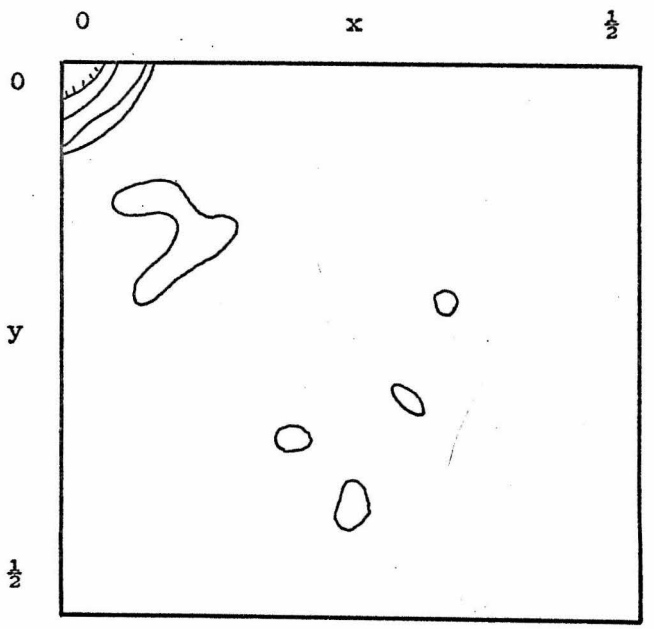

z= 5/48

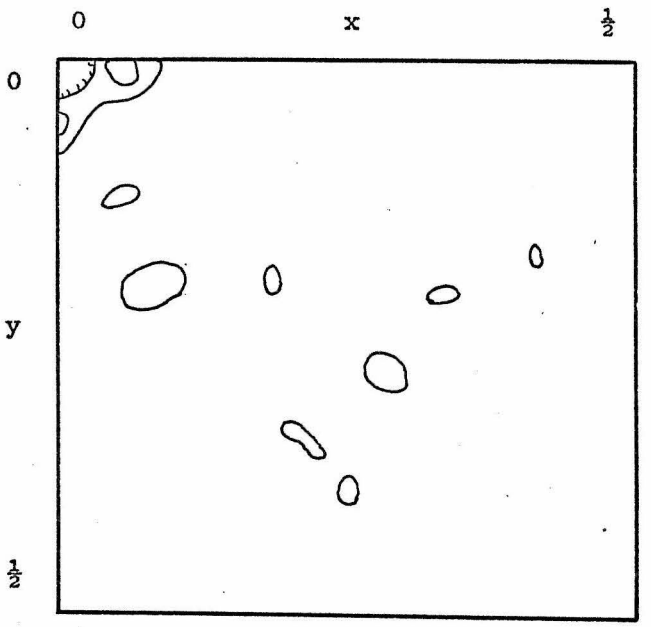

z= 6/48

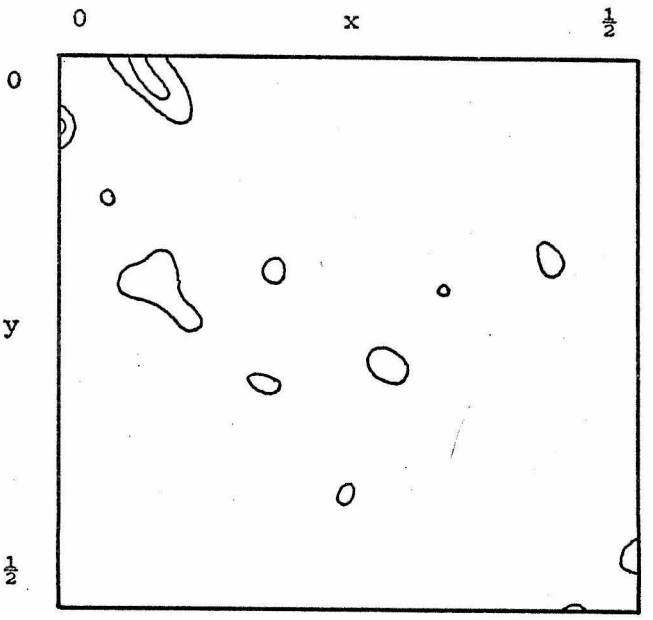

z= 7/48

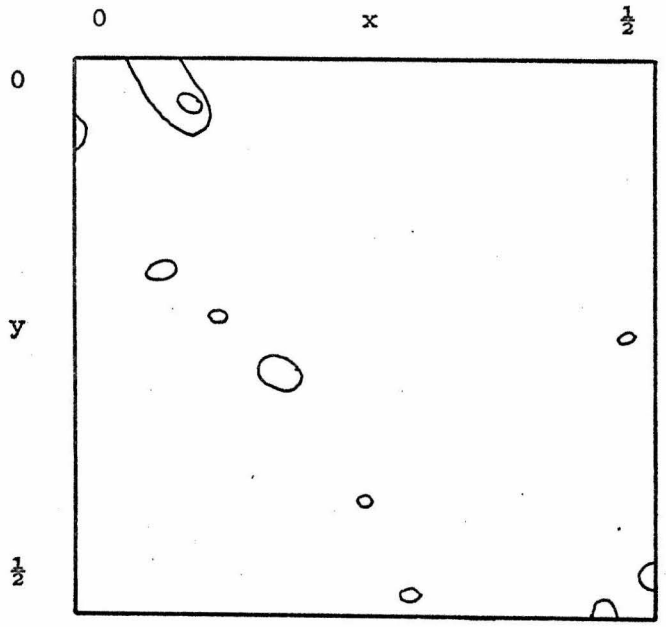

z= 8/48

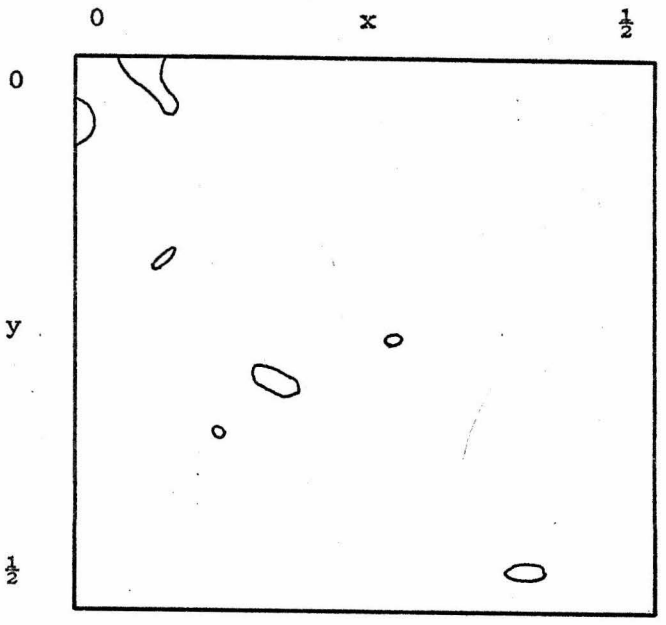

z= 9/48

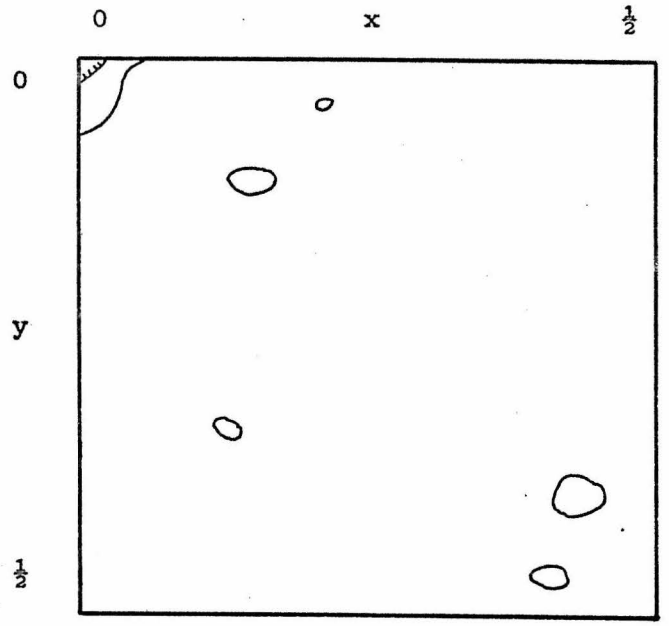

z= 10/48

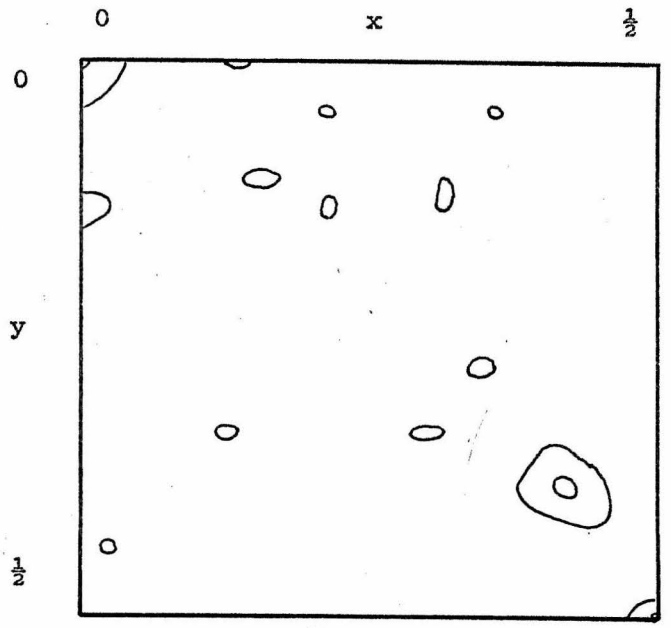

z= 11/48

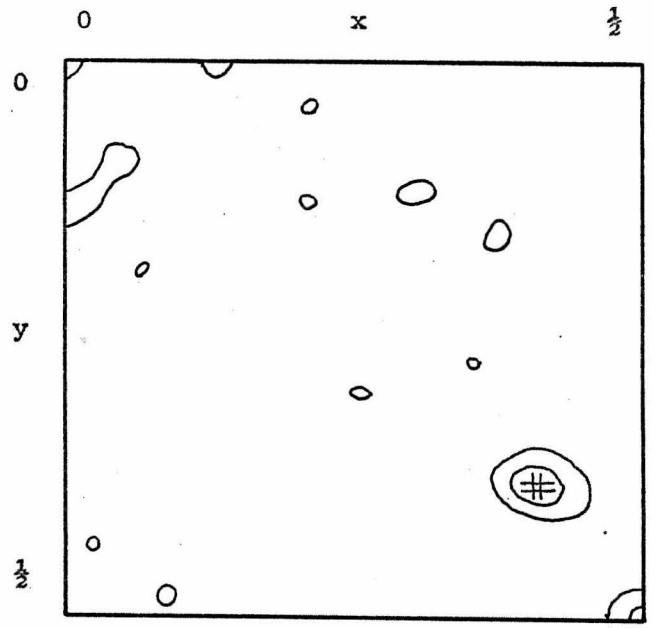

z= 12/48

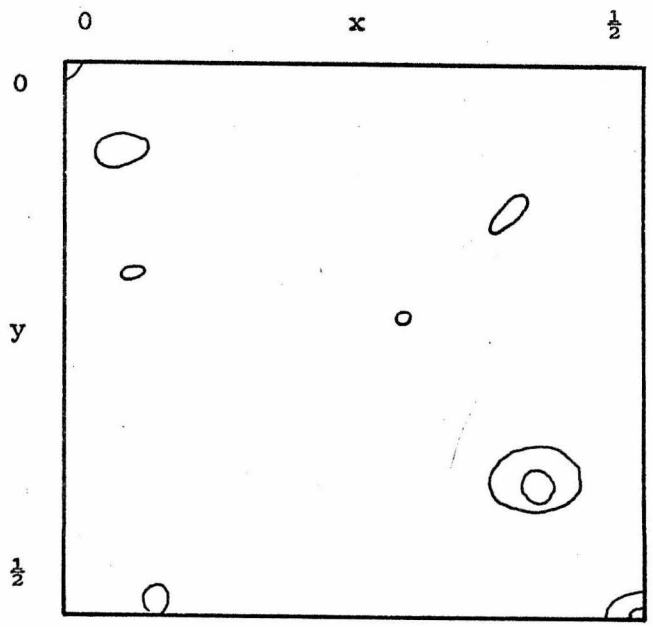

z= 13/48

= Double Weight Peak

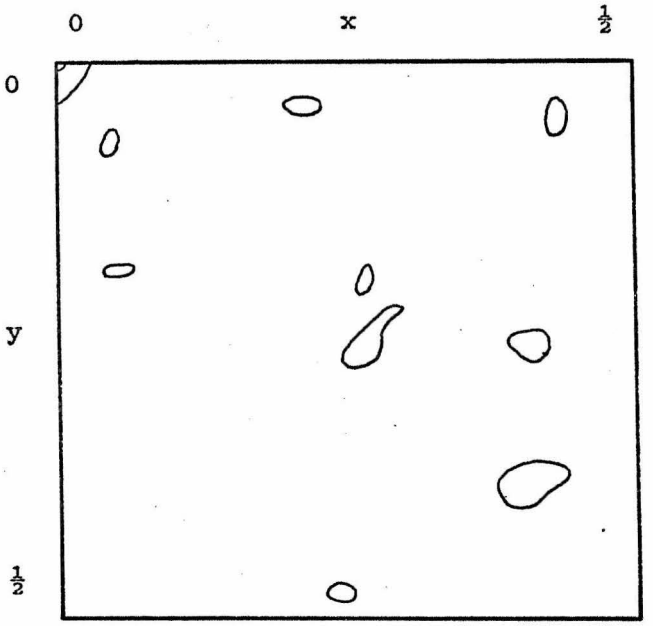

z= 14/48

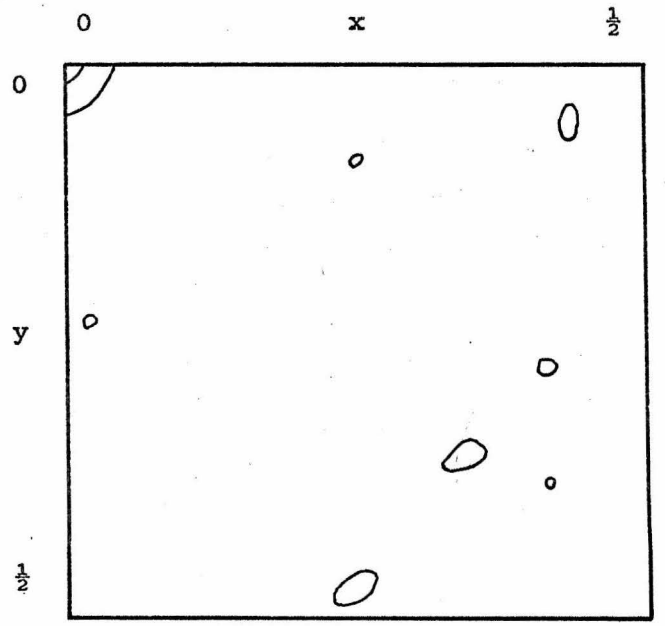

z= 15/48

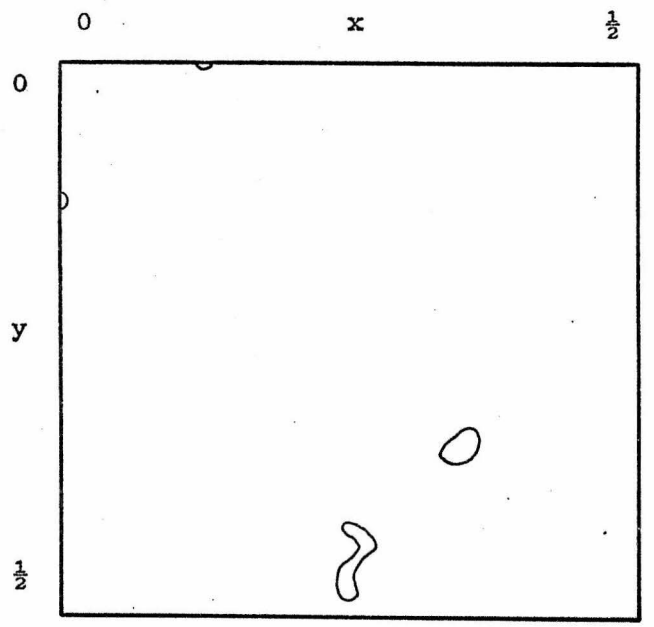

z= 16/48

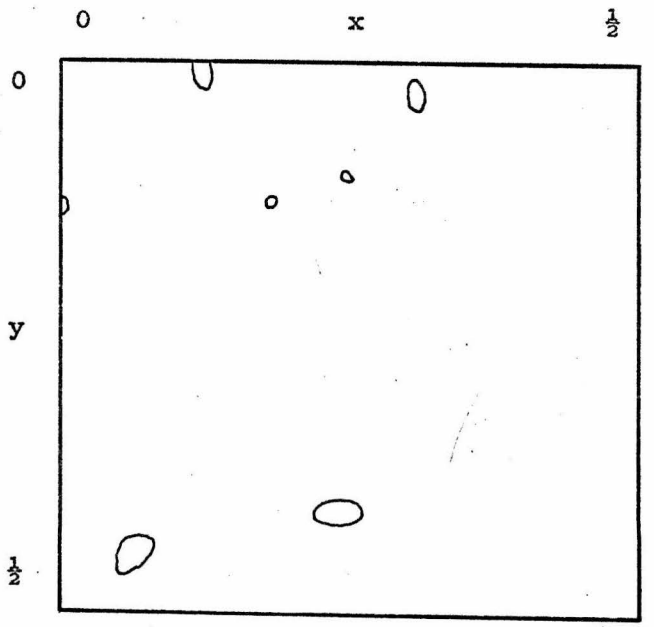

z= 17/48

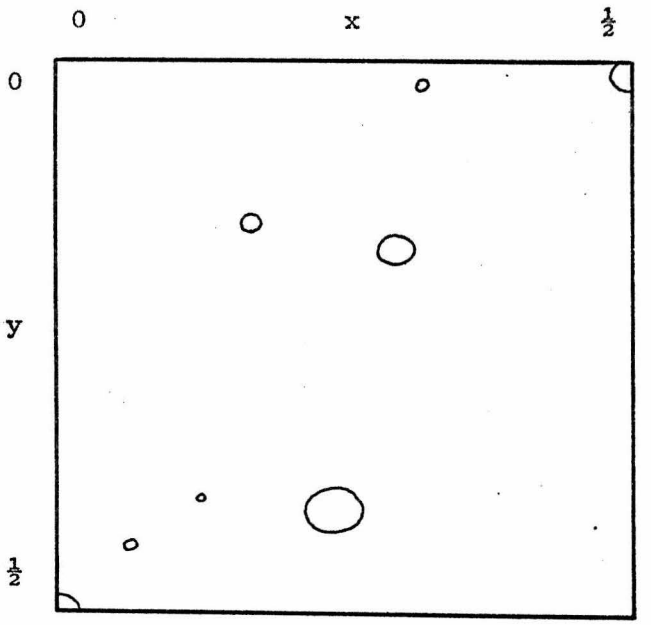

z= 18/48

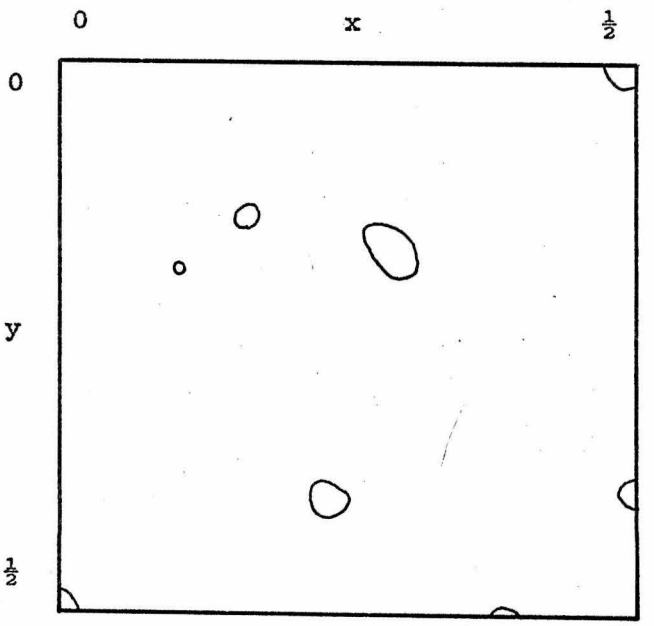

z= 19/48

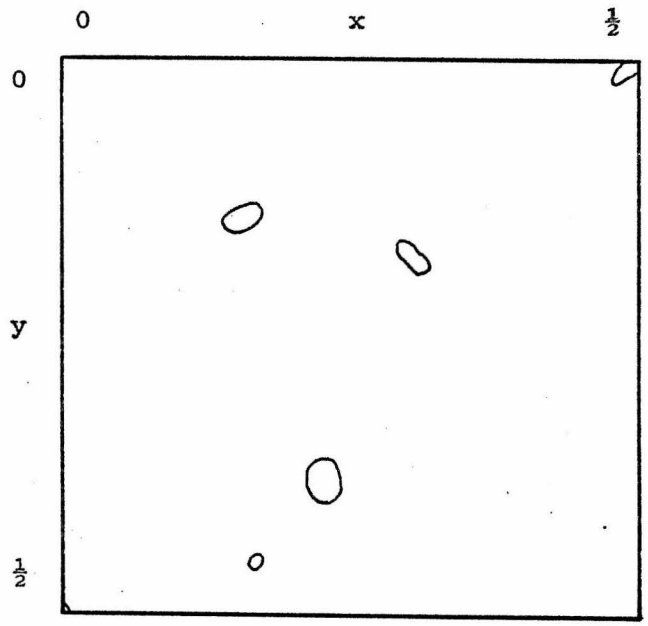

z= 20/48

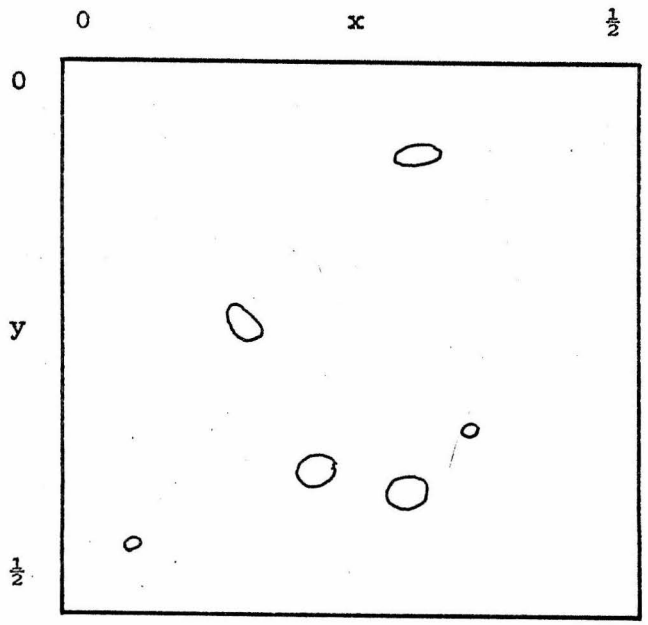

z= 21/48

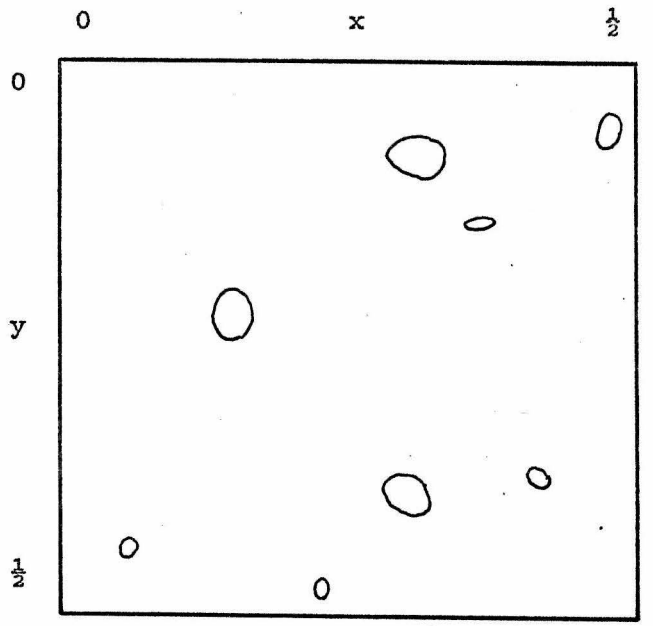

z= 22/48

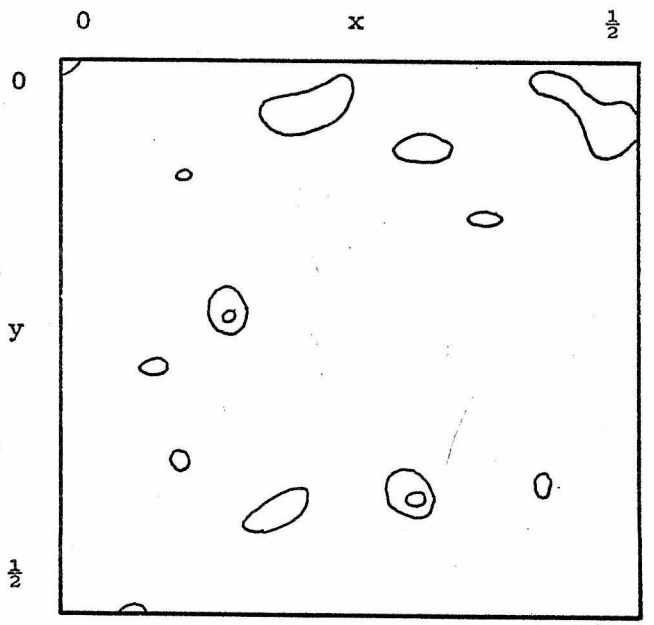

z= 23/48

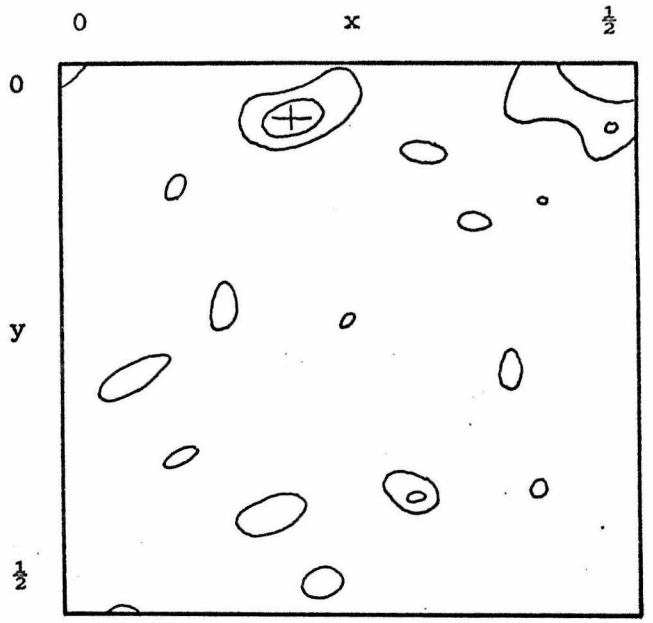

z= 24/48

+ = Single Weight Peak

APPENDIX VI

"CROSS" (ΔF MERCURY)(ΔF PLATINUM) PATTERSON MAP

The following Patterson map was calculated on the basis of the new native data set, the platinum derivative data set, and the mercury derivative data set. The coefficients used in the synthesis were (ΔF_{Pt}) x (ΔF_{Hg}). The contour interval was taken at 20 beginning at a contour height of 20. One eighth of a cell is shown: x from 0.0 to 0.5, y from 0.0 to 0.5, and z from 0.0 to 0.5.

The noise level in this Patterson map is extremely high as in the $(\Delta F)^2$ Patterson map for the mercury derivative. This is an indication of either non-isomorphism of the mercury derivative or of experimental errors in the mercury data set. From the appearance of the errors in the map, the latter seems more likely.

Knowing the x and y coordinates of the Pt and Hg atoms, and having assigned the z coordinate of the Pt atom at z = 0.000, the following peaks should appear in this map:

Peak Position		
.192	.198	z_{Hg}
.183	.386	$z_{Hg} + \frac{1}{4}$
.400	.240	$z_{Hg} + \frac{1}{2}$
.226	.198	$z_{Hg} - \frac{1}{4}$

These peaks are marked A, B, C, and D on the Patterson sections, and correspond to a value for z_{Hg} of ± 0.376.

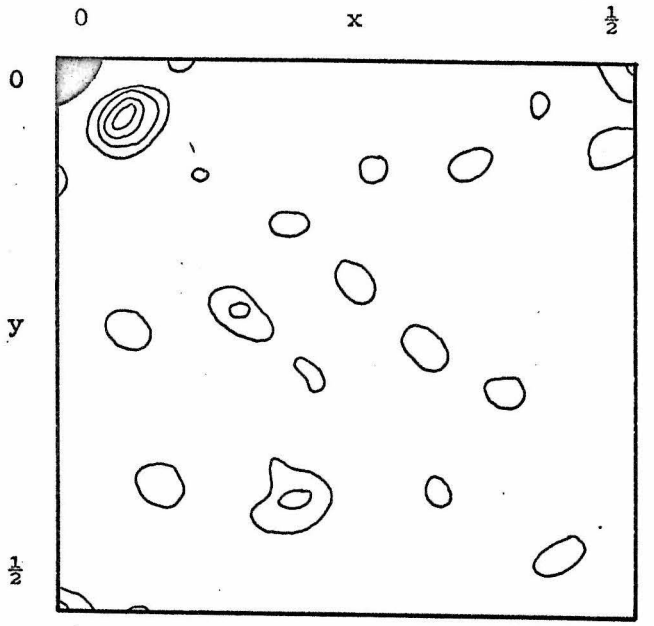

z= 0/48

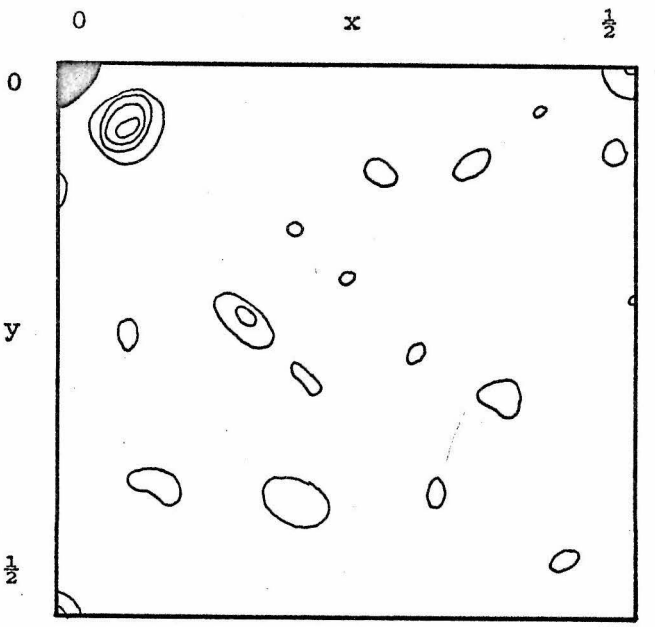

z= 1/48

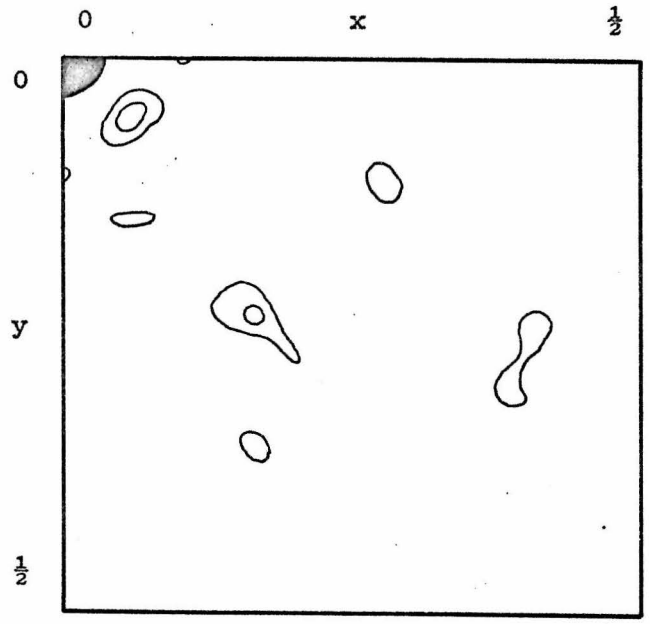

z= 2/48

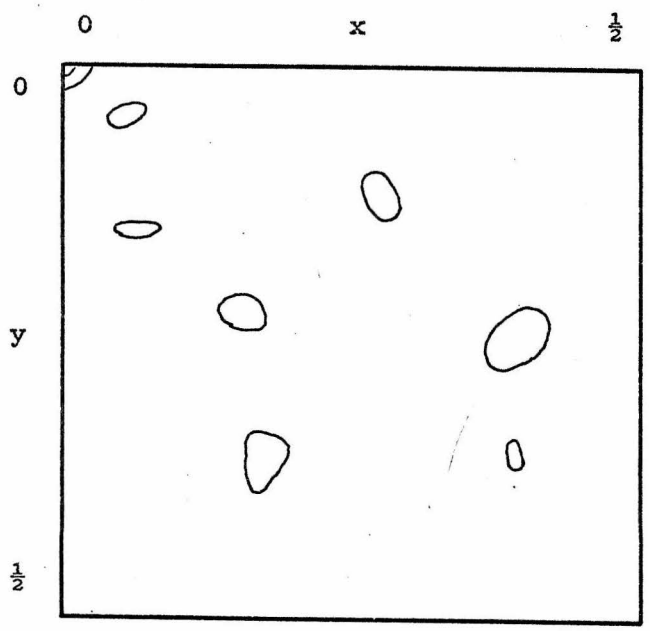

z= 3/48

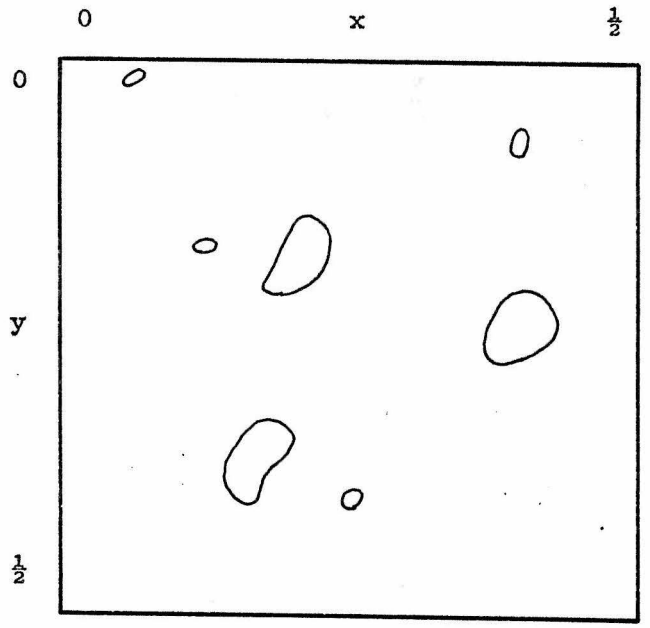

z= 4/48

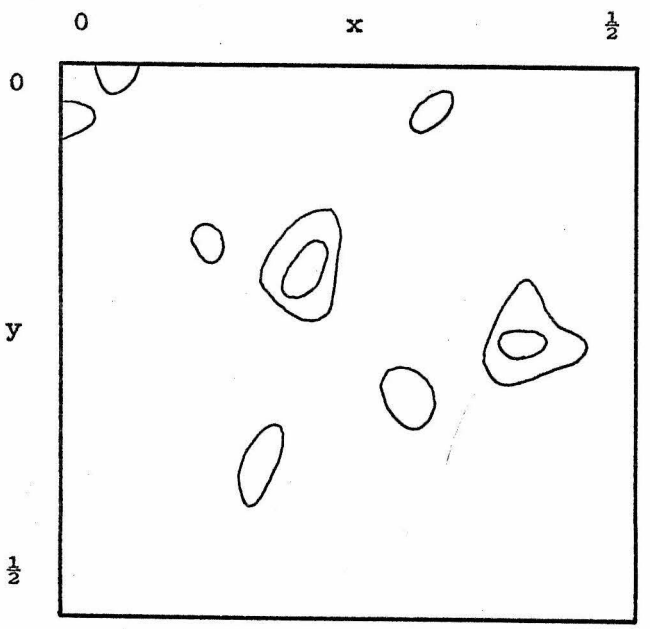

z= 5/48

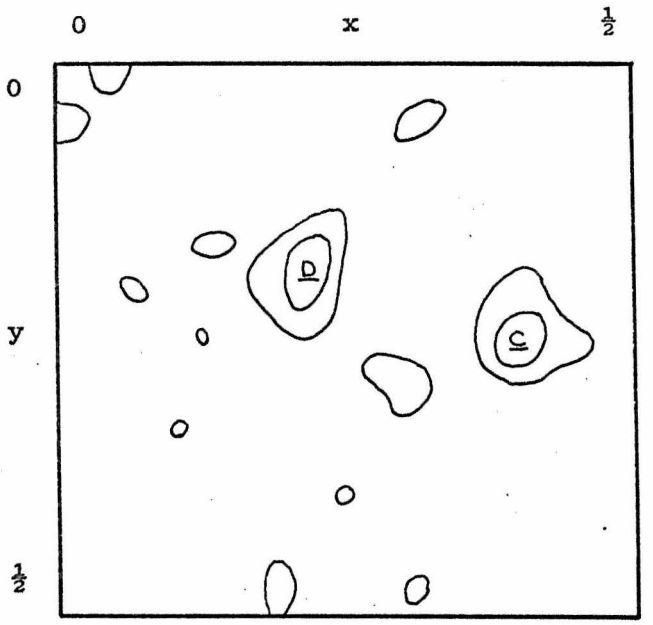

z= 6/48

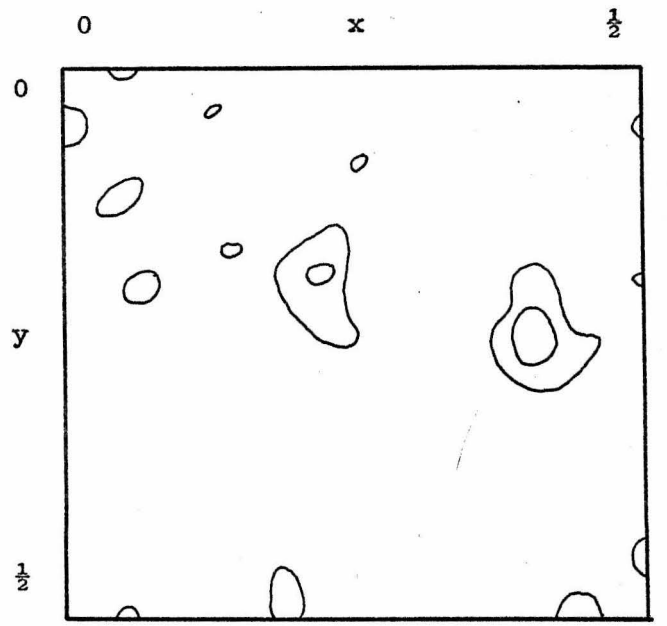

z= 7/48

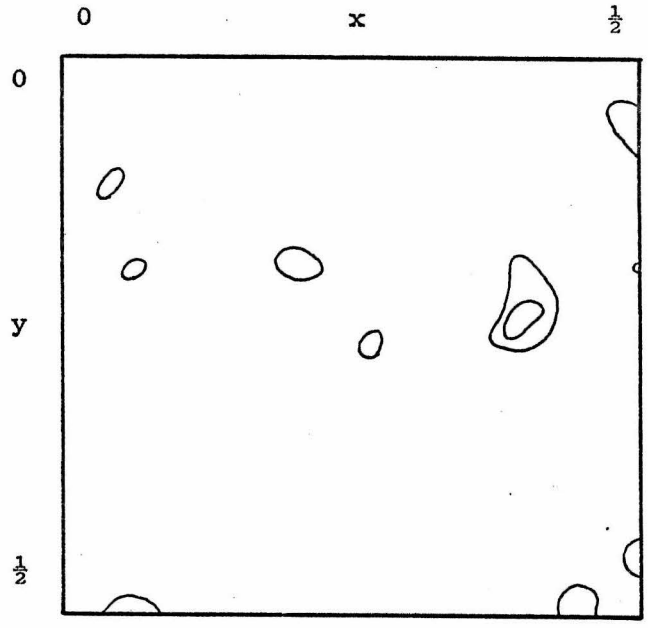

z= 8/48

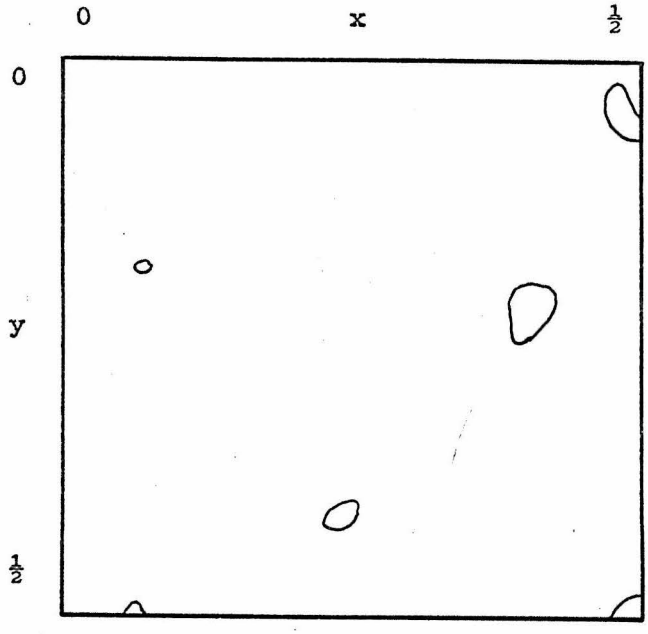

z= 9/48

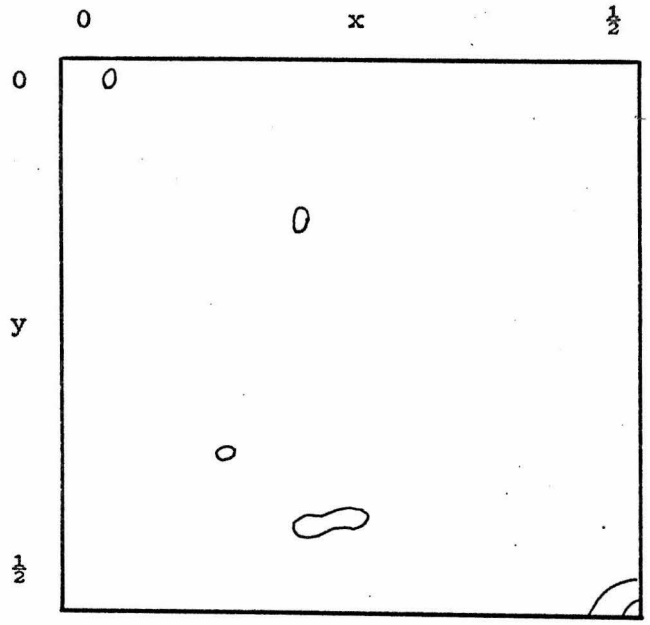

z= 10/48

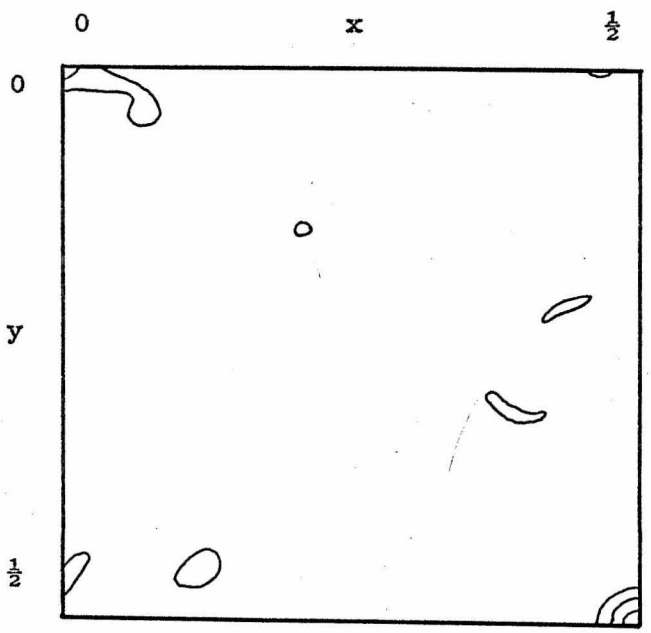

z= 11/48

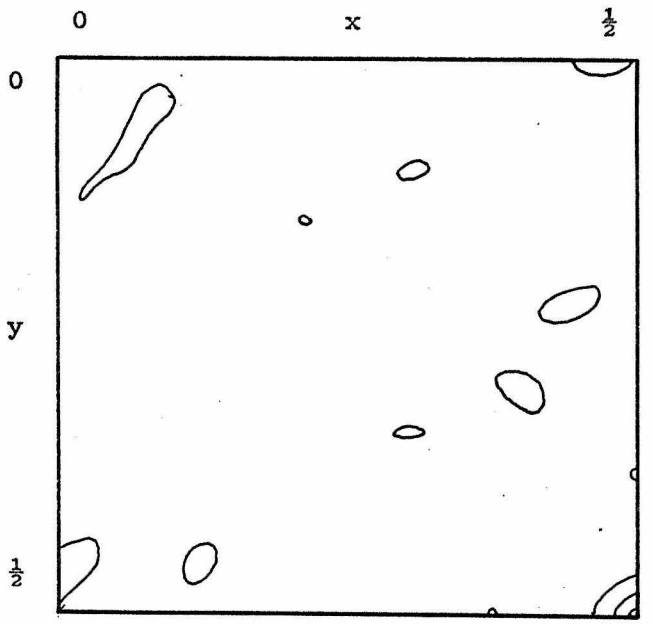

z= 12/48

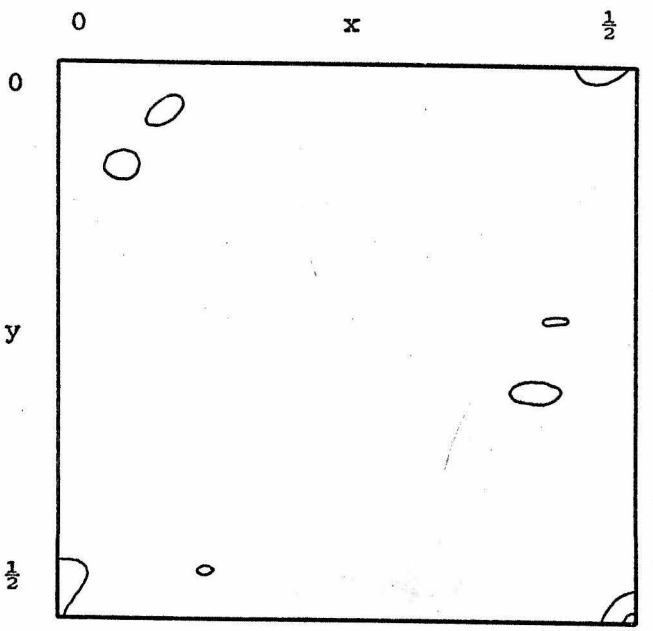

z= 13/48

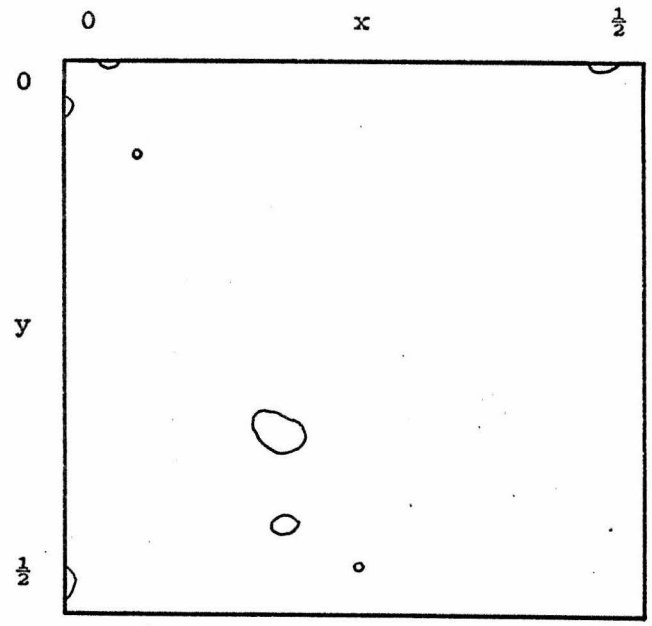

z= 14/48

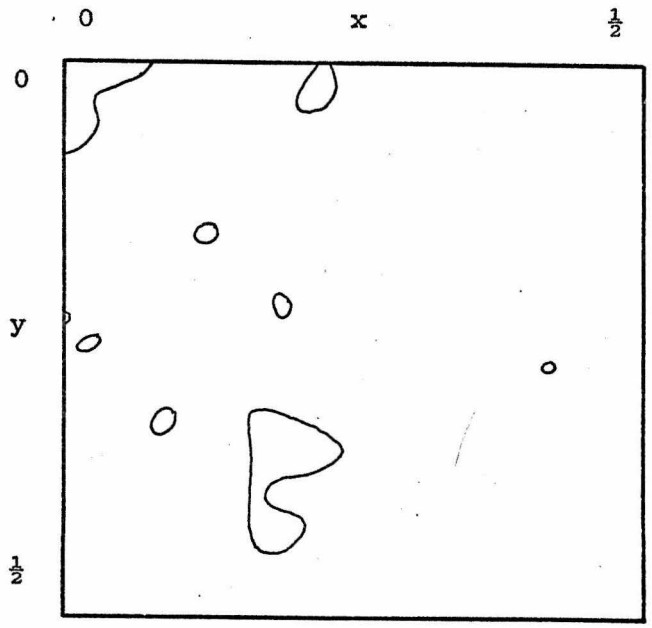

z= 15/48

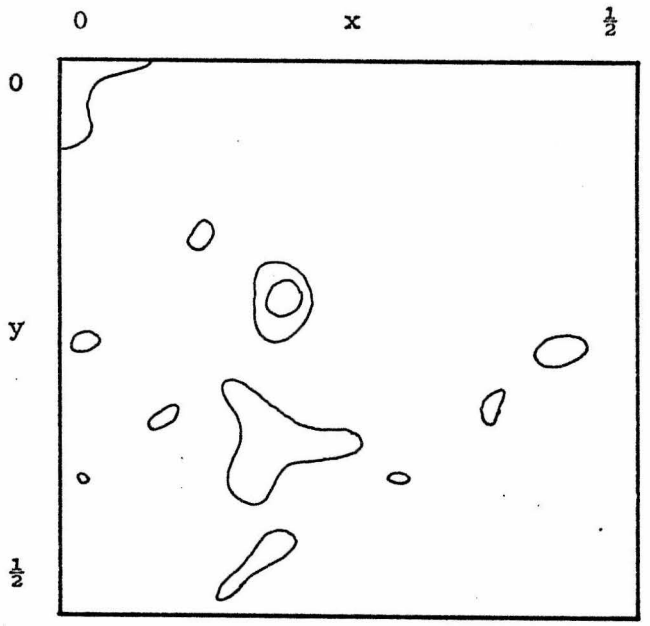

z= 16/48

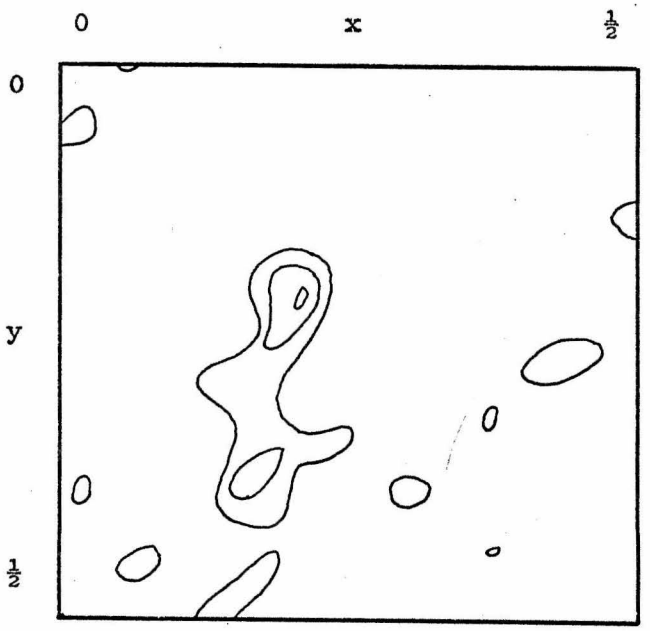

z= 17/48

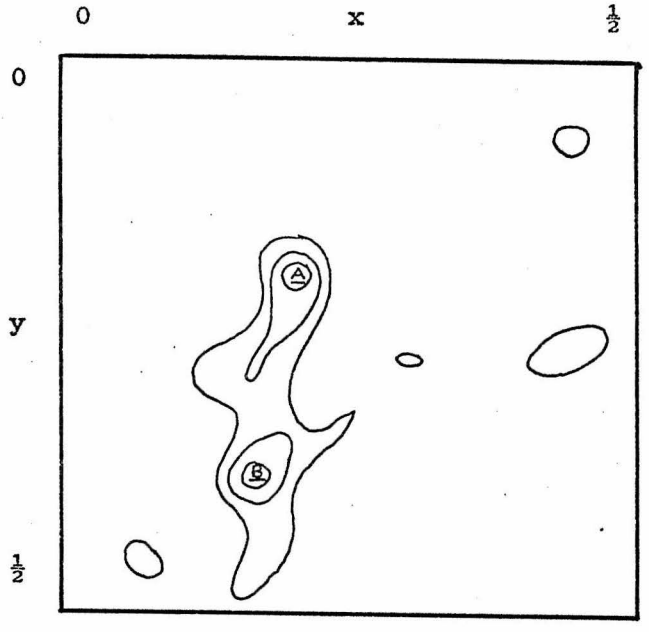

z= 18/48

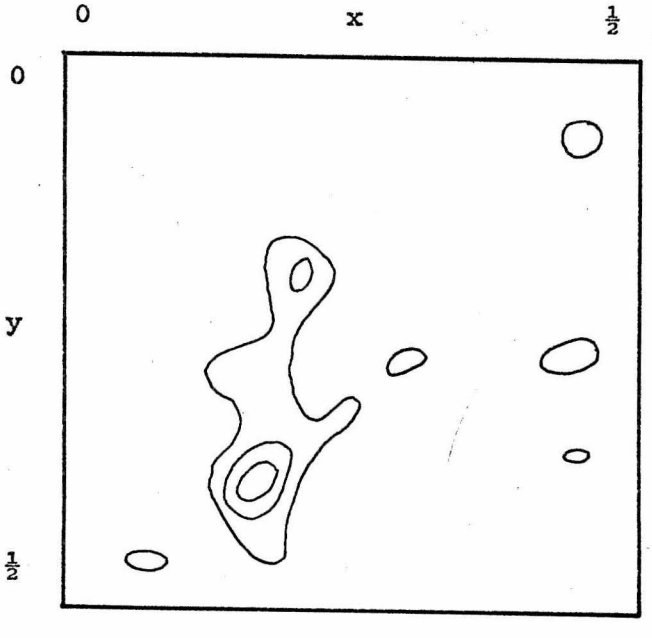

z= 19/48

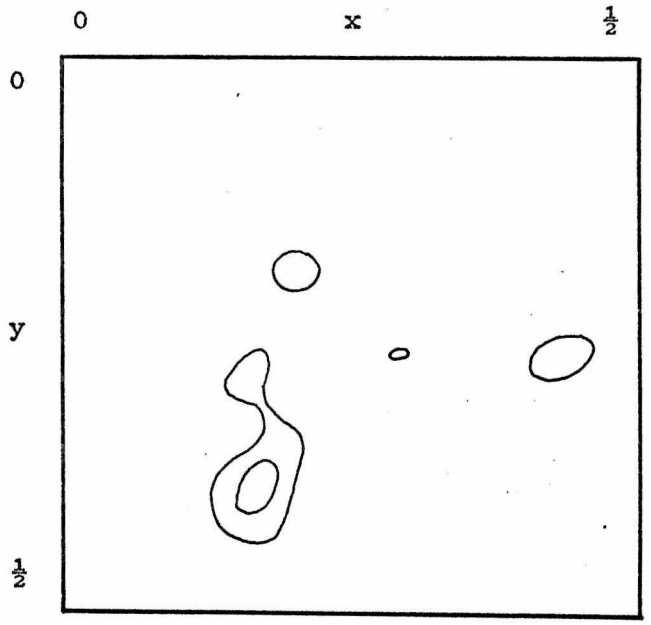

z= 20/48

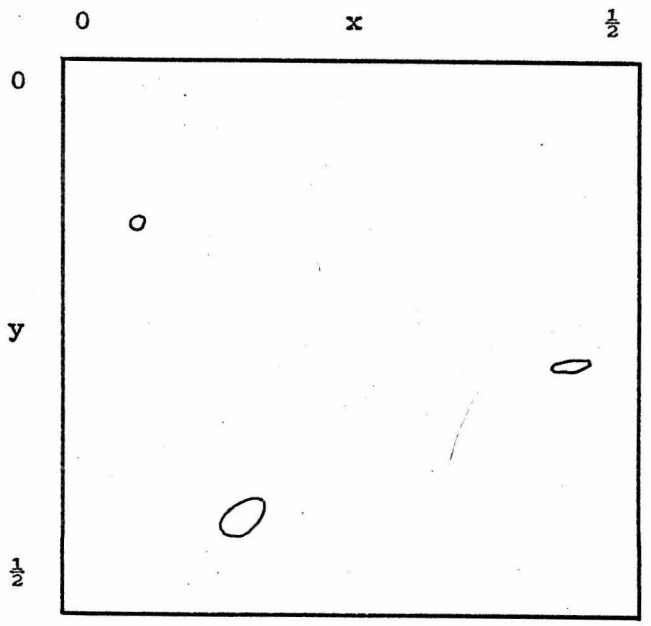

z= 21/48

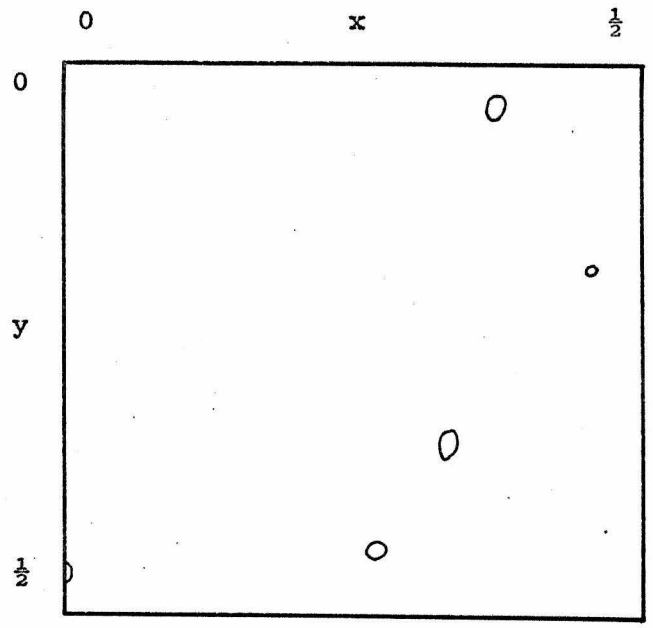

z= 22/48

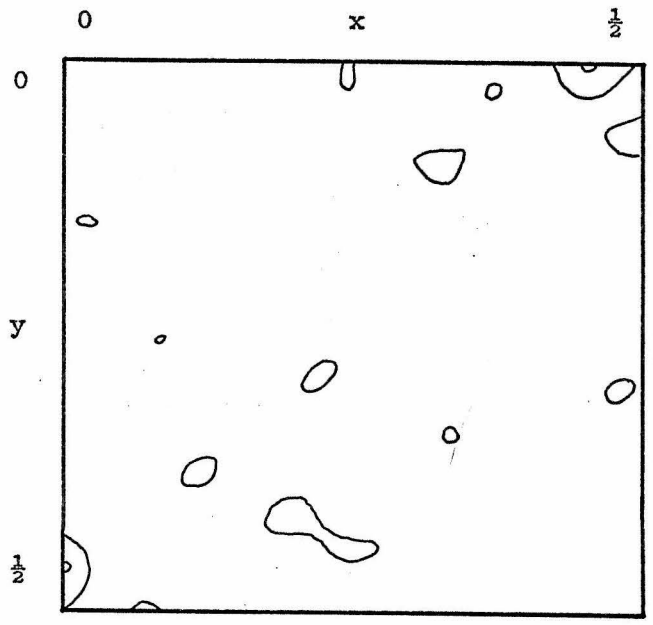

z= 23/48

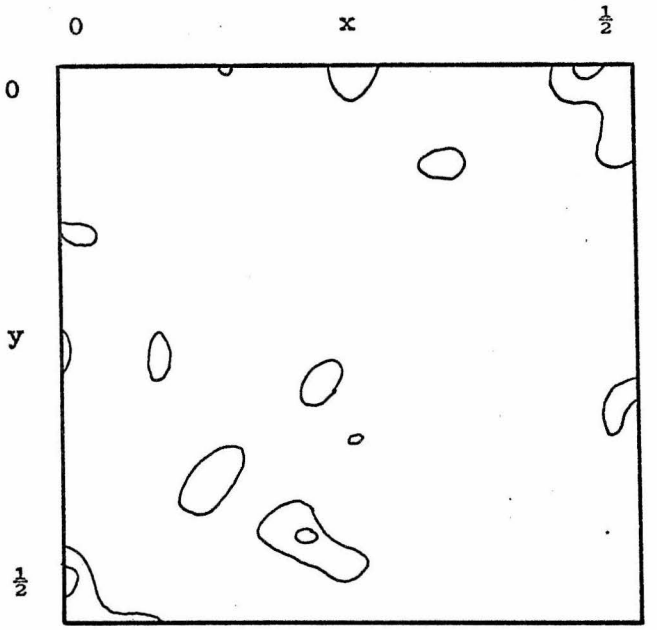

z= 24/48

APPENDIX VII

SINGLE ISOMORPHOUS REPLACEMENT FOURIER

The following Fourier map was calculated on the basis of the old native data set and the platinum derivative data set. The map is on an arbitrary scale with a contour interval of 50. The lowest contour is at height 50. The position of the Pt atom and the two possible positions of the Hg atom are marked. One complete asymmetric unit is shown: x from 0.0 to 1.0, y from 0.0 to 1.0, and z from 0.0 to 0.25. The scale is approximately 3.8 Å/cm.

This map allowed the determination of the molecular boundaries, the relative z separation of the Pt and Hg atoms, and the location of the heme group.

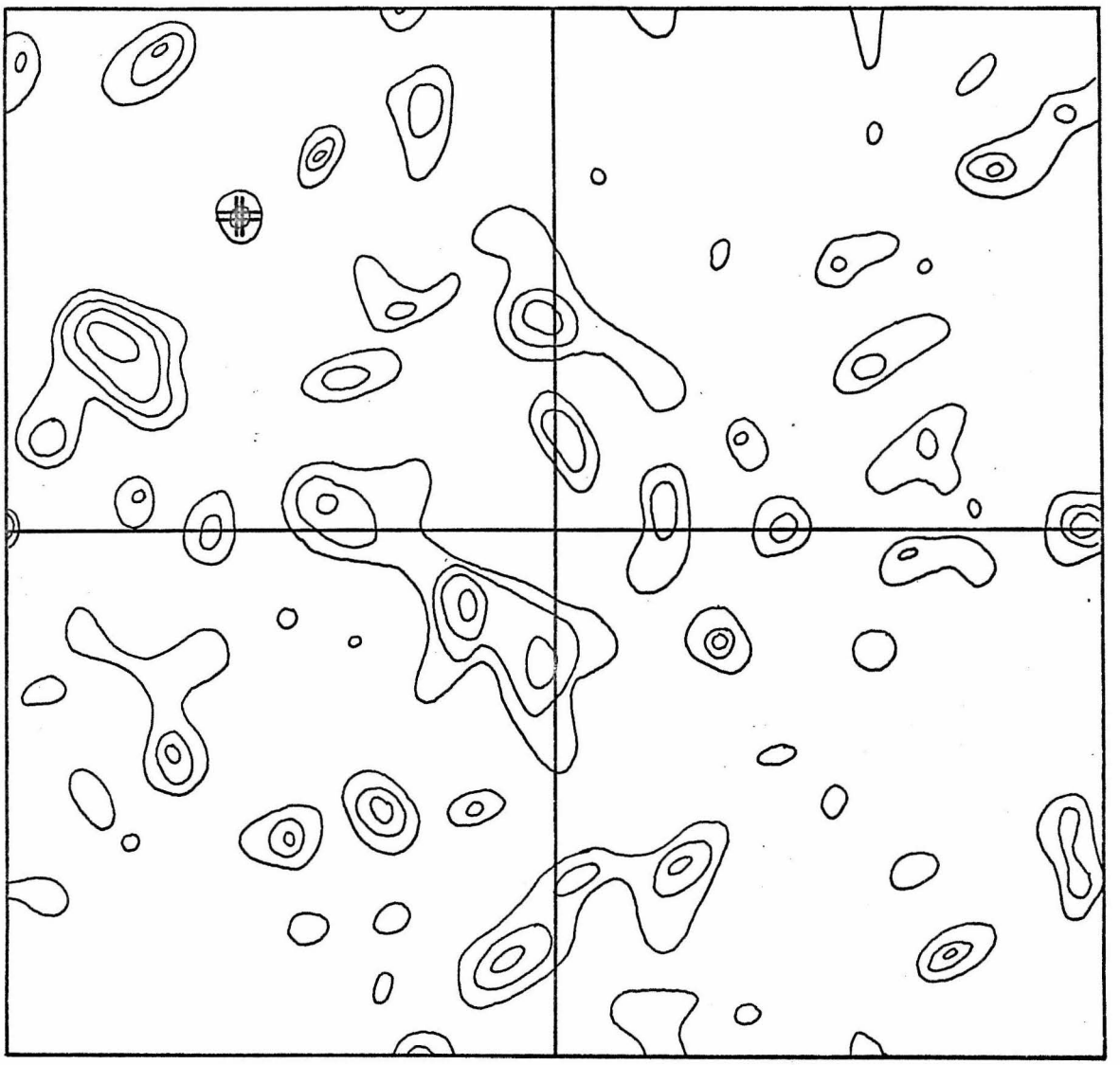

PLATINUM DERIVATIVE SINGLE ISOMORPHOUS REPLACEMENT FOURIER

Origin: Upper Left Hand Corner
x: Left to Right; 0.0 to 1.0
y: Top to Bottom; 0.0 to 1.0

$\#$ = Platinum Site

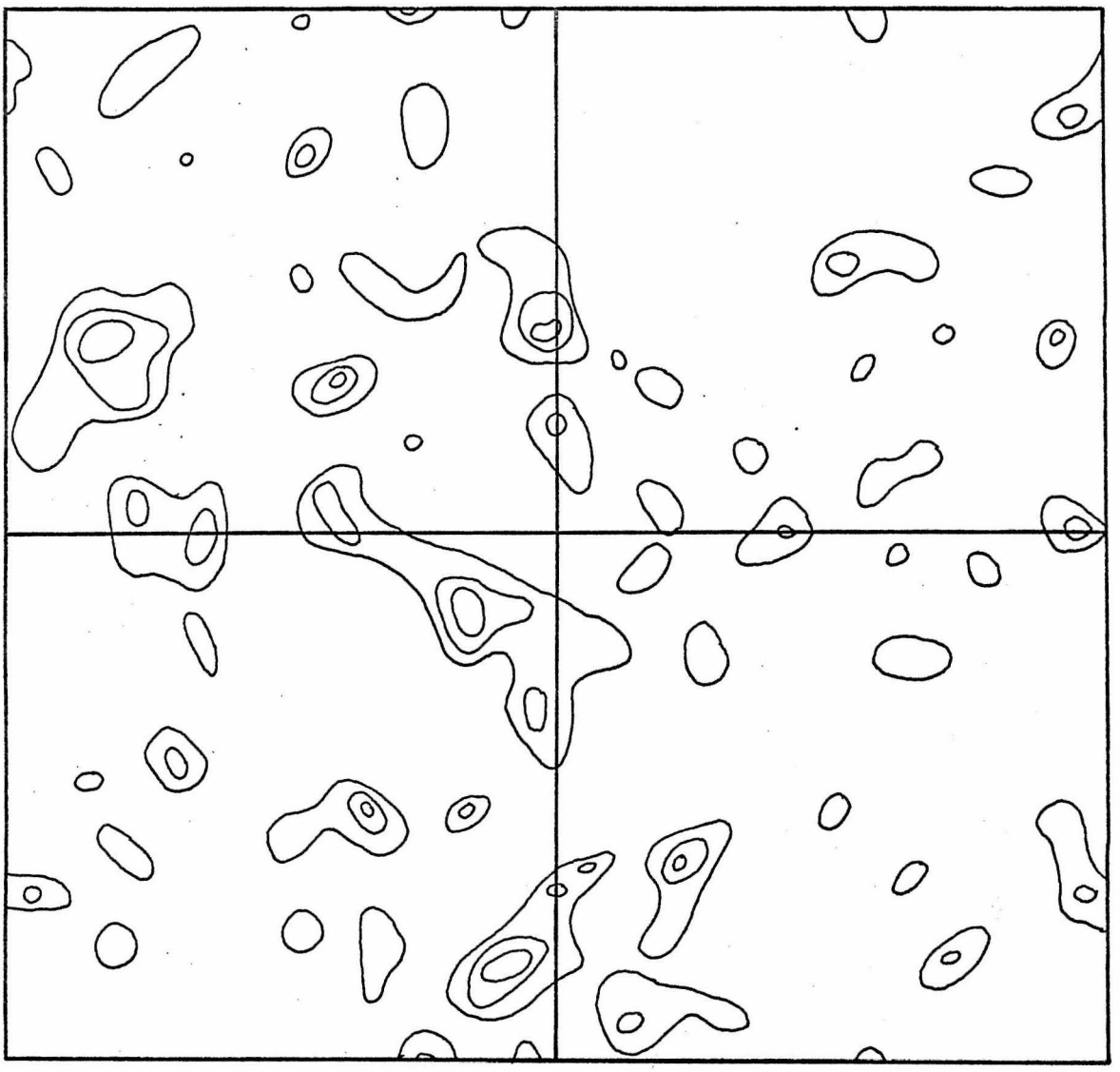

z= 1/48

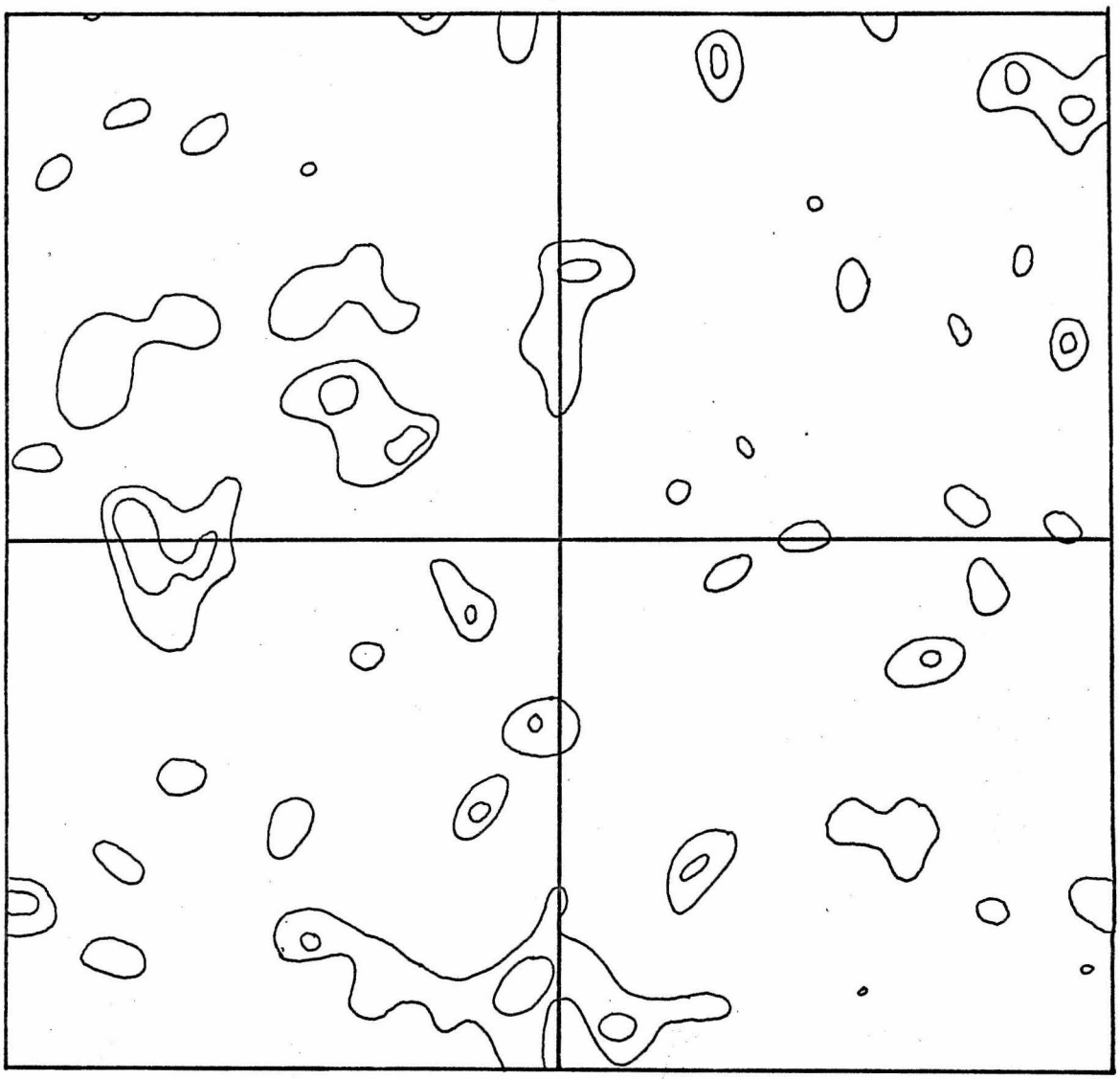

z= 2/48

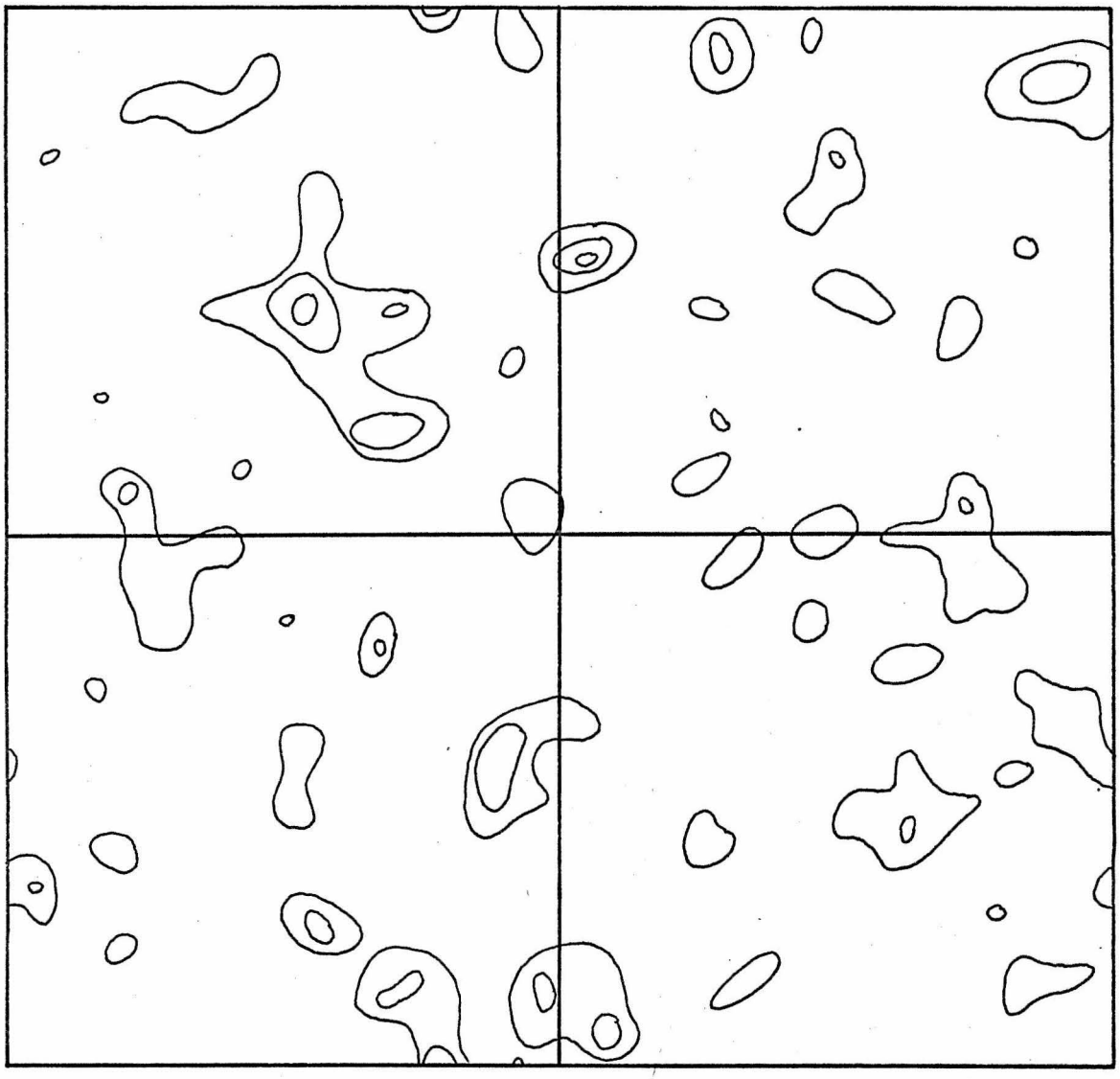

z= 3/48

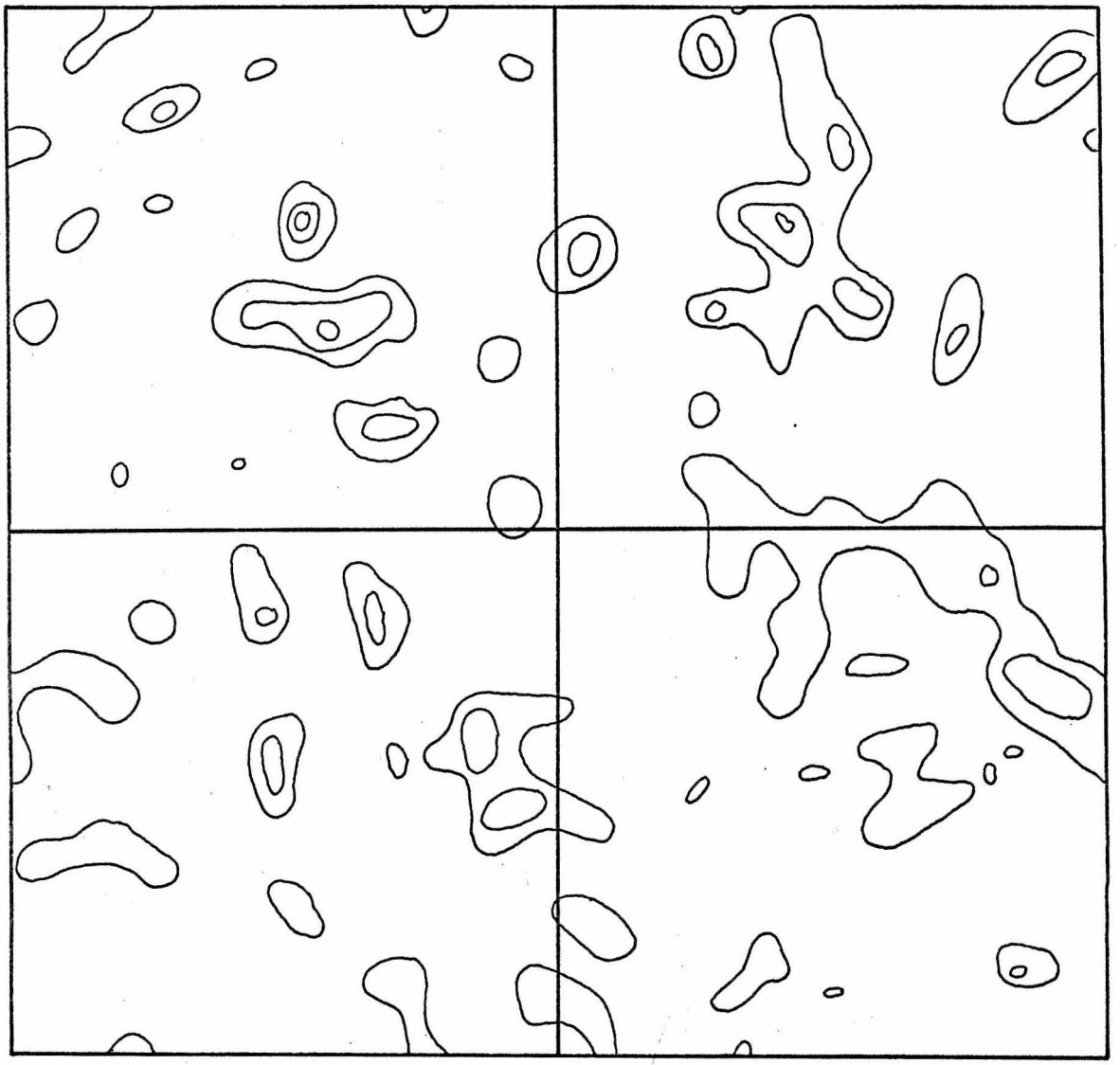

z= 4/48

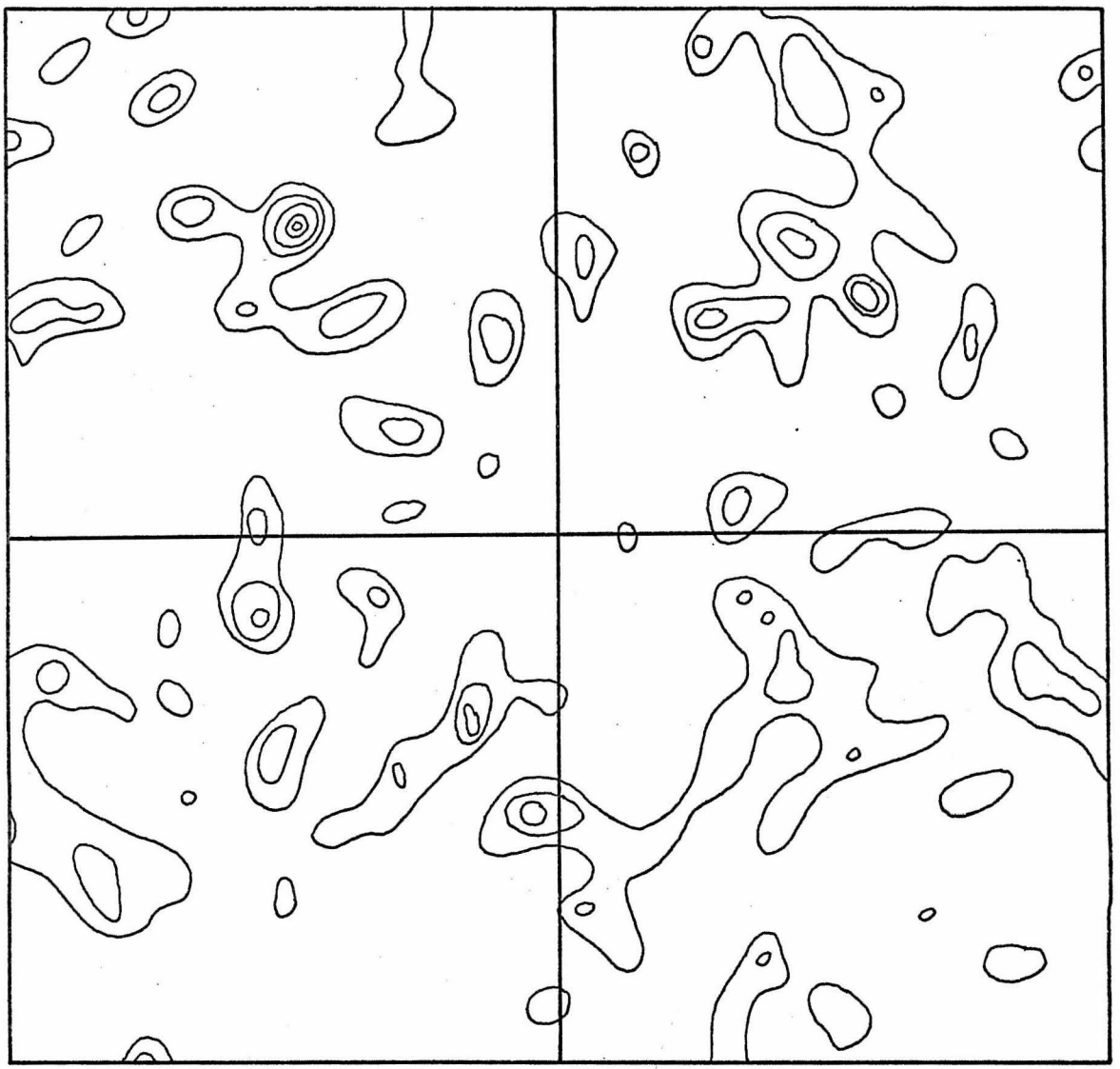

z= 5/48

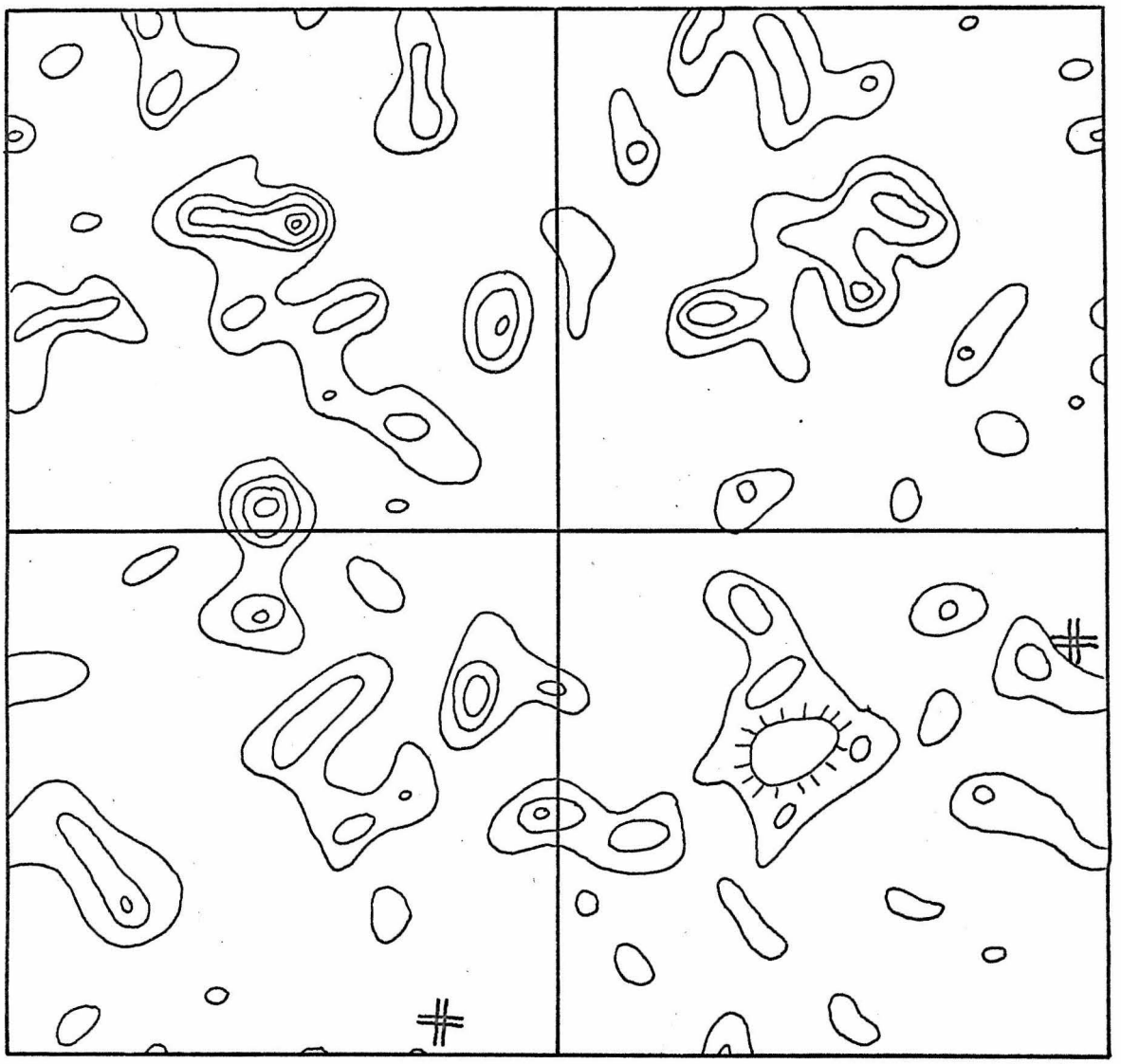

z= 6/48

= Two Possible Mercury Sites

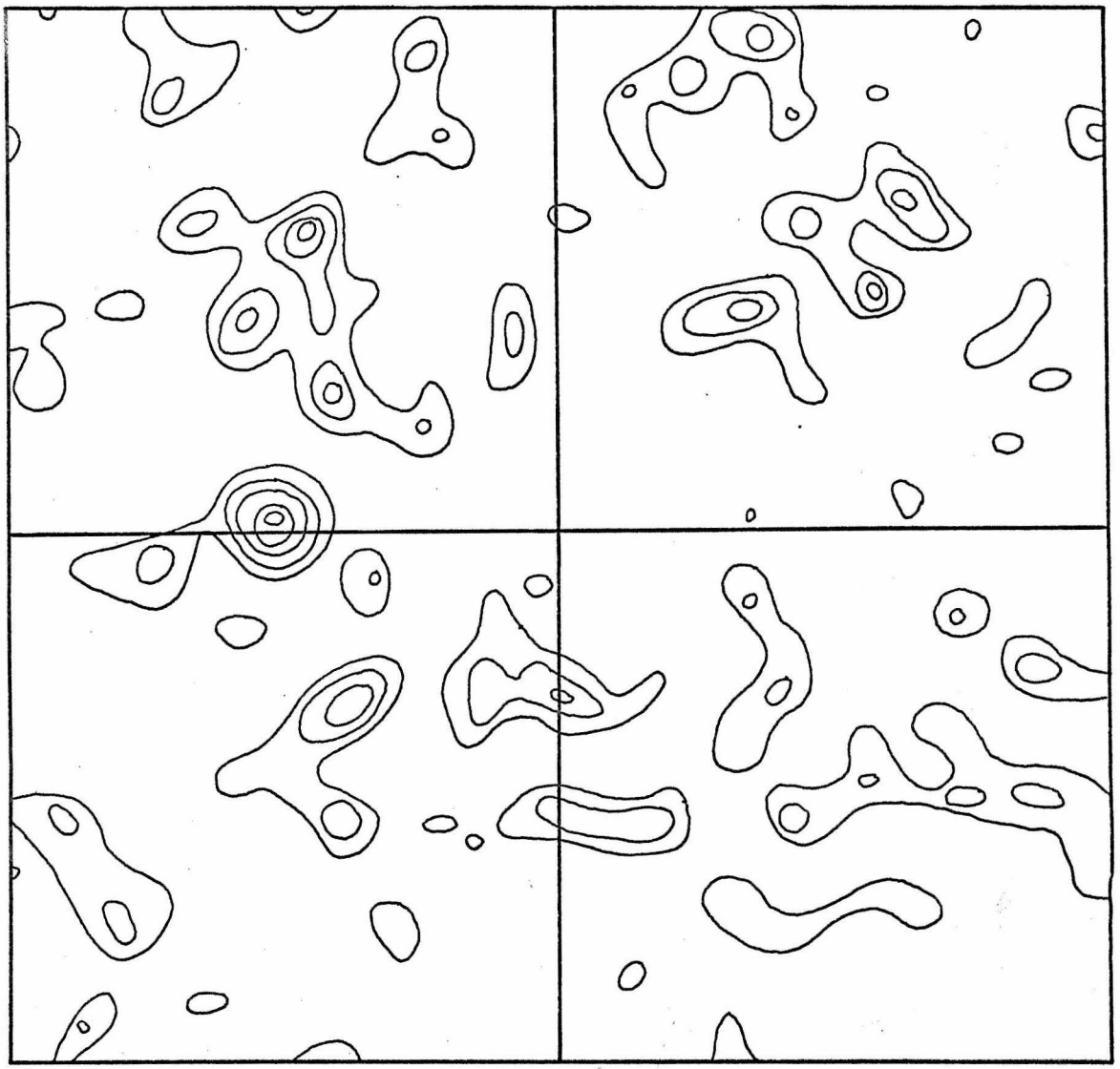

z= 7/48

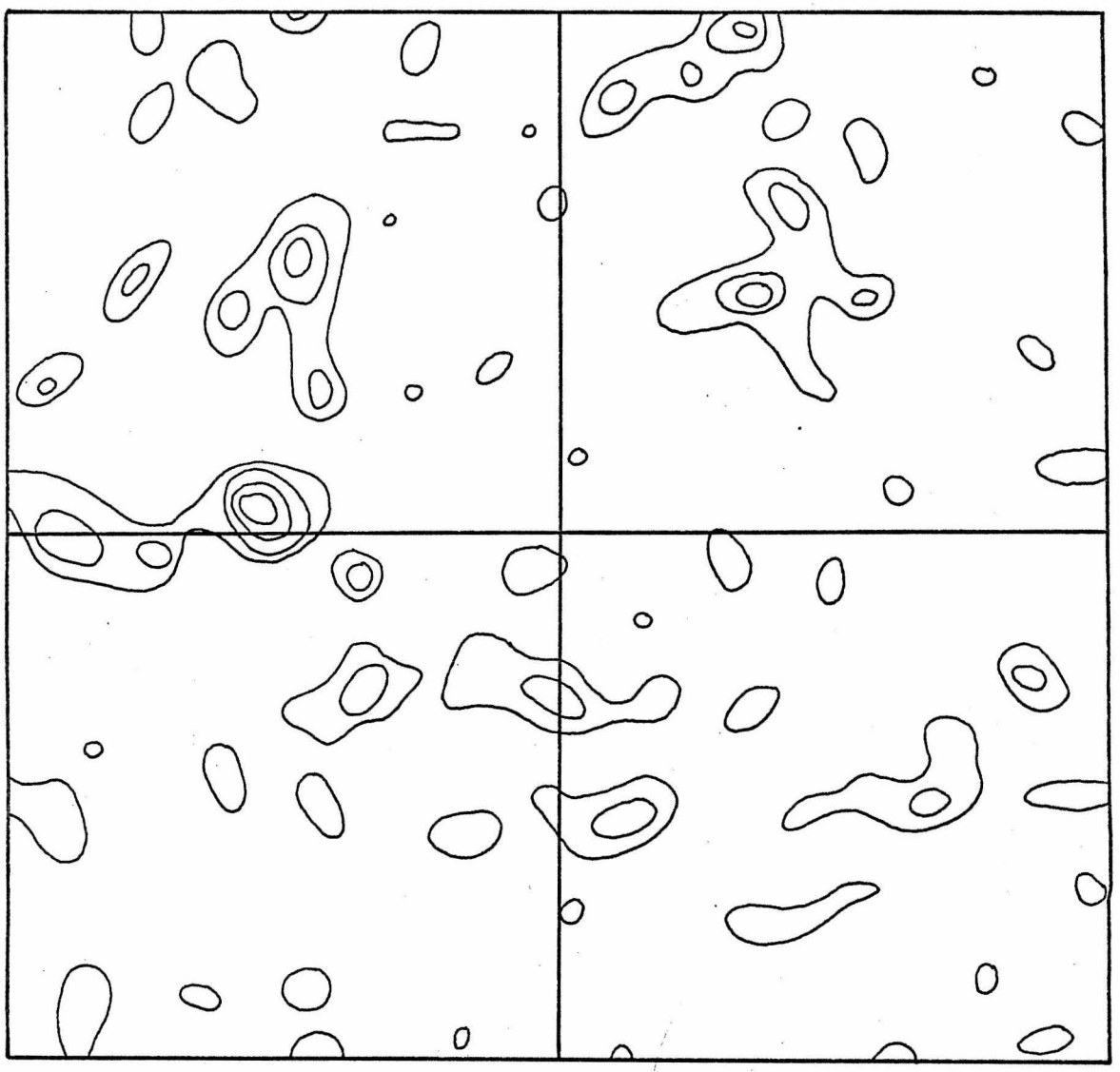

z= 8/48

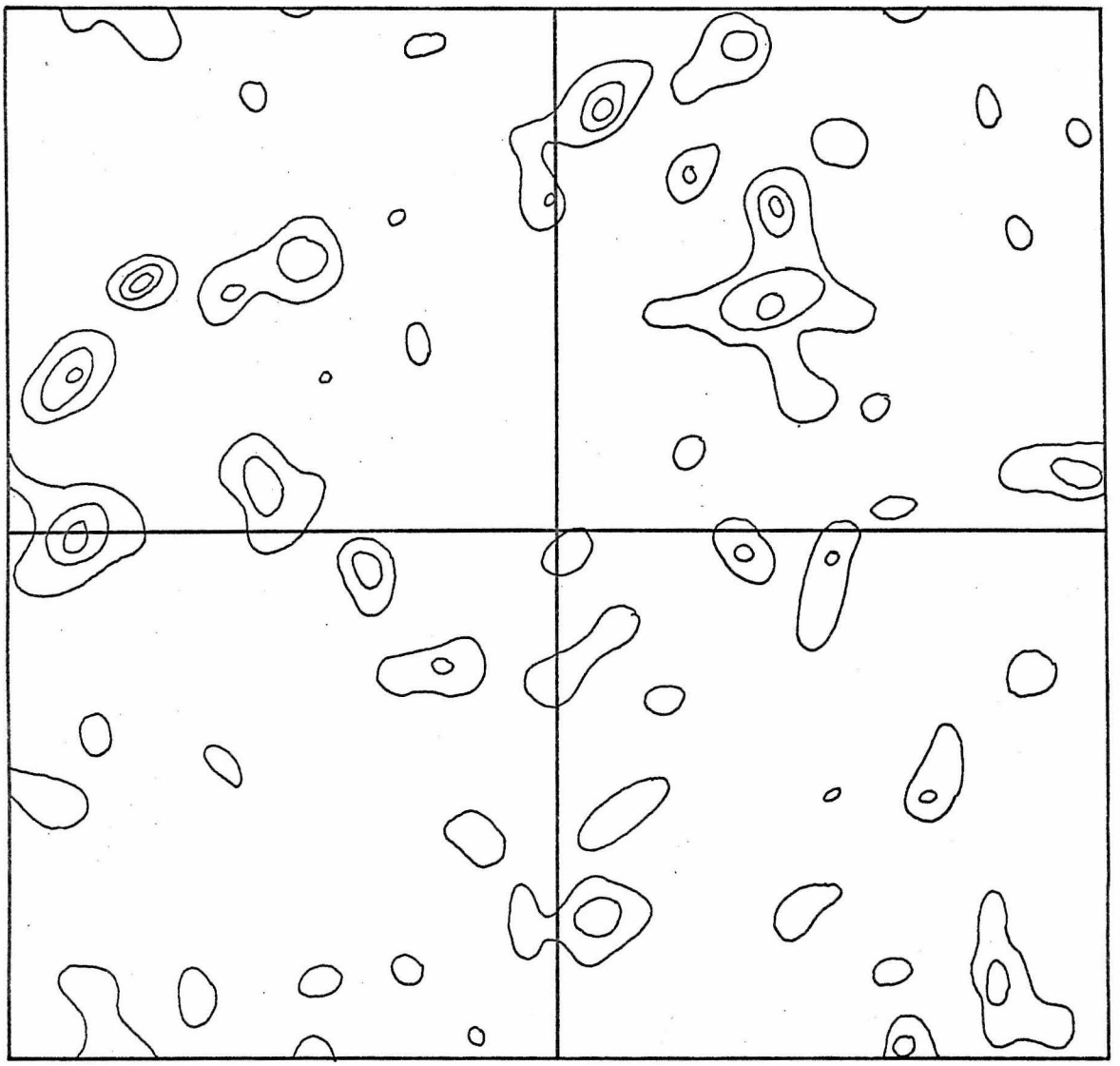

z= 9/48

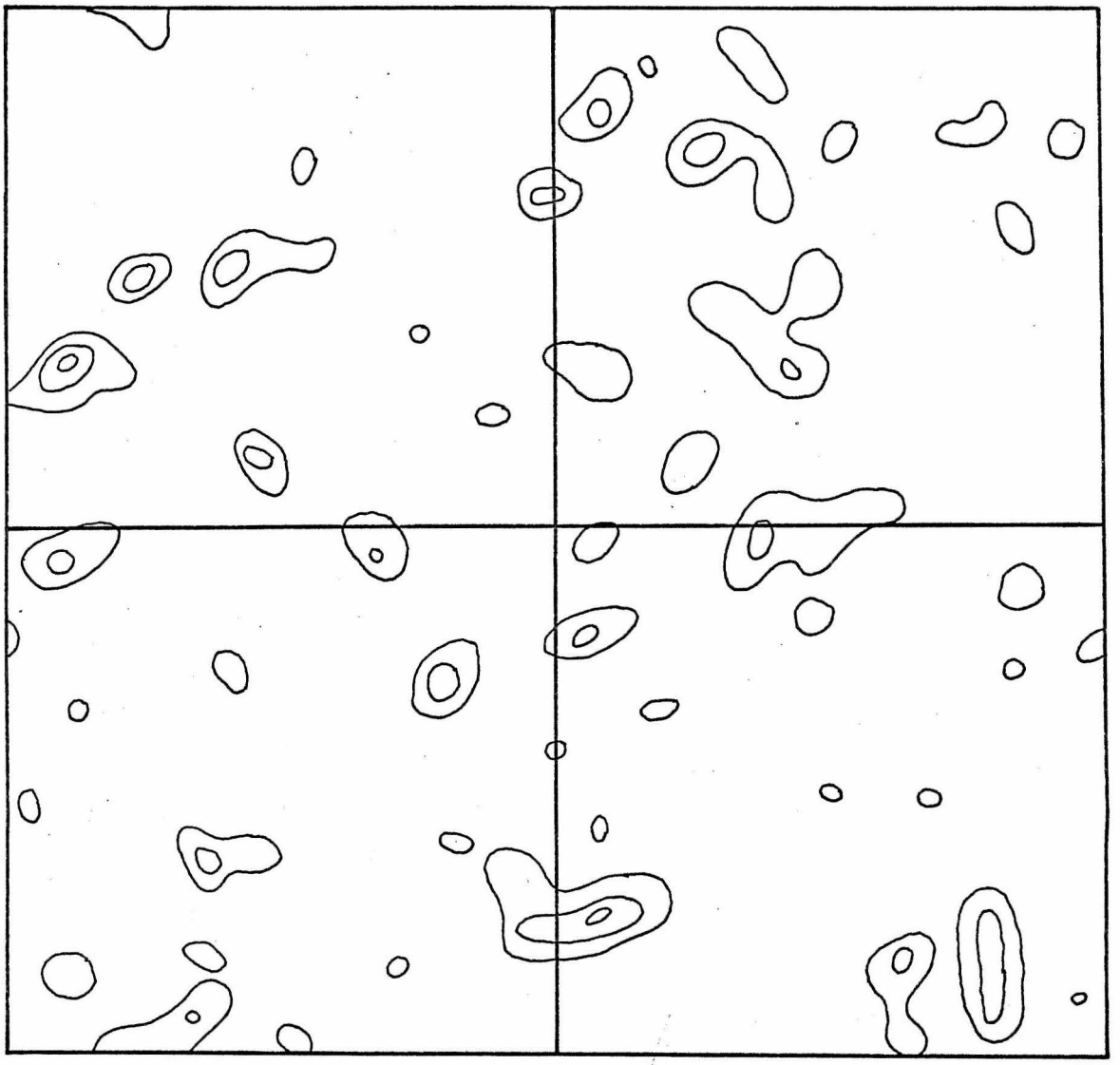

z= 10/48

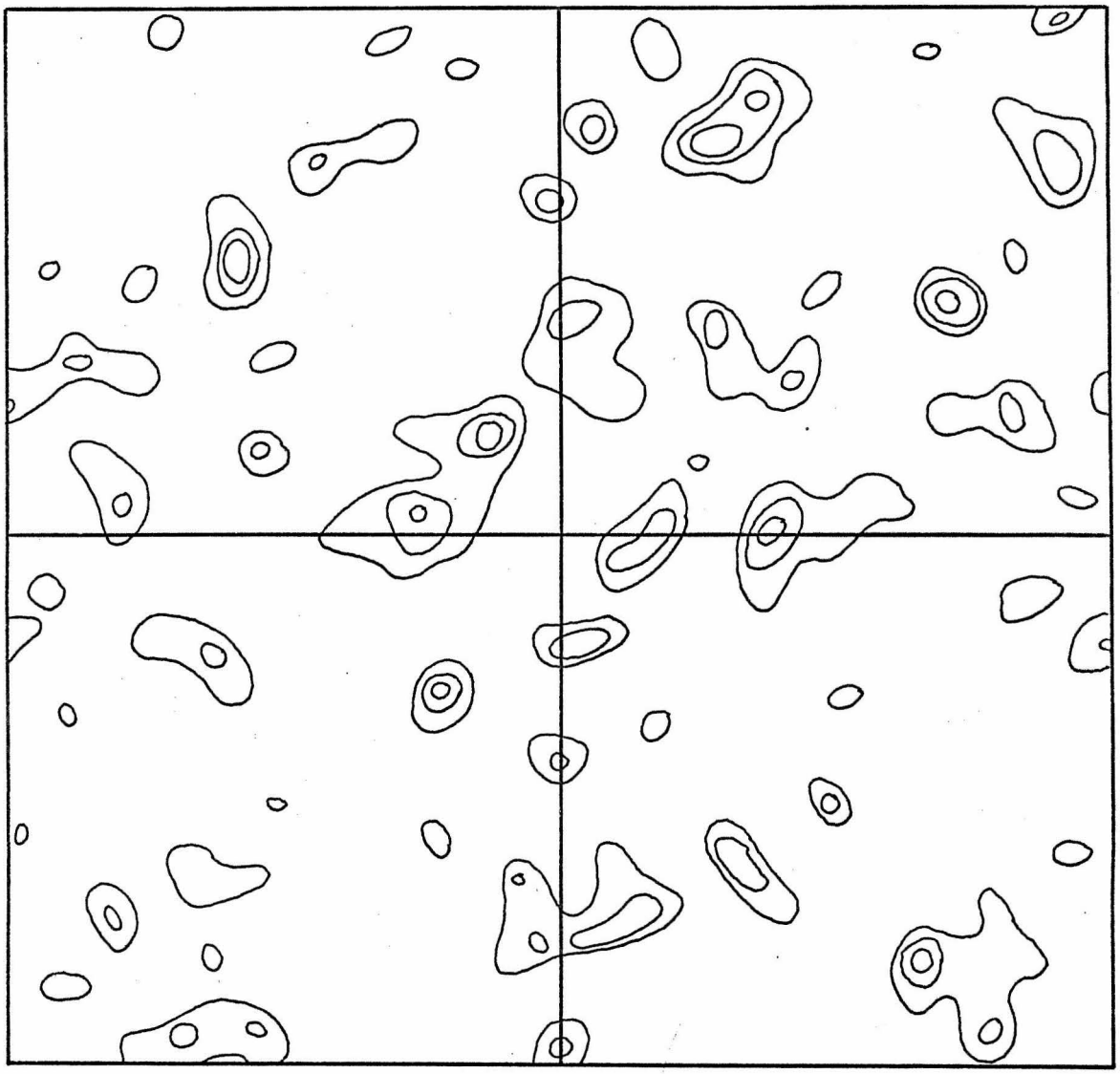

z= 11/48

APPENDIX VIII

TWO DERIVATIVE FOURIER

The following Fourier was calculated on the basis of the new native data set, the platinum derivative data set, and the mercury derivative data set. The map is on the same arbitrary scale as the single isomorphous replacement Fourier map. The contour interval is 50, starting at a height of 100. The contour at height 75 has been added to increase the conectivity of the map. One complete asymmetric unit is shown: x from 0.0 to 1.0, y from 0.0 to 1.0, and z from 0.0 to 0.25. The scale is approximately 3.8 Å/cm.

The most obvious feature of this map is the extremely well formed heme group, centered on section seven. The normal to the heme is parallel to the plane of the section. A space filling model of the heme and the adjacent, attached polypeptide chair fits these contours very well. The second most obvious feature of the map is the lack of indication of any α-helix in the structure. The molecule appears to be formed from extended chain with the hydrophobic residues located on the interior of the molecule.

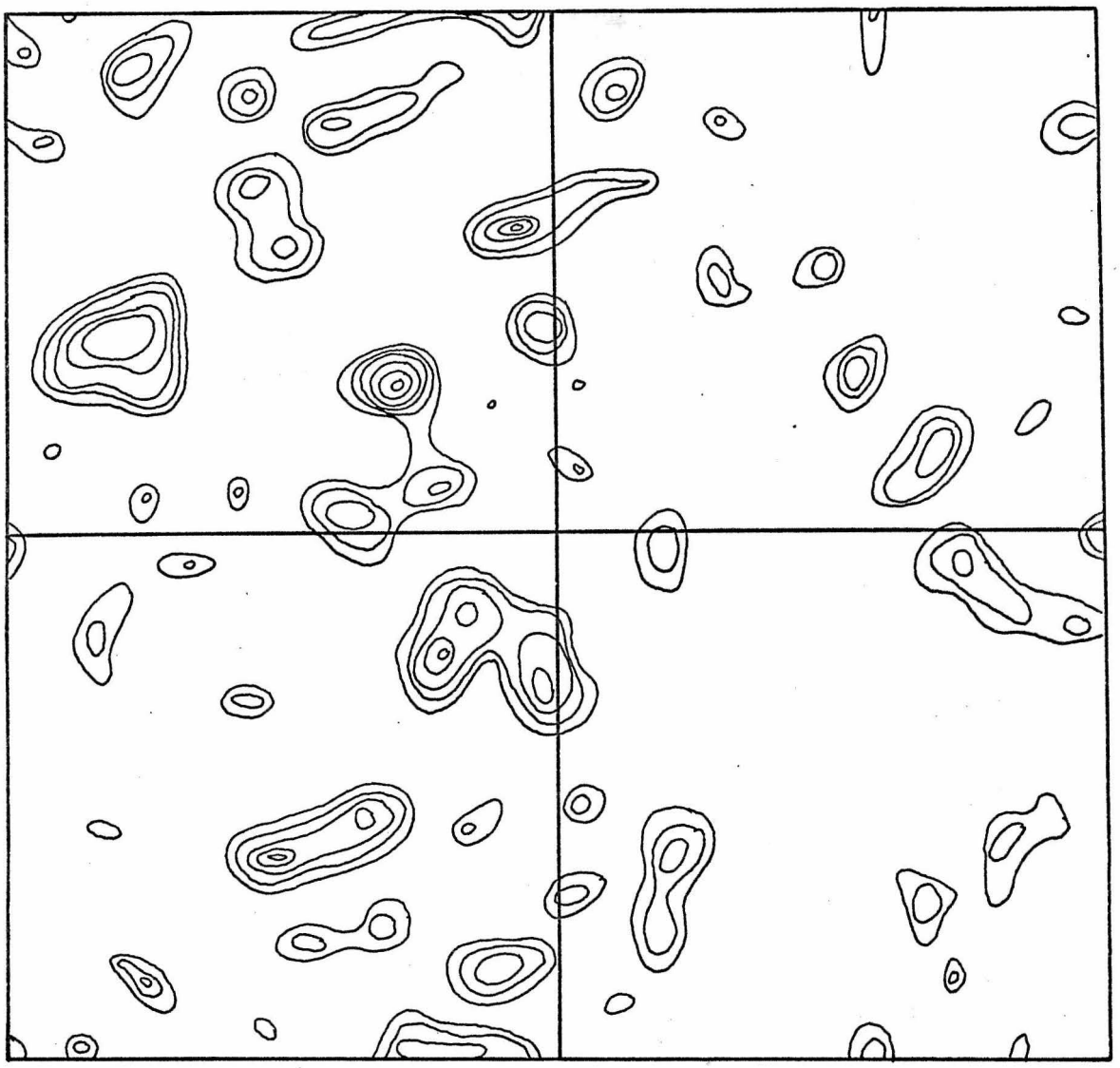

DOUBLE ISOMORPHOUS REPLACEMENT FOURIER BASED ON THE PLATINUM AND MERCURY DERIVATIVES

Origin: Upper Left Hand Corner
x: Left to Right; 0.0 to 1.0
y: Top to Bottom; 0.0 to 1.0

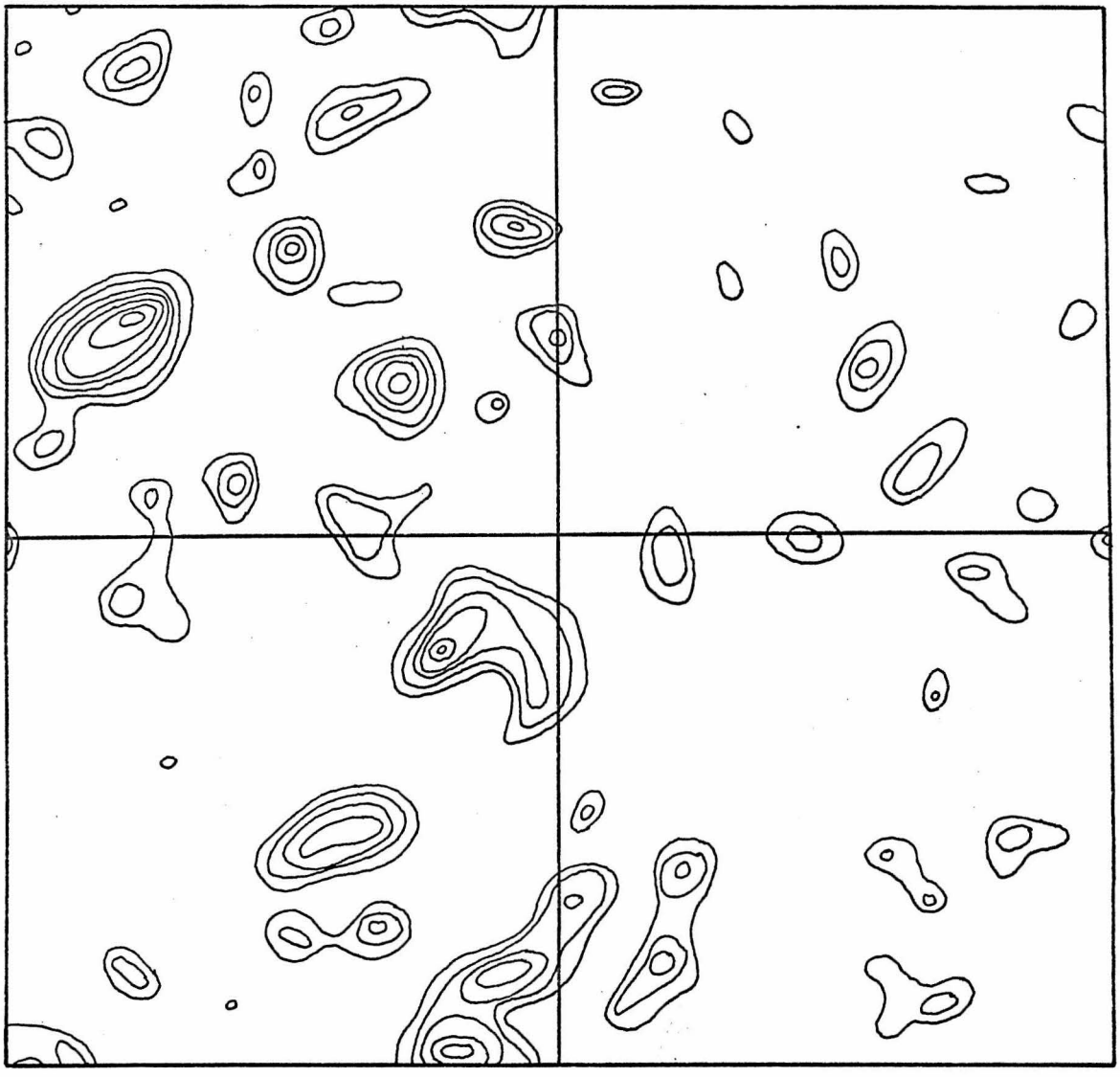

z= 1/48

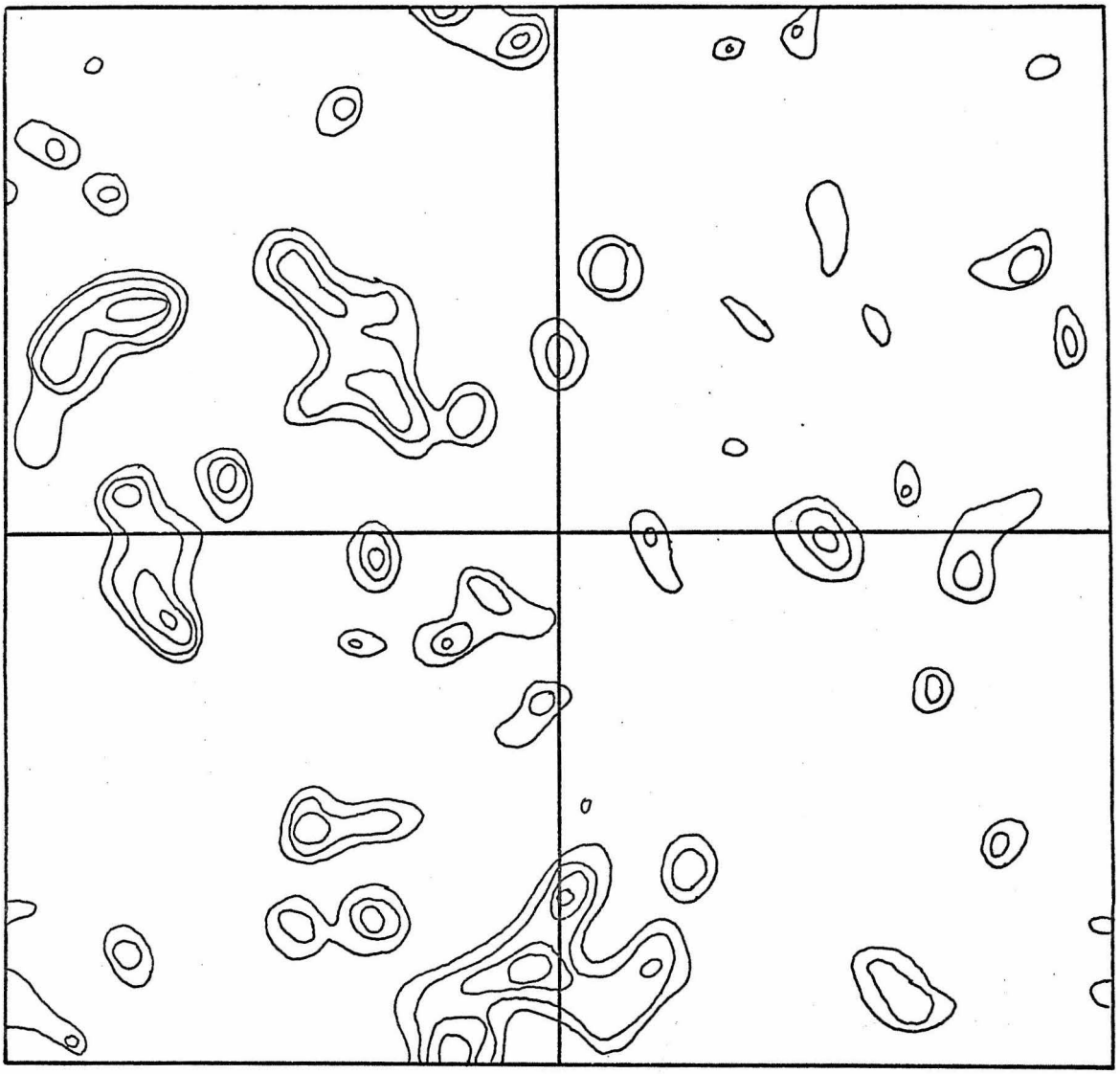

z= 2/48

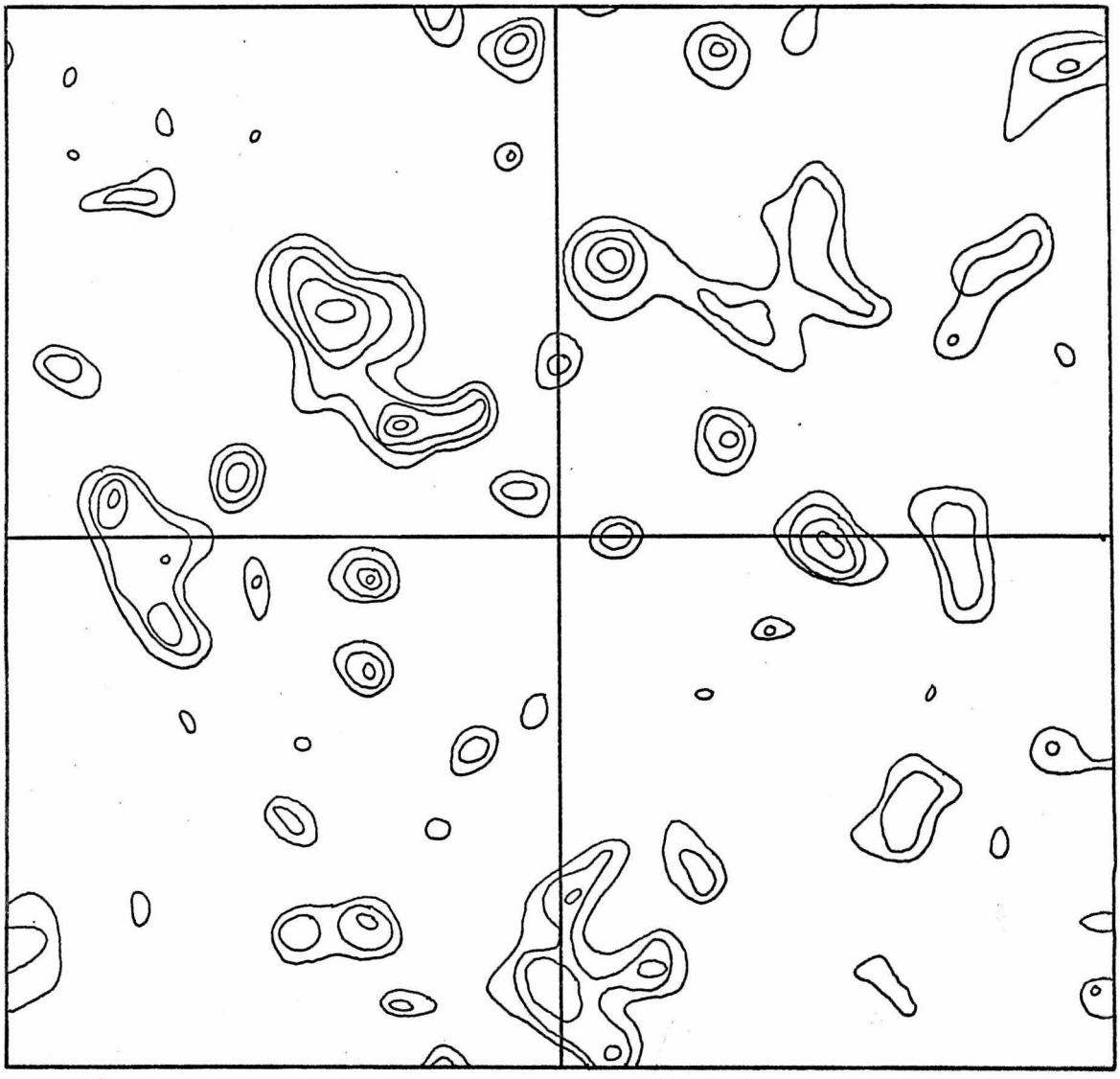

z= 3/48

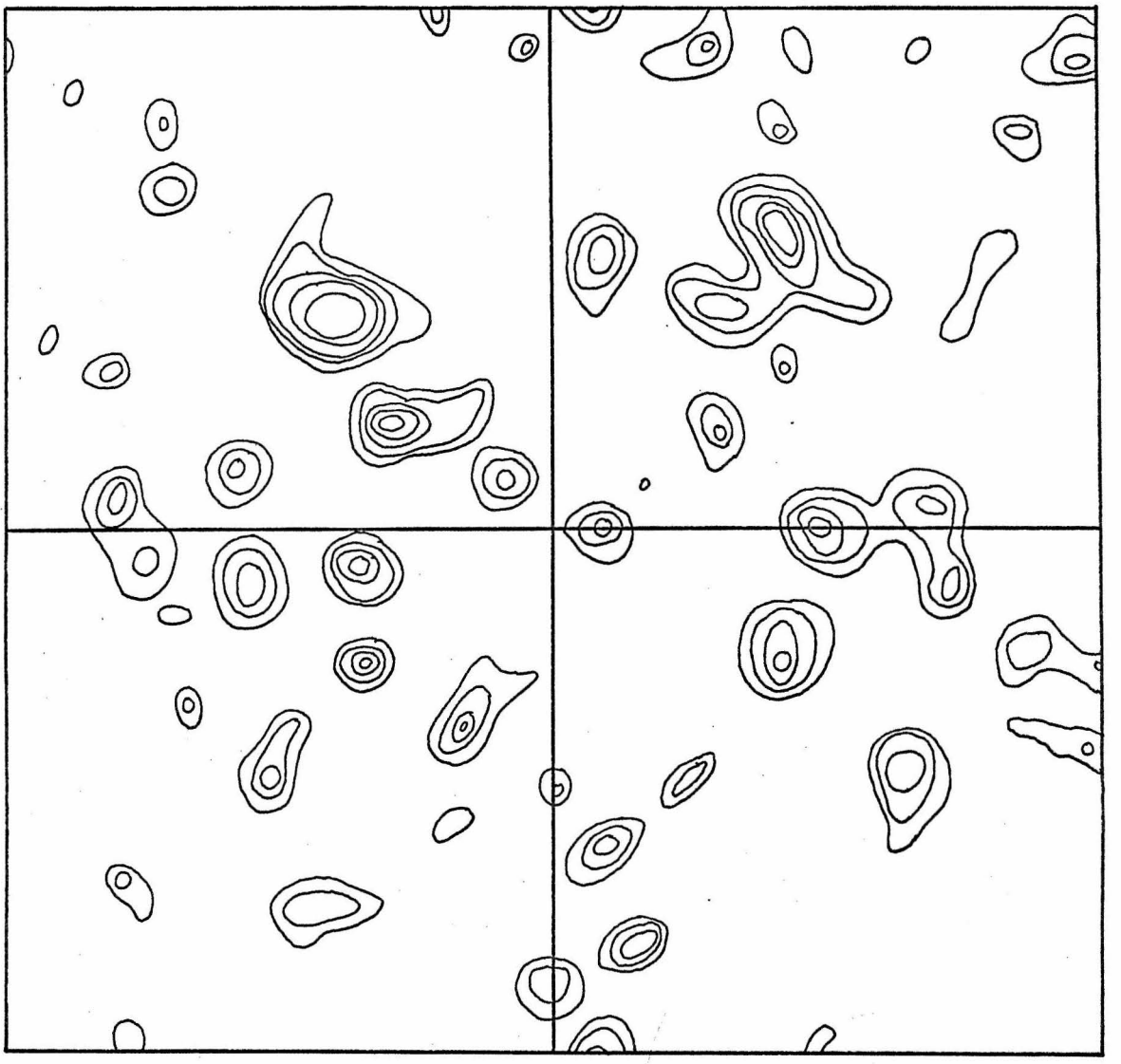

z= 4/48

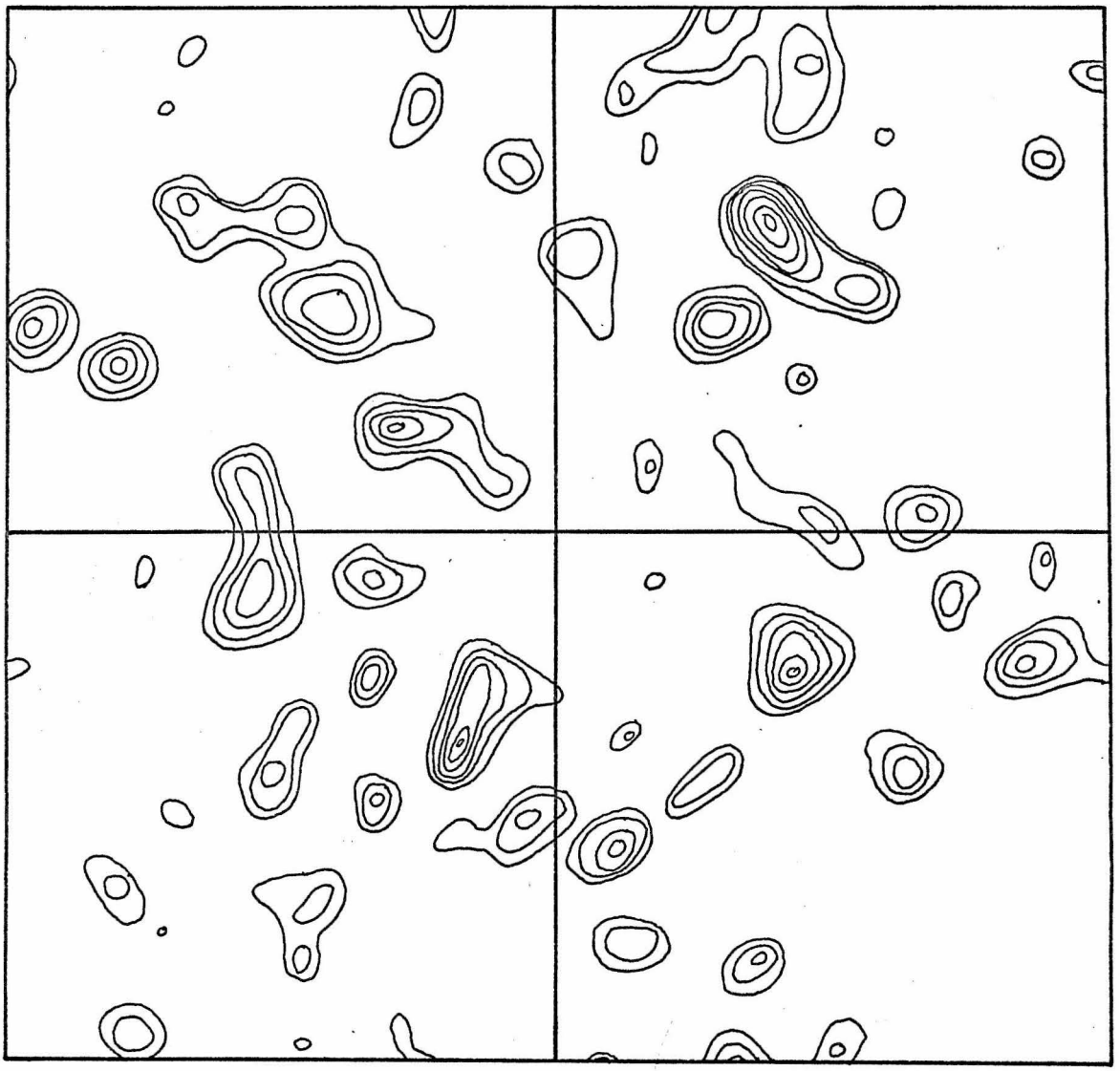

z= 5/48

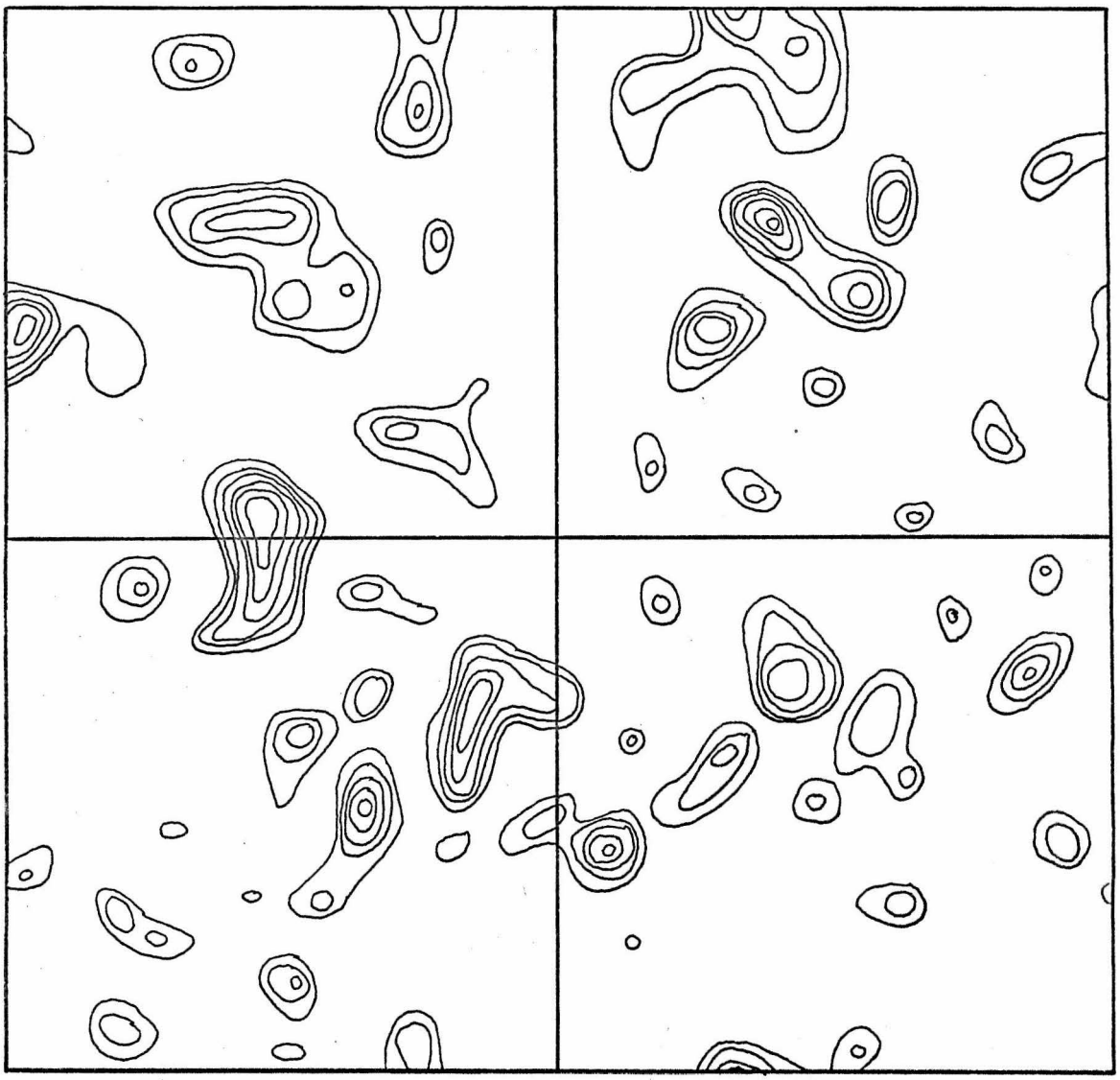

z= 6/48

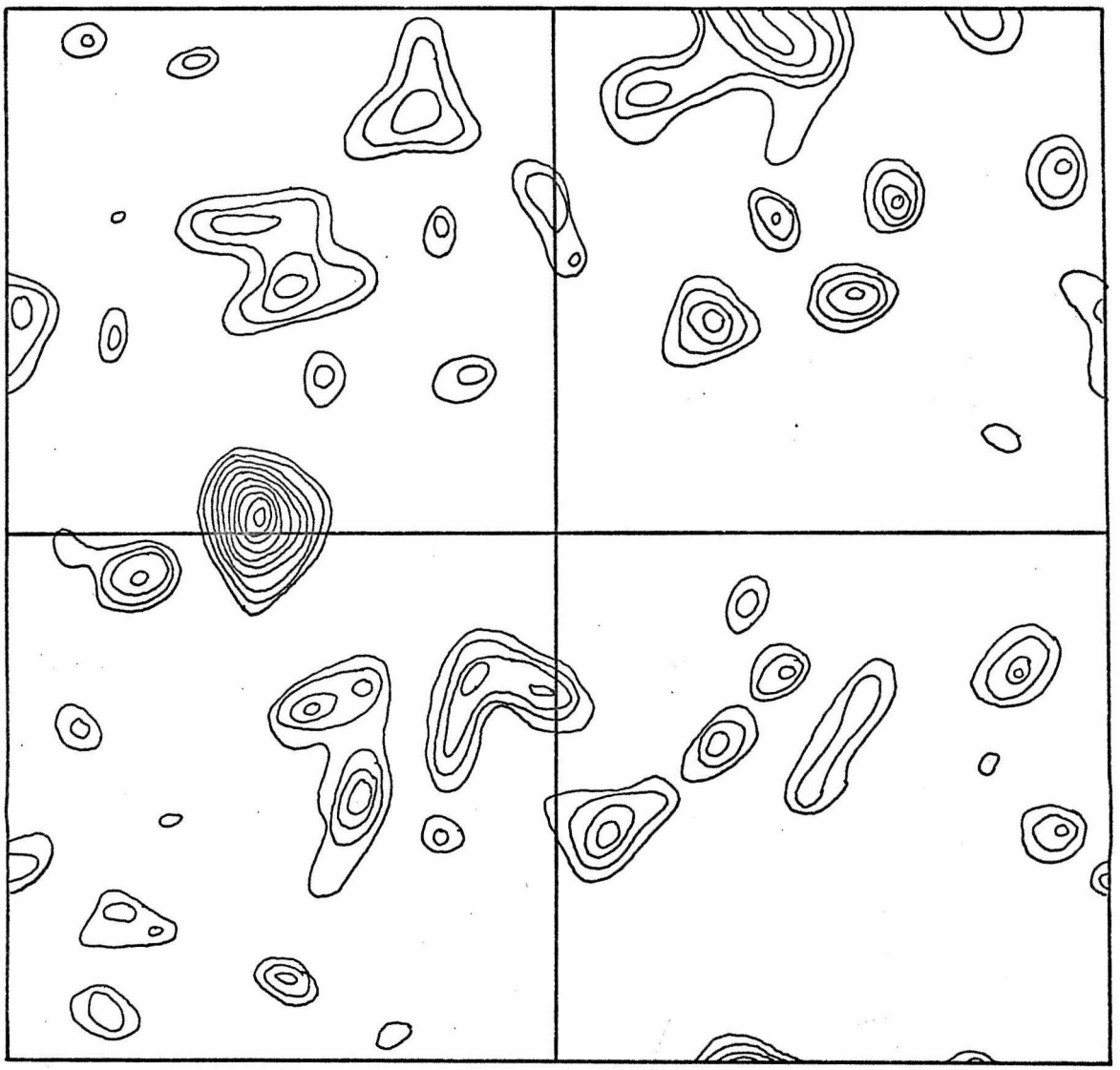

z= 7/48

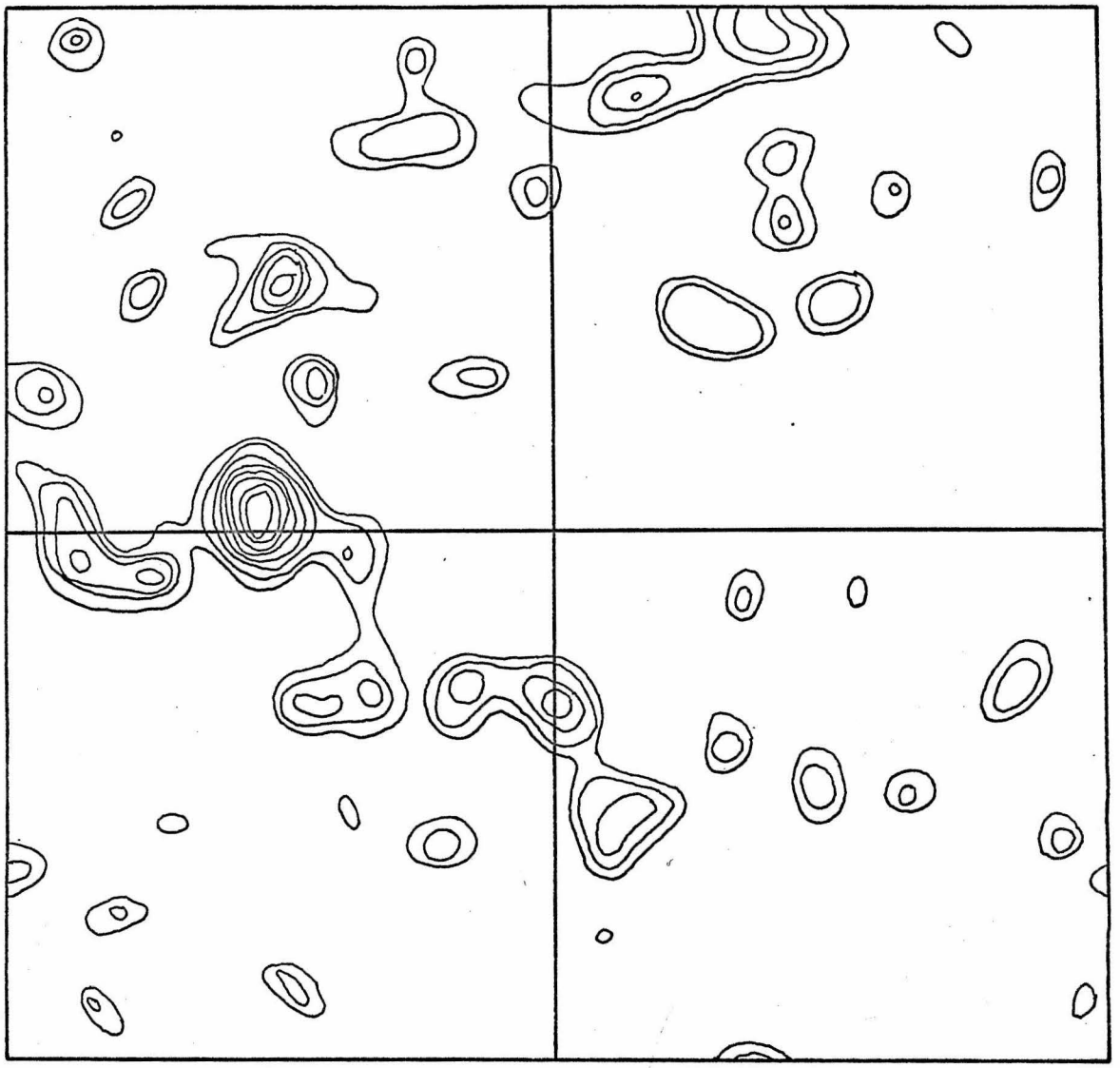

z= 8/48

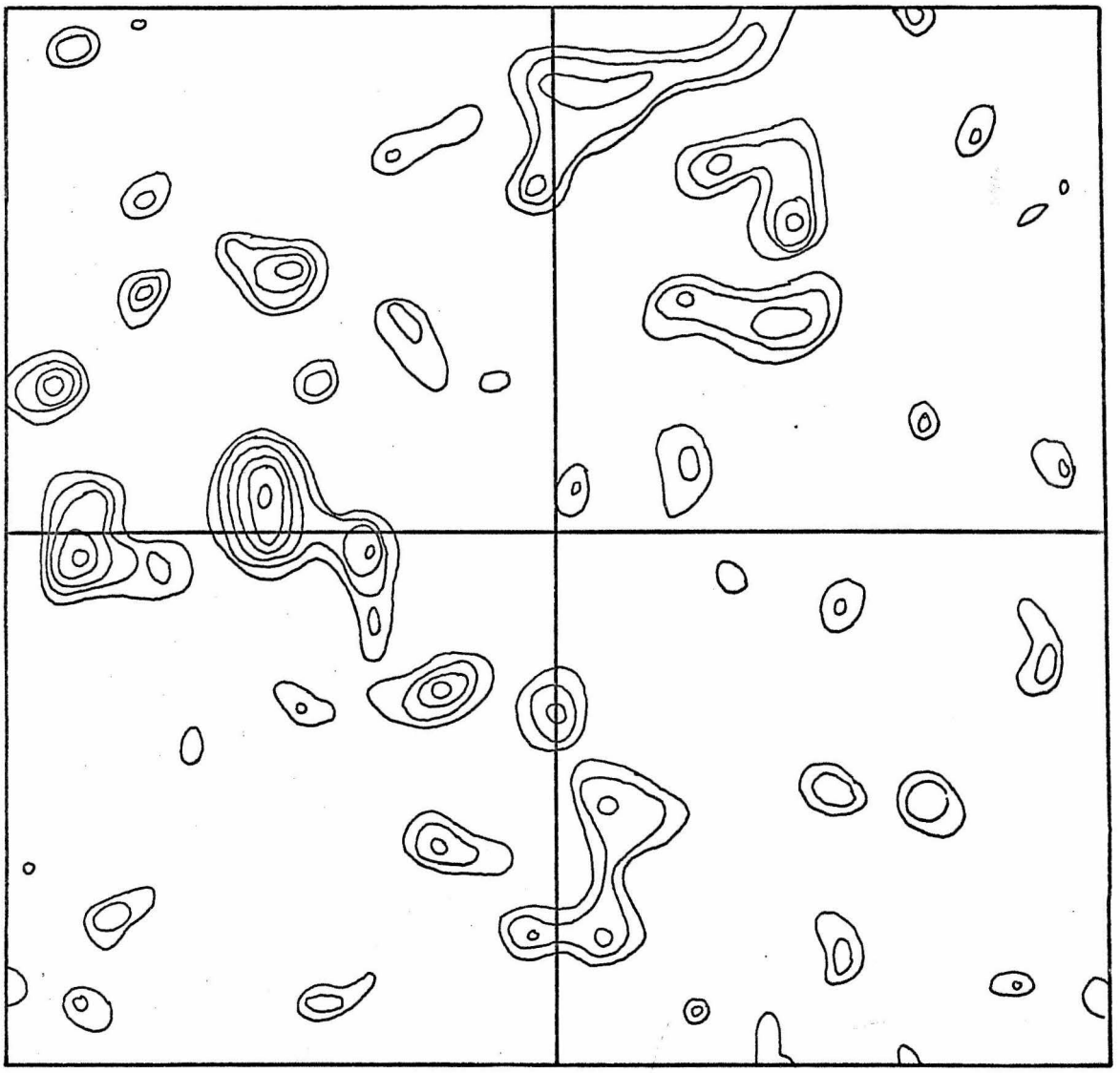

z= 9/48

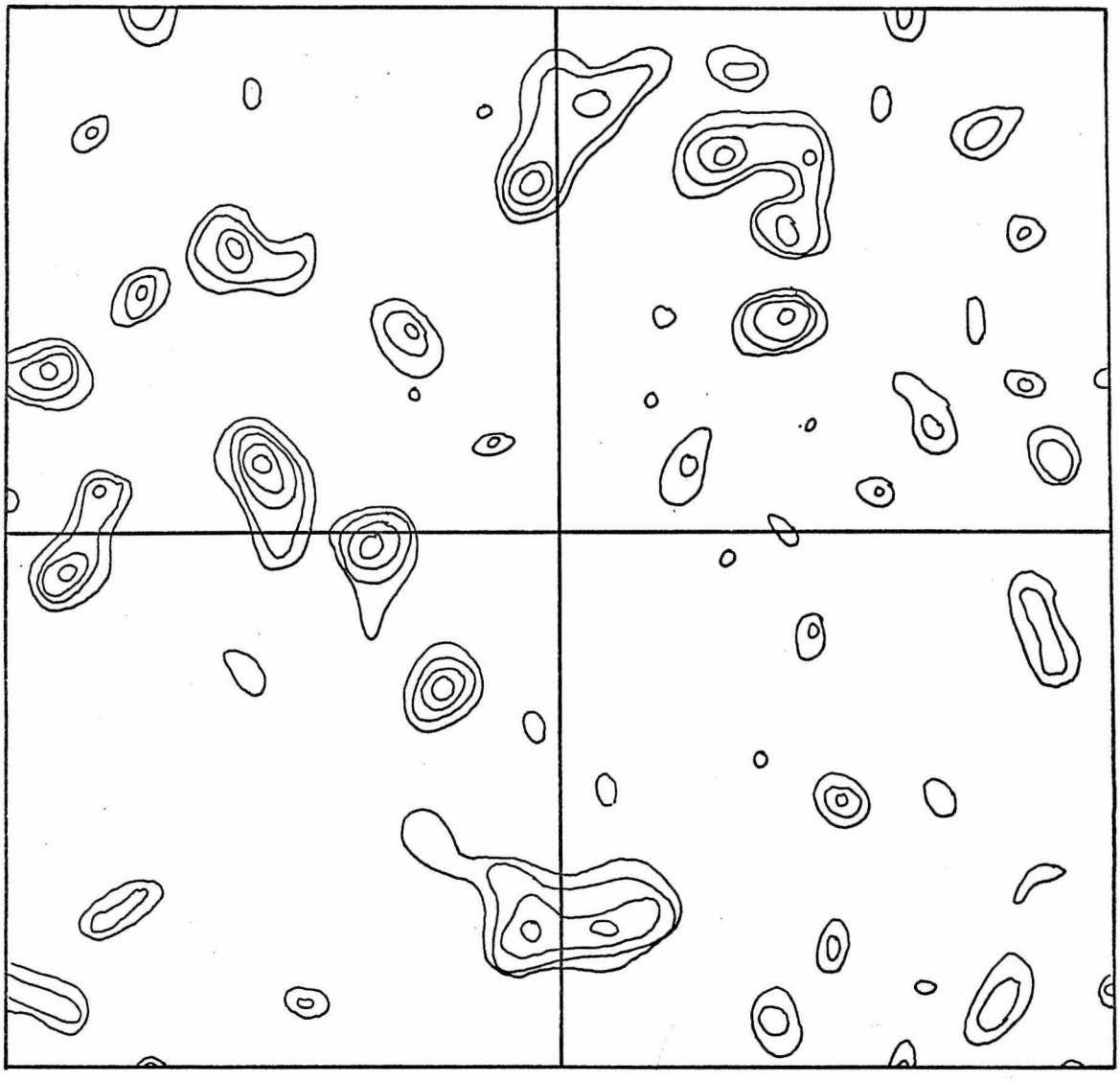

z= 10/48

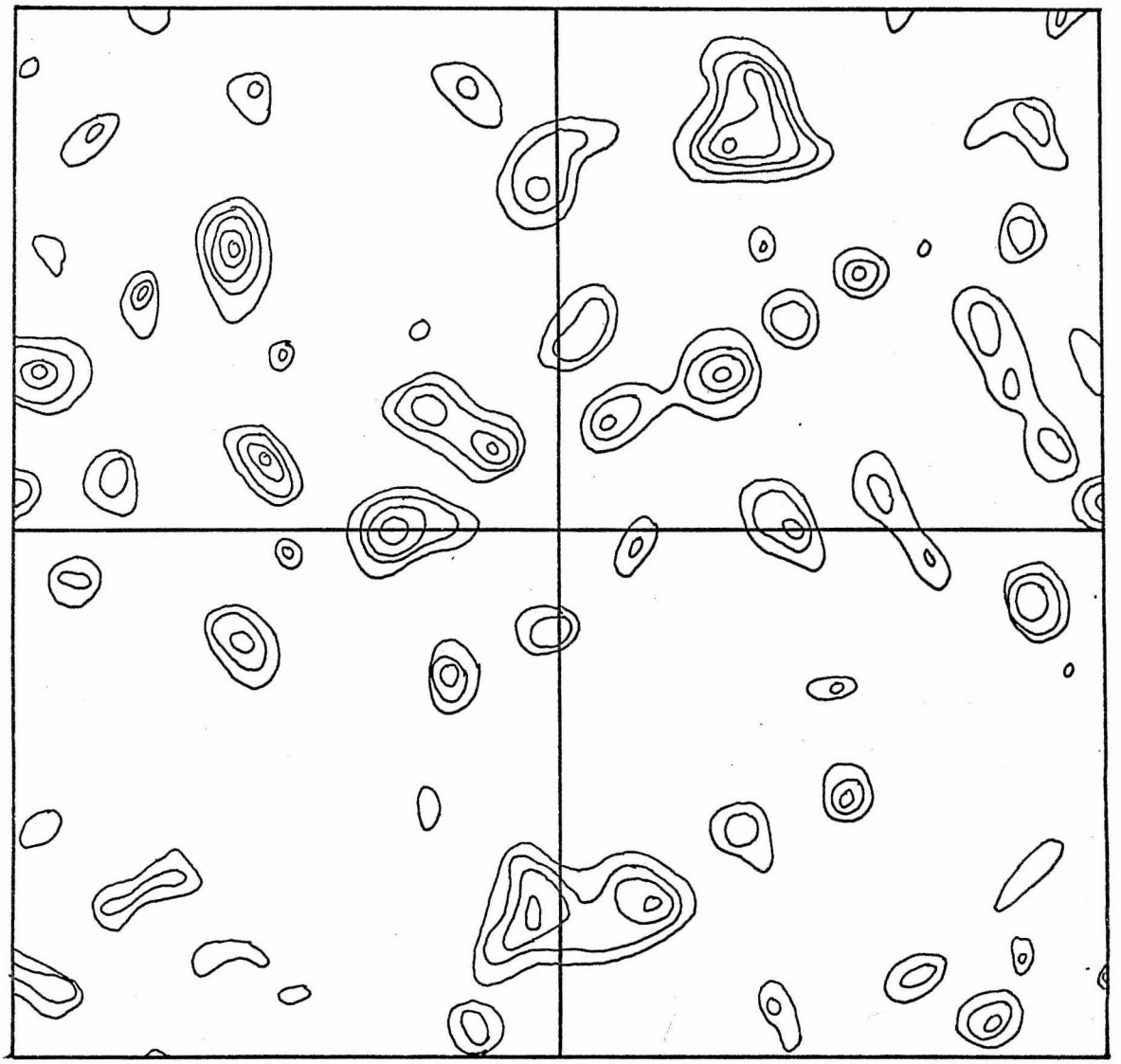

z= 11/48

APPENDIX IX

TWO DERIVATIVE FOURIER REFINED BY MEANS OF THE KARLE HAUPTMAN-TANGENT FORMULA

The following map is the Karle-Hauptman refined product of the two derivative Fourier in Appendix VIII. The map is on approximately the same scale as the two derivative Fourier. The contour interval is also the same. One complete asymmetric unit is shown: x from 0.0 to 1.0, y from 0.0 to 1.0, and z from 0.0 to 0.25.

This map is very similar to the two derivative Fourier. In general, the electron density has increased in those regions of the map which have been attributed to polypeptide. This is most clear in the polypeptide region joining the two cysteines which bind the heme group. In addition, the position attributed to Met 80, which is supposed to coordinate the 6'th coordination position of the Fe atom has become higher in this map.

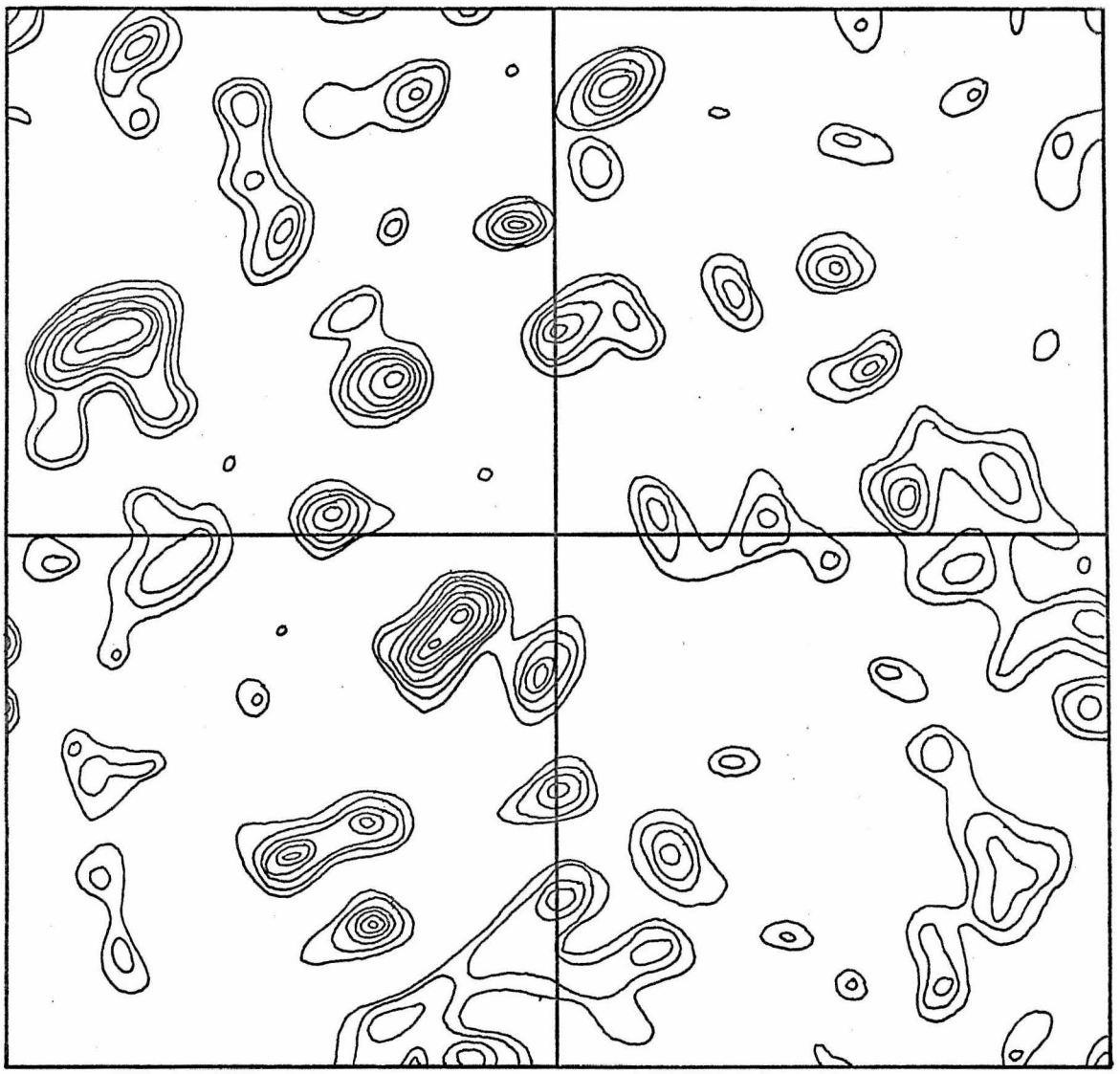

DOUBLE ISOMORPHOUS REPLACEMENT FOURIER REFINED
BY MEANS OF THE KARLE-HAUPTMAN TANGENT FORMULA

Origin: Upper Left Hand Corner
x: Left to Right; 0.0 to 1.0
y: Top to Bottom; 0.0 to 1.0

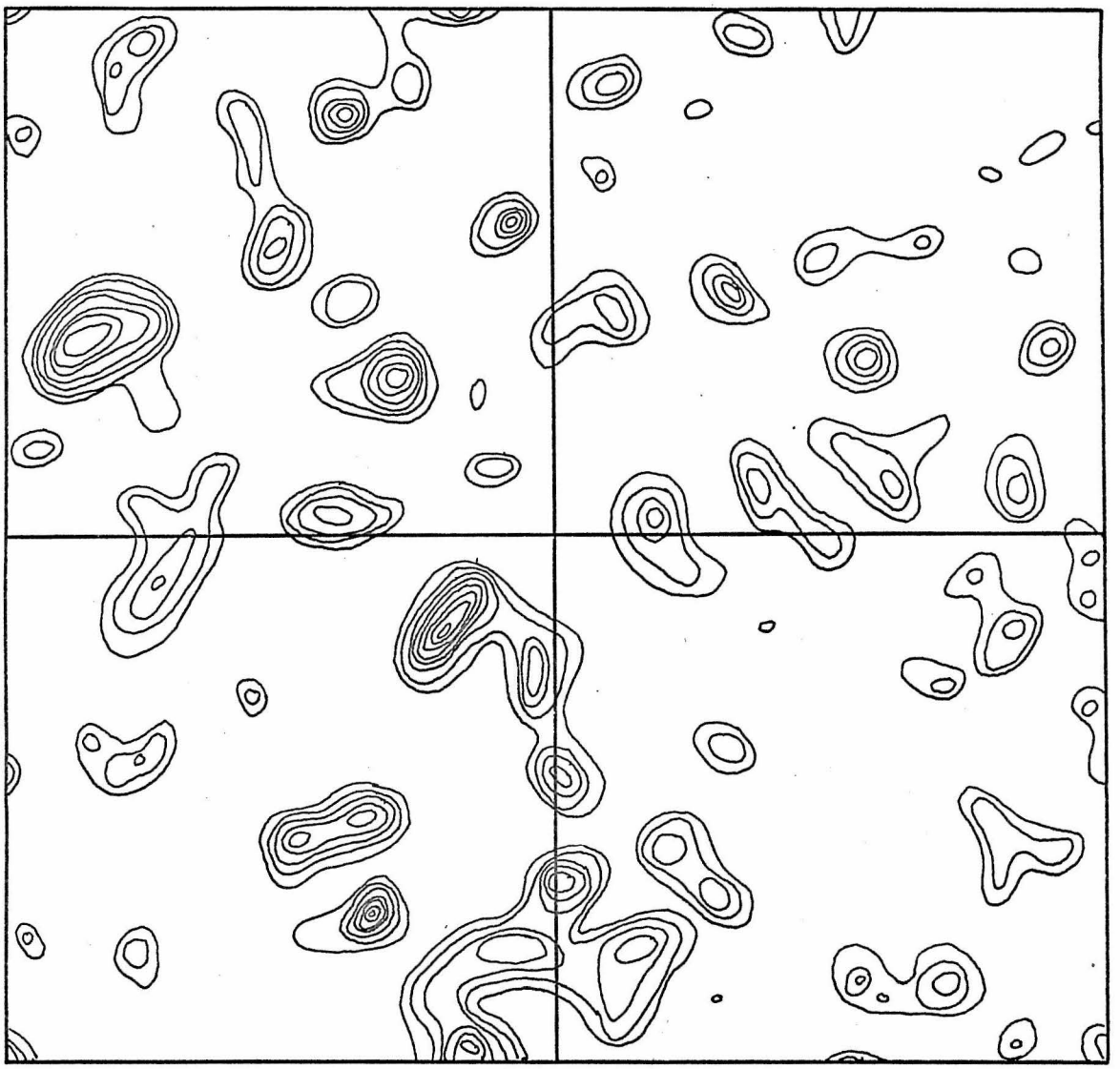

z= 1/48

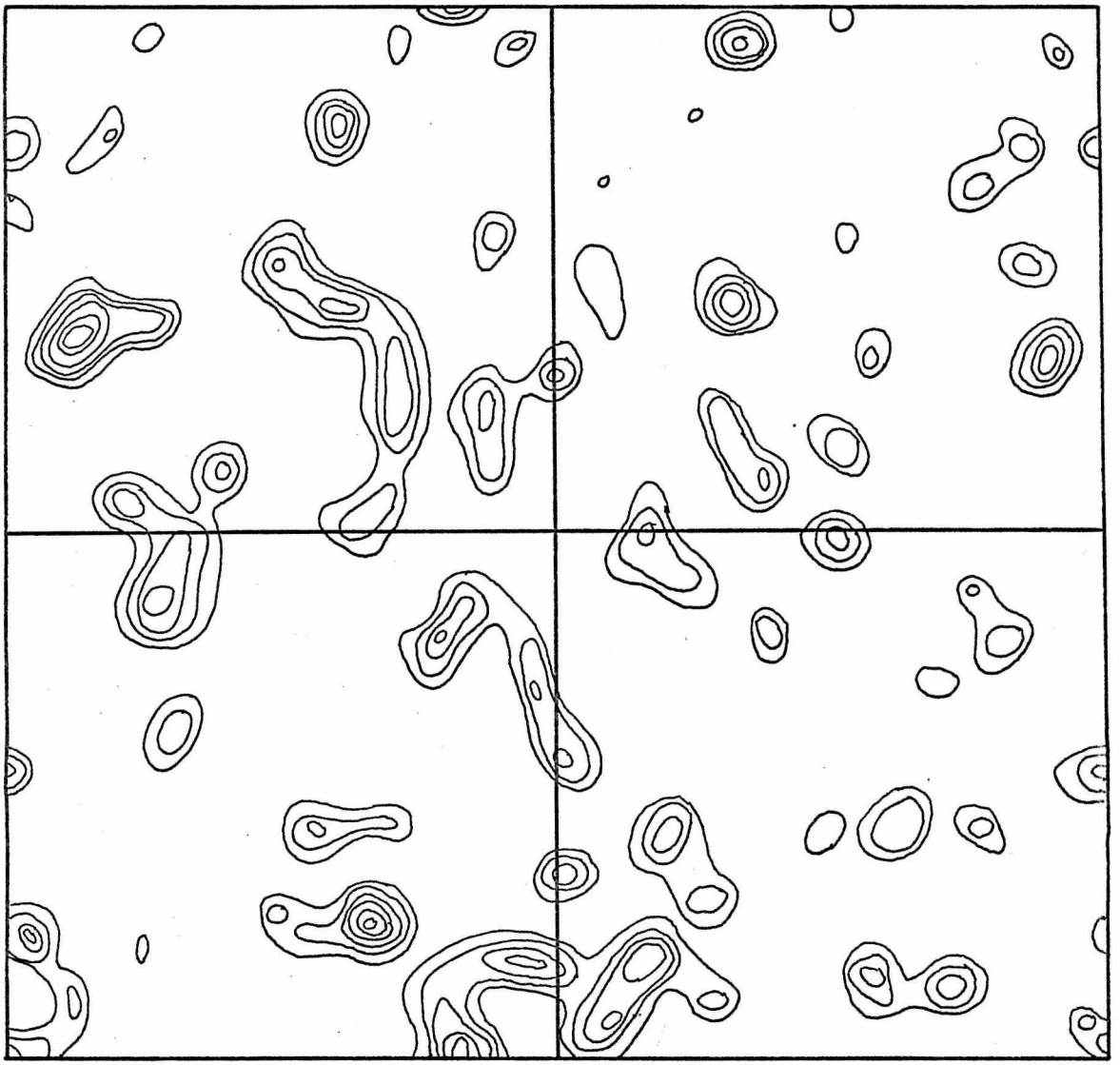

z= 2/48

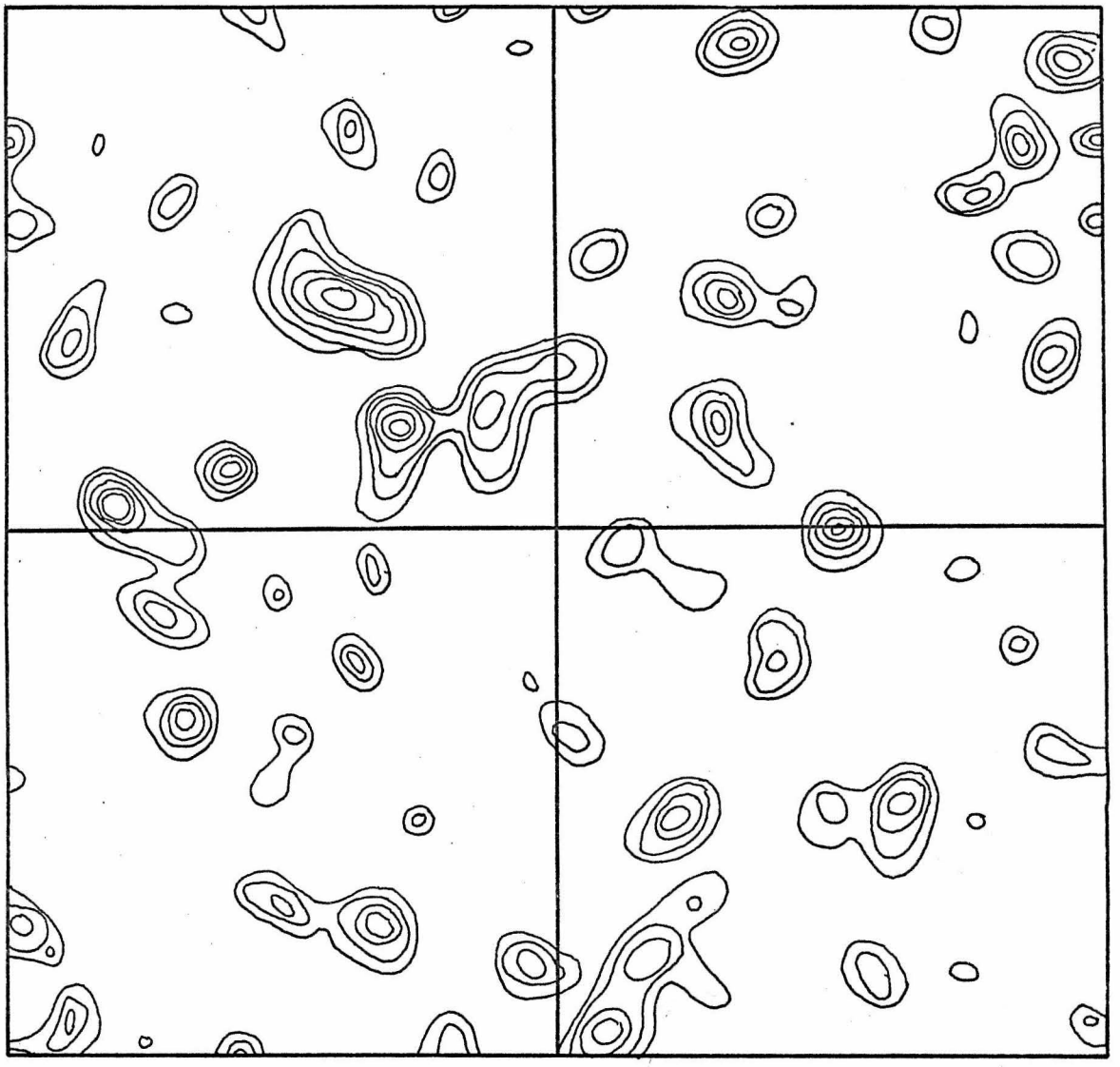

z= 3/48

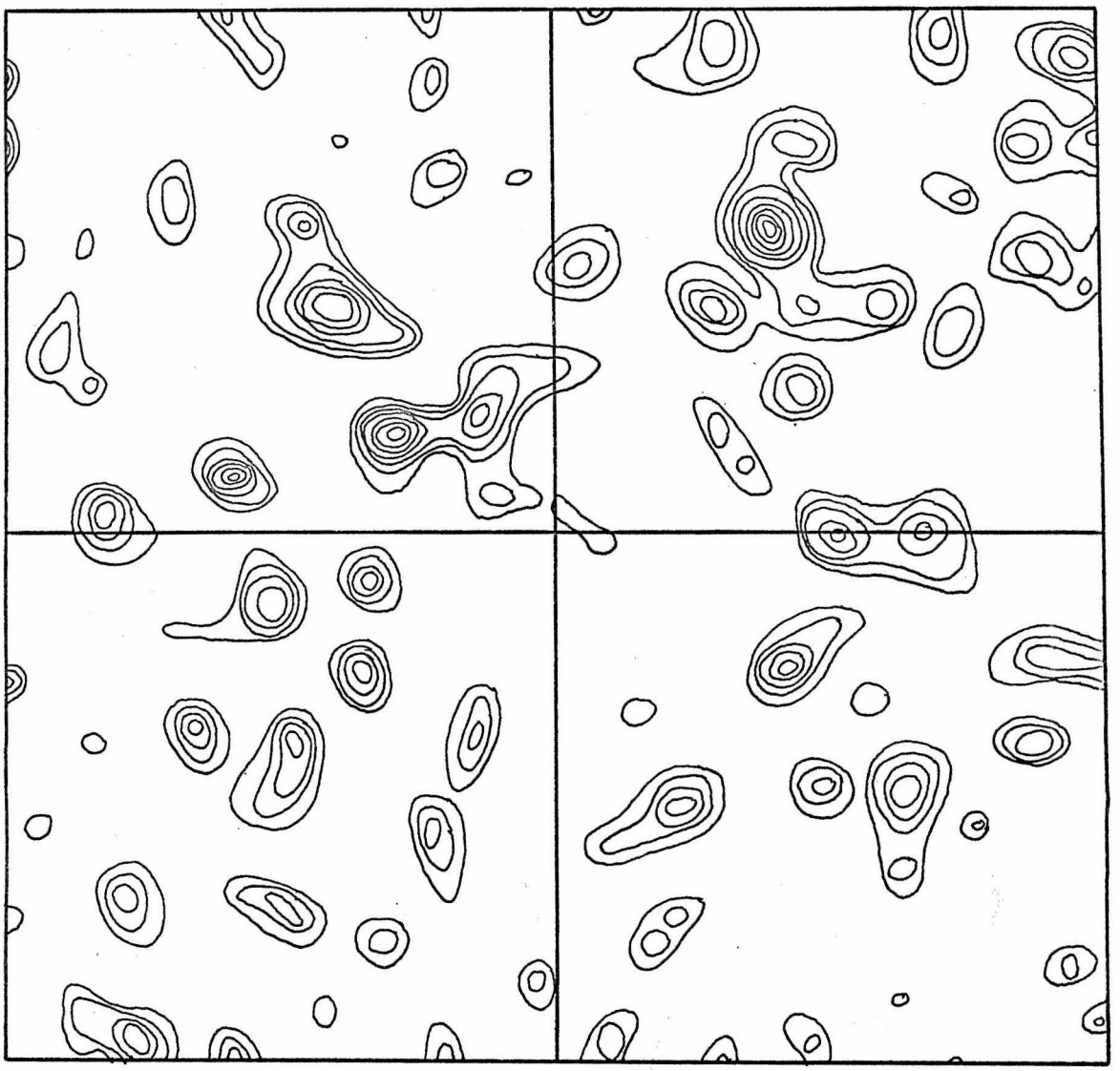

z= 4/48

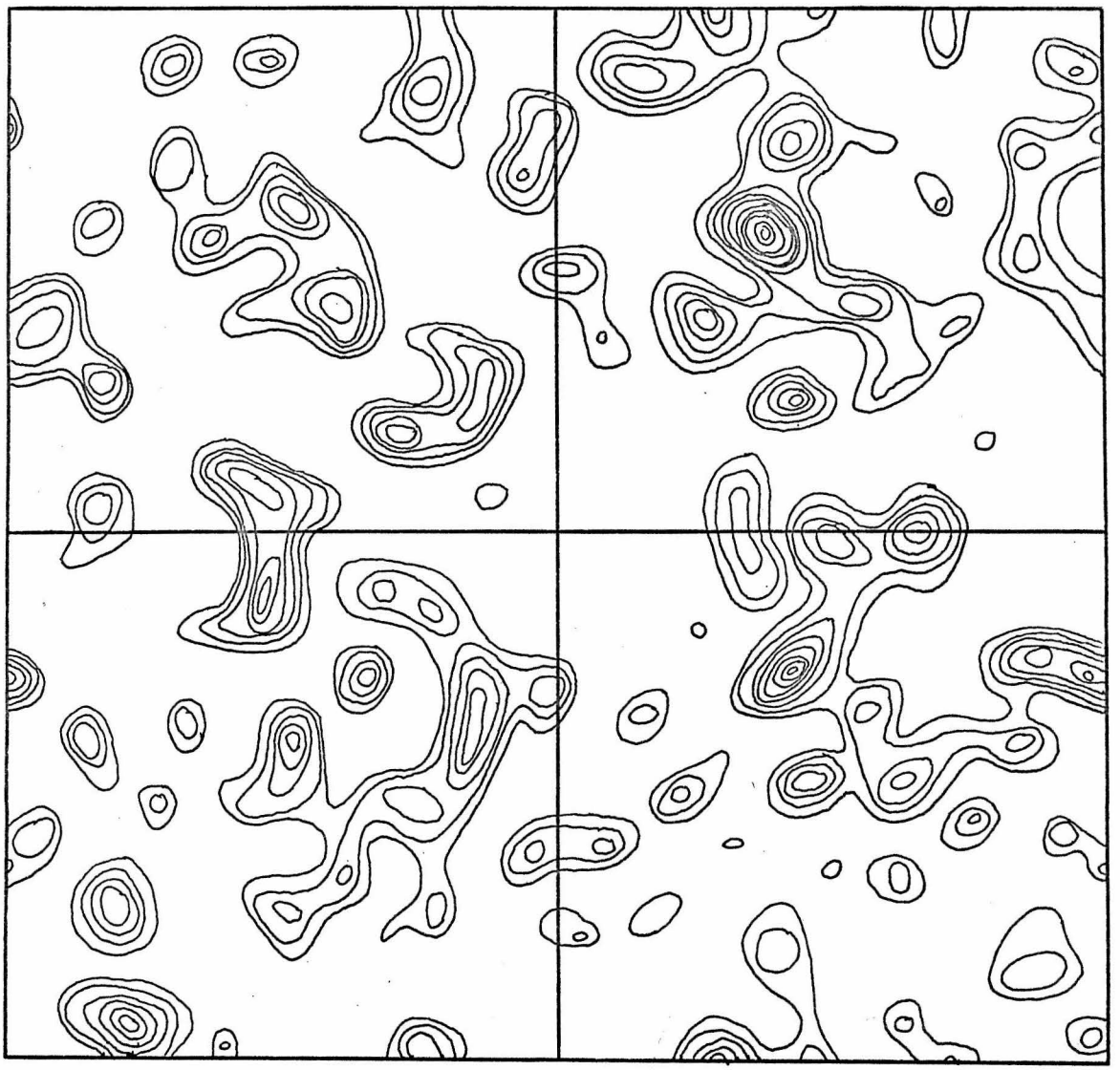

z= 5/48

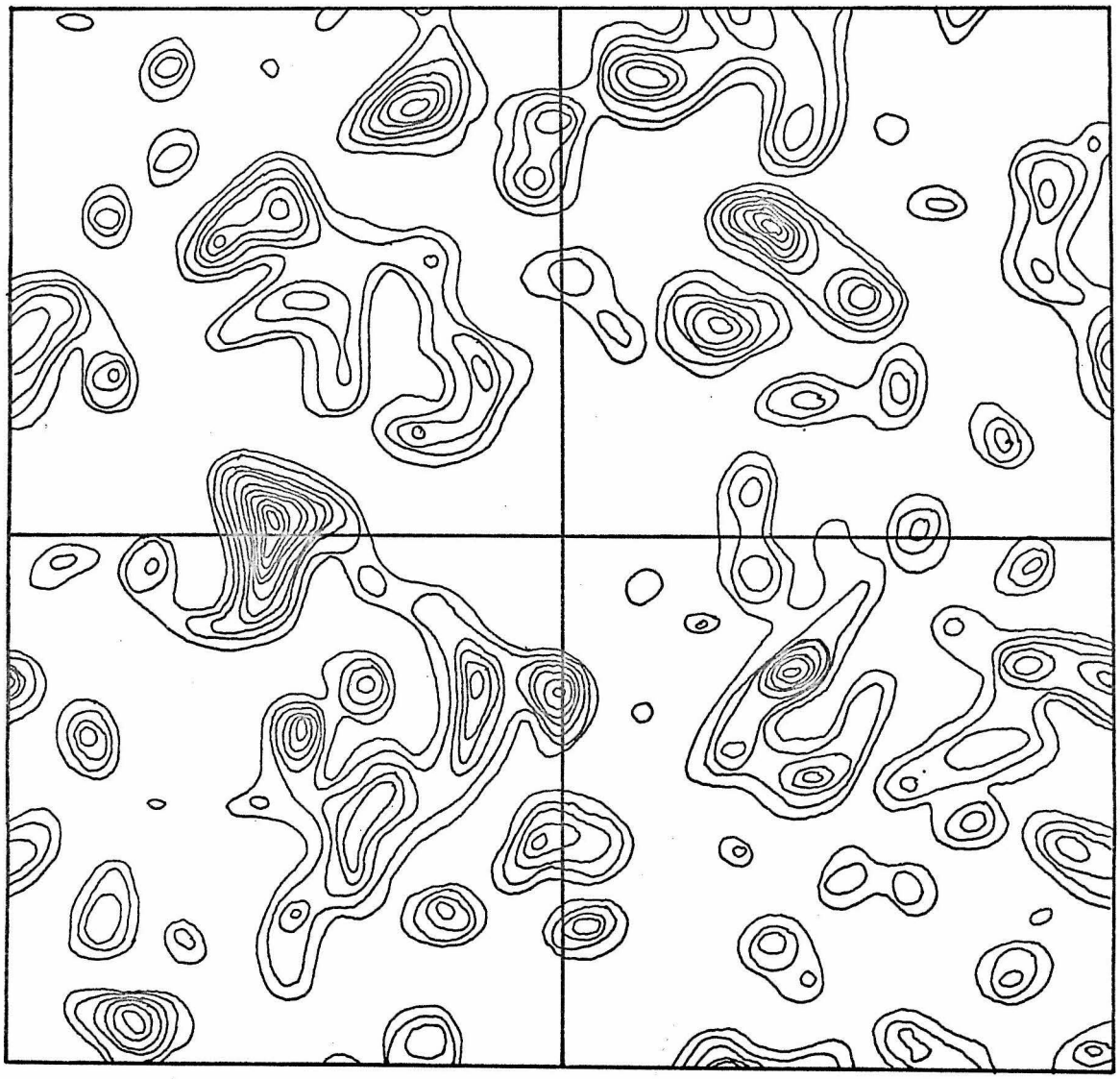

z= 6/48

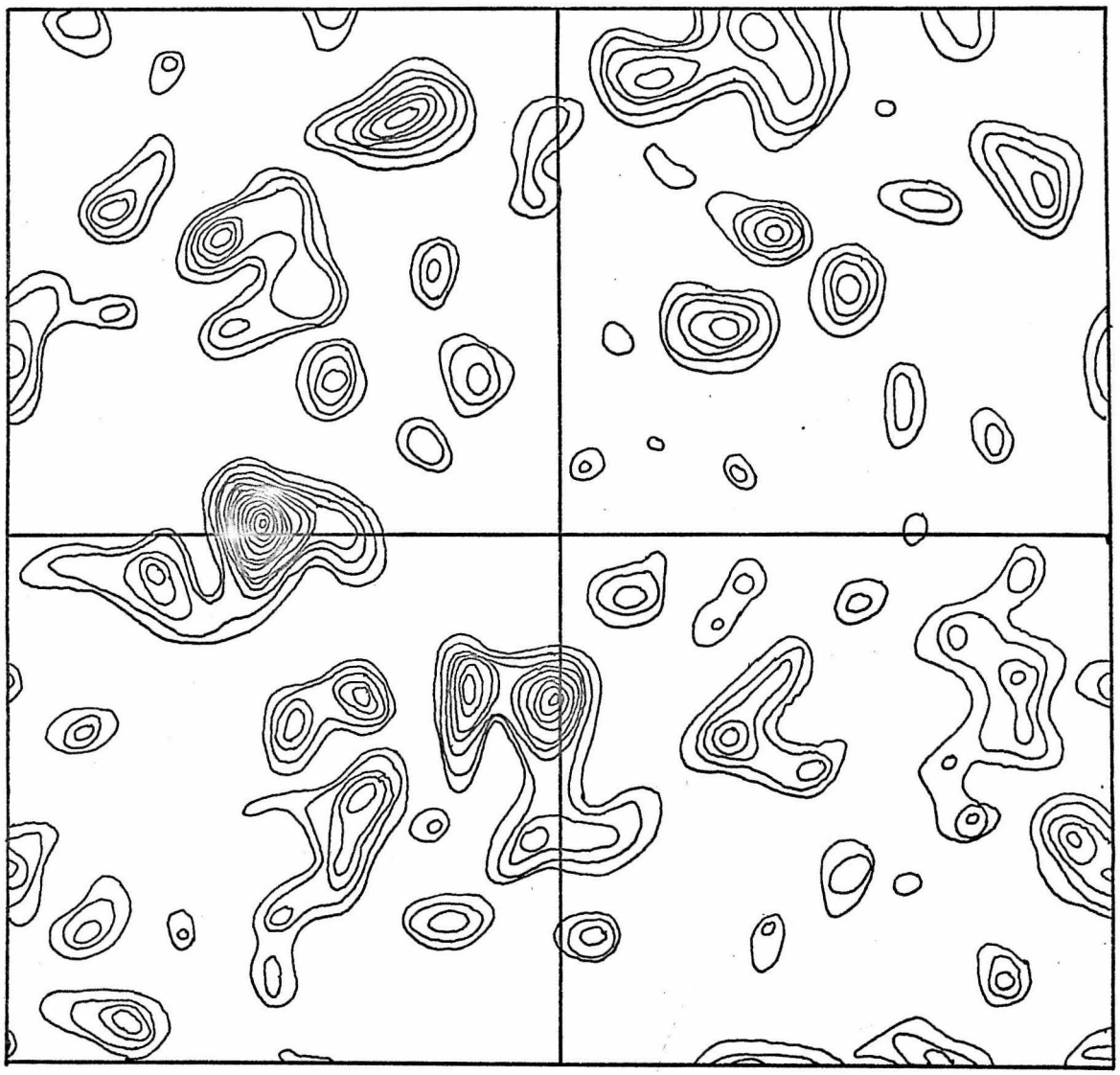

z= 7/48

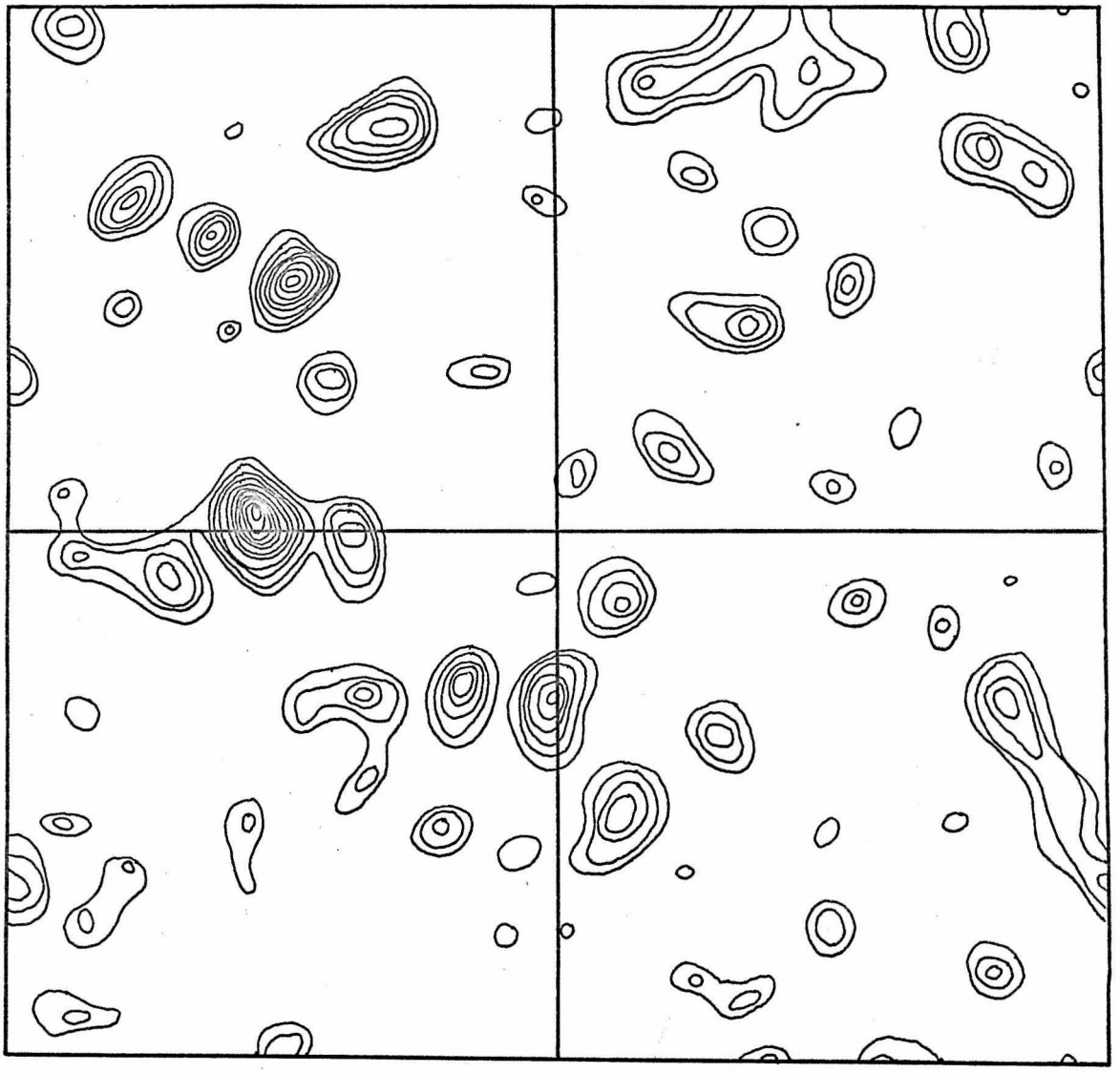

z= 8/48

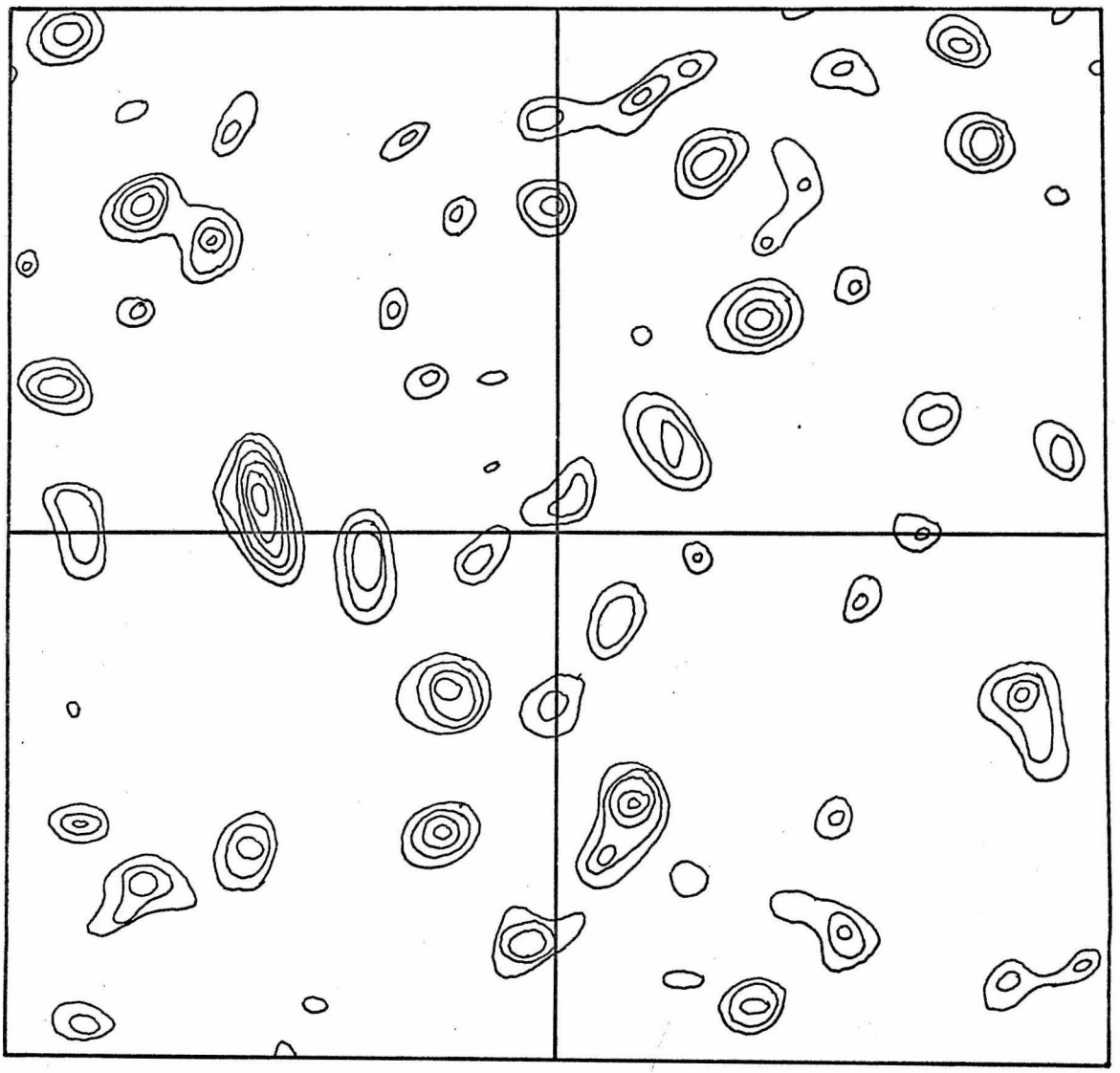

z= 9/48

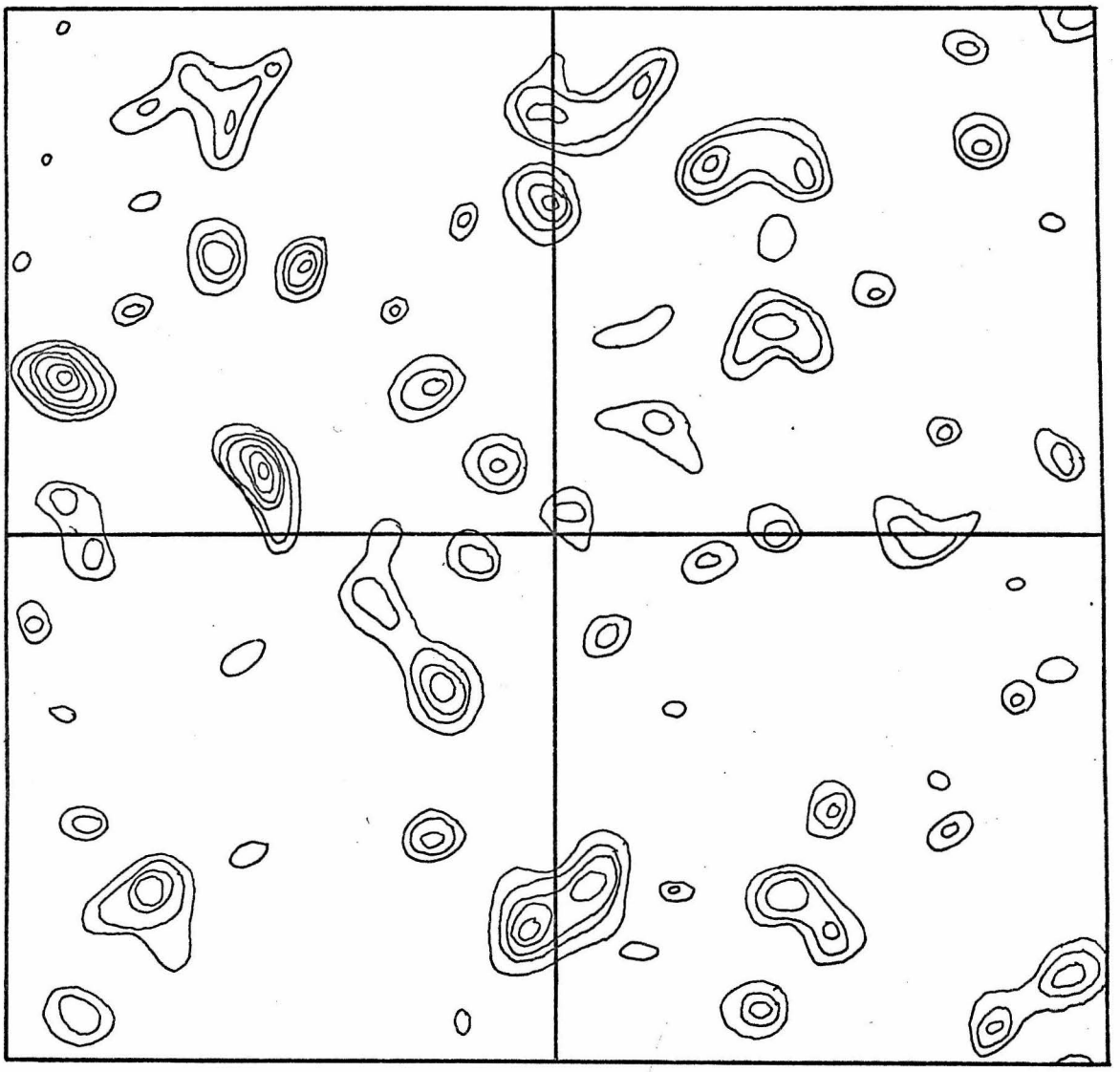

z= 10/48

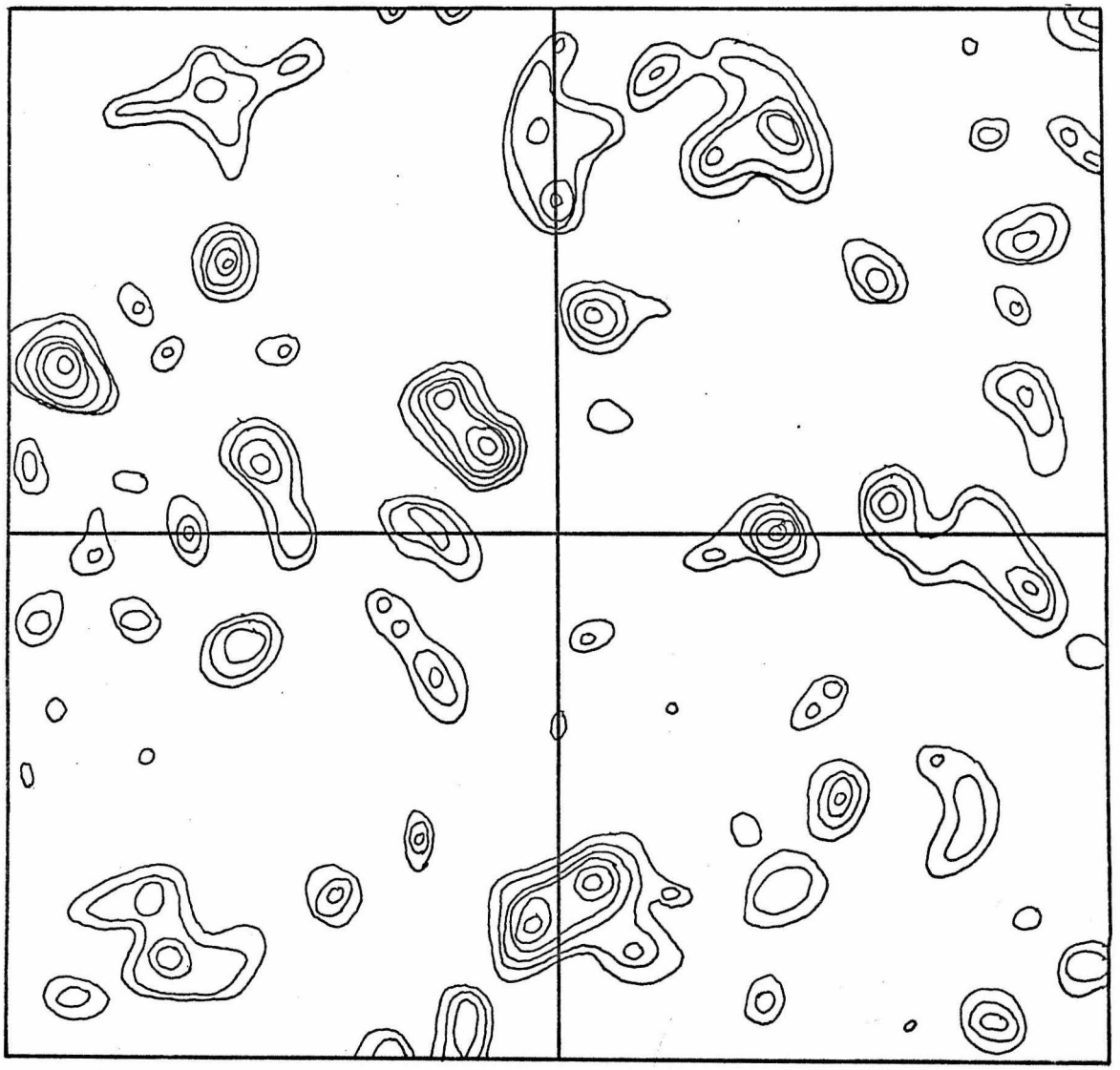

z= 11/48

BIBLIOGRAPHY

1. Ando, K., Matsubara, H., and Okunuki, K., Proc. Japan Acad., 41, 79, (1965).

2. Blout, E. R., In Polyamino Acids, Polypeptides and Proteins (M. A. Stahmann, ed.), p. 275. University of Wisconsin Press, Madison, Wisconsin.

3. Blow, D. M. and Crick, F. H. C., Acta Cryst., 12, 794, (1959).

4. Dickerson, R. E., Acta Cryst., 12, 610, (1959).

5. Dickerson, R. E., Kendrew, J. C. and Strandberg, B. E., Acta Cryst., 14, 1188, (1961).

6. Eaton, W. A., and Hochstrasser, R. M., J. Chem. Phys., in press.

7. Harbury, H. A., Cronin, J. A., Fanger, M. W., Hettinger, T. P., Murphy, A. J., Myer, Y. P., and Vinogradov, S. N., Proc. Nat. Acad. Sci. U.S.A., 54, 1658 (1965).

8. Kabat, D., J. Mol. Biol, 6 (11), 3443, (1967).

9. Karle, J., and Karle, I. L., Acta Cryst., 21, 849, (1966).

10. Kautzman, W., Advances in Protein Chem., Vol. 14, pp. 1-63, (1959).

11. Levin, O., Arch. Biochem. Biophys. (Suppl. 1), p. 301, (1962).

12. Levin, O., J. Mol. Biol., 6, 137, (1963).

13. Margoliash, E., Kimmel, J. R., Hill, R. L., and Schmidt, W. R., J. Biol. Chem., 237, 2148, (1962).

14. Margoliash, E., and Schejter, A., Advance. Protein Chem., 21, 113, (1966).

15. Margoliash, E., and Walasek, O. F., In Methods in Enzymology, Vol. 10 (S. P. Colowick and N. O. Kaplan, eds.)., Academic Press, New York.

16. Minakami, S., Titani, K., and Ishikura, H., J. Biochem. (Tokyo), 45, 341, (1958).

17. Okunuki, K., Wada, K., Matsubara, H., and Takemori, S., In Oxidases and Related Redox Systems (T. E. King, H. S. Mason, and M. Morrison, eds.), John Wiley and Sons, Inc., New York.

18. Sano, S., Nanzyo, N., and Rimington, C., Biochem. J. (London), 93, 270 (1964).

19. Stellwagen, E., J. Biol. Chem., 242, 602 (1967).

20. Takahashi, K., Titani, K., Furuno, K., Ishikura, H., and Minakami, S., J. Biochem. (Tokyo), 45, 375, (1958).

21. Titani, K., Ishikura, H., and Manakami S., J. Biochem. (Tokyo), 46, 151, (1959).

REFERENCES TO PUBLISHED PAPERS

I. Dickerson, R. E., Kopka, M. L., Varnum, J. C. and Weinzierl, J. E., "Bias, Feedback and Reliability in Isomorphous Phase Analysis", Acta Cryst. 23, 511-522, 1967.

II. Dickerson, R. E., Kopka, M. L., Borders, C. L., Jr., Varnum, J. and Weinzierl, J. E., "A Centrosymmetric Projection at 4 Å of Horse Heart Oxidized Cytochrome c", J. Mol. Biol. 29, 77-95, 1967.

III. Dickerson, R. E., Kopka, M. L., Weinzierl, J. E., Varnum, J., Eisenberg, D. and Margoliash, E., "Location of the Heme in Horse Heart Ferricytochrome c by X-ray Diffraction", J. Biol. Chem. 242, No. 12, 3015-3017, 1967.

IV. Dickerson, R. E., Kopka, M. L., Weinzierl, J. E., Varnum, J. C., Eisenberg, D. and Margoliash, E., "An Interpretation of a Two-Derivative, 4 Å Resolution Electron Density Map of Horse Heart Ferricytochrome C", Symposium on Cytochromes and Cytochrome Oxidases, ed. by K. Okunuki, in press.

V. Weinzierl, J. E., Eisenberg, D. and Dickerson, R. E., "Refinement of Protein Phases with the Karle-Hauptman Tangent Formula", Acta Cryst., (Received for Publication).

Reprinted from *Acta Crystallographica*, Vol. 23, Part 4. October 1967

PRINTED IN DENMARK

Acta Cryst. (1967). 23, 511

Bias, Feedback and Reliability in Isomorphous Phase Analysis

BY RICHARD E. DICKERSON, MARY L. KOPKA, JOAN C. VARNUM AND JON E. WEINZIERL

Gates and Crellin Laboratories of Chemistry, California Institute of Technology, Pasadena, California, U.S.A.*

(*Received* 2 *December* 1966)

The effect of assumed structural information about heavy atom sites on subsequent difference Fourier maps in the multiple isomorphous replacement phase analysis method is studied. Examples of good and bad derivatives of horse heart cytochrome C are used to illustrate the effect of the introduction of spurious derivatives into a phase analysis. Various means of discriminating between valid and invalid derivatives are compared, and suggested minimum standards for publication of a low resolution structure analysis are presented.

Introduction

In a conventional crystal structure analysis carried out at atomic resolution ($d_{min} = \lambda/s_{max} = \lambda/2 \sin\theta = 0{\cdot}771$ Å for Cu $K\alpha$), the test of the final structure is the degree to which the structure factors calculated from the model agree with those actually observed. The course of analysis – the manner in which the model is obtained – is relatively unimportant. Electron density maps are ultimately more for display than for illumination, and their interpretation is seldom in doubt.

A much different situation prevails in macromolecular structure analysis using multiple isomorphous replacement methods at resolutions short of the atomic level. Here individual atomic positions cannot be found, and the electron density map itself is the sole end product. This map must then be interpreted in terms of a sensible structure, and it becomes vital that the investigator should know exactly how accurate his map is

One of the characteristics of Fourier series which makes Fourier refinement possible in small structures is the feedback property – the property that once an atom is put into the structure factor calculation and made to contribute to the phases (or signs), the atom persists in subsequent electron density maps. The degree and kind of persistence offers a clue as to whether it was put in correctly or not. In a certain sense the phases are *more* important than the amplitudes. Trial phases used with true amplitudes will, under favorable conditions, give a structure intermediate between trial and true structure. Trial phases with unit or random amplitudes will often give the trial model back again. If the trial model is so incorrect that the measured amplitudes are essentially random for this model, then the resulting electron density map can reproduce the false model and create a false impression of correctness. The saving factor is that observed and calculated amplitudes will disagree and the false model can be recognized for what it is. It is this last check which is lacking in low resolution protein or macromolecular structure analyses.

* Contribution No. 3458 from the Gates and Crellin Laboratories of Chemistry.

The correctness of the electron density map in a multiple isomorphous replacement phase analysis depends upon how well the heavy atoms have been located and characterized. Heavy atoms are usually located initially by difference Patterson methods of one type or another, and then characterized (extent of substitution or effective atomic number, and radial fall-off factor or empirical form factor) by methods such as Wilson-type plots or least-squares refinement. From this information, trial phases can be calculated, which can then be used in difference Fourier maps to improve the interpretation of the original heavy atom derivatives or to pull in multiple-site derivatives whose difference Patterson maps were too complex to interpret by themselves.

The danger in this process is that if a wrong interpretation of a heavy atom parameter is made and then if this interpretation enters into the phase analysis, subsequent rechecks involving those phases in difference Fourier maps may tend to confirm the wrong heavy atom. The investigator may carry on unwittingly with this wrong set of phases, produce an incorrect low resolution map of the molecule, and then spend fruitless hours trying to fit known polypeptide chain to what is only noise and error.

The purpose of this study was to see the effect of incorrect bias on a multiple isomorphous replacement analysis, to find out how serious the Fourier feedback problem was, and to try to find some criteria for assessing the reliability of assumed heavy atom parameters. If the investigator has made an error, how soon and in what manner will the subsequent analysis tell him so?

Experimental

The data used in this study were from crystals of the parent horse heart cytochrome C and from four heavy-atom derivatives, containing platinum, mercury, the combination of both at once, and palladium. Cytochrome C was extracted from whole frozen horse hearts by a method developed by Margoliash (1967) and crystallized in one to ten weeks from 95% saturated ammonium sulfate, 1*M* in sodium chloride. The platinum derivative, designated Pt30w, was prepared by diffusing $PtCl_4^{2-}$ into the pregrown crystals at a 7·5:1 mole ratio at *p*H 6 and photographed after 30 weeks. The mercury derivative, designated Hg14w, was prepared in a similar manner by diffusing in mersalyl (the sodium salt of salyrganic acid) at *p*H 6·8 and a 10:1 molar excess of heavy atom and was photographed after 14 weeks of aging. The double derivative was prepared using Pt and Hg at *p*H 6·8 at molar ratios of 1:1 and 3:1, respectively, and was photographed after seven weeks. Palladium as $PdCl_4^{2-}$ or $PdCl_2$ produced no intensity changes in ammonium sulfate, but was found to produce large and characteristic changes in crystals which had first been transferred from sulfate to 4·3 *M* mixed phosphate buffer (2:1 metal/protein mole ratio, *p*H 5·7, aged five weeks). The change of crystal medium itself altered only the innermost reflections, of fourth order or less. Observed structure factor data are shown in Table 1.

Cytochrome was found to crystallize in tetragonal space group $P4_1$ with cell dimensions $a=b=58{\cdot}5$, $c=42{\cdot}3$ Å. After Lorentz–polarization correction, parent and derivative data were placed on the same scale by a Wilson-type plot of $\ln(\langle F_P\rangle/\langle F_{PH}\rangle)$ *versus* s^2, where F_P and F_{PH} are observed parent protein and heavy-atom derivative structure amplitudes and $s=2\sin\theta$. Heavy-atom positions were found from difference Patterson maps using $(\Delta F)^2=(|F_{PH}|-|F_P|)^2$ as coefficients. Scale factors for scaling up the heavy-atom derivative data relative to the parent data were calculated by using an expression derived by Kraut (1961) based upon the assumption that in a centrosymmetric projection the origin peak should be the same height in a ΔI difference Patterson map as in a $(\Delta F)^2$ difference Patterson map:

$$K=\sum_{hk} F_P^2/\sum_{hk} F_P F_{PH}\,.$$

In practice the scaled-up difference Patterson maps were little improved over the level-scale maps ($\Sigma F_P=\Sigma F_{PH}$) other than in having a somewhat quieter background. In no case was any significant detail obscured by the use of level scale. Heavy atom structure factors for single sites were calculated from:

$$f_H=2Ae^{-Bs}\{\cos 2\pi(hx+ky)+\cos 2\pi(hy-kx)\}\,.$$

The extent of substitution, A, and the radial fall-off factor, B, were found by first assuming values of 1·00 and zero, respectively, and then making a Wilson-type plot of $\ln(\langle|\Delta F|\rangle/\langle|f_H|\rangle)$ *versus* s. This was found to give a better straight line plot than s^2, implying a sharper-than-Gaussian radial fall-off of heavy atom contribution near the origin of the diffraction pattern, and a flatter-than-Gaussian profile for the added heavy group. The assumption is physically reasonable at this resolution and the practical distinction is small. Unrefined heavy atom parameters are given in Table 2.

Signs were determined first by inspection and then by the phase probability method of Blow & Crick (1959; Dickerson, Kendrew & Strandberg, 1961*a*). The program which was used alternates a phase determining cycle with one cycle of full-matrix least-squares refinement of heavy atom parameters against the fixed phases of the previous cycle, in a manner first used by Dickerson, Kendrew & Strandberg (1961*a*,*b*) with myoglobin, and subsequently programmed by Kraut, Sieker, High & Freer (1962) for chymotrypsinogen, Muirhead (1966) for haemoglobin, and Lipscomb, Coppola, Hartsuck, Ludwig, Muirhead, Searl & Steitz (1966) for carboxypeptidase. The program is summarized by Dickerson & Palmer (1967). However, except in the 'four-data' phase set used as a check, the parameters in this paper were deliberately *not* refined, and were those taken by inspection from the difference Patterson maps and Wilson plots.

Table 1. *Observed structure factors for parent cytochrome* C *and for heavy atom derivatives*

All data are on the same arbitrary scale. Missing data are represented by −1·00. *AS*=ammonium sulfate; 4·3=4·3 *M* mixed phosphate buffer; *N*=native cytochrome without heavy atoms.

h k	N in AS	Pt in AS	Hg in AS	Double in AS	N in 4.3	Pd in 4.3
1.·0.	23·60	−1·00	−1·00	−1·00	50·66	74·55
1. 1.	5·64	−1·00	23·53	−1·00	37·18	47·98
1. 2.	24·58	2·50	20·20	3·44	28·02	22·49
1. 3.	22·81	12·93	15·05	8·65	19·58	18·56
1. 4.	28·39	36·40	17·17	36·07	24·50	19·73
1. 5.	12·30	5·65	11·61	5·30	15·02	20·15
1. 6.	46·81	33·73	35·55	34·10	51·33	44·39
1. 7.	13·75	8·37	16·16	6·26	16·20	15·67
1. 8.	54·59	49·56	49·59	53·49	55·87	47·20
1. 9.	13·80	7·88	22·12	7·08	13·50	22·39
1.10.	30·66	32·49	34·24	34·62	32·62	26·23
1.11.	54·10	40·75	57·87	50·54	−1·00	59·15
1.12.	33·97	40·54	25·86	37·16	−1·00	29·84
1.13.	15·39	12·04	16·46	12·40	−1·00	24·47
1.14.	4·55	12·42	5·35	8·41	−1·00	6·46
1.15.	18·56	22·62	24·95	29·20	−1·00	17·83
2. 0.	2·27	30·00	20·91	15·21	13·10	25·39
2. 1.	2·45	2·39	4·24	−1·00	22·00	36·31
2. 2.	19·85	2·62	7·37	−1·00	36·03	35·99
2. 3.	30·41	38·34	34·64	38·48	27·29	45·42
2. 4.	141·55	125·55	144·13	180·31	163·83	154·04
2. 5.	16·75	4·76	17·27	5·45	6·46	9·90
2. 6.	46·45	40·86	40·50	43·11	46·24	56·46
2. 7.	16·97	6·88	16·26	7·59	16·80	15·40
2. 8.	10·34	7·43	12·32	6·81	13·21	7·22
2. 9.	48·58	41·10	35·75	39·63	49·51	46·84
2.10.	19·13	30·19	14·44	26·77	19·90	20·24
2.11.	19·01	20·15	23·84	22·49	−1·00	8·68
2.12.	20·08	7·76	23·53	11·59	−1·00	16·35
2.13.	54·42	55·81	46·86	62·09	−1·00	55·82
2.14.	52·90	57·40	53·93	63·89	−1·00	53·32
2.15.	21·20	25·02	24·14	28·65	−1·00	22·77
3. 0.	15·12	8·10	23·13?	−1·00	10·83	13·76
3. 1.	28·50	26·51	34·24	28·31	17·38	17·39
3. 2.	15·03	36·25	18·58	38·73	14·49	14·98
3. 3.	62·27	66·04	62·82	71·48	60·94	77·40
3. 4.	14·23	31·42	15·45	32·80	2·97	27·05
3. 5.	30·26	14·08	34·24	19·28	22·87	17·28
3. 6.	11·76	22·54	15·35	21·89	15·66	30·33
3. 7.	43·49	25·12	33·23	25·18	40·49	41·52
3. 8.	8·16	8·98	5·15	6·86	4·20	8·86
3. 9.	13·87	27·02	8·08	19·54	16·64	13·22
3.10.	4·67	12·61	10·20	7·62	4·68	6·07
3.11.	6·04	9·00	5·55	7·98	−1·00	6·27
3.12.	40·49	28·79	33·53	31·13	−1·00	40·91
3.13.	32·05	27·26	31·92	29·86	−1·00	25·92
3.14.	53·73	44·14	58·78	55·66	−1·00	59·66
3.15.	8·37	9·74	19·90	32·35	−1·00	22·27
4. 0.	43·94	48·85	44·74	54·96	37·68	42·57
4. 1.	39·57	25·42	23·23	24·34	41·25	39·26
4. 2.	14·58	24·66	16·26	22·80	2·83	23·02
4. 3.	48·88	42·91	48·18	47·68	47·25	39·48
4. 4.	15·70	13·80	4·44	11·46	10·34	5·55
4. 5.	7·49	10·78	9·80	7·29	9·01	15·07
4. 6.	5·31	10·05	14·44	6·28	17·00	10·16
4. 7.	27·47	22·78	20·60	23·29	29·99	22·94
4. 8.	36·01	28·52	30·10	28·10	34·50	30·88
4. 9.	32·58	27·24	25·65	26·94	39·31	36·12
4.10.	5·71	14·90	9·09	7·83	4·90	9·78
4.11.	11·74	13·96	5·55	9·67	−1·00	7·58
4.12.	4·73	9·52	5·55	8·31	−1·00	10·30
4.13.	16·49	16·61	20·30	17·18	−1·00	20·09
4.14.	19·70	13·80	24·74	16·84	−1·00	16·76
4.15.	8·45	7·35	−1·00	12·79	−1·00	−1·00
5. 0.	76·63	44·71	58·38	52·35	78·71	68·11
5. 1.	58·91	54·83	54·03	63·66	65·93	56·70
5. 2.	67·00	38·34	74·13	50·09	71·91	64·44
5. 3.	32·26	32·97	25·86	32·94	36·18	28·21
5. 4.	8·45	16·81	5·86	11·08	4·39	5·79
5. 5.	37·78	46·57	44·14	47·34	40·38	43·19
5. 6.	30·87	36·45	27·67	37·98	28·50	28·75
5. 7.	17·54	28·71	8·99	19·66	16·96	19·41
5. 8.	35·81	29·50	27·98	28·58	31·11	21·06
5. 9.	47·96	28·86	46·36	35·28	52·83	42·62
5.10.	36·03	38·27	38·68	39·07	38·68	39·06
5.11.	22·67	29·37	19·80	25·50	−1·00	8·38
5.12.	6·02	12·61	11·41	8·41	−1·00	6·55
5.13.	28·48	26·24	28·28	29·72	−1·00	35·32
5.14.	20·36	16·93	11·51	18·19	−1·00	6·11
5.15.	39·75	−1·00	−1·00	−1·00	−1·00	−1·00
6. 0.	20·49	22·87	18·79	22·66	16·65	13·93
6. 1.	4·71	6·56	16·36	5·77	9·16	8·86
6. 2.	5·40	6·36	4·65	5·92	3·43	5·79
6. 3.	8·01	5·49	4·75	6·09	10·88	14·91
6. 4.	10·27	18·45	5·86	12·95	7·77	6·24
6. 5.	28·78	22·73	27·47	21·57	27·62	24·70
6. 6.	19·37	7·97	11·21	6·85	21·20	20·20
6. 7.	32·18	23·38	31·51	24·05	31·88	28·00
6. 8.	14·03	17·44	14·64	15·06	4·60	16·02
6. 9.	5·36	8·80	5·55	7·84	4·91	6·21
6.10.	7·85	7·59	9·90	8·05	6·58	6·29
6.11.	34·10	35·42	39·29	39·87	−1·00	44·92
6.12.	41·91	44·42	48·28	48·40	−1·00	43·89
6.13.	9·66	9·86	10·40	8·34	−1·00	11·75
6.14.	35·30	29·93	35·96	26·44	−1·00	30·57
7. 0.	21·16	35·18	16·36	29·96	16·76	26·00
7. 1.	25·33	30·06	16·06	28·30	26·11	35·56
7. 2.	8·44	24·65	13·84	24·62	4·74	5·13
7. 3.	5·83	5·86	4·95	6·46	3·82	5·86
7. 4.	22·95	35·02	21·31	34·33	25·63	33·19
7. 5.	13·72	6·41	12·02	7·00	13·89	13·79
7. 6.	4·60	8·04	7·27	7·24	7·45	5·87
7. 7.	4·68	10·69	5·45	7·51	4·58	11·74
7. 8.	33·48	34·66	38·18	36·03	33·36	38·73
7. 9.	22·19	18·15	17·78	13·21	27·13	22·20
7.10.	23·36	24·45	23·43	23·67	25·29	20·45
7.11.	16·43	19·24	12·32	13·01	−1·00	14·96
7.12.	36·38	32·77	32·12	32·99	−1·00	21·87
7.13.	10·01	14·91	16·16	8·16	−1·00	17·28
7.14.	5·29	−1·00	−1·00	−1·00	−1·00	−1·00
8. 0.	35·73	25·70	41·01	27·37	35·17	32·66
8. 1.	16·86	20·72	15·76	17·70	19·50	8·43
8. 2.	23·11	10·96	9·29	6·81	22·78	27·77
8. 3.	8·95	15·86	8·58	8·34	4·20	13·68
8. 4.	27·17	15·32	32·12	18·73	19·64	19·18
8. 5.	26·97	30·64	21·71	30·78	28·74	34·79
8. 6.	11·26	6·98	11·82	7·53	12·02	6·03
8. 7.	55·27	60·85	61·71	64·55	62·55	68·44
8. 8.	14·08	18·90	5·55	16·35	15·52	8·70
8. 9.	21·30	26·23	19·69	22·36	18·80	12·77
8.10.	31·15	27·89	32·02	32·35	35·94	27·95
8.11.	16·06	18·26	17·17	17·80	−1·00	13·58
8.12.	10·62	8·02	6·56	8·21	−1·00	11·89
8.13.	50·67	44·33	44·74	39·96	−1·00	−1·00
9. 0.	4·51	11·36	6·36	7·07	4·27	5·65
9. 1.	21·43	29·13	33·53	34·98	23·36	25·27
9. 2.	37·04	24·38	34·64	27·33	40·89	33·45
9. 3.	19·85	13·82	29·19	12·93	21·01	13·43
9. 4.	14·64	20·94	11·51	13·47	12·88	21·90
9. 5.	36·62	27·30	32·32	27·83	35·86	28·62
9. 6.	42·54	40·51	50·30	45·50	45·85	47·68
9. 7.	4·75	7·51	5·55	7·98	5·05	5·74
9. 8.	14·31	16·84	21·31	12·88	13·28	21·04
9. 9.	17·82	17·80	13·03	8·33	17·05	9·67
9.10.	18·47	18·28	17·88	14·91	16·96	21·24
9.11.	6·09	9·81	9·09	8·31	−1·00	6·37
9.12.	4·19	7·96	4·95	8·07	−1·00	6·13
9.13.	−1·00	−1·00	−1·00	−1·00	−1·00	−1·00
10. 0.	10·31	9·82	5·45	12·13	4·60	6·66
10. 1.	4·68	8·42	6·16	7·54	4·61	6·04
10. 2.	8·31	26·03	6·97	16·82	8·04	15·44
10. 3.	4·67	7·09	5·45	7·62	4·68	6·07
10. 4.	39·17	19·29	29·49	23·36	43·23	32·92
10. 5.	13·22	17·99	18·68	18·45	8·57	12·38
10. 6.	29·08	21·80	25·65	13·31	31·15	17·60
10. 7.	8·19	9·33	21·71	8·19	9·79	14·75
10. 8.	45·26	38·05	48·28	40·85	55·86	47·53
10. 9.	12·28	20·07	12·52	14·60	8·88	11·89
10.10.	28·81	21·87	27·77	23·90	35·21	25·88
10.11.	21·90	20·96	25·96	18·02	−1·00	33·50
10.12.	49·59	−1·00	−1·00	22·13	−1·00	−1·00
11. 0.	20·74	20·94	20·40	15·06	−1·00	19·11
11. 1.	15·04	24·75	5·55	20·24	−1·00	14·05
11. 2.	9·42	12·58	12·83	7·93	−1·00	6·99
11. 3.	15·63	22·25	24·24	26·56	−1·00	22·09
11. 4.	4·75	11·33	5·55	8·06	−1·00	6·30
11. 5.	31·73	21·78	31·92	21·35	−1·00	27·50
11. 6.	54·51	48·47	53·83	53·71	−1·00	64·62
11. 7.	35·00	38·62	27·37	36·89	−1·00	26·22
11. 8.	8·33	8·15	5·45	8·43	−1·00	6·51
11. 9.	17·32	18·21	22·83	22·05	−1·00	21·89
11.10.	5·73	11·92	4·95	8·03	−1·00	6·11
11.11.	≤2·20	−1·00	−1·00	15·00	−1·00	−1·00
12. 0.	10·86	23·24	9·59	20·40	−1·00	10·51
12. 1.	4·74	9·26	5·55	8·14	−1·00	15·67
12. 2.	21·03	35·68	23·53	35·53	−1·00	26·25
12. 3.	28·08	21·92	25·15	24·69	−1·00	30·66
12. 4.	27·72	9·52	29·39	11·78	−1·00	23·86
12. 5.	27·52	29·46	33·23	30·73	−1·00	41·15
12. 6.	29·90	19·44	31·92	18·31	−1·00	22·99
12. 7.	4·55	12·09	5·35	8·37	−1·00	6·44
12. 8.	36·24	30·85	25·75	26·41	−1·00	26·81
12. 9.	31·73	29·07	31·11	30·48	−1·00	30·31
12.10.	23·39	−1·00	−1·00	7·43	−1·00	−1·00
13. 0.	7·74	12·90	8·58	15·13	−1·00	15·72
13. 1.	4·73	12·04	5·55	8·42	−1·00	7·21
13. 2.	33·19	28·64	24·44	21·82	−1·00	35·47
13. 3.	19·85	9·69	20·00	11·91	−1·00	16·81
13. 4.	29·97	35·67	21·92	37·01	−1·00	30·58
13. 5.	66·06	55·99	63·93	62·28	−1·00	61·31
13. 6.	22·97	15·35	18·48	15·24	−1·00	22·50
13. 7.	12·07	8·01	5·05	8·16	−1·00	6·21
13. 8.	4·02	13·35	4·75	7·83	−1·00	5·94
13. 9.	−1·00	−1·00	−1·00	−1·00	−1·00	−1·00
14. 0.	27·53	33·72	23·63	33·92	−1·00	33·37
14. 1.	16·64	20·99	18·28	19·84	−1·00	11·13
14. 2.	25·64	12·72	22·02	13·86	−1·00	17·85
14. 3.	4·46	8·14	15·25	8·34	−1·00	8·06
14. 4.	4·37	13·16	5·15	8·26	−1·00	6·30
14. 5.	4·19	7·90	4·95	8·19	−1·00	6·11
14. 6.	23·33	7·73	17·98	12·31	−1·00	21·79
14. 7.	17·33	−1·00	−1·00	−1·00	−1·00	−1·00
15. 0.	12·32	19·32	9·59	18·78	−1·00	12·26
15. 1.	5·64	11·71	11·92	−1·00	−1·00	12·38
15. 2.	9·06	14·72	4·75	16·23	−1·00	14·91
15. 3.	12·05	9·74	10·50	11·17	−1·00	−1·00
15. 4.	22·97	13·54	34·24	30·13	−1·00	−1·00
15. 5.	21·50	−1·00	−1·00	−1·00	−1·00	−1·00

Table 2. *Unrefined heavy atom parameters for cytochrome derivatives*

Derivative	*x*	*y*	*B*	*A*
Pt30w	0·220	0·200	7·46	8·15
Hg14w	0·020	0·400	8·63	5·80
Pd	0·150	0·030	7·75	4·45
	0·090	0·300	7·75	4·45
Erronium	0·280	0·280	7·58	5·90

Of the two general classes of derivative tests, real space tests (Patterson, Fourier and convolution methods) and reciprocal space tests (figures of merit, *R* factors and sign or phase agreement), this paper is concerned chiefly with the former. Reciprocal space criteria will be mentioned in passing where relevant. The most widely used such criterion is the 'figure of merit', *m*, an attenuation factor ranging between 0 and 1 which is both the weighting factor to the *F*'s or *ΔF*'s which insures the smallest r.m.s. error in electron density throughout a map (Blow & Crick, 1959), and the mean value of the cosine of the error in phase angle for the reflection in question (Dickerson *et al.*, 1961*b*).

A second widely used criterion is the Kraut *R* factor (Kraut *et al.*, 1962), defined by:

$$R_K \equiv \frac{\sum_{hkl} |\varepsilon_{hkl}|}{\sum_{hkl} |F_{PH}|}$$

where ε_{hkl} is the lack-of-closure error of the phase triangle of the derivative in question using the protein phase angle determined by all the derivatives together:

$$|\varepsilon_{hkl}| \equiv ||\mathbf{F}_{PH}| - |\mathbf{F}_P + \mathbf{f}_H|| \,.$$

A third criterion is the 'centric *R* factor' of Cullis, Muirhead, Perutz, Rossmann & North (1961):

$$R_C \equiv \frac{\sum_{hkl} ||\Delta F| - |f_H||}{\sum_{hkl} |\Delta F|}$$

where:

$$|\Delta F| = ||F_{PH}| - |F_P|| \,.$$